INFORMATION TO USERS

This manuscript has been reproduced from the microfilm master. UMI films the text directly from the original or copy submitted. Thus, some thesis and dissertation copies are in typewriter face, while others may be from any type of computer printer.

The quality of this reproduction is dependent upon the quality of the copy submitted. Broken or indistinct print, colored or poor quality illustrations and photographs, print bleedthrough, substandard margins, and improper alignment can adversely affect reproduction.

In the unlikely event that the author did not send UMI a complete manuscript and there are missing pages, these will be noted. Also, if unauthorized copyright material had to be removed, a note will indicate the deletion.

Oversize materials (e.g., maps, drawings, charts) are reproduced by sectioning the original, beginning at the upper left-hand corner and continuing from left to right in equal sections with small overlaps.

Photographs included in the original manuscript have been reproduced xerographically in this copy. Higher quality 6" x 9" black and white photographic prints are available for any photographs or illustrations appearing in this copy for an additional charge. Contact UMI directly to order.

Bell & Howell Information and Learning
300 North Zeeb Road, Ann Arbor, MI 48106-1346 USA
800-521-0600

UMI®

STUDIES OF ELECTRON-WITHDRAWING PHOSPHORUS LIGANDS FOR HYDROFORMYLATION, AND OF AN FE-CR METHOXYCARBYNE COMPLEX

By

WEI LUO

A dissertation submitted to the Graduate Faculty in Chemistry in partial fulfillment of the requirements for the degree of Doctor of Philosophy, The City University of New York

2000

This manuscript has been read and accepted for the Graduate Faculty in Chemistry in satisfaction of the dissertation requirement for the degree of Doctor of Philosophy.

1/20/00
Date

William H. Hersh
Professor William H. Hersh
Chair of Examining Committee

1/21/2000
Date

Gerald Koeppl
Professor Gerald Koeppl
Executive Officer

Professor William H. Hersh

Professor Harry D. Gafney

Professor Klaus G. Grohmann

Supervisory Committee

THE CITY UNIVERSITY OF NEW YORK

Abstract

STUDIES OF ELECTRON-WITHDRAWING PHOSPHORUS LIGANDS FOR HYDROFORMYLATION, AND OF AN FE-CR METHOXYCARBYNE COMPLEX

by

Wei Luo

Adviser: Professor William H. Hersh

Part 1: Three new iron-chromium heterodinuclear compounds, $[Cp(CO)Fe(\mu\text{-}CO)_2Cr(CO)(\eta^6\text{-}C_6H_6)]^-Na^+$ (**6-Na$^+$**), $[Cp(CO)Fe(\mu\text{-}CO)_2Cr(CO)(\eta^6\text{-}C_6H_6)]^-[PPN^+]$ (**6-PPN$^+$**) [PPN^+ = bis(triphenylphosphine)nitrogen(+1)] and $Cp(CO)Fe(\mu\text{-}COCH_3)(\mu\text{-}CO)Cr(CO)(\eta^6\text{-}C_6H_6)$ (**7**) were prepared. Cis/trans isomerization of **6-Na$^+$** was observed by ^1H and ^{13}C NMR to occur remarkably rapidly in CD_3CN. Isomerization of methoxycarbyne **7** is slower but still rapid by comparison to related compounds. Thermal decomposition of **7** at 50 °C in C_6D_6 with and without PPh_3 provides just the fourth example of oxygen to metal methyl migration in a methoxycarbyne complex. However, it is the first example in which a *methoxy*carbyne follows kinetics in which the values of the rate constants are independent of phosphine concentration. This decomposition

results in the cleavage of the iron-chromium bond. The use of these compounds in non-linear optical applications is considered, but the metal-metal cleavage may limit their utility in the preparation of novel mixed-metal materials.

Part 2: Hydroformylation of 1-hexene and 1-octene was carried out in THF using $Rh(acac)(CO)_2$ as a catalyst precursor in the presence of a variety of aminophosphine additives. The electron-withdrawing chelating ligand *N, N'*-bis(diphenylphosphino)-*N, N'*-di-*p*-toluenesulfonyl-1,2-ethanediamine (**diTosL**) gives the highest yields (>80%) and regioselectivity, favoring the formation of the linear aldehyde over the branched aldehyde by a ~10:1 ratio. A monodentate analog of **diTosL** and an N-methyl electron-donating analog each give rise to lower yields and much lower regioselectivity. Attempts to prepare modified **diTosL** analogs with more rigid backbone linkages failed due to the high degree of steric hindrance around both nitrogen atoms. Two new chelating analogs of 2-phenyl-1,3-di-*p*-toluenesulfonyl-1,3,2-diazaphospholidine (**TosL**) were also prepared, but they are insoluble in common hydroformylation solvents. In the solvent in which they are soluble, DMF, no hydroformylation is observed to occur. We propose that DMF is more strongly coordinating than these weakly

coordinating ligands towards rhodium, resulting in the loss of catalytic ability of the ligands.

Table of Contents

Lists of Tables

Part 1

Part 2

Lists of Plots and Spectra

Part 1

Part 2

Part 1.

Synthesis and Reaction of the Heterodinuclear Methoxycarbyne Complex $Cp(CO)Fe(\mu\text{-}COCH_3)(\mu\text{-}CO)Cr(CO)(\eta^6\text{-}C_6H_6)$, a Potential Precursor to Nonlinear Optical Materials

[Reproduced in part with permission from Luo, W.; Fong, R. H.; Hersh, W. H. *Organometallics*, **1997**, *16*, 4192-4199, Copyright 1997 American Chemical Society]

I. Introduction

We have been studying the chemistry of heteronuclear alkoxycarbyne complexes for many years since our report of **2**, the first neutral heterodinuclear methoxycarbyne (Scheme 1).[1-6] This and related compounds are synthesized by alkylation of heterodinuclear anions that have structures analogous to that of the well-known iron dimer $[CpFe(CO)_2]_2$.[7,8] That is, each contains two bridging carbonyl ligands, two terminal carbonyl ligands (or one nitrosyl ligand as in **5**), and each compound exists as a mixture of interconverting cis and trans isomers. The carbynes have the iron dimer structure as well, but with a bridging carbyne ligand in place of the μ-CO ligand. Each carbyne undergoes a novel thermal decomposition reaction in which the alkyl group migrates from oxygen to iron with concomitant cleavage of the metal-metal bond, as shown for carbynes **2**, **3**, and **5**. The initially formed iron product in principle could be the 18-electron complex $CpFe(CO)_2CH_3$, the unsaturated species $CpFe(CO)CH_3$, or more speculatively $CpFe{\equiv}COCH_3$.[5,9] In practice, the isoelectronic $MeCpMn(CO)_3$ and $CpCr(CO)_2NO$ molecules are ejected during the thermal decomposition,

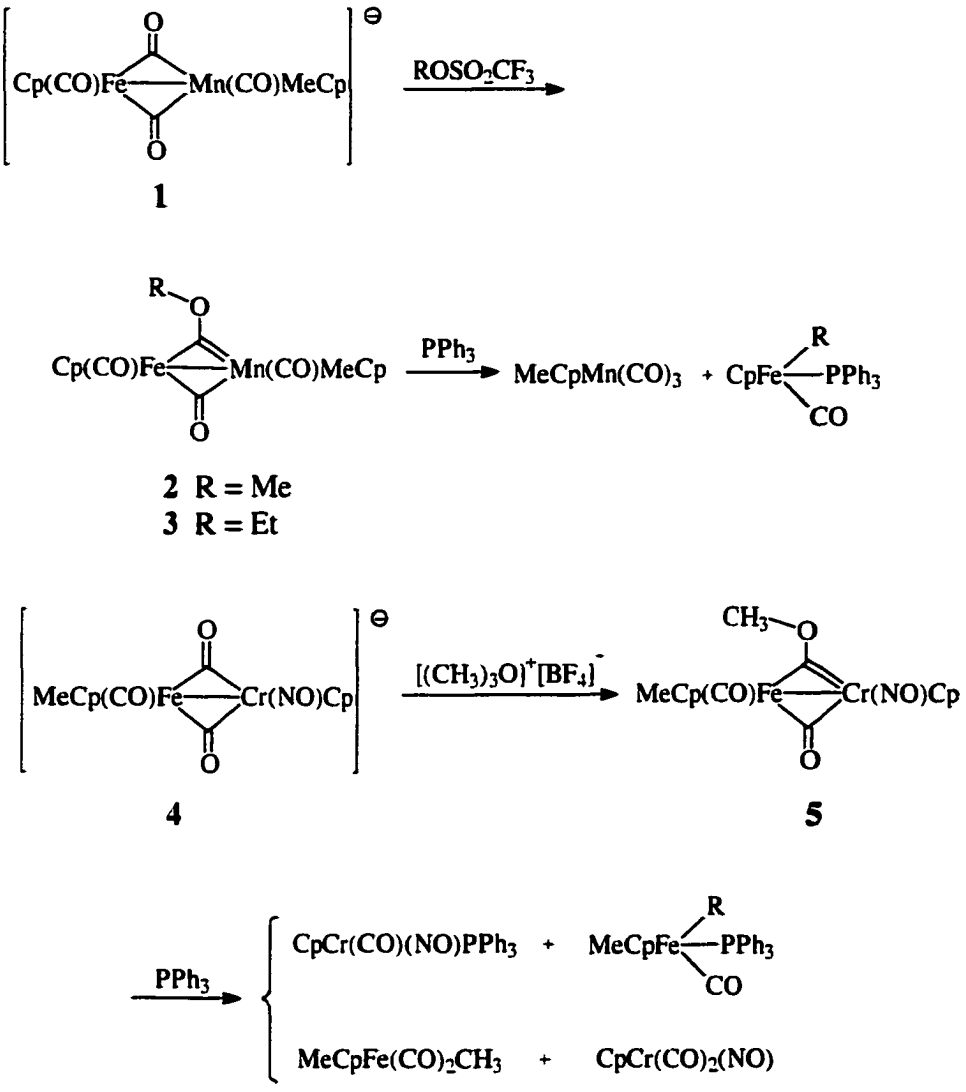

Scheme 1

requiring that $CpFe(CO)_2CH_3$ not be a stoichiometrically-formed primary product, and the alkyl is trapped as $CpFe(CO)(PPh_3)R$ (R = Me, Et). In **5** an additional pathway exists in which CpCr(CO)NO is ejected and then trapped by external PPh_3, so here $CpFe(CO)_2CH_3$ could form initially. Part of our effort has been directed at trying to understand these details in hopes that light might be shed on the mechanism of the alkyl migration step itself.

In addition to this mechanistic interest, such carbyne chemistry can provide a unique means by which to stitch together metals that might lead to materials with unique nonlinear optical [10-13] or magnetic properties.[14-16]

Nonlinear optics is the study of the interaction of intense electromagnetic fields with materials to produce modified fields that are different from the input field in frequency, phase, or amplitude. For nonlinear optical (NLO) properties molecular polarization is necessary.[17] For magnetic properties, paramagnetic metals such as Fe, Cr and Mn are desired.[18] Formation of bonds between different metals is well-known to lead to large perturbations in electronic properties,[19] but there are few studies examining NLO effects in mixed metal systems.[20] The dinuclear metal compounds synthesized in our lab such as **1** to **5** in Scheme 1 might be good candidates for the research.

NLO materials that are widely used in the telecommunications industry for high-band width optical switching and processing devices[21] are often prepared using single-crystal methods that are costly. A potentially simpler and lower cost approach, to be carried out in collaboration with Professors Harry Gafney, Peter Wong, and Tak Cheung, involved the use of Porous Vycor Glass (PVG) that would incorporate the transition metal compounds to attempt to produce new NLO and/or magneto-optical materials that retain high optical transparency. Organometallic compounds would be loaded on PVG, which is a proprietary borosilicate glass with high surface area and ~ 100 Å pores and cavities, by dipping the glass into a solution of the compound, followed by solvent removal under vacuum.[22] Photolysis or thermolysis would then lead to deposition of metal clusters or their oxides on or inside the PVG[15] to form the new magneto-optical material.

Second harmonic generation (SHG) is an NLO process that results in the conversion of an input optical wave into an output wave of half the input wavelength. For example, when an infrared laser (λ = 1064 nm) illuminates an SHG active material, a green light (λ = 532 nm) is emitted. At the outset of this project, we planned to have the SHG properties of metal compounds tested by Professor Cheung at Queensborough Community College using a 1064 nm laser. In order to gain experience with the experimental set-up and

to compare new compounds to well-known SHG-active materials, Professor Cheung tested compounds in the solid state using the Kurtz and Perry[23] powder method; he planned to later compare SHG properties for materials loaded on the PVG. For qualitative results and for the initial survey work, a thin layer (~ 0.2 mm) of powdered sample was placed on a microscope slide and held in place with transparent tape, and then placed in the laser path. As expected, the SHG-active reference material $LiNbO_3$ gave rise to a green light while the SHG-inactive reference material NaCl did not.[24] Since most organometallics are air and/or water sensitive, $LiNbO_3$ and NaCl samples were also prepared by packing the powders in a melting-point capillary with a diameter of about 1 mm which was then sealed with a flame. These samples also behaved as expected with Professor Cheung's set-up.

Professor Cheung then proceeded to test organometallic compounds that were available in our lab, including $W(CO)_6$, $(C_6H_6)Cr(CO)_3$, $[Na][Cp(CO)Fe(\mu\text{-}CO)_2Cr(CO)(C_6H_6)]$, $Me_3PW(CO)_5$, $Ph_3PW(CO)_5$, *p*-$MeC_6H_4CNW(CO)_5$, and $[Na][Cp(CO)Fe(\mu\text{-}CO)_2Mn(CO)Cp]$. The first compound, $W(CO)_6$, is a nonpolar, centrosymmetric octahedral molecule and was expected not to give any SHG,[17] and the second compound, $(C_6H_6)Cr(CO)_3$, crystallizes in a centrosymmetric space group and so also was expected not to give any SHG.[11] We presume, although we cannot be

certain, that the other crystals are also centrosymmetric, since this is the most likely possibility.[11]

Surprisingly, *all* of the organometallic compounds, including $W(CO)_6$, gave rise to a green light as seen for $LiNbO_3$, and then burned in seconds! Two control experiments were run to check if the compounds were simply absorbing IR light and then burning due to the accumulation of heat in the relatively thick layer of sample. However, in one, SHG-active urea powder[24] tightly packed in a 5-mm glass tube did not burn but just turned hot, and in the second, a thin layer (~ 0.5 mm) of 10% $W(CO)_6$ in NaCl on a slide still burned. No rational explanation for these results was ever obtained, although Professor Cheung suspected the novel results were due to the unusually high power of the laser used. The NLO studies were dropped from my thesis.

In any event, we were left without any means to measure SHG in our organometallic compounds, and so our attention was switched to the synthesis of a new heterodinuclear methoxy carbyne and its thermal decomposition chemistry since this might have relevance for the PVG deposition work if it were to be resumed. The new carbyne, $Cp(CO)Fe(\mu\text{-}COCH_3)(\mu\text{-}CO)Cr(CO)(\eta^6\text{-}C_6H_6)$,[25] was first described in 1985 by Raymond H. Fong, a former student of Dr. Hersh. In this thesis, I will describe the

completion of this work, including the synthesis and characterization of this carbyne, and the study of its decomposition chemistry in the presence and absence of PPh_3. The results show that the iron-chromium bond undergoes cleavage upon heating to give $(C_6H_6)Cr(CO)_3$ as the major chromium decomposition product under all conditions. Without PPh_3, $CpFe(CO)_2CH_3$ is the major iron decomposition product while in the presence of PPh_3 $CpFe(CO)(PPh_3)CH_3$ becomes predominant. A mechanism for the decomposition will be proposed. This work has been published in full.[26]

II. Results and Discussion

Synthesis of a Dinuclear Iron-Chromium Anion. A 1:1 molar ratio of solid $CpFe(CO)_2Na\cdot$~0.5THF and $(\eta^6\text{-}C_6H_6)Cr(CO)_2(CH_3CN)$ were combined in THF, and the solution was stirred at room temperature under a nitrogen atmosphere. After 3 hours, the reaction was judged to be complete on the basis of monitoring the appearance of a new carbonyl band in the infrared spectrum at 1615 cm^{-1}. Following solvent removal and washing with benzene, the desired anion, $[Cp(CO)Fe(\mu\text{-}CO)_2Cr(CO)(\eta^6\text{-}C_6H_6)]^-Na^+$ (**6-Na$^+$**) was isolated in 77% yield as a black solid (eq 1). In THF, the infrared spectrum was complicated by

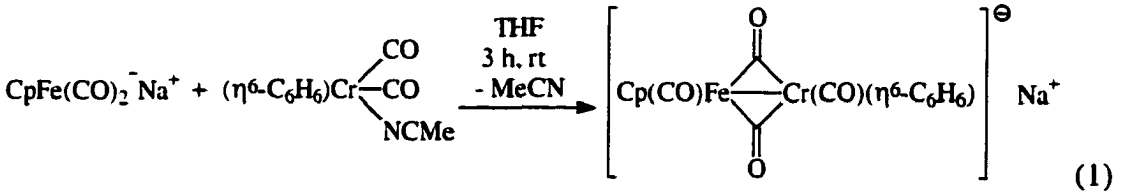

6-Na$^+$ (1)

ion-pairing but in acetonitrile it exhibited three strong bands at 1885, 1813, and 1661 cm^{-1}, corresponding to the two terminal and one bridging CO ligands. The room temperature ^1H and ^{13}C NMR spectra of **6-Na$^+$** in CD_3CN exhibited one C_6H_6 and one Cp signal, as well as signals indicating the presence of 1.3 equiv of Na^+-coordinated THF; peaks in the ^{13}C NMR

spectrum due to the carbonyl ligands could not be identified (see the variable-temperature NMR section below).

Metathesis of **6-Na**$^+$ with PPN^+Cl^- [PPN^+ = bis(triphenylphosphine)nitrogen(+1)] gave the corresponding **6-PPN**$^+$ salt. Its IR spectrum in THF simplified to four carbonyl bands at 1894, 1861, 1823, and 1678 cm^{-1}, while in acetonitrile it was virtually identical to that of the sodium salt. The room temperature ^1H NMR spectrum exhibited signals at δ 4.62 (s, 6H) and 4.33 (s, 5H) ppm due to the C_6H_6 and Cp ligands, respectively, and at 7.67-7.44 ppm due to the phenyl protons, while the ^{13}C NMR similarly exhibited signals due to a single set of C_6H_6, Cp, and PPN^+ carbons; like the Na^+ spectrum, no carbonyl ligands were visible. Integration of the ^1H NMR spectrum consistently gave more phenyl protons than warranted (40% excess under standard acquisition conditions), in part due to long relaxation times of the benzene and cyclopentadienyl ligands. Even increasing the relaxation delay to greater then 20 s did not suffice, but cutting the ^1H flip angle from the usual 30° down to 3° gave constant integrals for 1-20 s relaxation delays. Nevertheless, at best a 10% excess of phenyl protons was still present. Consistent with this, suitable elemental analyses could not be obtained for **6-PPN**$^+$, but the low carbon analysis is not consistent with the presence of impurities such as $CpFe(CO)_2^-PPN^+$ or

PPN^+Cl^- which have the requisite extra phenyl protons but are higher rather than lower in the percentage of carbon. Both **6-PPN$^+$** and **6-Na$^+$** were found to be unstable in methylene chloride, so this solvent could not be used for recrystallization and further purification could not be accomplished. Interestingly, **4-PPN$^+$** was also found to be unstable in methylene chloride.

Synthesis of an Iron-Chromium Methoxycarbyne. Alkylation of the heterodinuclear anion was carried out by rapid addition of 1 equiv of $(CH_3)_3O^+BF_4^-$ to a CH_3CN solution of **6-Na$^+$**. After 5 min of stirring followed by solvent removal, the desired carbyne **7** was obtained as a brown solid that was contaminated by substantial amounts of $[CpFe(CO)_2]_2$ and $(C_6H_6)Cr(CO)_3$ (eq 2). Purification by chromatography could not be carried out due to decomposition of the carbyne product on a silica gel column. Nonetheless, subsequent workup followed by two recrystallizations from CH_2Cl_2/hexane gave a spectroscopically pure material. Similar to the anion **6-PPN$^+$**, a suitable elemental analysis could not be obtained, although in this case the cause is undoubtedly due to the thermal instability of the carbyne. The overall yield after the two recrystallizations was 29%. While this is significantly lower than that obtained for iron-manganese carbynes **2** and **3**, it is higher than that obtained for the iron-chromium carbyne **5**. This effect presumably is due to the higher nucleophilicity of the bridging CO ligands in

the non-nitrosyl anion **6**, as reflected in the lower CO stretching frequencies (see below).

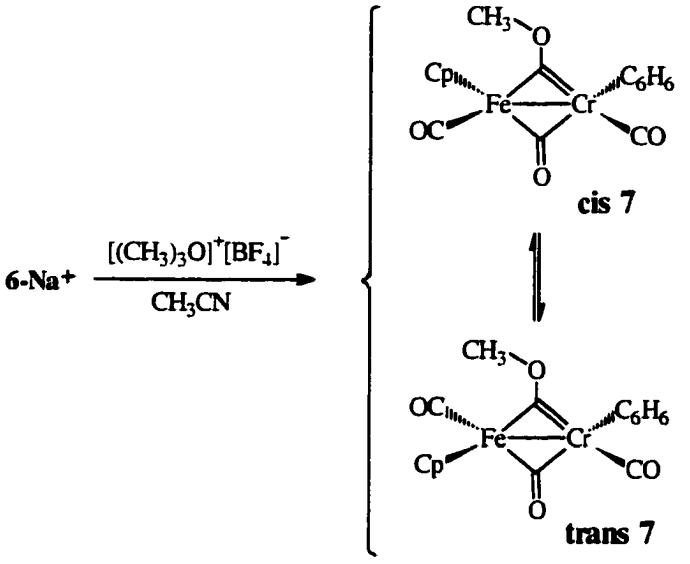

(2)

The IR spectrum of **7** exhibits strong bands at 1943 and 1876 cm^{-1} for the two terminal CO ligands and one strong band at 1736 cm^{-1} for the bridging carbonyl. These bands are consistent with retention of the iron dimer type structure and absence of the negative charge (see below).

Both the ^{1}H and ^{13}C NMR spectra clearly exhibit broad lines due to a dynamic process as indicated in eq 2. The room temperature ^{1}H NMR spectrum in C_6D_6 for instance was not particularly informative, consisting of broad peaks at 4.56 and 4.41 ppm due to the overlapping and interconverting

Table 1. Infrared Stretching Frequencies in Dimuclear $[CpFe(CO)_2]_2$ Analogs

compound (solvent)	Fe—Cr	M'—Cr	μ—CO	Cr—NO
1-PPN$^+$ (CH_2Cl_2)	1899	1832	1671	
4-PPN$^+$ (CH_3CN)	1891		1698	1558
6-PPN$^+$ (CH_3CN)	1886	1812	1661	
$[CpFe(CO)_2]_2$ (CH_2Cl_2)	1996	1954	1773	
2 (THF)	1954	1907	1774	
***cis*-5** (C_6H_6)	1966		1794	1659
7 (CH_2Cl_2)	1943	1876	1736	

cyclopentadienyl and benzene ligands and a sharp peak at 4.25 ppm due to the methoxy group. In CD_2Cl_2, a broad but more informative spectrum was obtained, exhibiting peaks at 5.32, 4.87, and 4.66 ppm that on the basis of relative integrals are due to the benzene, methoxy, and Cp ligands, respectively. The room temperature ^{13}C NMR spectrum (CD_2Cl_2) exhibited a peak at 392.2 ppm that is typical of μ-carbyne resonances; for instance, that in **2** is at 391 ppm and that in **5** is at 428 ppm.[4,5] The methyl from the alkylating reagent is clearly incorporated as a methoxy group, as judged by the new methoxy signal at 71.5 ppm. In addition, signals indicative of two terminal CO ligands (236.7 ppm, Cr-CO; 215.0 ppm, Fe-CO) and one bridging CO (285.2 ppm) were observed. Two broad peaks were observed for the Cp and benzene peaks at 85.77 and 97.39 ppm, respectively, but in addition, two much smaller broad peaks at 98.84 and 88.05 ppm suggested the presence of a second isomer in a 75:25 ratio. The intensities of the other bands were too small to allow peaks for the second isomer to be observed above the noise, with the exception of the methoxy peak, but presumably methoxy peaks for the two isomers overlap as observed previously.[4]

Infrared Spectra of Iron Dimer Analogs. Infrared data are collected in Table 1 for the heterodinuclear anions and carbynes that have been discussed above, along with that of the iron dimer $[CpFe(CO)_2]_2$. The carbonyl bands

of **6-PPN**$^+$ are each about 10-20 cm^{-1} lower than those of **1-PPN**$^+$, and the value for the bridging CO ligands in **6-PPN**$^+$ is nearly 40 cm^{-1} lower than that for **4-PPN**$^+$. The lower CO stretching frequencies indicate the presence of more negative charge on these ligands. Presumably, the strongly π-acidic NO ligand in **4-PPN**$^+$ removes electron density from the bridging CO ligands more than the terminal CrCO ligand does in **6-PPN**$^+$, and the neutral benzene ligand of **6** permits a lower oxidation state than the anionic Cp^- ligand of **1** and **4** does. The bands of **6-PPN**$^+$ are all lower than those of the isoelectronic and isostructural iron dimer $[CpFe(CO)_2]_2$ by >100 cm^{-1} due to the negative charge; those at 1885 and 1661 cm^{-1} are ~110 cm^{-1} lower than those in the iron dimer at 1996 and 1773 cm^{-1}, while the third band is ~140 cm^{-1} lower than that in the iron dimer at 1954 cm^{-1} and, therefore, may be due to the CrCO ligand.

All of the terminal carbonyl ligands exhibit lower frequencies in the carbynes than those seen in the iron dimer, so it is reasonable to conclude that the carbyne ligand is not as electron-withdrawing as a bridging carbonyl ligand. The remaining bridging carbonyl ligand in **2** has the same frequency as the μ-CO of the iron dimer while that in **5** is higher. In contrast, the bridging carbonyl ligand in **7** is much lower in frequency, as is the terminal carbonyl ligand on Cr at 1876 cm^{-1}. Here, once again then, the (η^6-C_6H_6)Cr

fragment appears to be more electron-rich than the MeCpMn or CpCr(NO) fragments.

Variable-Temperature NMR Spectra of Anion 6-Na^+ and Methoxycarbyne 7. While the purity of the PPN^+ salt of **6** is higher than that of the Na^+ salt, the solubility is much lower and suitable ^{13}C NMR spectra could not be obtained. The Na^+ salt, as judged from the IR spectrum in acetonitrile, is not ion-paired, so except for the question of purity it would be expected to give useful spectra of the heterodinuclear anion. At room temperature, both salts gave a single peak for each of the benzene and cyclopentadienyl moieties in the ^1H and ^{13}C NMR spectra as described above. Upon cooling **6-Na^+** to -50 °C, each singlet split into two broad singlets in a 63:37 ratio, consistent with the presence of interconverting cis and trans isomers, as previously observed for the Fe-Mn anion.[4] Spectra were simulated using the chemical shifts and isomer ratios at -50 °C, giving in the ^{13}C NMR (for cis to trans isomerization) $k_{ct} = 12 \pm 2\ s^{-1}$ at -50 °C but requiring $k_{ct} \geq 15{,}000\ s^{-1}$ at 22 °C to fit the coalesced spectrum. A lower rate suffices to simulate the room temperature ^1H NMR spectrum, where coalescence occurs by –20 °C at $k_{ct} = 500 \pm 50\ s^{-1}$, but there is no difference in the simulated spectra at 22 °C for $k_{ct} \geq 5000\ s^{-1}$ since the fast-exchange limit has already been reached. A linear plot of $\ln(k_{ct}/T)$ vs. $1/T$ was

obtained, giving $\Delta G^{\ddagger}$(300 K) = 11.5 ± 0.6 kcal/mol, $\Delta H^{\ddagger}$ = 12.6 ± 0.3 kcal/mol, and $\Delta S^{\ddagger}$ = 3.7 ± 1.4 eu. By comparison, the rate constant for **1-PPN**$^{+}$ in CD_2Cl_2 at 297 K was 14 ± 1 s^{-1}, with $\Delta G^{\ddagger}$ (300 K) = 15.8 ± 0.4 kcal/mol. The barrier for cis/trans isomerization of **6-Na**$^{+}$ is remarkable in that it is the lowest we know of for a compound of the iron dimer structure. The next lowest is $[CpFe(CO)_2]_2$ itself, for which $\Delta G^{\ddagger}$(220 K) ≈ 12 kcal/mol. While we can only speculate as to the cause, it is possible that the Na^{+} ion is responsible rather than some intrinsic property of the organometallic anion. Finally, bands for only a single of bridging and terminal CO ligands were observed in the ^{13}C NMR spectrum at –50 °C, which we presume are due to the cis isomer alone. The trans isomer, as proposed previously,[4,27,28] allows rapid interconversion of the bridging and terminal CO ligands, hence preventing their observation despite the absence of cis-trans isomerization.

The spectra of methoxycarbyne **7** were the most straightforward in CD_2Cl_2, as described above, so we start here. Cooling to –20 °C gives a simple ^{1}H NMR spectrum consistent with the presence of two isomers in an 82:18 ratio; each of the benzene, methoxy, and cyclopentadienyl signals is split into two bands. In the ^{13}C NMR, a similar cis-trans ratio was observed for the benzene and Cp bands as well as the terminal CO peaks. At this temperature, the peaks are quite sharp and separate bands for the cis and

trans isomers were observed for all carbons, except the bridging carbonyl and carbyne (including the methoxy) ligands; the intensities of the peaks due to the bridging carbon atoms were low, however, and the isomer peaks could be below the noise level. Carbynes **2** and **5** exhibited resolved peaks (typical $\Delta\nu \approx 1$ ppm) for most carbons in the two isomers, the exceptions being the methoxy carbon and terminal FeCO in **2**. Spectra were simulated using both the chemical shifts and isomer ratios in the ^{1}H and ^{13}C NMR spectra at –20 °C, and in sharp contrast to anion **6**, $k_{ct} < 1\ s^{-1}$ at –20 °C and less than 55 s^{-1} at 22 °C, where the ^{1}H NMR peaks are past coalescence but the ^{13}C peaks are resolved albeit still broadened.

The room temperature ^{1}H NMR spectra in toluene-d_8 were virtually identical to those in C_6D_6 described above. As seen in Figure, cooling results in decoalescence of both the very broad band just downfield of the sharp methoxy resonance as well as the large broad downfield peak to give four new bands at 0 °C; by –10 °C, even the methoxy peak begins to be resolved into two bands. Integration of the – 20 °C spectrum is consistent with assignment of the bands at 4.2 ppm to the methoxy peaks of the two isomers, the bands at 4.45 and 4.32 to the benzene and Cp peaks of the

Figure : Variable-temperature ^{1}H NMR spectra (400 MHz) of 7 in toluene-d_8

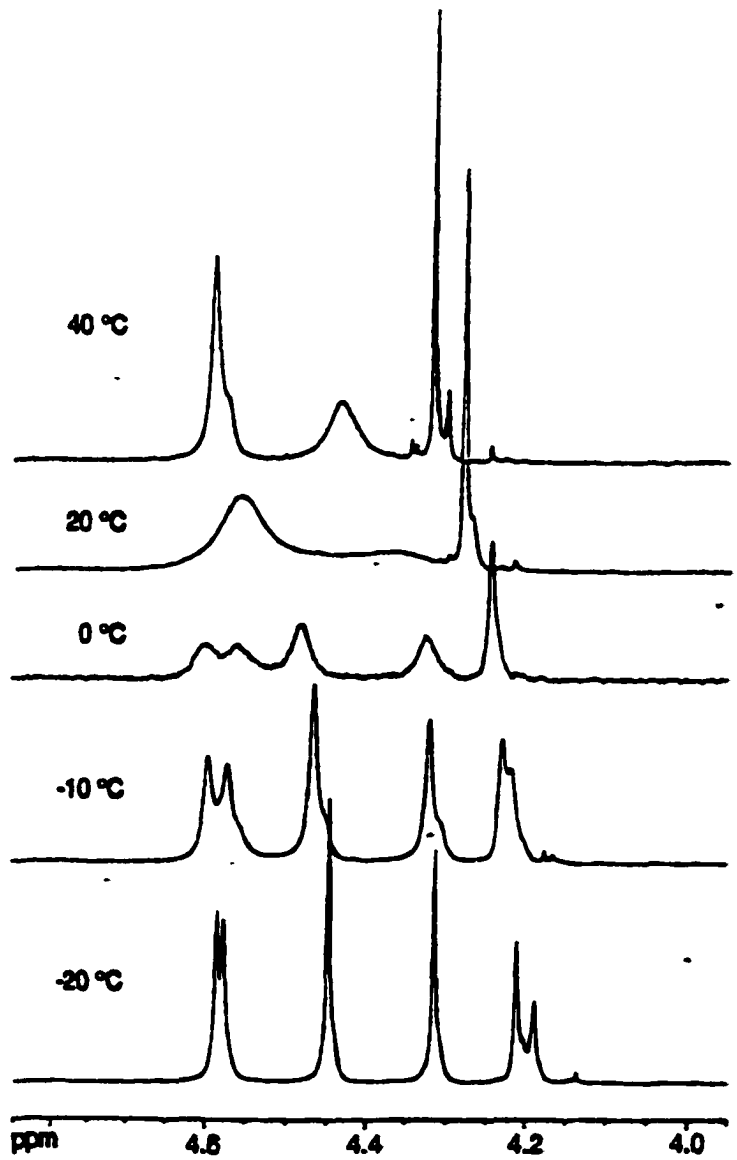

major isomer, and the two downfield bands to those of the minor isomer. The variable-temperature spectra were simulated using the temperature-dependent integrated isomer ratios and chemical shifts. Without the latter in particular, the spectra could not be fit, and near perfect linear correlations of chemical shifts with the three lowest temperatures were observed, allowing simple extrapolation. The broad spectra could be simulated regardless of which of the peaks at 4.59 and 4.58 ppm was assigned to the benzene and Cp peaks of the minor isomer, but assignment of the peak at 4.59 ppm as a benzene rather than a Cp peak was made both on the basis of height, but also because it is the only assignment that correctly fits the temperature-dependent chemical shifts. Warming above room temperature sharpens the three bands, and data were collected even at 40 °C without significant thermal decomposition.

The derived barrier for cis/trans isomerization of **7** is $\Delta G^{\ddagger}$(300 K) = 14.3 ± 1.8 kcal/mol in toluene-d_8 and $\Delta G^{\ddagger}$(300 K) = 15.2 ± 1.9 in CD_2Cl_2. Direct inspection of the rate constants suggests the difference is statistically significant; for instance, in CD_2Cl_2 $k_{ct} = 0.6 \pm 0.4$ and 25 ± 5 s^{-1} at –20 and +22 °C in the ^{1}H NMR, while in toluene-d_8 $k_{ct} = 2.0 \pm 0.5$ and 180 ± 40 s^{-1} at –20 and +20 °C. For carbyne **2**, $\Delta G^{\ddagger}$(300 K) = 16.4 ± 0.7 kcal/mol, while carbyne **5** did not undergo exchange at a measurable rate and the cis and

trans isomers were chromatographically separated.[5] As noted above, all compounds with the iron dimer structure have higher barriers than that seen in **6-Na**$^+$ and most have higher barriers than **7** as well. It is reasonable to assume, therefore, that the low barrier for **6-Na**$^+$ is at least in part a reflection of its structure rather than an artifact of the particular solvent and cation present. It is possible that the relatively electron-rich nature of **6-Na**$^+$ and **7** is in some way responsible for the low barriers, but further speculation is unwarranted.

The identity of the major isomer in both **6** and **7** cannot be determined with certainty. Since methylene chloride (dielectric constant = 9.1) is more polar than toluene (dielectric constant = 2.38), the simplest hypothesis[4,29,30] is that the cis isomer is favored in both methylene chloride (82:18 cis/trans ratio at –20 °C) and toluene (59:41 cis/trans ratio at –20 °C); alternatively, the lower polarity of toluene could lead to a crossover of isomer stability and the trans isomer could be dominant. However, integration of the toluene-d_8 ^{1}H NMR spectra shows that as the temperature is increased, so is the relative ratio of the minor isomer (i.e., 52:48 cis:trans at 0 °C), consistent with it being the thermodynamically disfavored trans isomer. Similar ratios were seen for **2** at room temperature in methylene chloride (74:26) and benzene (68:32), although no variation in the cis-trans ratio was observed over a

temperature range comparable to that used here.[4] The 63:37 isomer ratio observed for **6-Na**$^+$ in acetonitrile at –50 °C does not shed any light on the identity of the isomers; previous work with the PPN^+ and Ph_3PMe^+ salts of **1** and **4** showed these ratios to be both cation and temperature dependent.[4,5]

Thermal Decomposition of Methoxycarbyne 7. Heating carbyne **7** in a sealed NMR tube in benzene-d_6 at 50 °C resulted in complete decomposition in 15 hours in both the absence and presence of PPh_3. The reactions are shown in Scheme 2, and the product data and rate constants are collected in Table 2. Products were identified by comparison of the ^1H, ^{13}C, and ^{31}P NMR chemical shifts to those of authentic samples; details may be found in the Experimental Section.

The qualitative results of the decomposition of **7** are similar to those previously observed for **2**, **3**, and **5**. The key result is that, once again, oxygen to iron methyl migration is observed, with concomitant bond cleavage to give mononuclear products. In the absence of PPh_3, large amounts of a black precipitate form since the system is deficient in donor ligand; decomposition releases CO, presumably, which is scavenged by the remaining products. The yield of (benzene)$Cr(CO)_3$ is the highest, which suggests that chromium is either more effective in scavenging CO or that it

Scheme 2

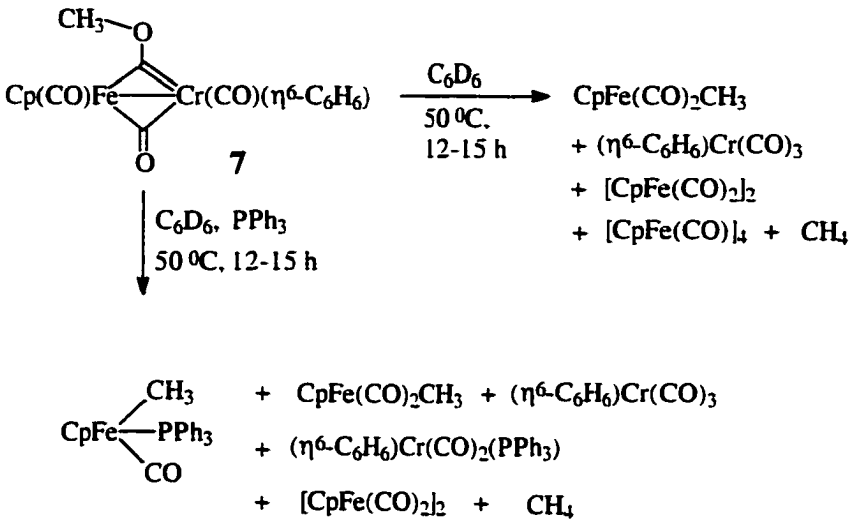

Table 2. Yield (%) and Rate Constant data for The Thermal Decomposition of 7[a]

	[PPh_3]			
product	0	0.19	0.38	0.59
$(C_6H_6)Cr(CO)_3$	38	55	55	72
$(C_6H_6)Cr(CO)_2(PPh_3)$		14	20	12
$CpFe(CO)_2(CH_3)$	18	7	10	11
$CpFe(CO)(PPh_3)(CH_3)$		35	41	36
$[CpFe(CO)_2]_2$	8	16	10	6
$[CpFe(CO)_2]_4$	4	0	0	0
CH4	2	2	2	2
total Cr	38	70	75	83
total Fe	30	58	61	52
rate constant[b]	8.66 ± 0.39	8.47 ± 0.15	7.09 ± 0.09	8.00 ± 0.16

[a] Concentrations of 7 for the four runs were 0.015, 0.026, 0.0110, and 0.0112 M.
[b] First-order rate constant for the decomposition of 7 at 50 0.1 °C in C_6D_6, $x10^5$ s^{-1}.

is the kinetic product of the methyl migration and Fe-Cr bond cleavage. This would then yield $CpFe(CO)CH_3$, which could scavenge CO to give a low yield of $CpFe(CO)_2CH_3$, lose the methyl radical to give the cluster $[CpFe(CO)]_4$, or do both to give the iron dimer $[CpFe(CO)_2]_2$; consistent with this, low yields of methane were observed.

In the presence of PPh_3, a stoichiometric reaction to give (benzene)$Cr(CO)_3$ and $CpFe(CO)(PPh_3)CH_3$ is possible, but chromium products still form in higher yield than do the iron products. Indeed, formation of both (benzene)$Cr(CO)_3$ and a smaller amount of (benzene)$Cr(CO)_2PPh_3$ suggests the presence of one reaction pathway that ejects (benzene)$Cr(CO)_3$ from the carbyne and one that ejects (benzene)$Cr(CO)_2$ which is then trapped by PPh_3. Under the reaction conditions, preformed (benzene)$Cr(CO)_3$ would react with PPh_3 to give (benzene)$Cr(CO)_2PPh_3$, but in less than 10% yield. Actual yields (based on total chromium) of 14-27% show that a pathway for the formation of (benzene)$Cr(CO)_2PPh_3$ from carbyne **7** must exist, but the difference is small. The two pathways were observed for iron-chromium carbyne **5** but not for the iron-manganese carbynes **2** and **3**, where only $MeCpMn(CO)_3$ and $CpFe(CO)(PPh_3)R$ formed. In the case of the iron adduct,

$CpFe(CO)(PPh_3)CH_3$ would not be expected to form from $CpFe(CO)CH_3$ and PPh_3 under the reaction conditions.[31]

The rates of the decomposition reactions were followed in order to determine their dependence (if any) on PPh_3. Within experimental error, the rate of decomposition of **7** is first order and independent of $[PPh_3]$, averaging $(8.1 \pm 0.6) \times 10^{-5}\ s^{-1}$ over a range of phosphine concentration from 0 to 0.59M. Previously, the only instance of this behavior was exhibited by *ethoxycarbyne* **3**. Both **2** and **5** exhibited phosphine-dependent pathways to give a different product, namely the $MePPh_3^+$ salt of the initial dinuclear anion via dealkylation of the carbyne by PPh_3. Consistent with this absence of a rate dependence on $[PPh_3]$, very little precipitate was observed in the PPh_3 reactions of **7**, unlike those with **2** and **5**, and isolation of the small amount of residue confirmed that it was not **6-PPh$_3$Me$^+$** nor any other Cp or benzene containing material. As noted repeatedly above, the IR data is consistent with **6-PPN$^+$** being relatively electron-rich, so this phosphine-induced dealkylation route may be inhibited.

The major mystery in the data collected is that as the phosphine concentration increases, the ratio of $CpFe(CO)(PPh_3)CH_3$ to $CpFe(CO)_2CH_3$ *decreases* rather than increases as might be expected. It is important to assess the certainty of this trend. While it is clear that the ratio goes roughly

from 5 to 4 to 3 as [PPh_3] goes from 0.19 to 0.38 to 0.59 M, examination of the percent yields might suggest that this ratio is an artifact, since both the $CpFe(CO)_2CH_3$ and $CpFe(CO)(PPh_3)CH_3$ yields vary little (from 7 to 11% for the former and from 35 to 41% for the latter). However, direct examination of the spectra clearly shows that the trend is real, both by comparison of the ratio of the Cp peaks and in the methyl region where $CpFe(CO)_2CH_3$ gives a singlet in the midst of the $CpFe(CO)(PPh_3)CH_3$ doublet in the high [PPh_3] runs but is buried in the low [PPh_3] run.

Mechanistic Proposals. A mechanism that is sonsistent with the results described here and previously is shown in Scheme 3. Three key experimental observations are incorporated into this mechanism. First, **7** undergoes cis/trans isomerization; at 50 °C, the calculated rate constant $k_{ct} \approx$ 1900 s^{-1} and the activation barrier $\Delta G_{ct}^{\ddagger}$ (50°C) = 14.1 ± 1.9 kcal/mol. The calculated cis:trans ratio is 45:55 at this temperature, with a corresponding thermodynamic energy difference of less than 0.3 kcal/mol. Second, the rate of decomposition of **7** is first-order and independent of phosphine concentration, with $k_{dec} = (8.1 \pm 0.6) \times 10^{-5}$ s^{-1} giving an activation barrier

Scheme 3

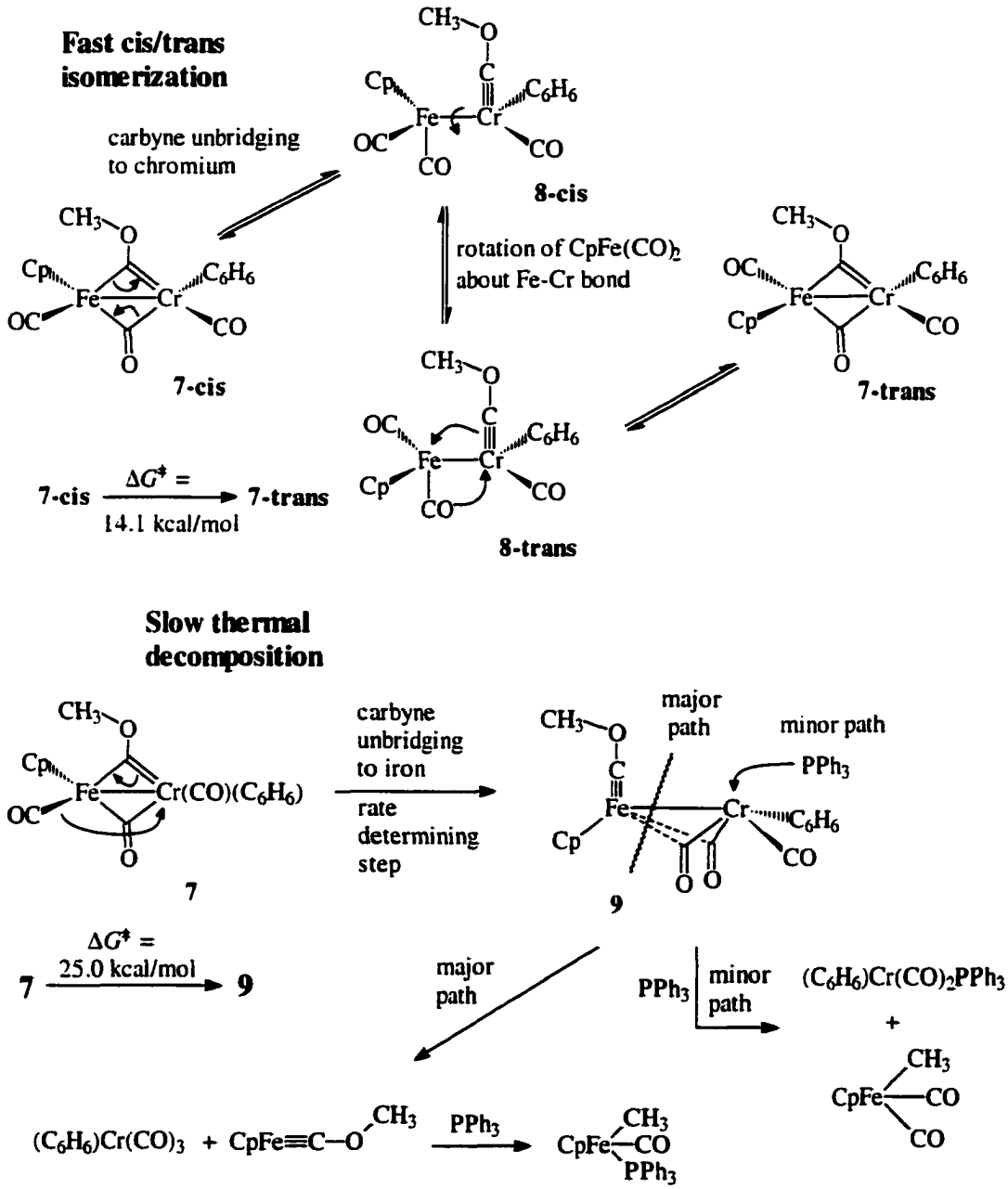

$\Delta G_{dec}^{\ddagger}$ (50°C) = 25.0 ± 0.1 kcal/mol. Third, the ratio of $CpFe(CO)(PPh_3)CH_3$ to $CpFe(CO)_2CH_3$ decreases as [PPh_3] increases. As will be described below, these facts are best accounted for by the presence of two intermediates, one a low-energy intermediate involved in cis/trans isomerization and the other a high-energy intermediate formed from **7** which gives rise to products in subsequent non-rate-determining steps.

Cis/trans isomerization of $[CpFe(CO)_2]_2$ has been proposed to proceed via the unbridged intermediate $Cp(CO)_2Fe—Fe(CO)_2Cp$,[28] and a wide variety of iron dimer analogs with non-carbonyl bridges undergo such isomerization at comparable rates.[4] The simplest assumption is that all of these isomerizations proceed via the same mechanism, so if this is assumed to be the case for **7** as well, then an iron-chromium single-bonded intermediate must be present. Unlike the iron dimer case, however, unbridging of the carbyne ligand of **7** to either metals should have different energy barriers and can have different stereochemical outcomes as well. We have previously proposed that cis-trans isomerization occurs via unbridging of the carbyne to a single metal, since only in this way is NMR-exchange of diastereotopic protons (when present) prevented.[4] Here, we propose exclusive carbyne unbridging to chromium to give intermediate **8**, as shown in Scheme 3, since only in this way can an intermediate form that

incorporates two 18-electron metal centers. The activation energy is roughly comparable to that seen in the iron dimer, and one might suppose that unbridging to iron to give formally 19-electron iron and 17-electron chromium centers would be disfavored. Of course, the 14 kcal/mol barrier to cis/trans isomerization includes rotation about the metal-metal bond as well as unbridging, so one cannot dismiss the possibility that unbridging to both metals occurs but that the 17-electron/19-electron intermediate simply does not undergo bond rotation.

Under the reaction conditions, cis/trans isomerization is rapid and similar amounts of each isomer are present, and we presume that thermal decomposition of **7** occurs from both isomers. Since PPh_3 is incorporated in the products without involvement in the rate-determining step, an intermediate having a barrier to its formation of the full 25 kcal/mol is required. We propose that carbyne unbridging to iron with concomitant CO bridging occurs to give **9**. The structure is proposed based on analogy to known semibridged heterodinuclear compounds[32-35] and presumably is higher in energy than **8** due to the 17/19-electron imbalance, even though it is ameliorated by the presence of semibridging carbonyl ligands.

The third experimental observation noted above requires a partitioning of the carbyne decomposition into two pathways *after* the phosphine-

independent rate-determining step, and so an irreversibly-formed intermediate must be involved. In the absence of phosphine, the major pathway leads to (benzene)$Cr(CO)_3$ and the proposed iron carbyne intermediate $CpFe{\equiv}COCH_3$.[5,9] This iron species is electron-deficient and must abstract CO in order to yield $CpFe(CO)_2CH_3$. Some of this CO must ultimately come from the (benzene)$Cr(CO)_3$, and so its yield is somewhat lower in the absence of PPh_3 than in the three runs in which PPh_3 is added. The key point is that the minor pathway requires trapping of intermediate **9** by PPh_3 to give the *alternate* pair of products, which includes $CpFe(CO)_2CH_3$. At high phosphine concentration, relatively more of these minor products should form, leading to the counterintuitive result that more $CpFe(CO)_2CH_3$ relative to $CpFe(CO)(PPh_3)CH_3$ forms at higher phosphine concentrations. As an alternative mechanism, one might suppose that the 25 kcal/mol step leads directly to metal-metal bond cleavage to give (benzene)$Cr(CO)_3$ and $CpFe{\equiv}COCH_3$ or (benzene)$Cr(CO)_2$ and $CpFe(CO)_2CH_3$. If this were the case, however, there likely would be no dependence of product ratios on PPh_3 concentration. We have previously described kinetic evidence in the thermal decomposition of carbyne **5** that similarly is best accounted for by the presence of a metal-metal bonded intermediate analogous to **9**.[5]

The mechanism involving **9** should have two other consequences: similar amounts of (benzene)$Cr(CO)_2PPh_3$ and $CpFe(CO)_2CH_3$ should form and less (benzene)$Cr(CO)_3$ should form at higher phosphine concentrations. The first consequence is very roughly observed; about half as much $CpFe(CO)_2CH_3$ as (benzene)$Cr(CO)_2PPh_3$ forms, although some of the excess chromium adduct could arise from direct thermal reaction of (benzene)$Cr(CO)_3$ with PPh_3. At present, we have no explanation for the failure to account for the second consequence.

The actual rate of decomposition of **7** may be compared to the first-order, phosphine-independent pathways observed for the other carbynes: 1.0×10^{-4} s^{-1} at 75 °C for **2**, 1.0×10^{-4} s^{-1} at 65 °C for **3**, and 6.5×10^{-4} s^{-1} at 50 °C for **5**. The rate of 8×10^{-5} s^{-1} at 50 °C for **7** is nearly the same as those for the iron-manganese carbynes **2** and **3** but at higher temperatures and is an order of magnitude slower than that of the iron-chromium carbyne **5** at the same temperature. These rates can be converted to activation energies to give a better, albeit still rough, guide to relative reactivity: at the reaction temperatures noted above, $\Delta G^{\ddagger} = 23.7$ kcal/mol for **5**, 25.0 kcal/mol for **7**, 26.1 kcal/mol for **3**, and 26.8 kcal/mol for **2**. Clearly, the isoelectronic fragments that make up the non-iron portion of these carbynes can be ranked in order of the stability they impact as MeCpMn(CO) > (benzene)Cr(CO) >

CpCr(NO). While the differences are modest, they are experimentally significant: we would predict, for instance, that the ethoxycarbyne analog of **5** would be difficult to isolate, and the larger array of products and apparent intermediates observed in the decomposition of **5** and **7** is due to their greater reactivity.

III. Conclusion

In conclusion, the experimental observations for the current study as well as those previously described are most readily explained by the presence of different barriers to carbyne unbridging to either metal. One of the resultant energetically different intermediates is involved in cis-trans isomerization, the other in thermal decomposition. Phosphine attack with concomitant metal-metal bond cleavage can occur on the high-energy decomposition intermediate competitive with phosphine-independent fragmentation. The details of the novel methyl migration reaction itself remain unknown.

Our initial question, regarding the utility of using a carbyne to stitch together metals that might lead to unique materials, similarly remains unanswered. The cleavage of the metal-metal bond on the surface of the PVG might also occur after heating as in the solution, so it is unclear if the two metals would remain adjacent to each other. The surface of the PVG is anionic. When the carbyne is loaded on the PVG, the oxide anion on the surface could act like PPh_3, participating in the thermal decomposition and resulting in binding of the metal species, such as the 16-electron intermediate, $CpFe{\equiv}COCH_3$, to the surface of the glass, and thus hold the metals in place. However, if the two metal atoms are able to migrate independently on the surface after heating, it might be difficult to prepare

novel mixed-metal materials. A more structured collaborative approach is needed to answer these questions, including setting up methods for NLO activity analysis, and examination of simpler metal compounds and mixtures before the mixed-metal systems are tackled.

IV. Experimental Section

General Considerations. All manipulations of air-sensitive compounds were carried out in a Vacuum Atmospheres inert-atmosphere drybox under recirculating nitrogen. NMR spectra were recorded on a Bruker DPX-400 spectrometer; chemical shifts are reported relative to residual hydrogen in C_6D_6 (δ 7.15), $C_2D_2Cl_2$ (δ 5.32), CD_3CN (δ 1.93), $C_6D_5CD_3$ (δ 7.15), and to carbon in C_6D_6 at 128.0 ppm, $C_2D_2Cl_2$ at 53.8 ppm, or CD_3CN at 1.3 ppm. NMR line-shape analyses were carried out using gNMR (Cherwell Scientific Publishing, Inc.) on a Macintosh computer. Infrared spectra were obtained on a Mattson Galaxy 4020 FT-IR. Elemental analyses were performed by Desert Analytics, Tucson, AZ.

All solvents were treated under nitrogen. Acetonitrile was purified by sequential distillation from calcium hydride and phosphorus pentoxide. Benzene and tetrahydrofuran were distilled from sodium benzophenone ketyl. Hexane was purified by washing successively with the following solutions and water: 5% nitric acid in sulfuric acid, water, sodium bicarbonate solution, and water. The washed hexane was then dried over calcium chloride and distilled from *n*-butyllithium in hexane. Methylene chloride was distilled from phosphorus pentoxide; CD_2Cl_2 was vacuum-transferred from phosphorus pentoxide. CD_3CN was dried over 4-Å

molecular sieves and vacuum-transferred prior to use; benzene-d_6 and toluene-d_8 were vacuum-transferred from sodium benzophenone ketyl.

Celite was dried in an over at 140 °C overnight prior to use. Trimethyloxonium tetrafluoroborate (Lancaster Synthesis) was used as received. $CpFe(CO)_3^-Na^+ \bullet \sim 0.5THF$,[4] $CpFe(CO)(PPh_3)(CH_3)$,[4,31,36] $(C_6H_6)Cr(CO)(CH_3CN)$,[37] $(C_6H_6)Cr(CO)_2(PPh_3)$,[38] $(C_6H_6)Cr(CO)_3$,[39] and PPN^+Cl^- [40] were prepared according to published procedures.

$[Cp(CO)Fe(\mu\text{-}CO)_2Cr(CO)(C_6H_6)]^-Na^+$ (6-Na^+). To a mixture of solid $CpFe(CO)_3^-Na^+ \bullet \sim 0.5THF$ (0.951 g, 4.03 mmol) and $(C_6H_6)Cr(CO)(CH_3CN)$ (0.961 g, 4.23 mmol) was added 100 mL of THF. The solution was stirred at room temperature for 3 h and filtered through Celite, and the solvent was removed on a vacuum line. The resultant black solid was purified by stirring for a few minutes with benzene, filtering, and then washing several times with 5-mL portions of benzene until these washes were nearly colorless, yielding 1.48 g (77% yield based on Fe and the presence of 1.3 equiv THF by ^1H NMR (CD_3CN)) of product as a black solid. IR (THF): 1968 (w), 1902 (m), 1889 (m), 1833 (m), 1709 (w), 1615 (br, m) cm^{-1}. IR (CH_3CN): 2018 (w), 1964 (w), 1885 (s), 1813 (m), 1661 (s) cm^{-1}. ^1H NMR (CD_3CN, 27 °C): δ 4.64 (s, 6H), 4.34 (s, 5H), 3.63, 1.79 (THF). ^1H NMR (CD_3CN, -50 °C): δ 4.76, 4.67 (C_6H_6, 63:37 cis:trans), 4.42, 4.29 (Cp, 63:37 cis:trans).

^{13}C NMR (CD_3CN, 27 °C): δ 93.42 (C_6H_6), 86.86 (Cp), 68.27, 26.19 (THF). ^{13}C NMR (CD_3CN, -50 °C): δ 311.63 (μ-CO), 242.72 (CrCO), 217.85 (FeCO), 94.04 (C_6H_6, trans), 92.50 (C_6H_6, cis), 87.71 (Cp, trans), 85.58 (Cp, cis), 67.81, 25.76 (THF) ppm.

$[Cp(CO)Fe(\mu\text{-}CO)_2Cr(CO)(C_6H_6)]^-PPN^+$ (6-PPN^+). To a mixture of 0.200 g (0.417 mmol) of **6-Na^+**•1.3THF and 0.239 g (0.417 mmol) of PPNCl was added 25 mL of THF. The solution was stirred at room temperature for 30 min and filtered on a medium frit, and the solvent was removed on a vacuum line. The resultant solid was purified by stirring for a few minutes with 5 mL of benzene, filtering, and then washing several times with 3 mL portions of benzene until these washes were nearly colorless, yielding 0.273 g (73% yield) of product as a black solid. IR (CH_3CN): 1886 (s), 1812 (m), 1661 (s) cm^{-1}. ^1H NMR (CD_3CN): δ 7.67-7.44 (m, 37H), 4.62 (s, 6H), 4.33 (s,5H). ^{13}C NMR (CD_3CN): PPN^+ at δ 134.57 (C_4), 133.22 (quintet, $^2J_{PC}$ = 12 Hz, $^5J_{PC}$ = 0 Hz, $^2J_{PP}$ = 7 Hz, C_3), 130.34 (quintet, $^2J_{PC}$ = 13.5 Hz, $^4J_{PC}$ = 0 Hz, $^2J_{PP}$ = 7 Hz, C_2), 128.18 (d, $^1J_{PC}$ = 109.1 Hz, C_1), 93.12 (C_6H_6), 86.83 (Cp). Anal. Calcd for $C_{51}H_{41}CrFeP_2NO_4$: C, 67.94; H, 4.58; N, 1.55. Found: C, 66.06; H, 4.40; N, 1.57.

$Cp(CO)Fe(\mu\text{-}CO)(\mu\text{-}COMe)Cr(CO)(C_6H_6)$ (7). A solution of 0.278 g (1.88 mmol) of Me_3OBF_4 dissolved in ~1 mL of CH_3CN was added in one

portion to a solution of 0.902 g (1.88 mmol) of **6-Na$^+$**•1.3 THF in 35 mL of CH_3CN. After the mixture was stirred at room temperature for 5 min, the solvent was removed on a vacuum line; 35 mL of benzene was added to the resultant solid to extract the product, and the solution was filtered through Celite. Following the solvent removal on the vacuum line, the crude product was recrystallized twice from 1:2 CH_2Cl_2/hexane to give 0.205 g (29% yield) of **7** as a black solid. IR (CH_2Cl_2): 1943 (s), 1875 (m), 1736 (m) cm^{-1}. ^1H NMR (CD_2Cl_2, 20 °C): δ 5.31 (C_6H_6), 4.86 (MeO), 4.65 (Cp). ^1H NMR (CD_2Cl_2, -20 °C): δ 5.35, 5.28 (s, 6H, 82:18 cis:trans), 4.89, 4.82 (s, 3H, 18:82 trans:cis), 4.65, 4.59 (s, 5H, 82:18 cis:trans). ^1H NMR (toluene-d_8, -20 °C): δ 4.45 (s, 6H), 4.32 (s, 5H), 4.21 (s, 3H) (cis isomer, 59%); δ 4.59 (s), 4.58 (s) (total 11H), 4.19 (s, 3H) (trans isomer, 41%).). ^{13}C NMR (CD_2Cl_2, -20 °C): δ 390.41 (carbyne carbon), 286.74 (μ-CO), 236.70 (CrCO, cis), 235.85 (CrCO, trans), 214.87 (FeCO, cis), 214.32 (FeCO, trans), 98.73 (C_6H_6, trans), 97.27 (C_6H_6, cis), 87.87 (Cp, trans), 85.54 (Cp, cis), 71.50 (CH_3). Anal. Calcd for $C_{16}H_{14}CrFeO_4$: C, 50.82; H, 3.73. Found: C, 49.68; H, 3.55.

^1H NMR Experiments. In the glovebox, solid PPh_3 (for the reactions in which it was used) and 1,4-dichlorobenzene (~6:1 molar ratio to carbyne, added as an internal standard for yield calculations) were loaded into an

NMR tube sealed to a 14/20 ground glass joint, while the carbyne was dissolved in a small amount of C_6D_6 and transferred and rinsed into the tube. C_6D_6 was added to a height of ~5 cm, a vacuum stopcock was fitted to the tube, and the tube was attached to a vacuum line. The tube was submitted to three freeze-pump-thaw cycles and sealed with a torch in order to prevent any air oxidation and to prevent any loss of the solvent and any volatile products. The sample was heated in a VWR 1160 water bath at 50.4 ± 0.1 °C and was quenched by immersing in an ice bath. The tube was centrifuged prior to recording each NMR spectrum. The volume in mL was calculated according to the equation $V = \pi(0.205)^2h$, where h is the height of the solvent measured in cm immediately after removal from the hot bath, and the inside radius of the NMR tube is 0.205 cm. Each kinetic run was followed for at least 3 half-lives.

The major difficulty was in quantifying the chromium products, since the benzene peaks of (benzene)$Cr(CO)_2L$ (L = CO, PPh_3) overlap precisely at 4.28 ppm in the ^1H NMR spectrum; a 1:1 mixture exhibits this single symmetrical peak in the ^1H NMR spectrum, a single peak in the ^{31}P NMR spectrum at 92.39 ppm, and in the ^{13}C NMR spectrum benzene peaks in a ~1:1 ratio for (benzene)$Cr(CO)_3$ (92.33 ppm) and (benzene)$Cr(CO)_2PPh_3$ (89.40 ppm). Combined yields could be obtained with reasonable

confidence, but the relative ratios were determined by comparing the ratio of (benzene)$Cr(CO)_2PPh_3$ (92.39 ppm) and $CpFe(CO)(PPh_3)CH_3$ (86.07 ppm) in the ^{31}P NMR and then subtracting the derived yield of (benzene)$Cr(CO)_2PPh_3$ from the combined yield to give the amount of (benzene)$Cr(CO)_3$. In the control experiment described in the text in which (benzene)$Cr(CO)_3$ (0.013 M) was heated with PPh_3 (0.40 M; P:Cr = 32:1) at 50 °C for 14 h, ~7.5 ± 1.5% of the mixture was (benzene)$Cr(CO)_2PPh_3$, as judged by ^{13}C NMR.

V. References

(1) Fong, R. H.; Hersh, W. H. *Organometallics* **1985**, *4*, 1468-1470.

(2) Fong, R. H.; Hersh, W. H. *J. Am. Chem. Soc.* **1987**, *109*, 2843-2845.

(3) Fong, R. H.; Hersh, W. H. *Organometallics* **1988**, *7*, 794-796.

(4) Fong, R. H.; Lin, C. H.; Idmoumaz, H.; Hersh, W. H. *Organometallics* **1993**, *12*, 503-516.

(5) Wang, B.; Hersh, W. H.; Rheingold, A. L. *Organometallics* **1993**, *12*, 1319-1330.

(6) Idmoumaz, H.; Lin, C. H.; Hersh, W. H. *Organometallics* **1995**, *14*, 4051-4063.

(7) Bryan, R. F.; Greene, P. T. *J. Chem. Soc. (A)* **1970**, 3064-3068.

(8) Bryan, R. F.; Greene, P. T.; Newlands, M. J.; Field, D. S. *J. Chem. Soc. (A)* **1970**, 3068-3074.

(9) Hersh, W. H. In *Transition Metal Carbyne Compleses*; F. R. Kreissl, Ed.; Nato ASI Series C: Mathematical and Physical Sciences, Vol. 392; Kluwer Academic Publishers: Dordrecht, 1993; pp 149-150.

(10) Frazier, C. C.; Harvey, M. A.; Cockerham, M. P.; Hand, H. M.; Chauchard, E. A.; Lee, C. H. *J. Phys. Chem.* **1986**, *90*, 5703-5706.

(11) Tam, W.; Eaton, D. F.; Calabrese, J. C.; Williams, I. D.; Wang, Y.; Anderson, A. G. *Chem. Mater.* **1989**, *1*, 128-140.

(12) Long, N. J. *Angew. Chem., Int. Ed. Engl.* **1995**, *34*, 21-38.

(13) Kanis, D. R.; Ratner, M. A.; Marks, T. J. *J. Am. Chem. Soc.* **1992**, *114*, 10338-10357.

(14) Ziolo, R. F.; Giannelis, E. P.; Weinstein, B. A.; O'Horo, M. P.; Ganguly, B. N.; Mehrotra, V.; Russell, M. W.; Huffman, D. R. *Science* **1992**, *257*, 219-223.

(15) Sunil, D.; Sokolov, J.; Rafailovich, M. H.; Duan, X.; Gafney, H. D. *Inorg. Chem.* **1993**, *32*, 4489-4490.

(16) Stroscio, J. A.; Pierce, D. T.; Unguris, J.; Celotta, R. J. *J Vac Sci Technol B* **1994**, *12*, 1789-1792.

(17) Kanis, D. R.; Ratner, M. A.; Marks, T. J. *Chem. Rev.* **1994**, *94*, 195-242.

(18) Lacroix, P. G.; Clement, R,; Nakatani, K.; Zyss, J.; Ledoux, I. *Science* **1994**, *263*, 658-60.

(19) Rodriguez, J. A.; Goodman, D. W. *Science* **1992**, *257*, 897-903.

(20) Laidlaw, W. M.; Denning, R. G; Verbiest, T.; Chauchard, E.; Persoons, A. *Nature* **1993**, *363*, 58-60

(21) Williams, D. J. *Angew. Chem. Int. Ed. Engl.* **1984**, *23*, 690-703

(22) Wong, P. K. *J. Phys. Chem.* **1971**, *75*, 201-7.

(23) Kurtz, S. K.; Perry, T. T. *J. Appl. Phys.* **1968**, *39(8)*, 3798-3813.

(24) Eaton, D. F. *Science* **1991**, *253*, 281.

(25) Fong, R. H. Ph. D. thesis **1987**.

(26) Luo, W.; Fong, R. H.; Hersh, W. H. *Organometallics*, **1997**, *16*, 4192-4199.

(27) Adams, R. D.; Cotton, F. A. *J. Am. Chem. Soc.* **1973**, *95*, 6589-6594.

(28) Farrugia, L. J.; Mustoo, L. *Organometallics* **1992**, *11*, 2941-2944.

(29) Bullitt, J. G.; Cotton, F. A.; Marks, T. J. *Inorg. Chem.* **1972**, *11*, 671-676.

(30) Kirchner, R. M.; Marks, T. J.; Kristoff, J. S.; Ibers, J. A. *J. Am. Chem. Soc.* **1973**, *95*, 6602-6613.

(31) Su, S. R.; Wojcicki, A. *J. Organomet. Chem.* **1971**, *27*, 231-240.

(32) Leonhard, K.; Werner, H. *Angew. Chem., Int. Ed. Engl.* **1977**, *16*, 649-650.

(33) Werner, H.; Juthani, B. *J. Organomet. Chem.* **1981**, *209*, 211-218.

(34) Werner, H. *Pure Appl. Chem.* **1982**, *54*, 177-188.

(35) Aldridge, M. L.; Green, M.; Howard, J. A. K.; Pain, G. N.; Porter, S. J.; Stone, F. G. A.; Woodward, P. *J. Chem. Soc., Dalton Trans.* **1982**, 1333-1340.

(36) Treichel, P. M.; Shubkin, R. L.; Barnett, K. W.; Reichard, D. *Inorg. Chem.* **1966**, *5*, 1177-1181.

(37) Knoll, L.; Reiss, K.; Schäfer, J.; Klüfers, P. *J. Organomet. Chem.* **1980**, *193*, C40-C42.

(38) Strohmeier, W.; Barbeau, C.; von Hobe, D. *Chem. Ber.* **1963**, *96*, 3254-3259.

(39) Mahaffy, C. A. L.; Pauson, P. L. *Reagents for Transition Metal* **1990**, *28*, 136-147.

(40) Ruff, J. K.; Schlientz, W. J. *Inorganic Syntheses* **1974**, *15*, 84-90.

Table 3: Kinetic Data – Thermal Decomposition of 7 without PPh_3

	A	B	C	D	E	F
1	time data (MAX 30 POINTS)		CONCENTRATION DATA		calculated	calculated
2	in seconds	or minutes	peak	reference	time (sec)	ln(peak/ref)
3		0.0000	108.0000	115.5000	0.00	-0.067139
4		30.0000	102.0000	145.0000	1800.00	-0.351761
5		60.0000	80.0000	145.5000	3600.00	-0.598149
6		90.0000	63.5000	145.0000	5400.00	-0.825694
7		120.0000	49.3000	145.2000	7200.00	-1.080188
8		180.0000	36.0000	145.5000	10800.00	-1.396657
9		240.0000	26.1000	144.9000	14400.00	-1.714109
10		360.0000	17.7000	144.6000	21600.00	-2.100407
11		540.0000	6.3000	144.1000	32400.00	-3.129958
12		720.0000	3.0000	144.6000	43200.00	-3.875359
13	RATE =	8.536E-05			R =	0.993428
14	±	3.278E-06			R squared =	0.986900
15	slope =	-8.5361E-05	±	3.278E-06		
16	intercept =	-0.315479	±	0.063936		
17						
18	last point not really integrated:					
19	RATE =	9.002E-05			R =	0.990420
20	±	4.437E-06			R squared =	0.980932
21	slope =	-9.0021E-05	±	4.437E-06		
22	intercept =	-0.279333	±	0.065108		
23						
24	1st point also odd - integral, and consistent with other data points -					
25	eliminate 1st and last point:					
26	RATE =	8.661E-05			R =	0.992991
27	±	3.897E-06			R squared =	0.986031
28	slope =	-8.6613E-05	±	3.897E-06		
29	intercept =	-0.347263	±	0.060640		
30						
31						
32	rate	half-life	half-lives followed:			
33	8.536E-05	8120.22	5.32			
34	9.002E-05	7699.82	4.21			
35	8.661E-05	8002.77	3.82			

Table 4: Kinetic Data – Thermal Decomposition of 7 with PPh_3 (0.19 M)

	A	B	C	D	E	F
1	time data (MAX 30 POINTS)		CONCENTRATION DATA		calculated	calculated
2	in seconds	or minutes	peak	reference	time (sec)	ln(peak/ref)
3		0.0000	71.0000	141.0000	0.00	-0.686080
4		30.0000	78.5000	141.5000	1800.00	-0.589201
5		60.0000	69.0000	145.0000	3600.00	-0.742627
6		90.0000	60.0000	143.6000	5400.00	-0.872687
7		120.0000	51.1000	144.0000	7200.00	-1.036029
8		180.0000	37.5000	143.9000	10800.00	-1.344778
9		240.0000	26.2000	142.0000	14400.00	-1.690068
10		360.0000	13.9000	144.0000	21600.00	-2.337924
11		480.0000	8.5000	142.5000	28800.00	-2.819276
12		720.0000	1.5000	141.8000	43200.00	-4.548953
13	RATE =	9.051E-05			R =	0.994033
14		± 3.311E-06			R squared =	0.988102
15	slope =	-9.0515E-05	±	3.311E-06		
16	intercept =	-0.428522	±	0.062673		
17						
18	skip 12 hr point (questionable from NMR):					
19	RATE =	8.124E-05			R =	0.994356
20		± 3.065E-06			R squared =	0.988744
21	slope =	-8.1245E-05	±	3.065E-06		
22	intercept =	-0.501573	±	0.042334		
23						
24	skip 1st and last point - 1st point clearly smaller than 2nd point					
25	RATE =	8.472E-05			R =	0.998871
26		± 1.523E-06			R squared =	0.997743
27	slope =	-8.4715E-05	±	1.523E-06		
28	intercept =	-0.437908	±	0.022312		
29						
30	rate	half-life	half-lives followed:			
31	9.051E-05	7657.85	5.64			
32	8.124E-05	8531.58	3.38			
33	8.472E-05	8182.10	3.30			

Table 5: Kinetic Data – Thermal Decomposition of 7 with PPh_3 (0.38 M)

	A	B	C	D	E	F
1	time data (MAX 30 POINTS)		CONCENTRATION DATA		calculated	calculated
2	in seconds	or minutes	peak	reference	time (sec)	ln(peak/ref)
3		0.0000	95.5000	141.3000	0.00	-0.391759
4		30.0000	96.8000	143.3000	1800.00	-0.392293
5		60.0000	85.4000	141.0000	3600.00	-0.501414
6		94.0000	75.2000	141.9000	5640.00	-0.634971
7		120.0000	65.9000	142.3000	7200.00	-0.769799
8		180.0000	54.0000	142.0000	10800.00	-0.966843
9		240.0000	40.8000	144.0000	14400.00	-1.261131
10		360.0000	24.8000	141.5000	21600.00	-1.741456
11		540.0000	10.8000	140.9000	32400.00	-2.568504
12		720.0000	4.3000	141.9000	43200.00	-3.496508
13					•••	•••
14	RATE =	7.283E-05			R =	0.997653
15	±	1.666E-06			R squared =	0.995311
16	slope =	-7.2828E-05	±	1.666E-06		
17	intercept =	-0.248221	±	0.032507		
18						
19						
20	skip first point (low):					
21	RATE =	7.422E-05			R =	0.998892
22	±	1.236E-06			R squared =	0.997786
23	slope =	-7.4222E-05	±	1.236E-06		
24	intercept =	-0.210484	±	0.025421		
25						
26	skip first and last point:					
27	RATE =	7.094E-05			R =	0.999417
28	±	9.163E-07			R squared =	0.998834
29	slope =	-7.0943E-05	±	9.163E-07		
30	intercept =	-0.240470	±	0.014270		
31						
32	rate	half-life	half-lives followed:			
33	7.283E-05	9517.65	4.54			
34	7.422E-05	9338.85	4.43			
35	7.094E-05	9770.52	3.13			
36						
37						
38						
39						

Table 6: Kinetic Data – Thermal Decomposition of 7 with PPh_3 (0.59 M)

	A	B	C	D	E	F
1	time data (MAX 30 POINTS)		CONCENTRATION DATA		calculated	calculated
2	in seconds	or minutes	peak	reference	time (sec)	ln(peak/ref)
3		0.0000	87.2000	138.5000	0.00	-0.462666
4		30.0000	83.0000	138.5000	1800.00	-0.512030
5		60.0000	73.0000	139.0000	3600.00	-0.644014
6		90.0000	65.5000	138.9000	5400.00	-0.751704
7		120.0000	53.9000	133.5000	7200.00	-0.906971
8		180.0000	39.5000	134.0000	10800.00	-1.221539
9		240.0000	30.0000	134.5000	14400.00	-1.500367
10		360.0000	19.2000	138.8000	21600.00	-1.978124
11		540.0000	6.8000	134.5000	32400.00	-2.984642
12		720.0000	5.5000	135.0000	43200.00	-3.200527
13					...	...
14	RATE =	6.956E-05			R =	0.991058
15	±	3.122E-06			R squared =	0.982196
16	slope =	-6.9563E-05	±	3.122E-06		
17	intercept =	-0.439593	±	0.060887		
18						
19	without last point:					
20	RATE =	7.848E-05			R =	0.997814
21	±	1.837E-06			R squared =	0.995633
22	slope =	-7.8475E-05	±	1.837E-06		
23	intercept =	-0.370475	±	0.026960		
24						
25	without first and last point:					
26	RATE =	7.996E-05			R =	0.998684
27	±	1.552E-06			R squared =	0.997369
28	slope =	-7.9956E-05	±	1.552E-06		
29	intercept =	-0.340962	±	0.024156		
30						
31	rate	half-life	half-lives followed:			
32	6.956E-05	9964.30	4.34			
33	7.848E-05	8832.70	3.67			
34	7.996E-05	8669.14	3.53			

Plot I: Thermal Decomposition of 7 without PPh_3

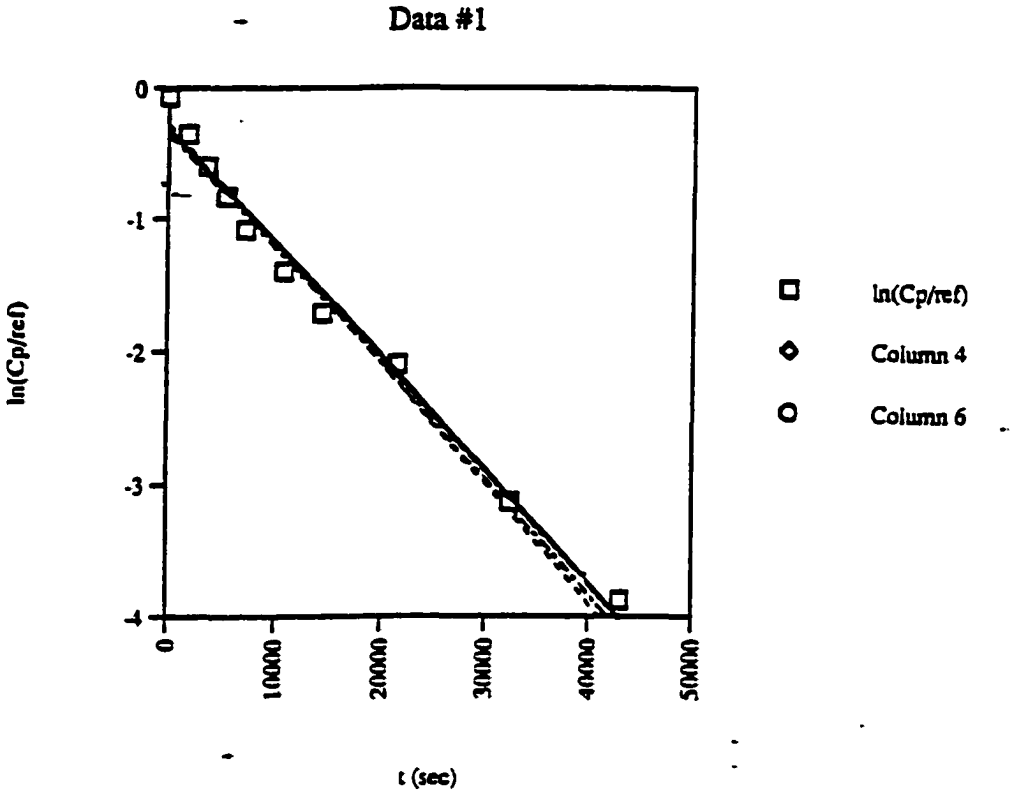

y = -8.5361E-05x - 3.1548E-01 r = 9.9343E-01 all data

y = -9.0021E-05x - 2.7933E-01 w/o 12 hr point

y = -8.6613E-05x - 3.4726E-01 w/o 1st and last point

Plot II: Thermal Decomposition of 7 with PPh_3 (0.19 M)

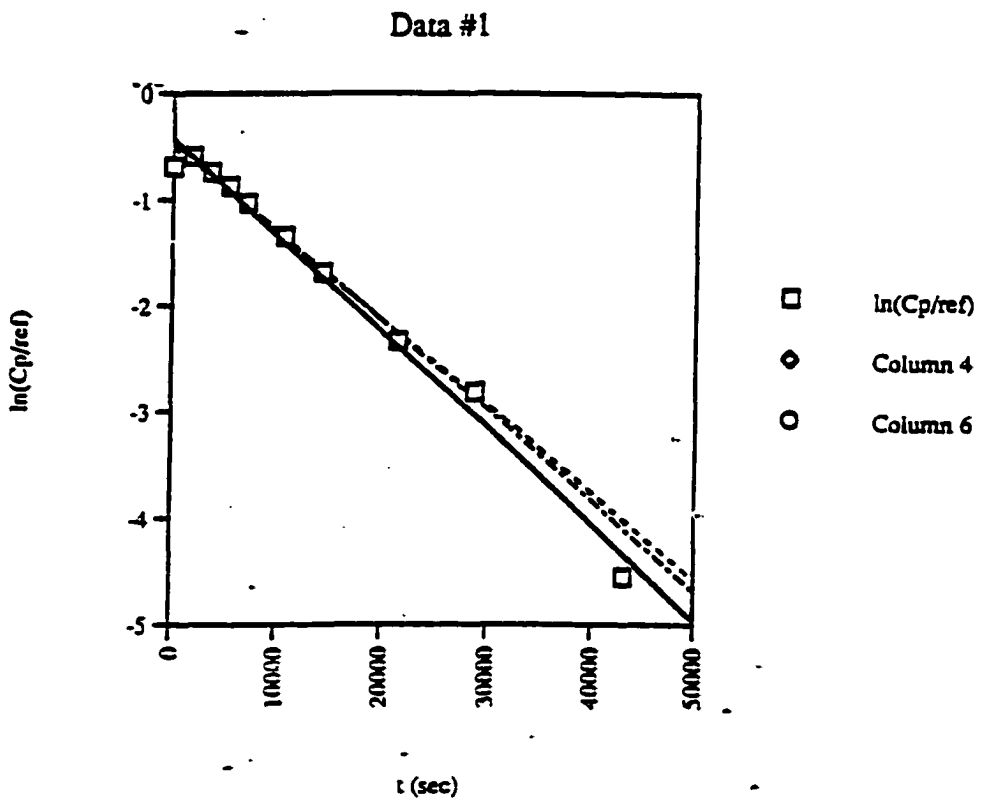

y = -9.0515E-05x - 4.2852E-01 12 hr data

y = -8.1245E-05x - 5.0157E-01 8 hr data

y = -8.4715E-05x - 4.3791E-01 8 hr, skip 1st pt

Figure 1-1. IR of 6-Na^+ in THF

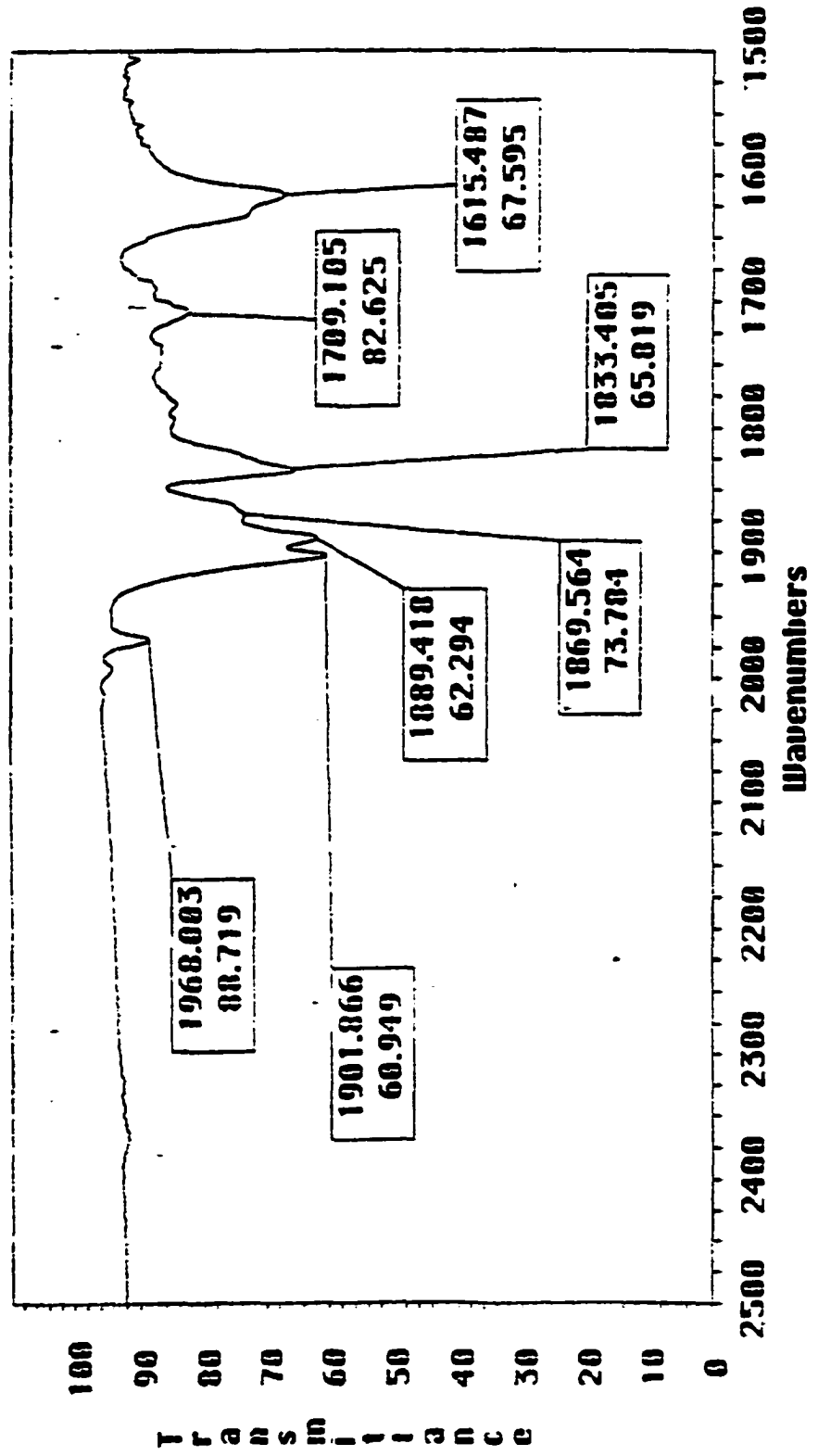

Figure 1-2. IR of 6-Na^+ in CH_3CN

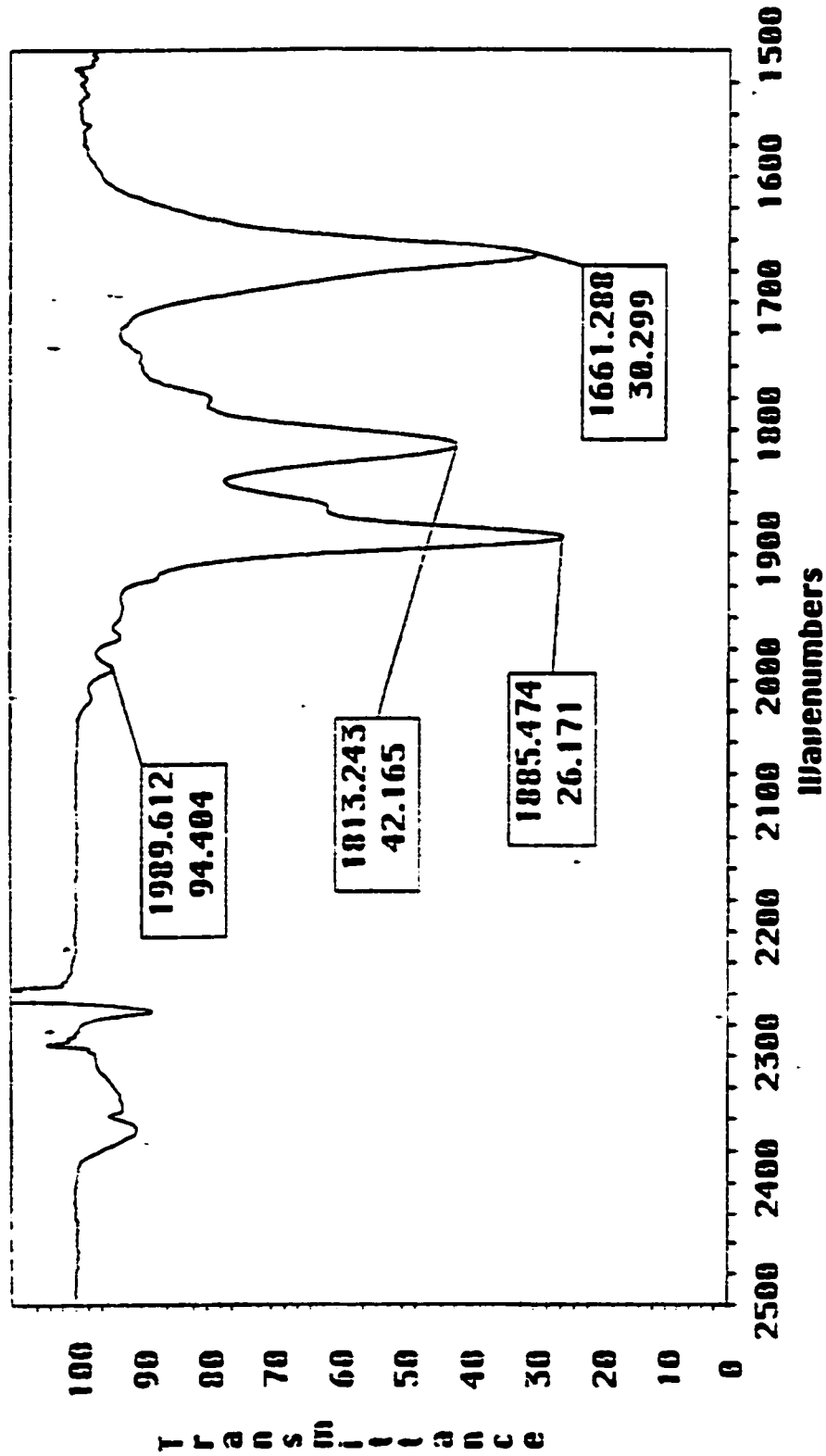

Figure 1-3. ^{1}H NMR (CD_3CN, 27 °C) of **6-Na$^+$**.

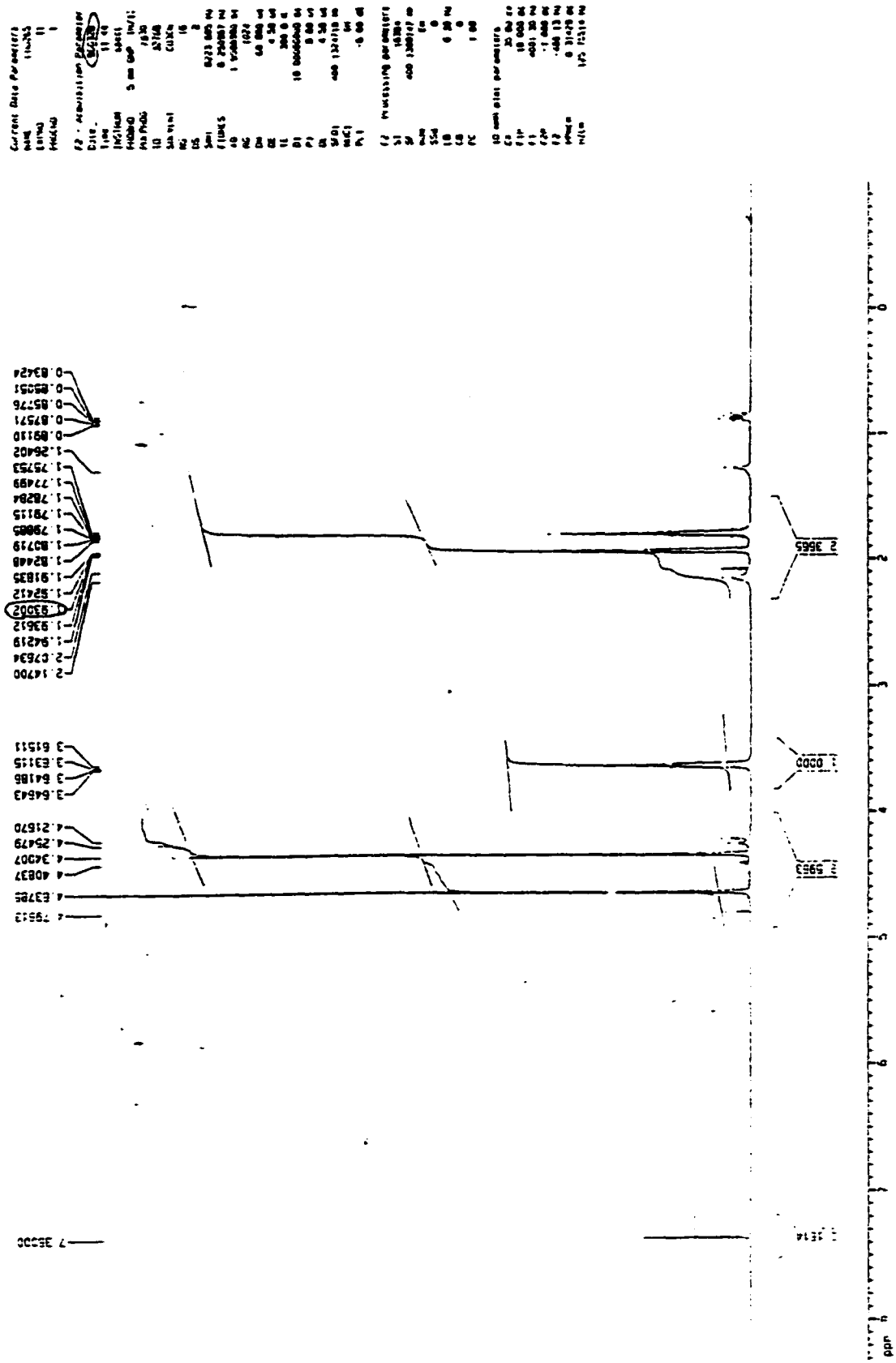

Figure 1-4. ^{1}H NMR (CD_3CN, -50 °C) of **6-Na$^+$** (full scale)

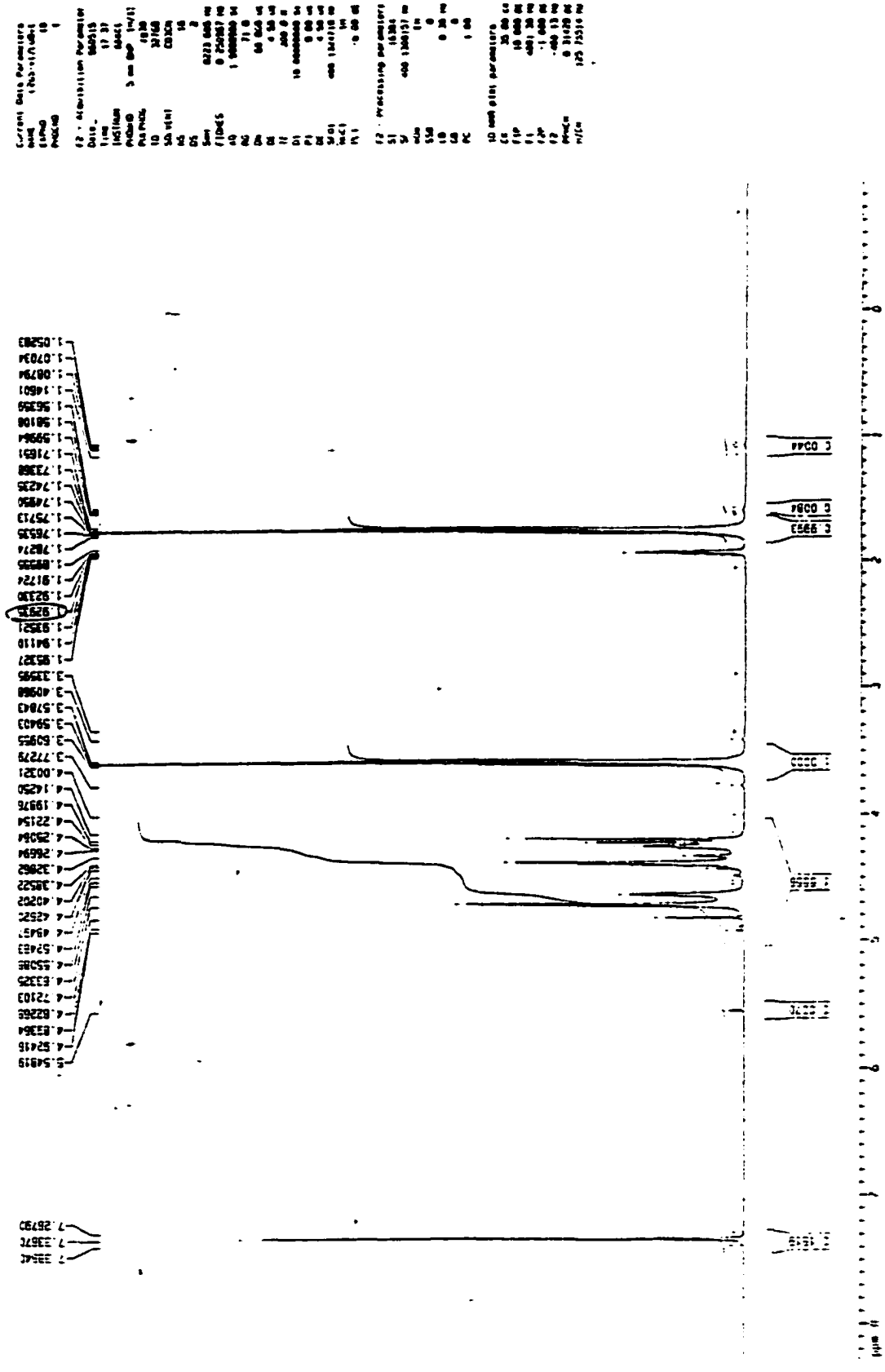

Figure 1-5. ^{1}H NMR (CD_3CN, -50 °C) of **6-Na**$^{-}$ (expanded scale)

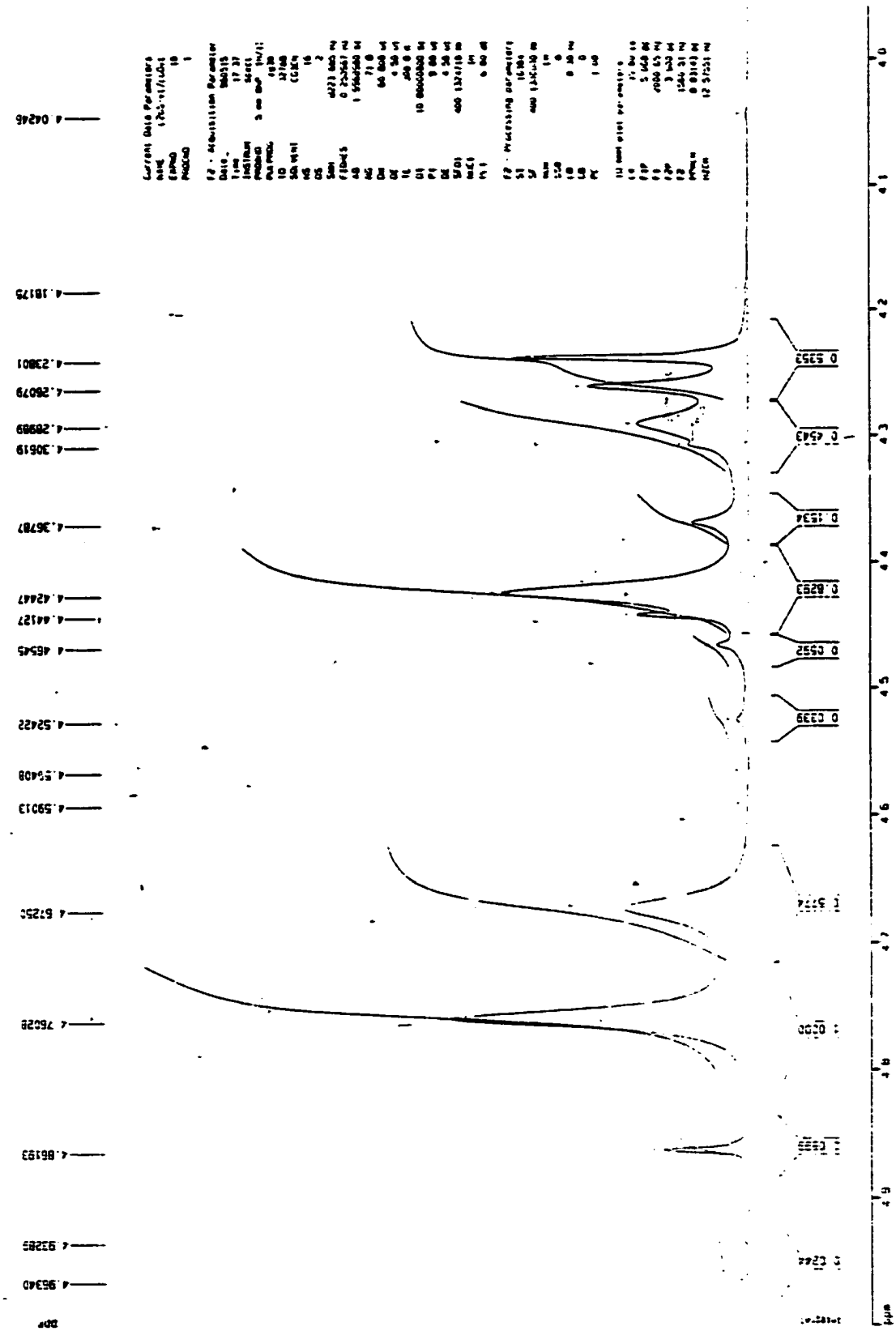

Figure 1-6. ^{13}C NMR (CD_3CN, 27 °C) of **6-Na$^+$**.

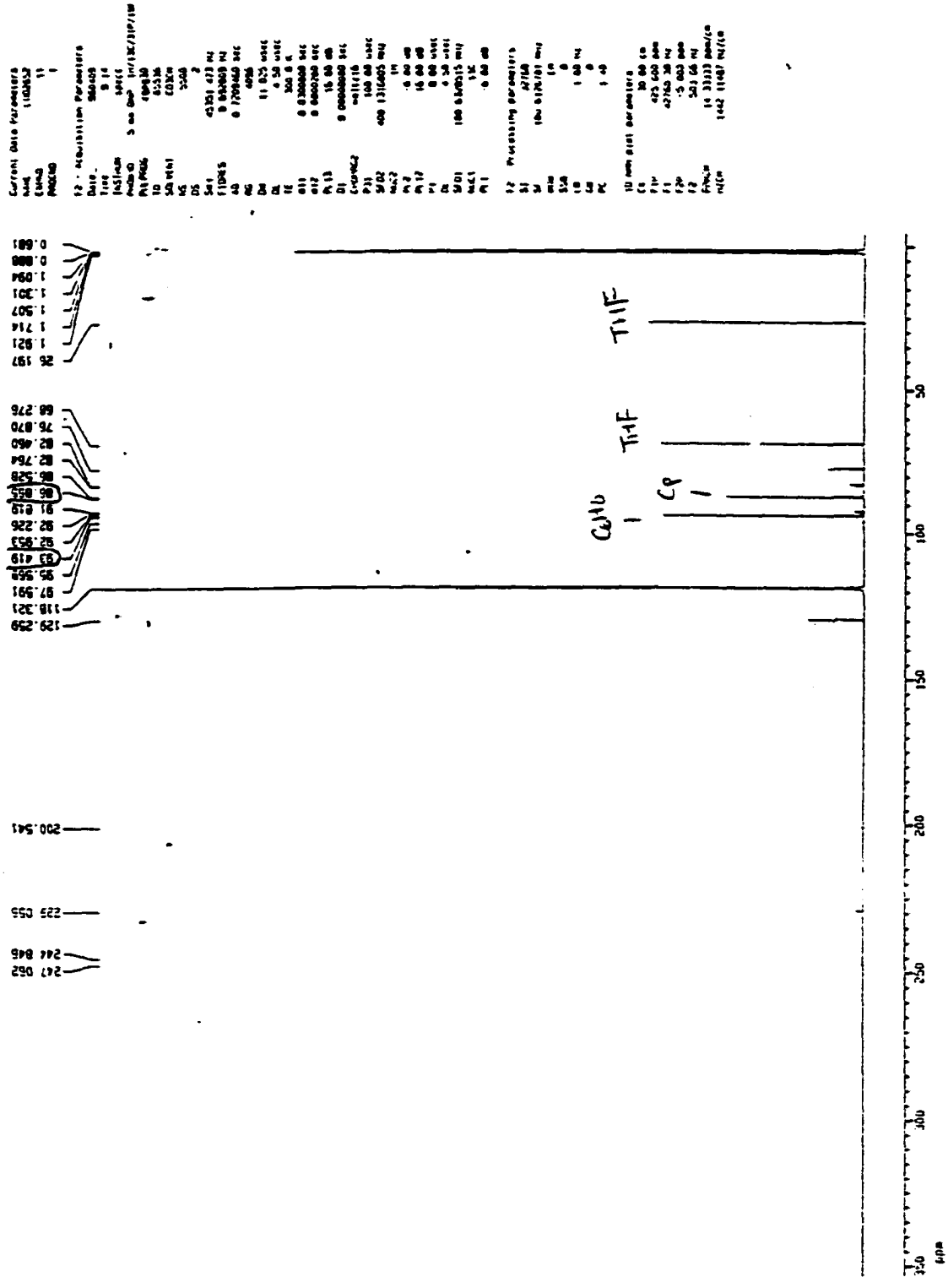

Figure 1-7. ^{13}C NMR (CD_3CN, -50 °C) of 6-Na^+ (full scale)

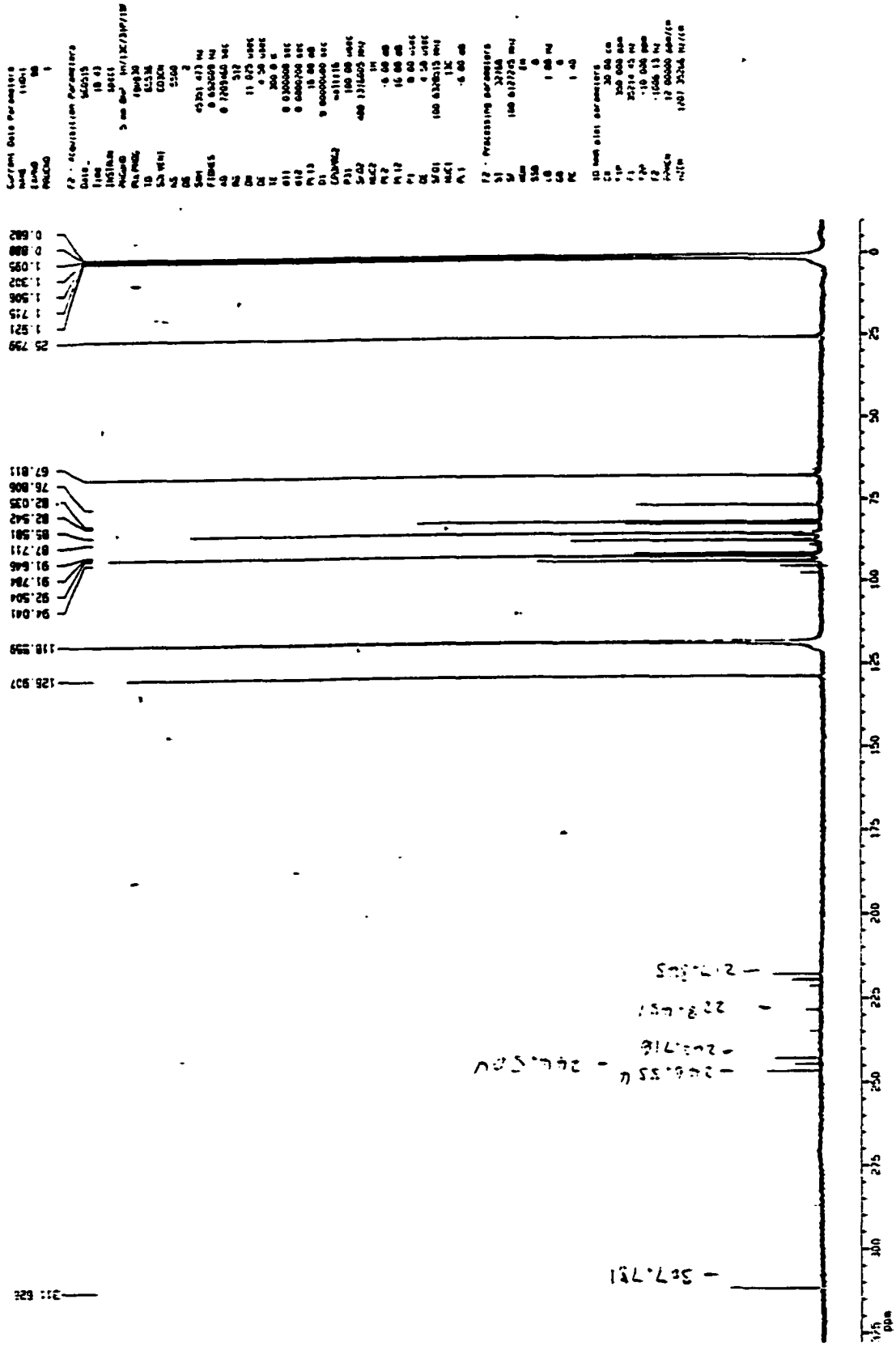

Figure 1-8. ^{13}C NMR (CD_3CN, -50 °C) of **6-Na$^+$** (60~150 ppm)

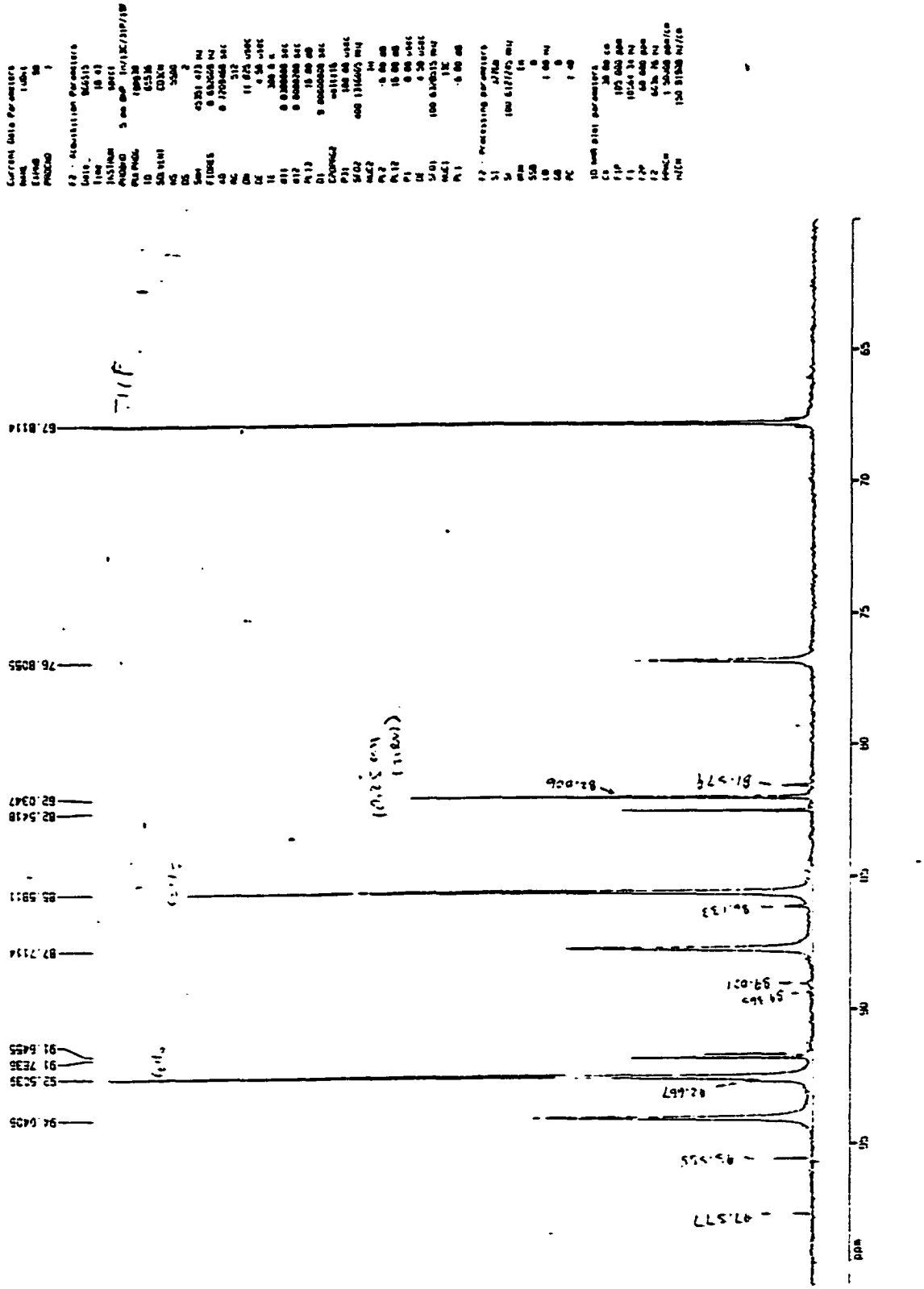

Figure 1-9. ^{13}C NMR (CD_3CN, -50 °C) of **6-Na$^+$** (195~315 ppm)

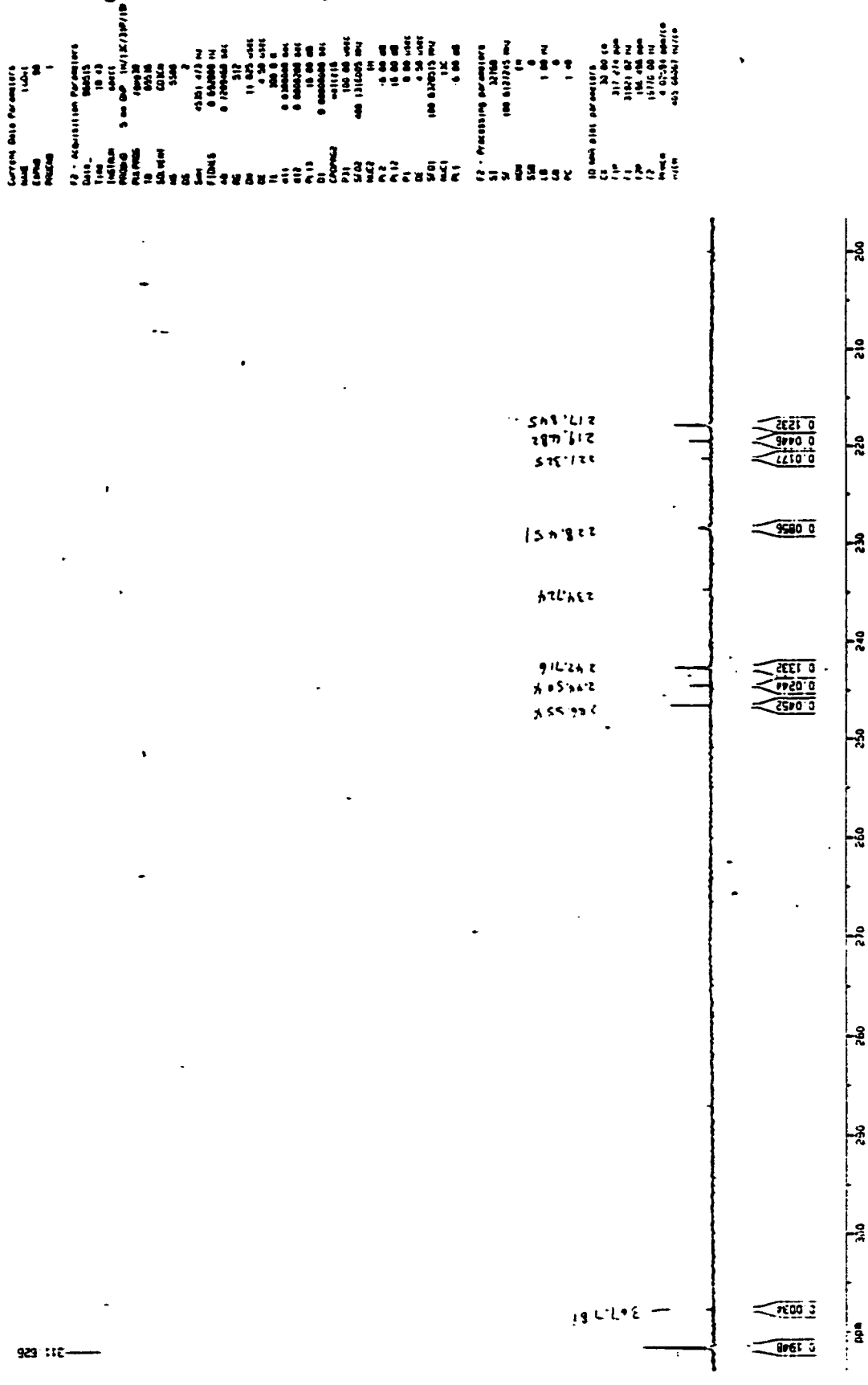

Figure 2-1. IR (CH_3CN) of **6-PPN**$^+$.

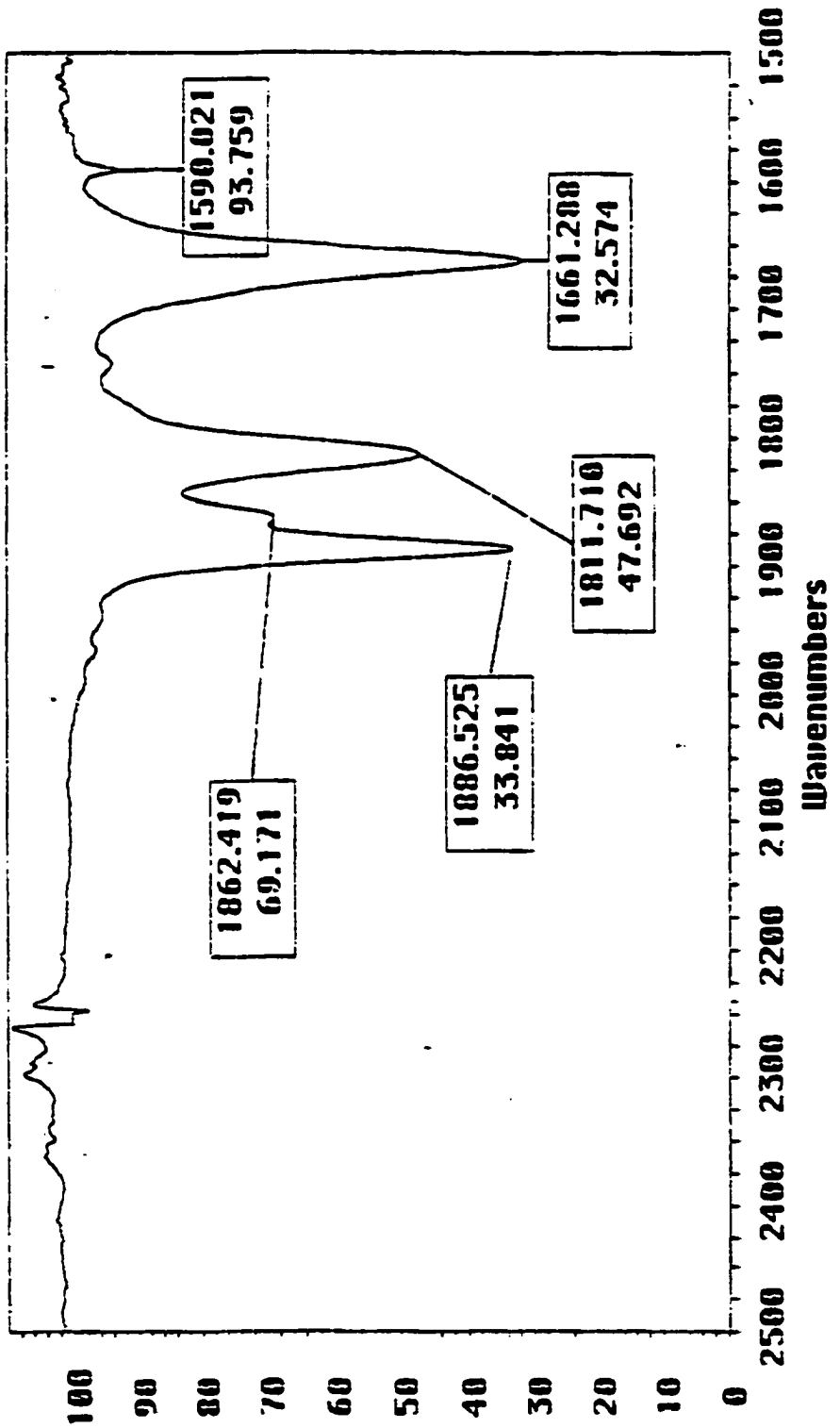

Figure 2-2. ^{1}H NMR (CD_3CN) of **6-PPN^{+}**. (relaxation delay [RD] 10 seconds)

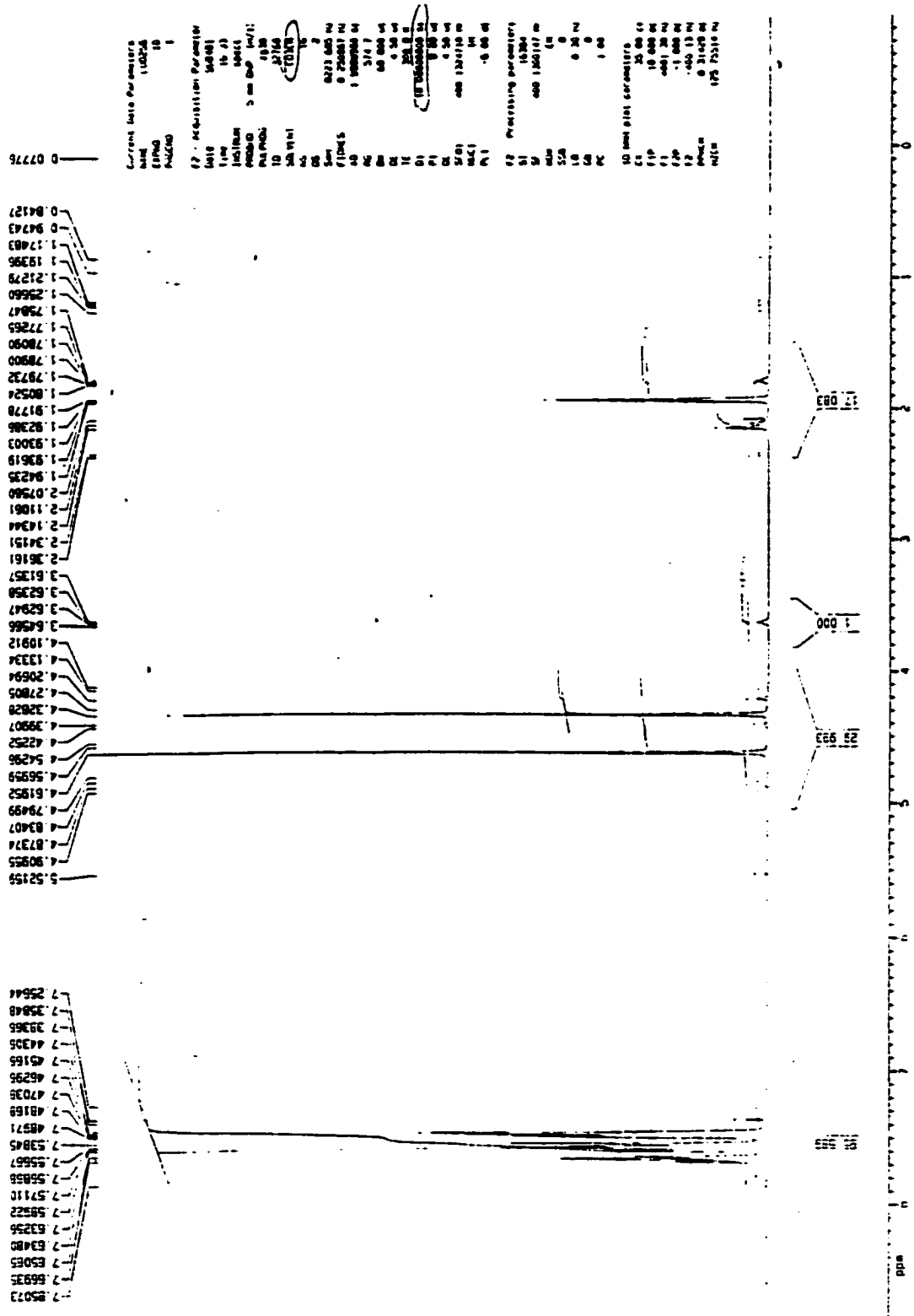

Figure 2-3. ^{1}H NMR (CD_3CN) of **6-PPN^{+}**. (RD = 20 seconds)

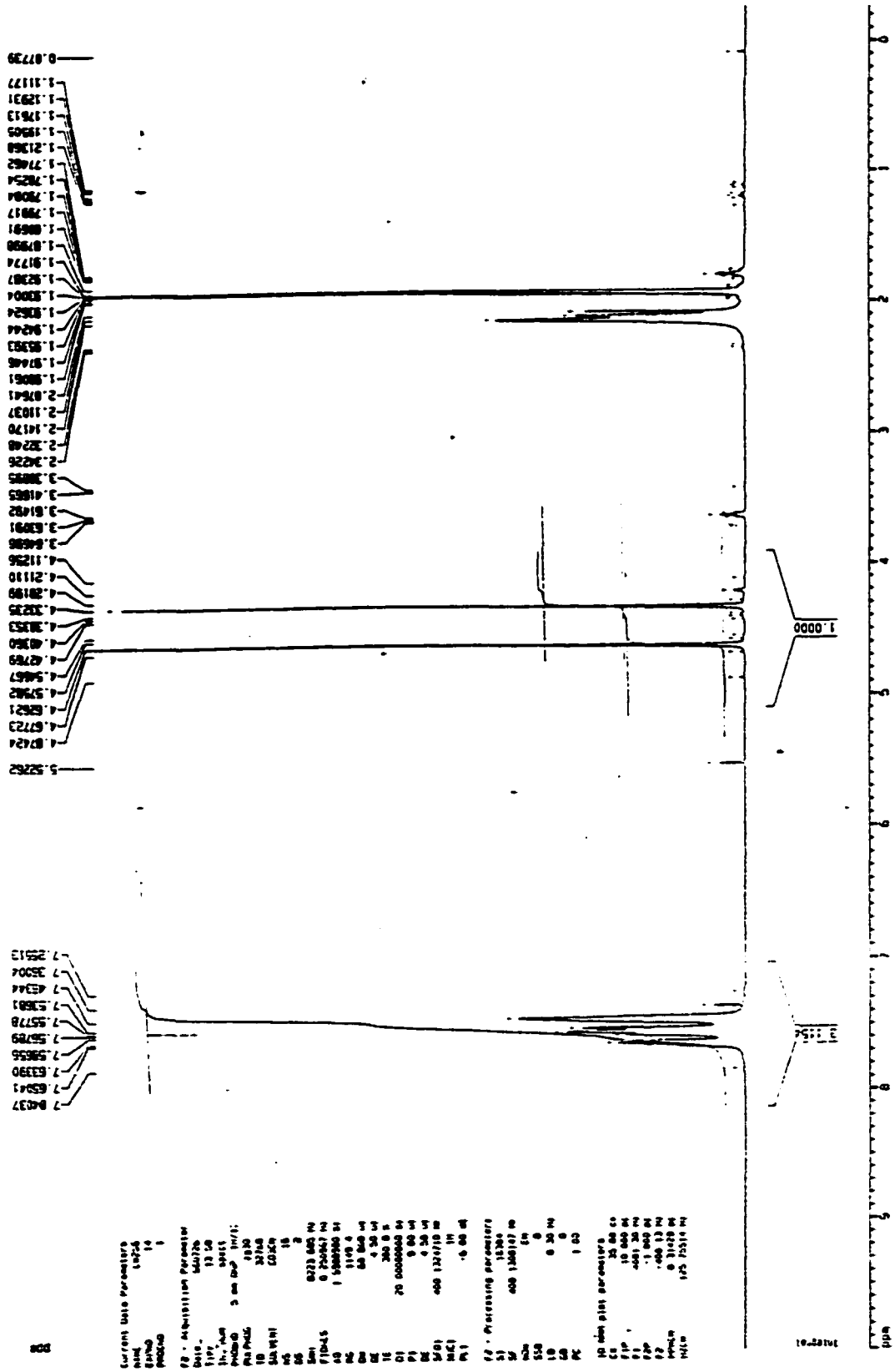

Figure 2-4. ^{1}H NMR (CD_3CN) of **6-PPN^{+}**. (RD = 20 seconds; ^{1}H flip angle = 3°)

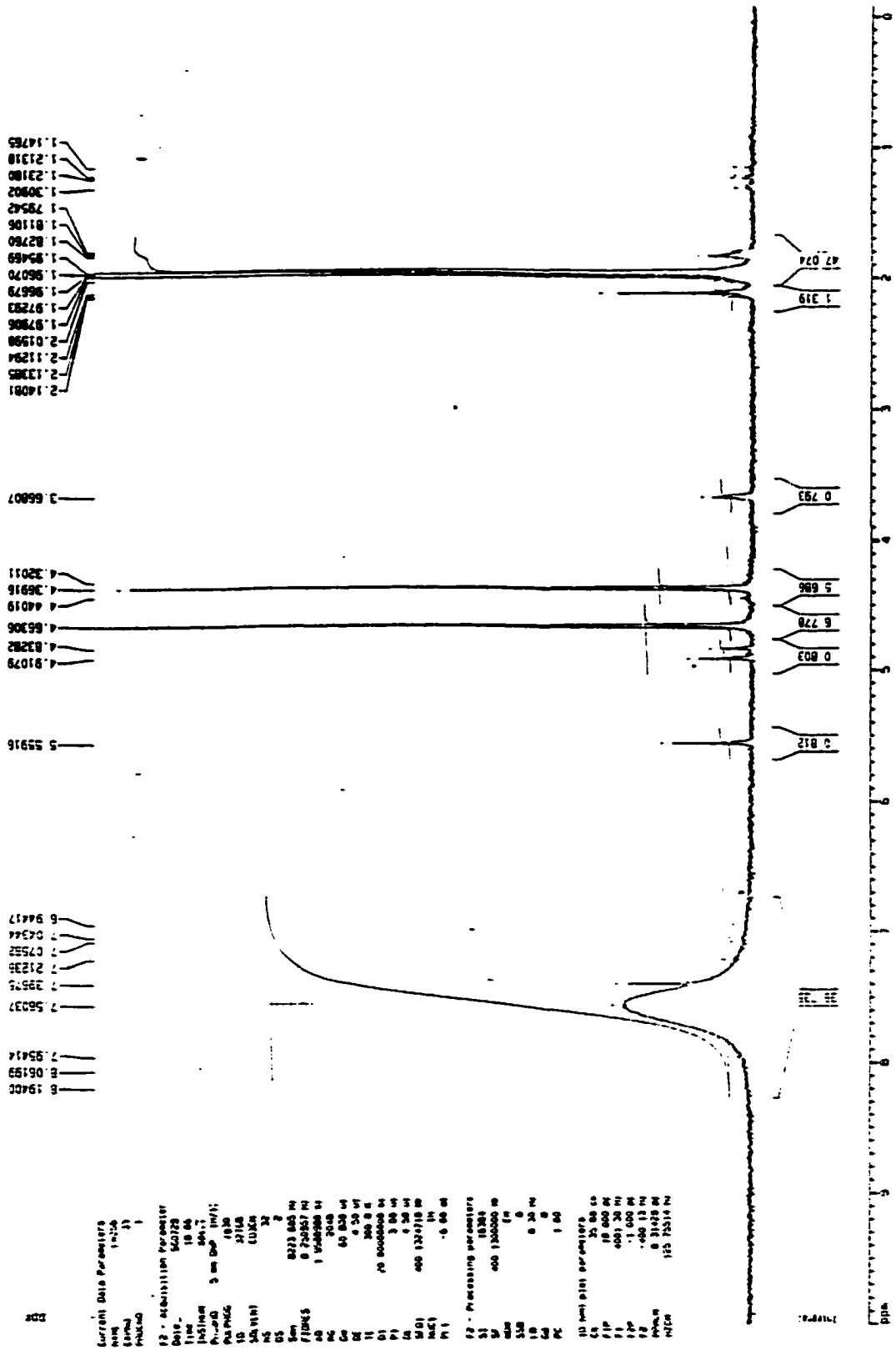

Figure 2-5. ^{31}P NMR (CD_3CN) of **6-PPN$^+$**.

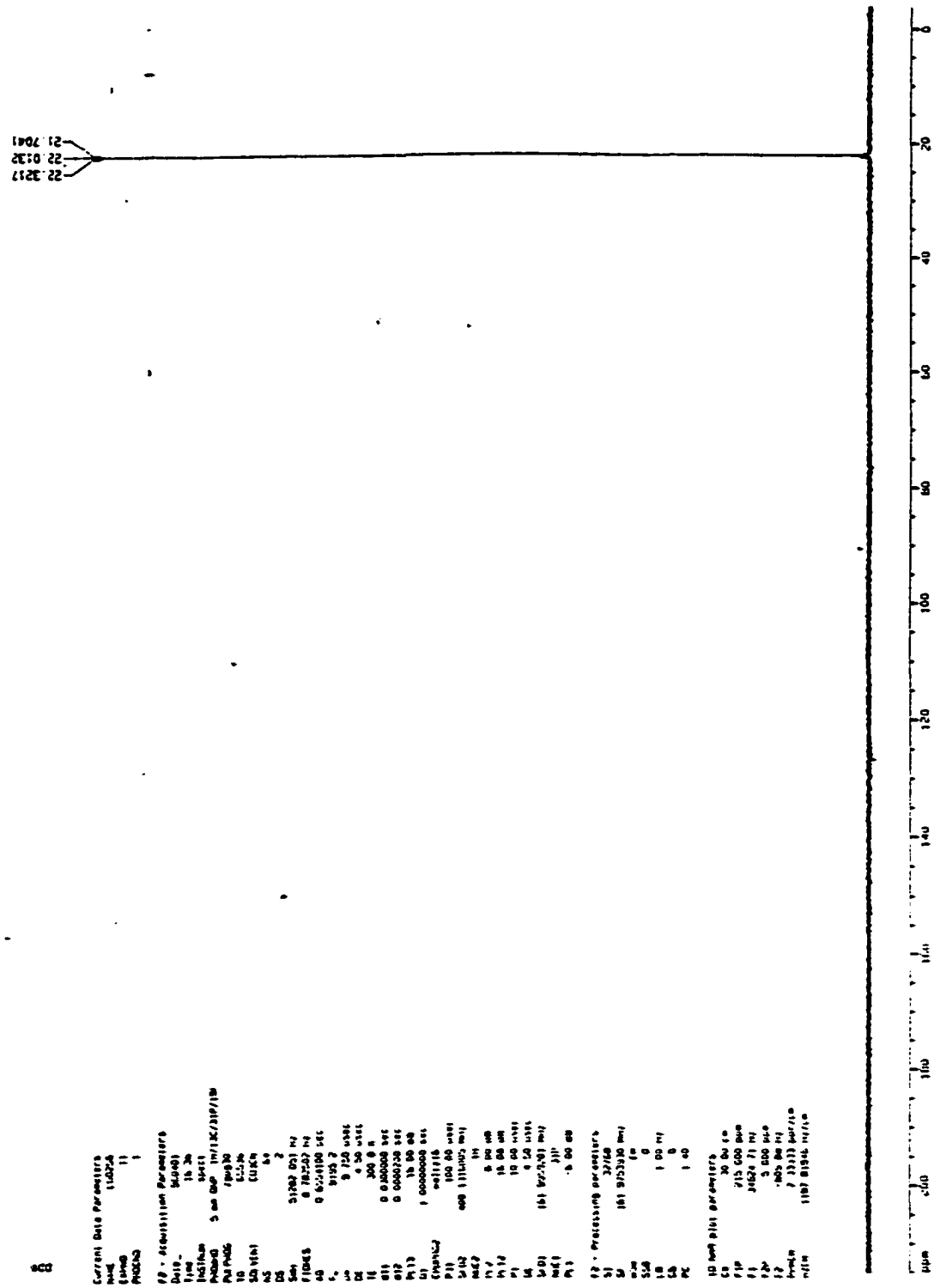

Figure 2-6. ^{13}C NMR (CD_3CN) of **6-PPN$^+$**. (full scale)

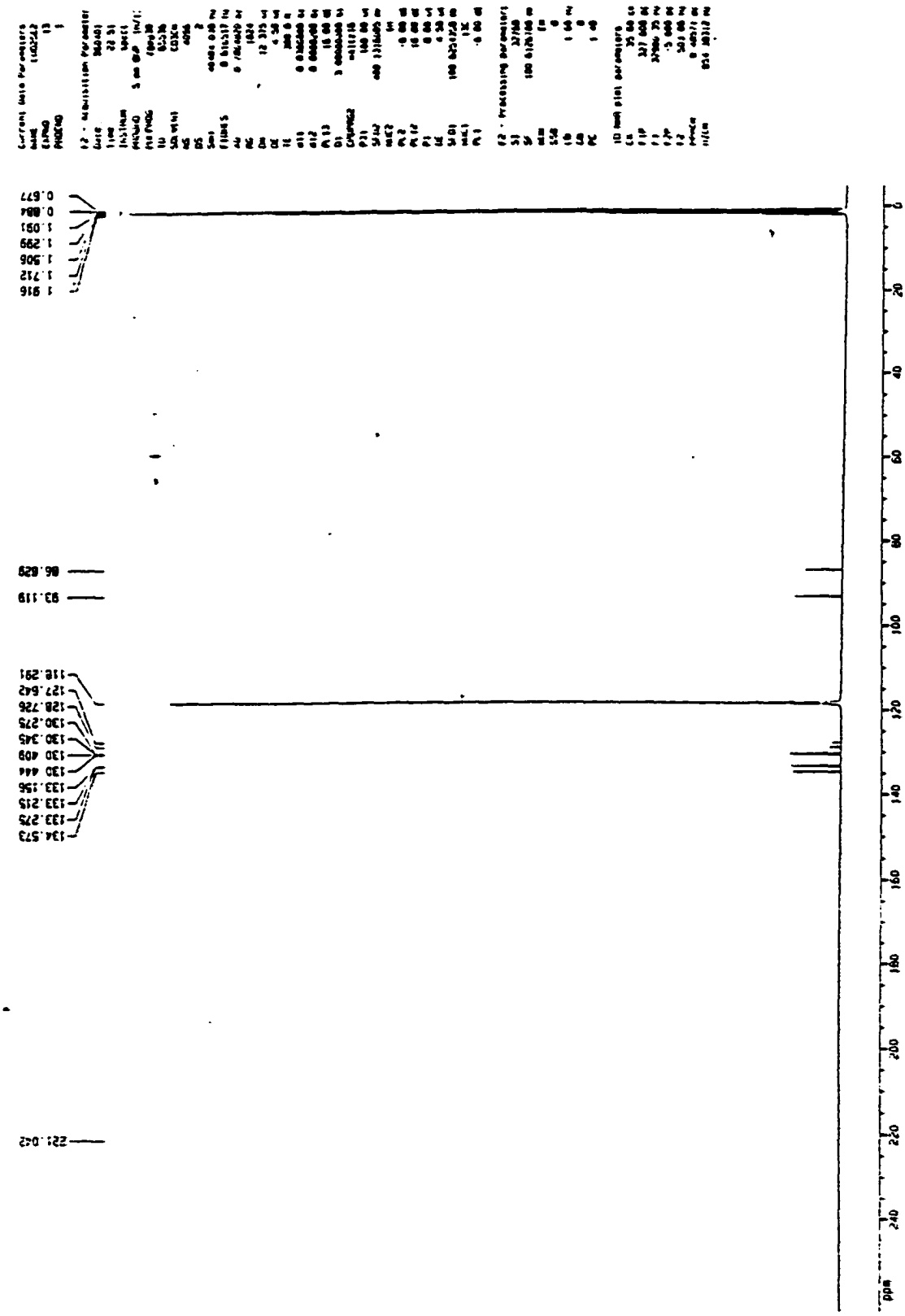

Figure 2-7. ^{13}C NMR (CD_3CN) of **6-PPN$^+$**. (126~136 ppm)

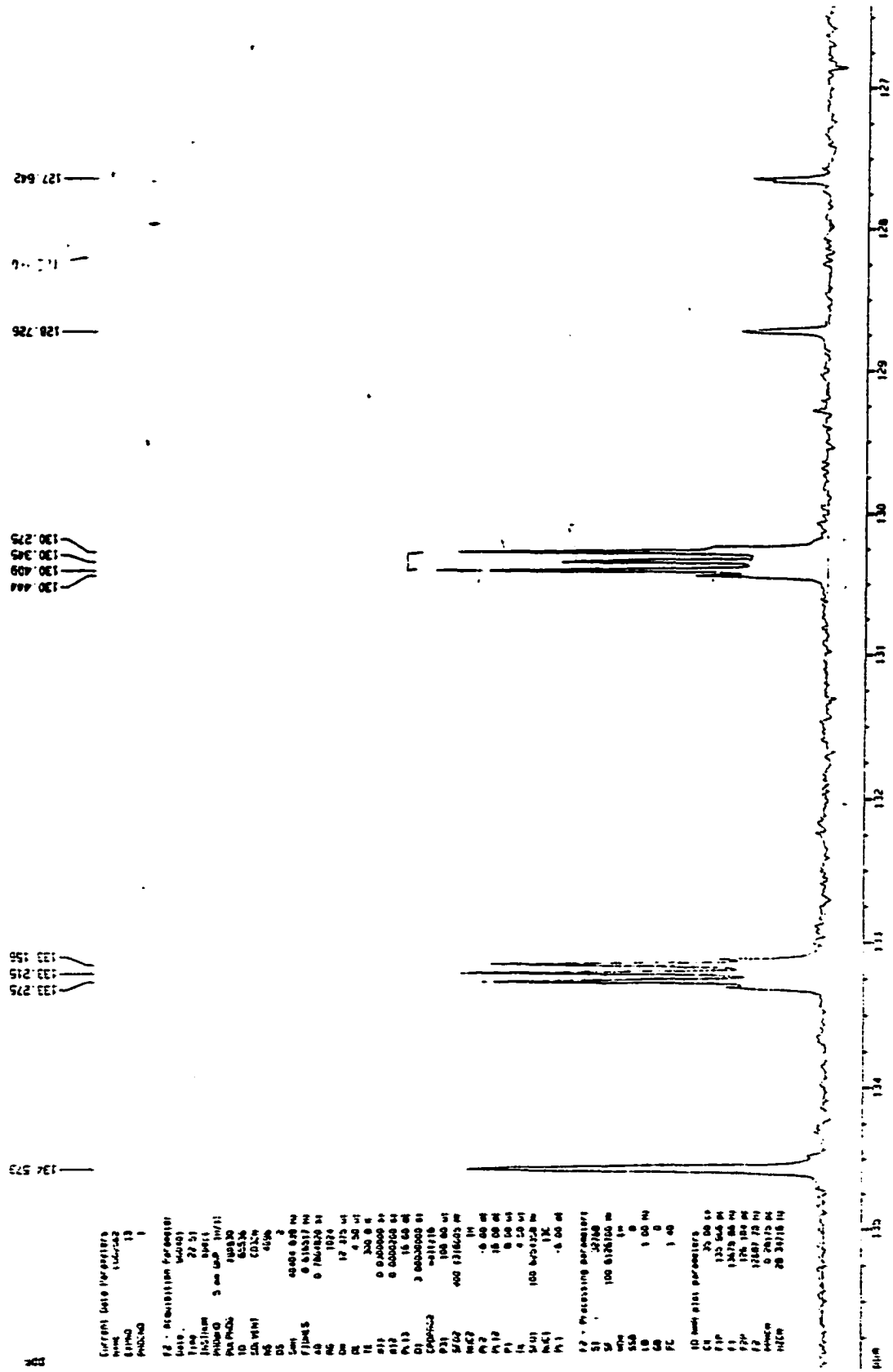

Figure 3-1. IR (CH_2Cl_2) of **Methoxycarbyne (7)**.

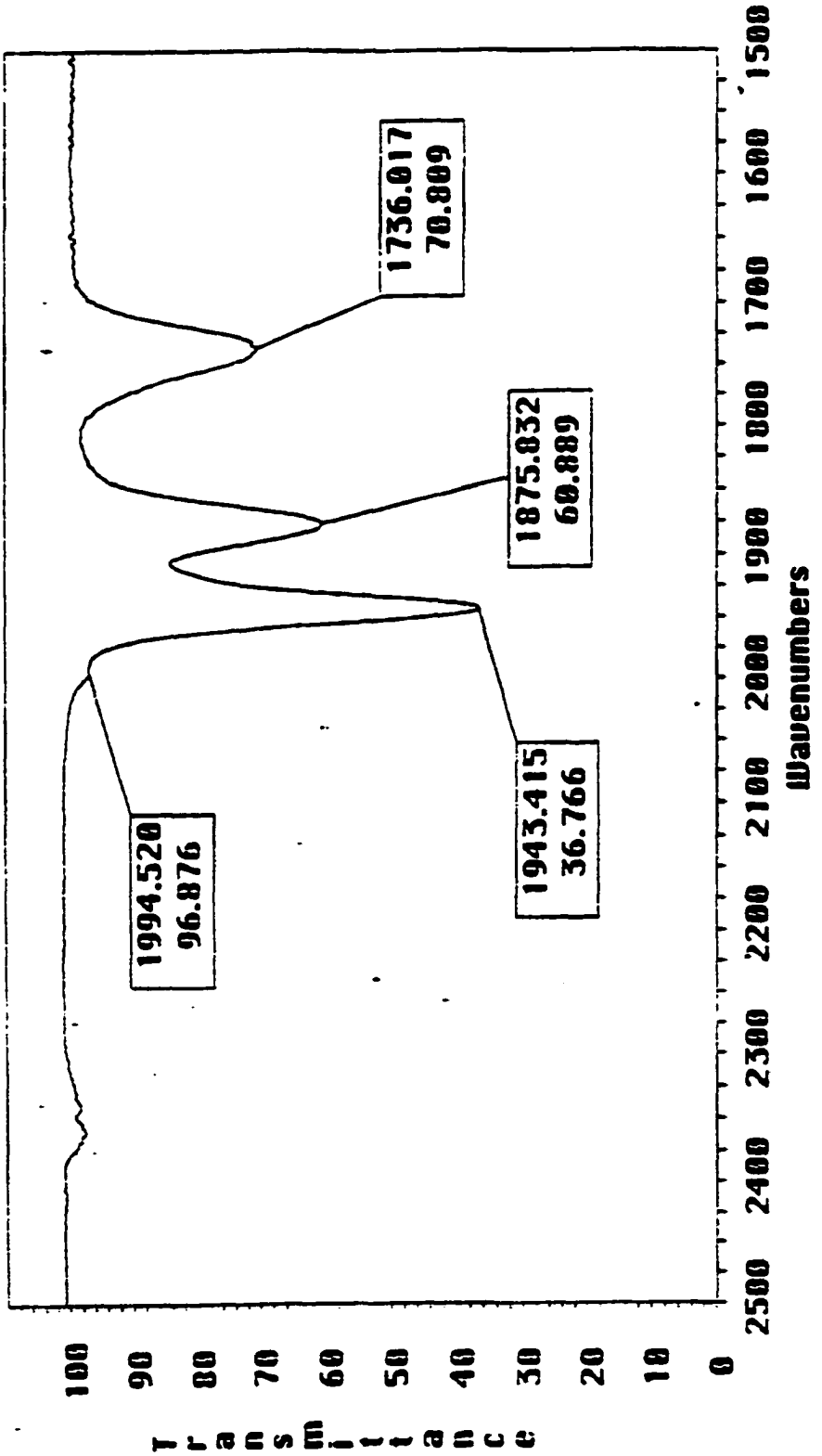

Figure 3-2. ^{1}H NMR (CD_2Cl_2, 20 °C) of **Methoxycarbyne (7).**

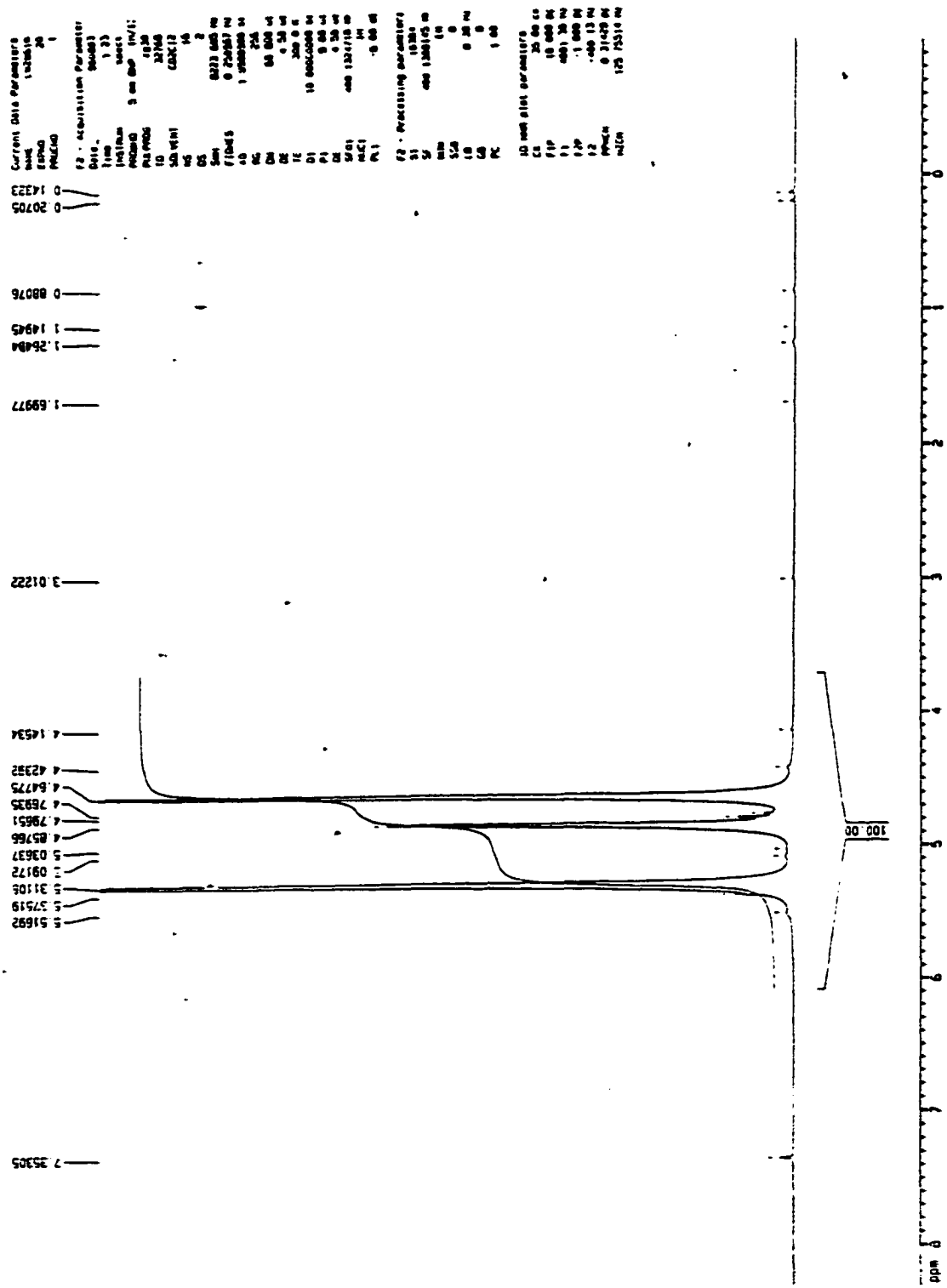

Figure 3-3. ^{1}H NMR (CD_2Cl_2, -20 °C) of **Methoxycarbyne (7)**.

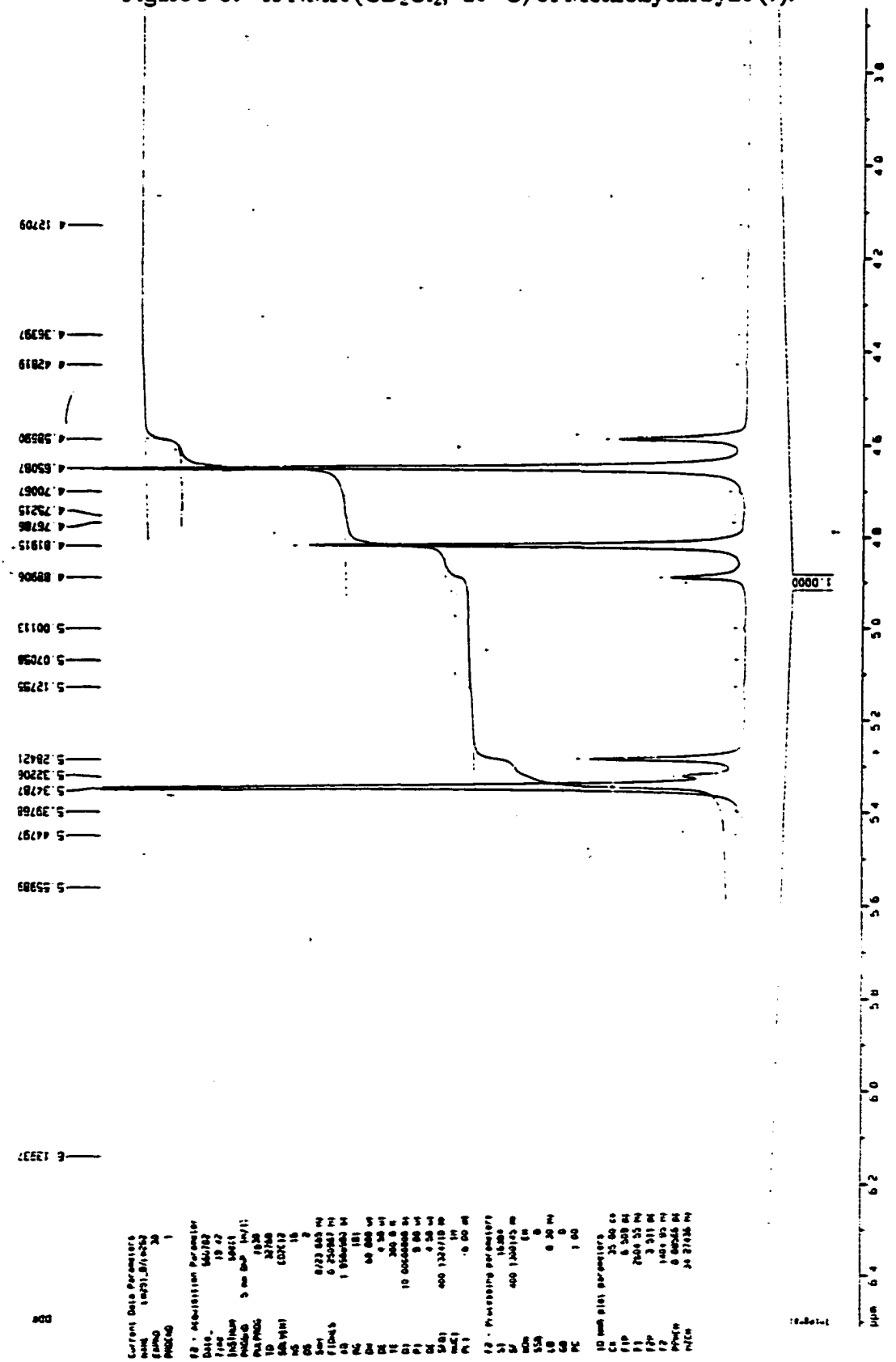

Figure 3-4. ^{1}H NMR (Toluene-d_8, -20 °C) of **Methoxycarbyne (7)**.

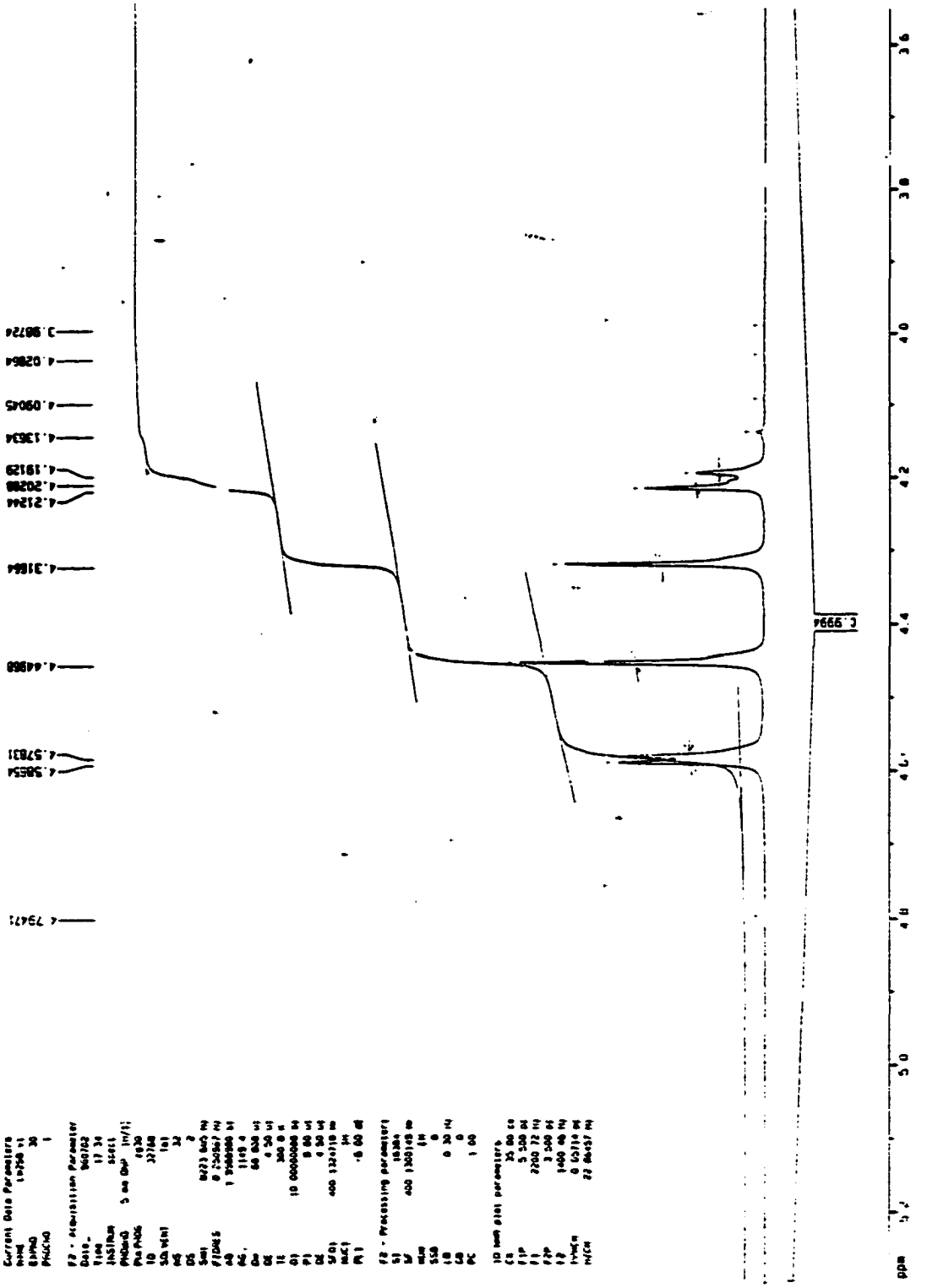

Figure 3-5. ^{1}H NMR (Toluene-d_8, -10 °C) of **Methoxycarbyne (7)**.

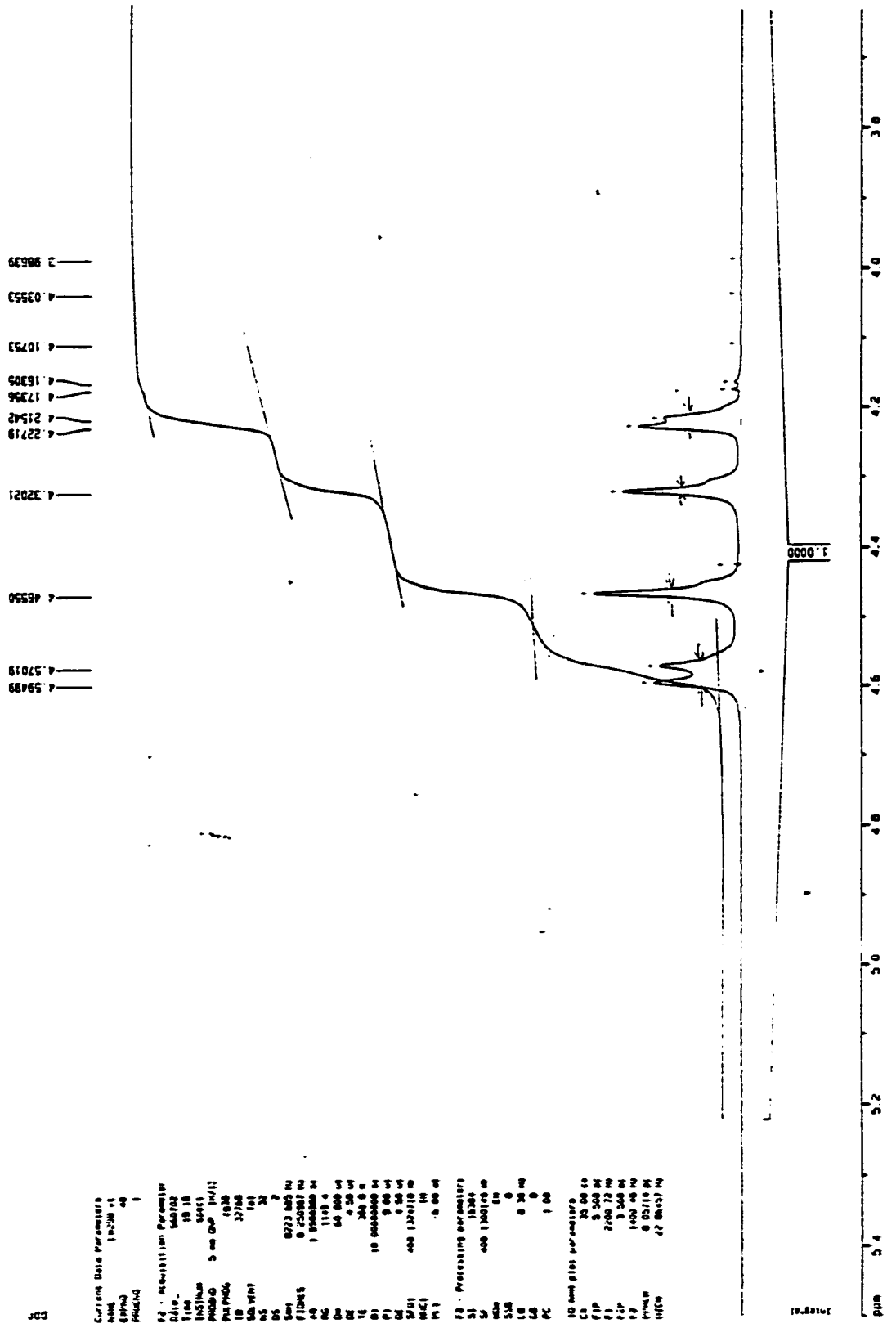

Figure 3-6. ^{1}H NMR (Toluene-d_8, 0 °C) of **Methoxycarbyne (7)**.

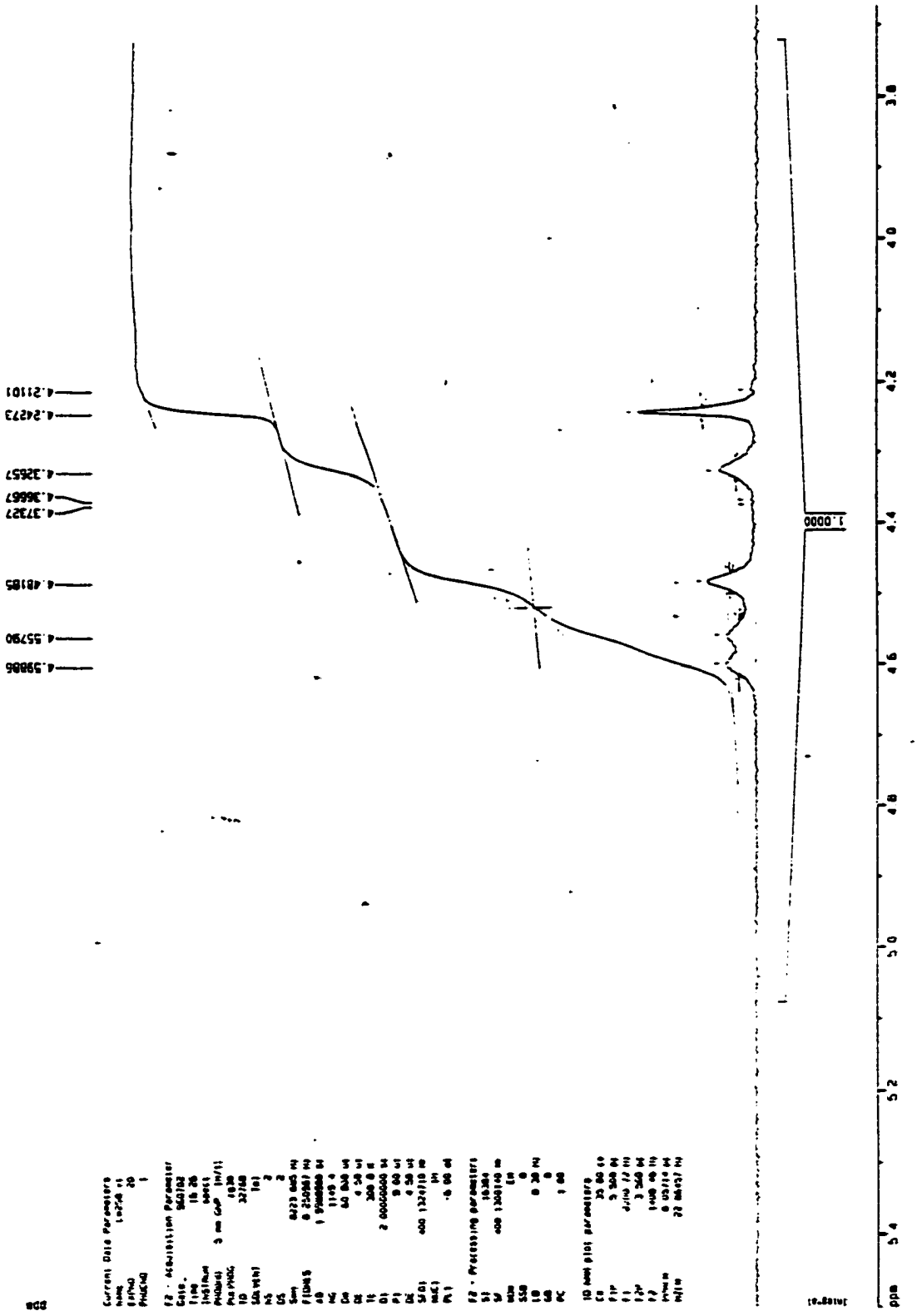

Figure 3-7. ^{1}H NMR (Toluene-d_8, 20 °C) of **Methoxycarbyne (7)**.

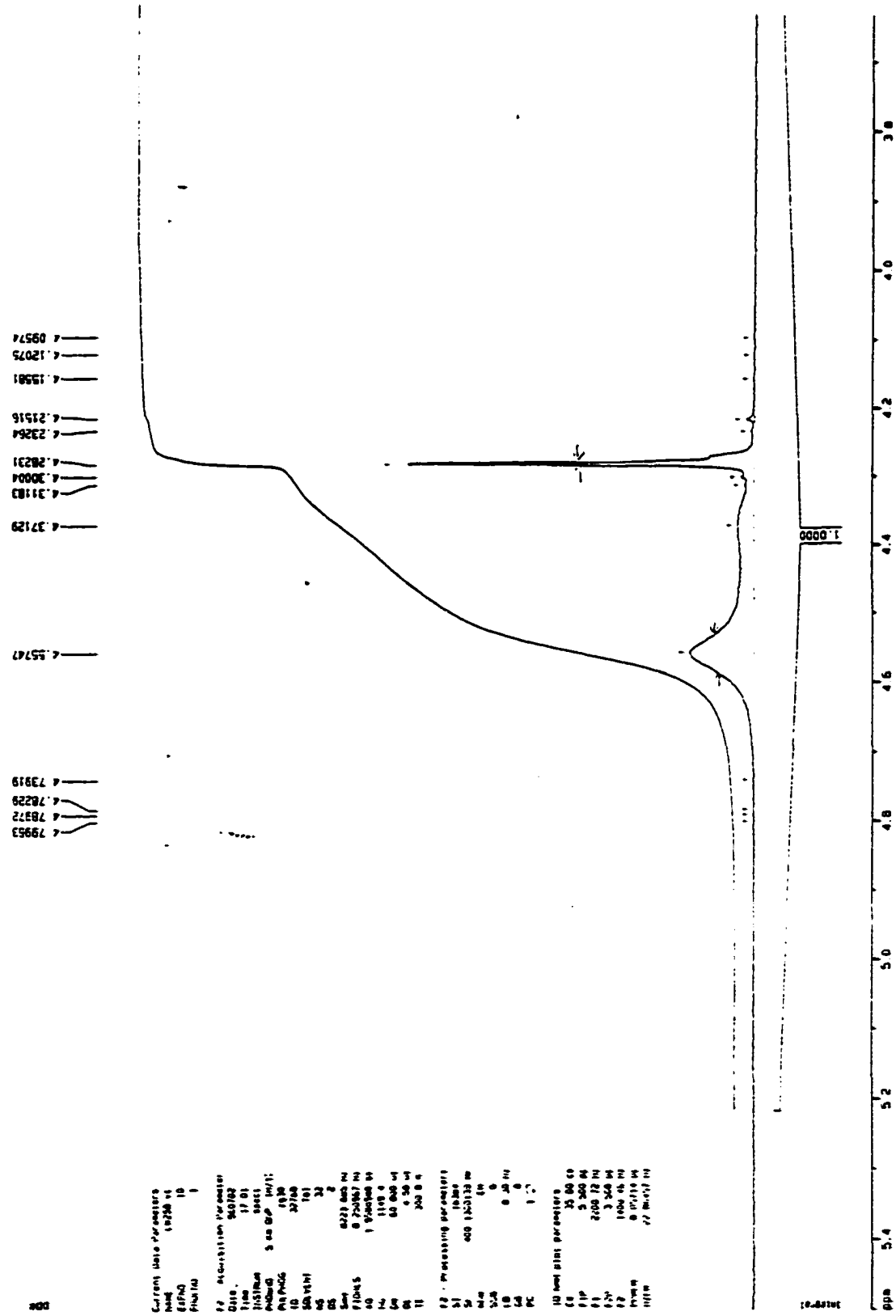

Figure 3-8. ^{1}H NMR (Toluene-d_8, 40 °C) of **Methoxycarbyne (7)**.

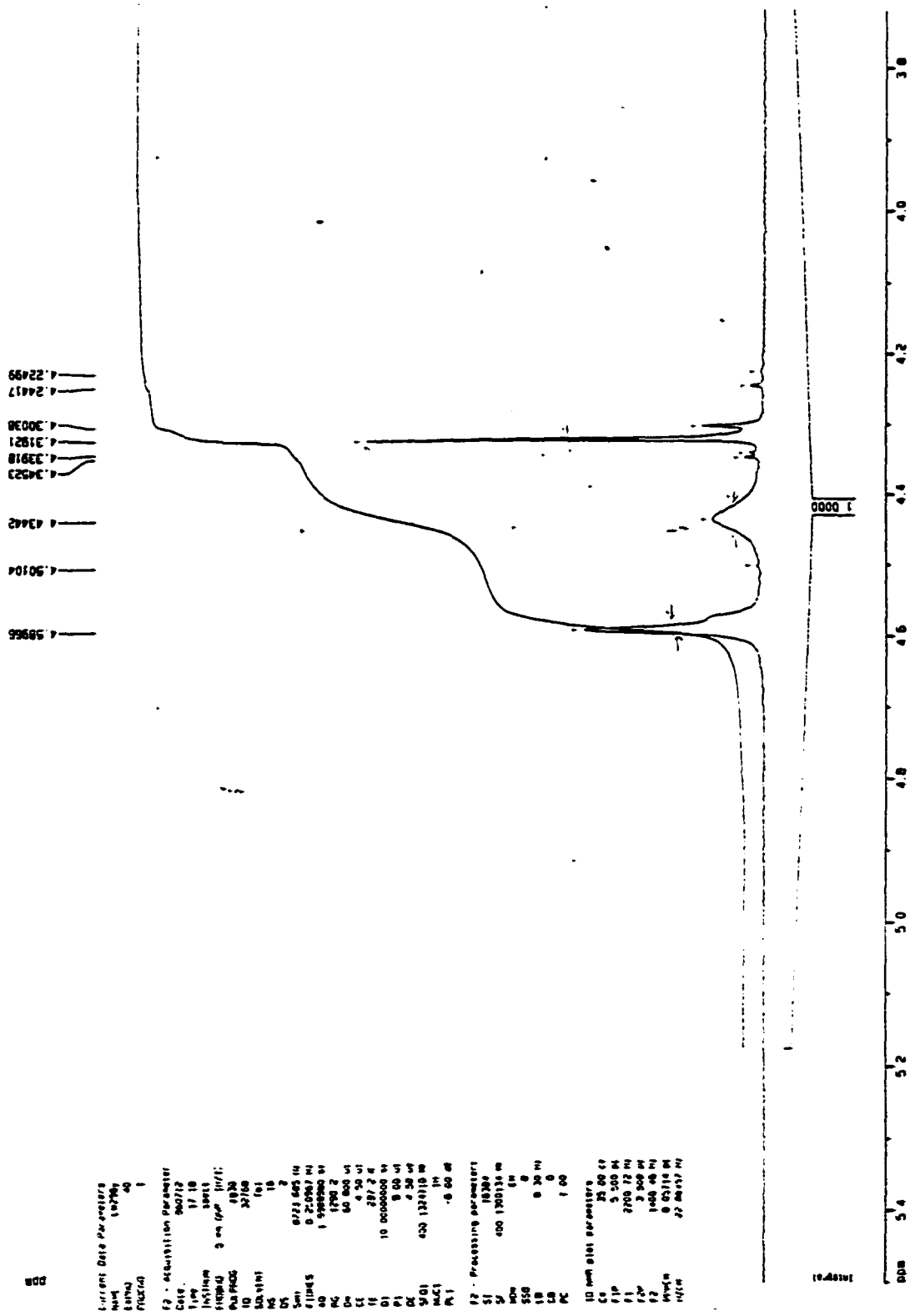

Figure 3-9. ^{13}C NMR (CD_2Cl_2, -20 °C) of **Methoxycarbyne (7)**.

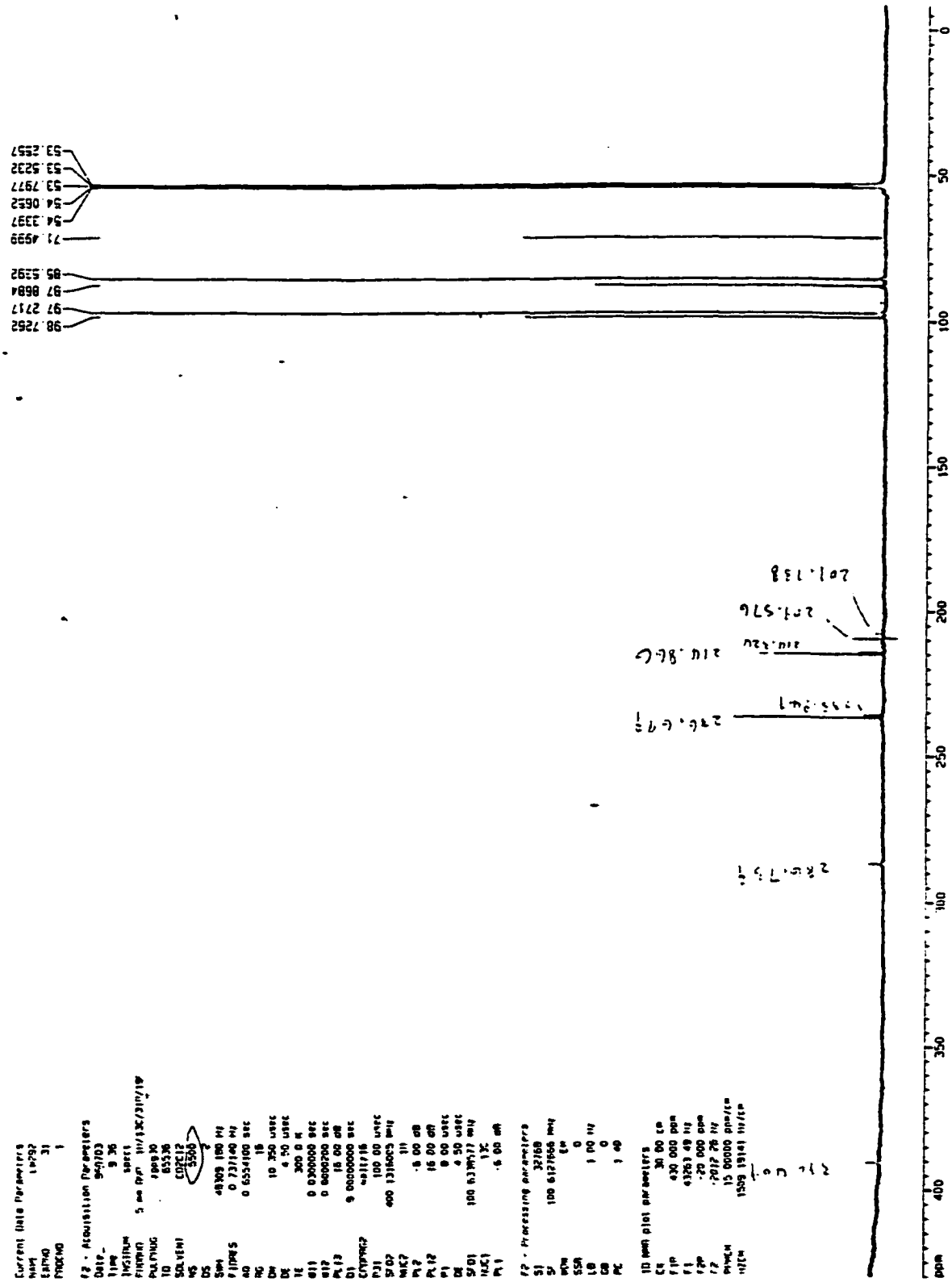

Figure 4-1. Reaction of (7) + PPh_3 (0.19 M) at beginning, 20 °C. ^1H NMR (C_6D_6)

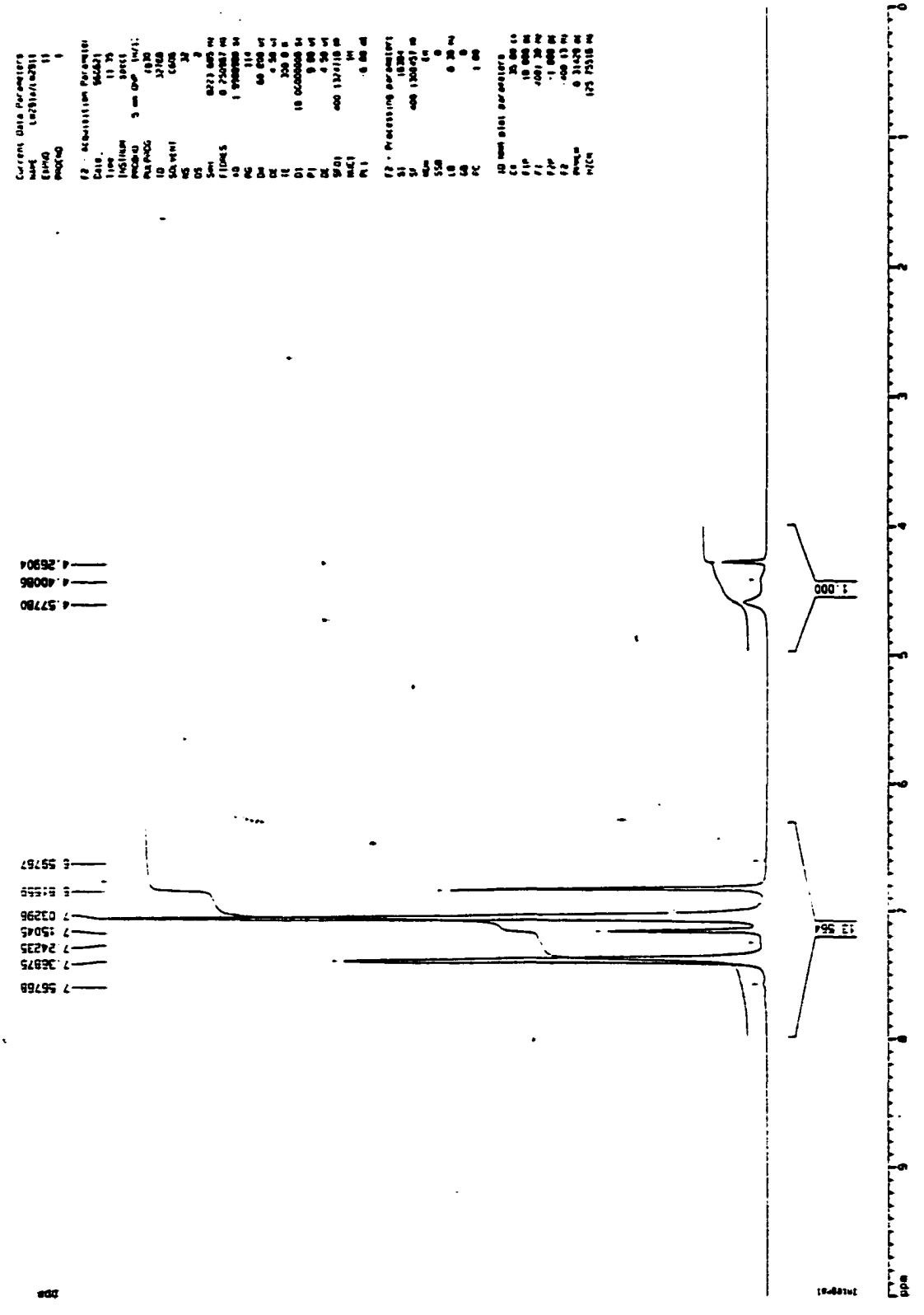

Figure 4-2. Reaction of (7) + PPh_3 (0.19 M) at 50 °C for 30 min. ^1H NMR (C_6D_6)

Figure 4-3. Reaction of (7) + PPh_3 (0.19 M) at 50 °C for 1 hour. ^1H NMR (C_6D_6)

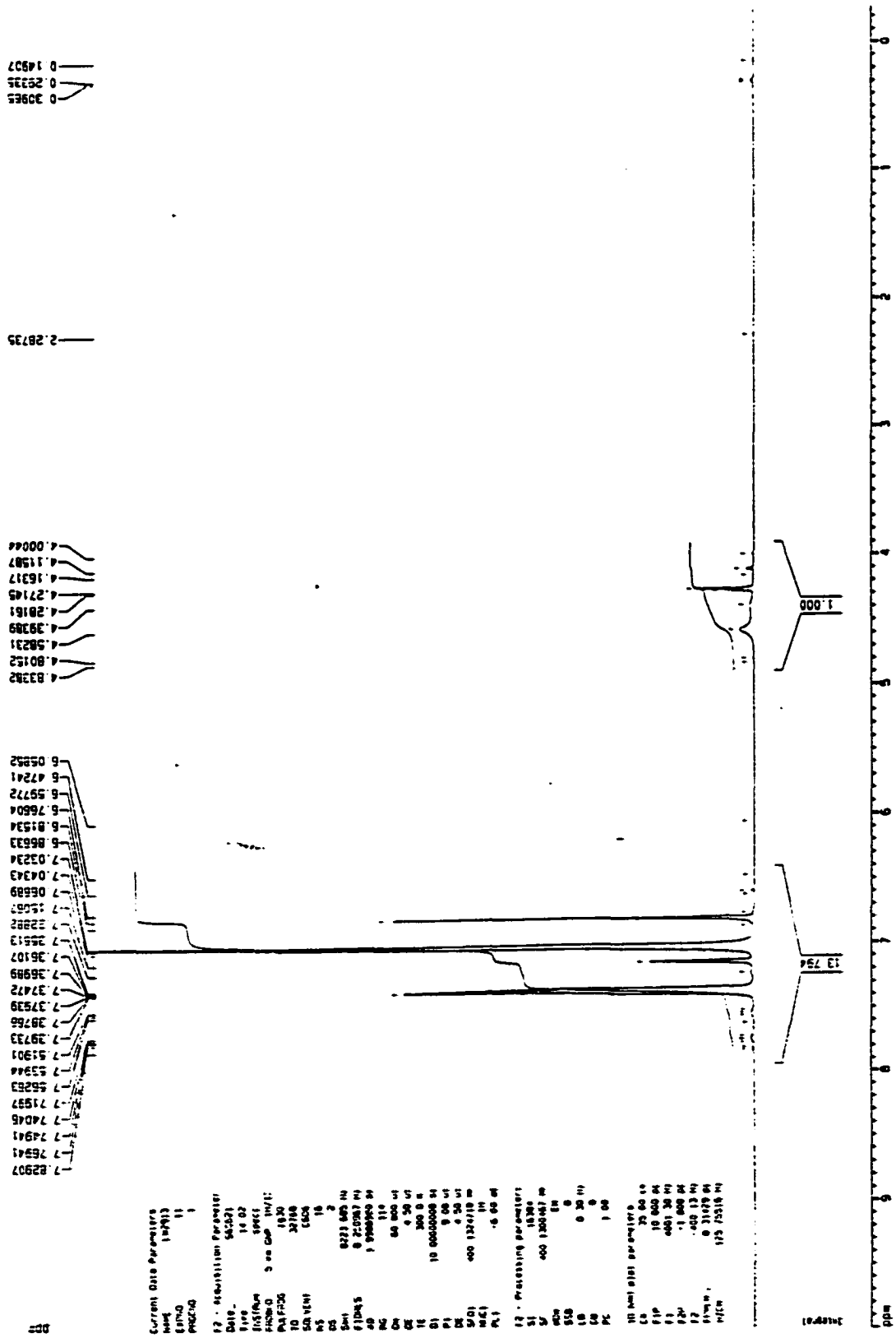

Figure 4-4. Reaction of (7) + PPh_3 (0.19 M)at 50 °C for 1.5 hour. ^1H NMR (C_6D_6)

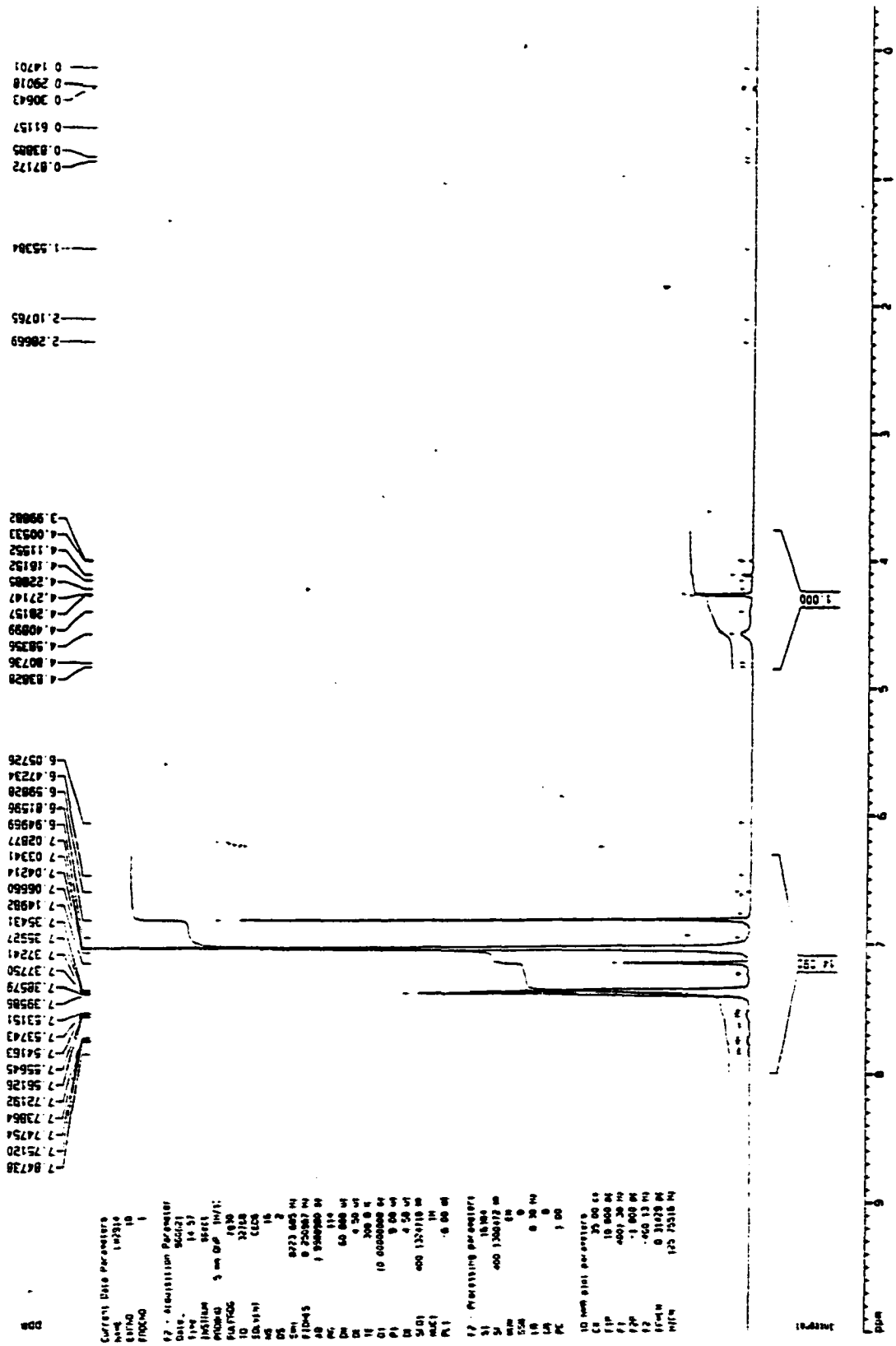

Figure 4-5. Reaction of (7) + PPh_3 (0.19 M) at 50 °C for 2 hours. ^1H NMR (C_6D_6)

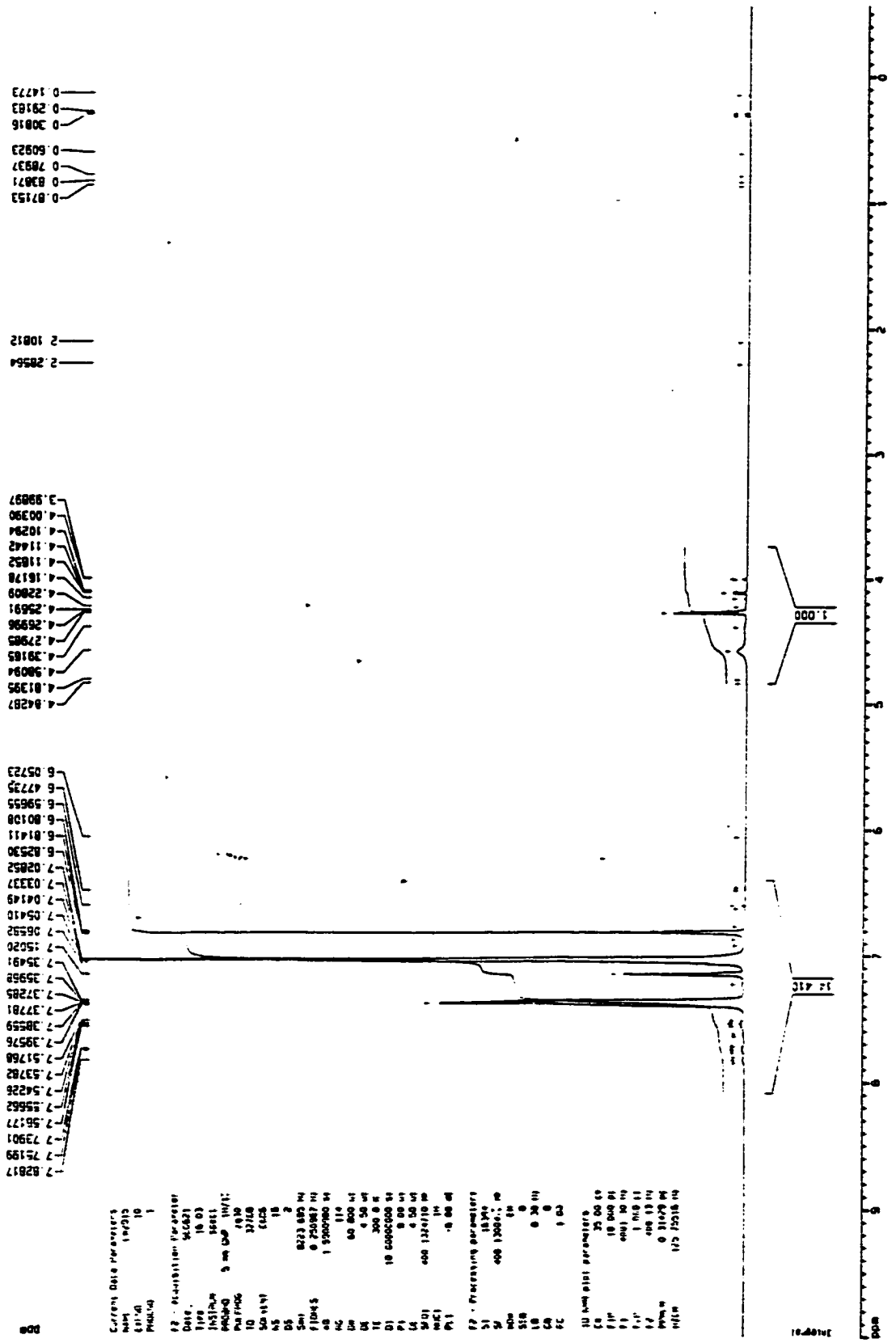

Figure 4-6. Reaction of (7) + PPh_3 (0.19 M) at 50 °C for 3 hours. ^1H NMR (C_6D_6)

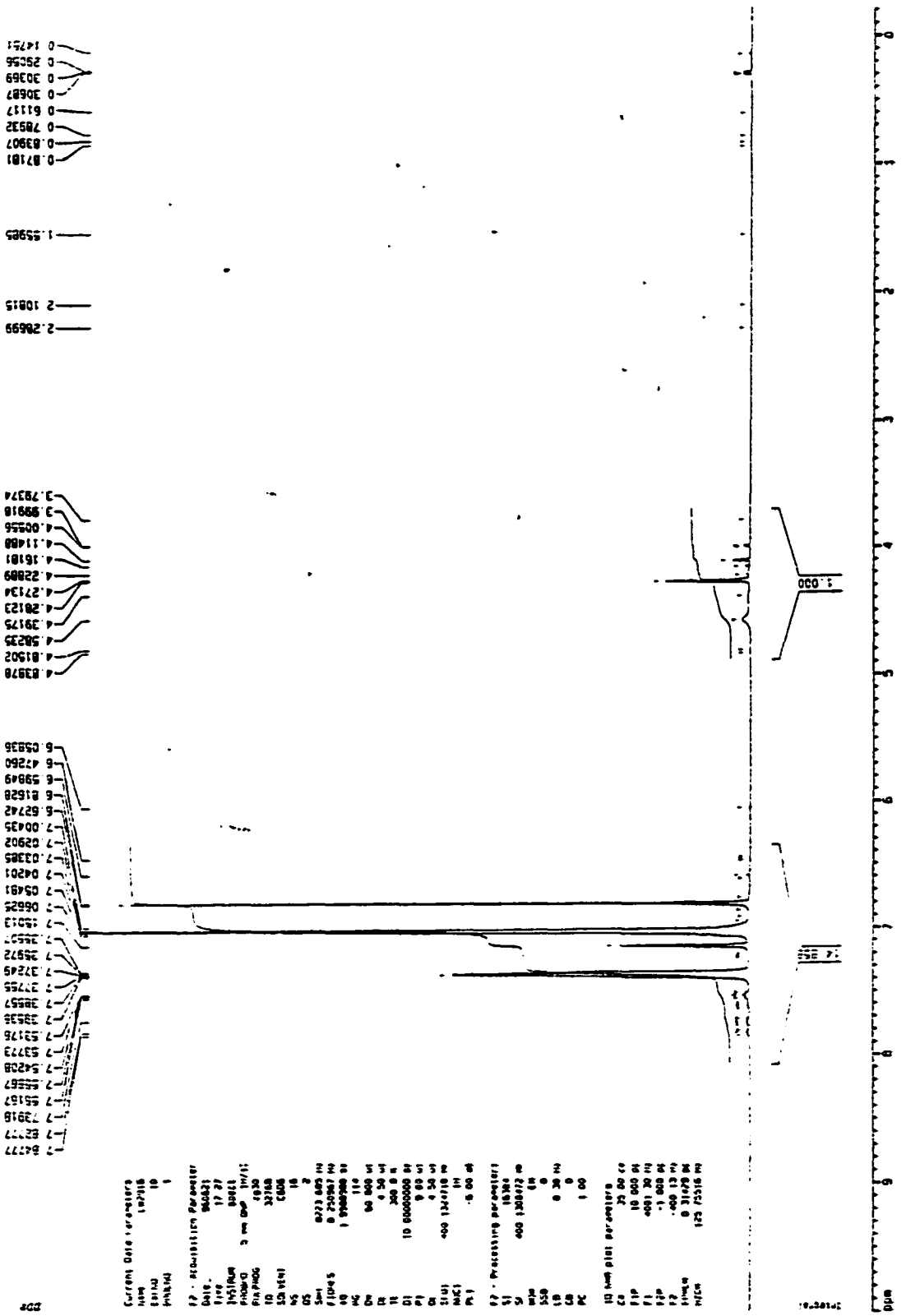

Figure 4-7. Reaction of (7) + PPh_3 (0.19 M) at 50 °C for 4 hours. ^1H NMR (C_6D_6)

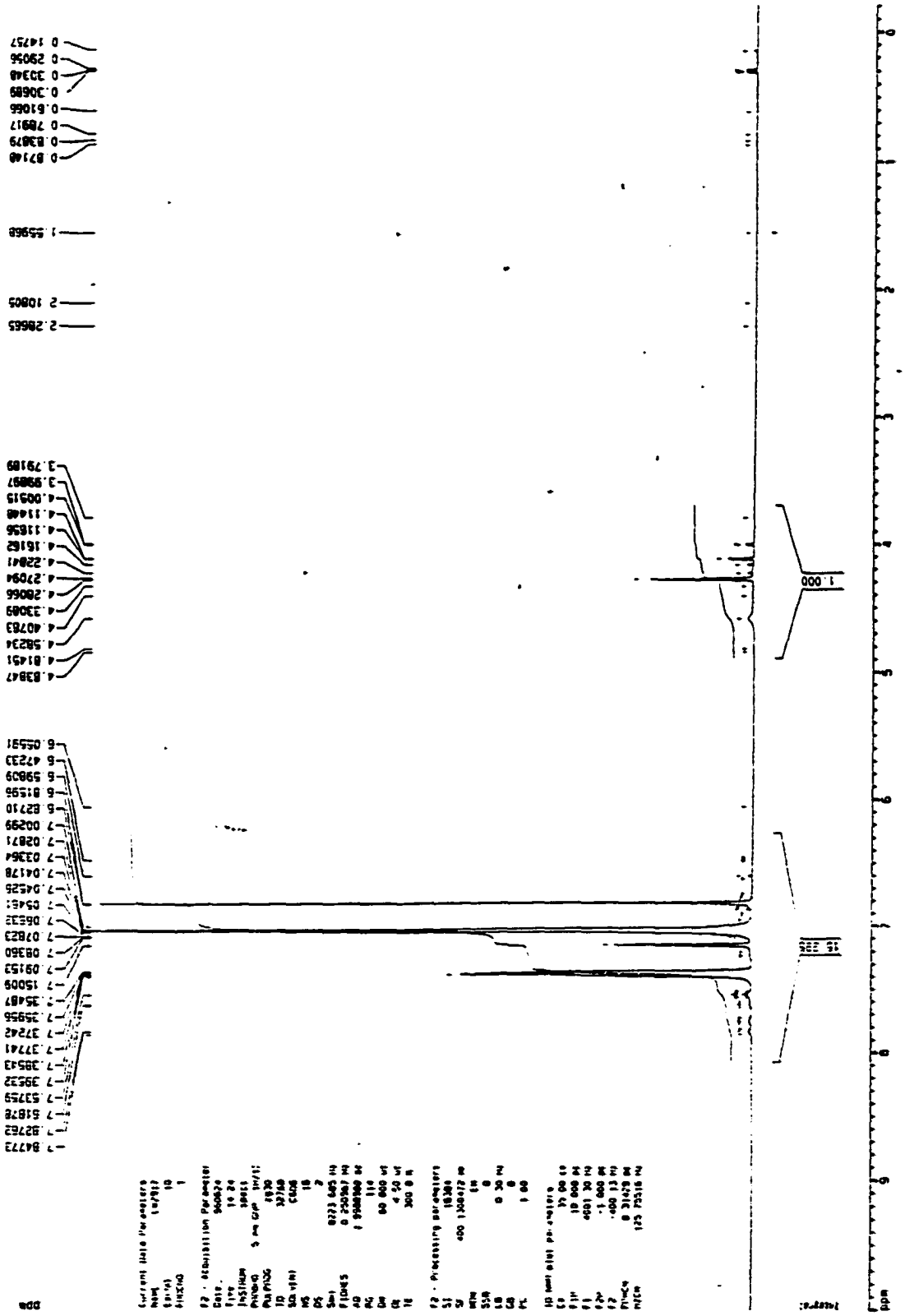

Figure 4-8. Reaction of (7) + PPh_3 (0.19 M) at 50 °C for 6 hours. ^1H NMR (C_6D_6)

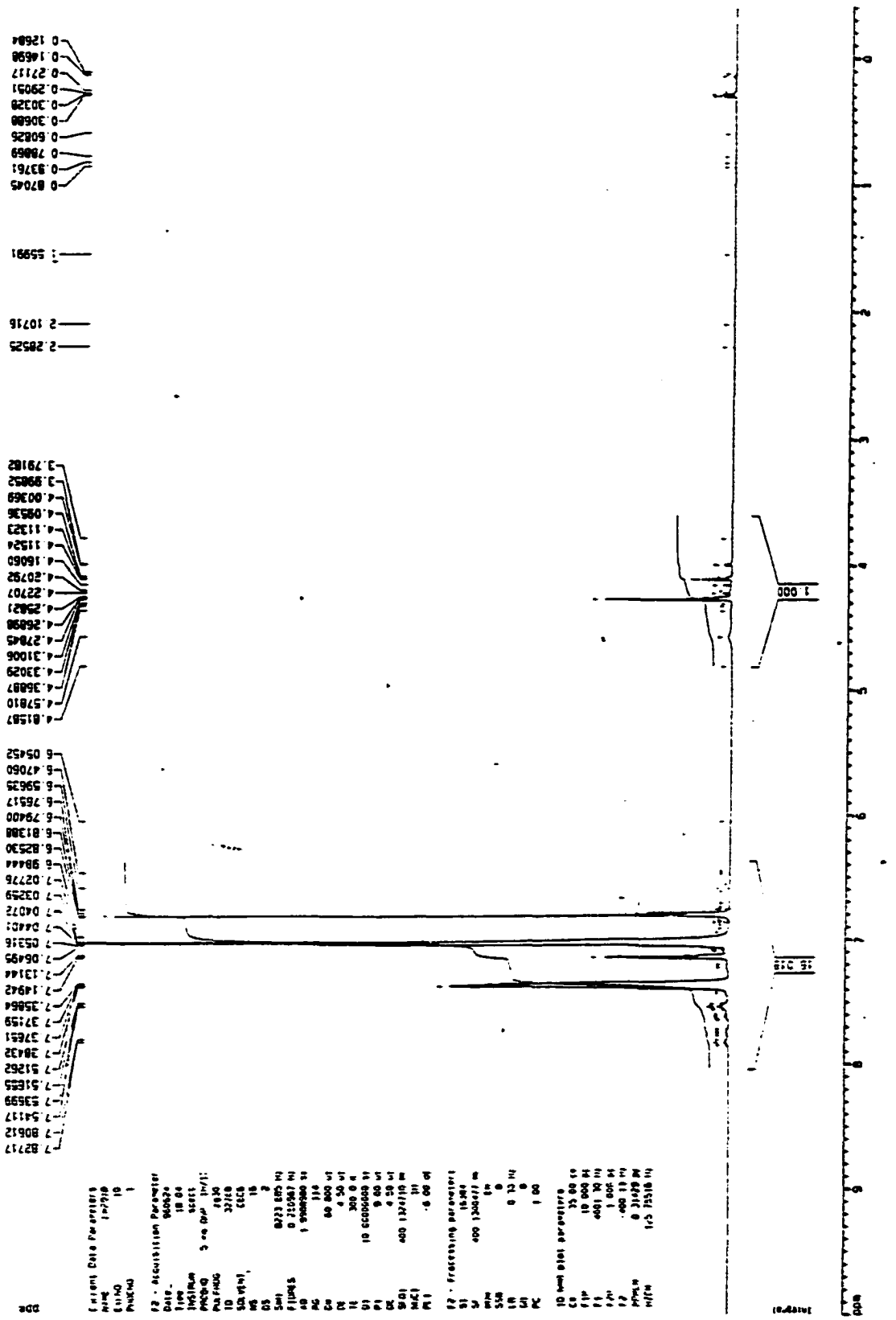

Figure 4-9. Reaction of (7) + PPh_3 (0.19 M) at 50 °C for 8 hours. ^1H NMR (C_6D_6)

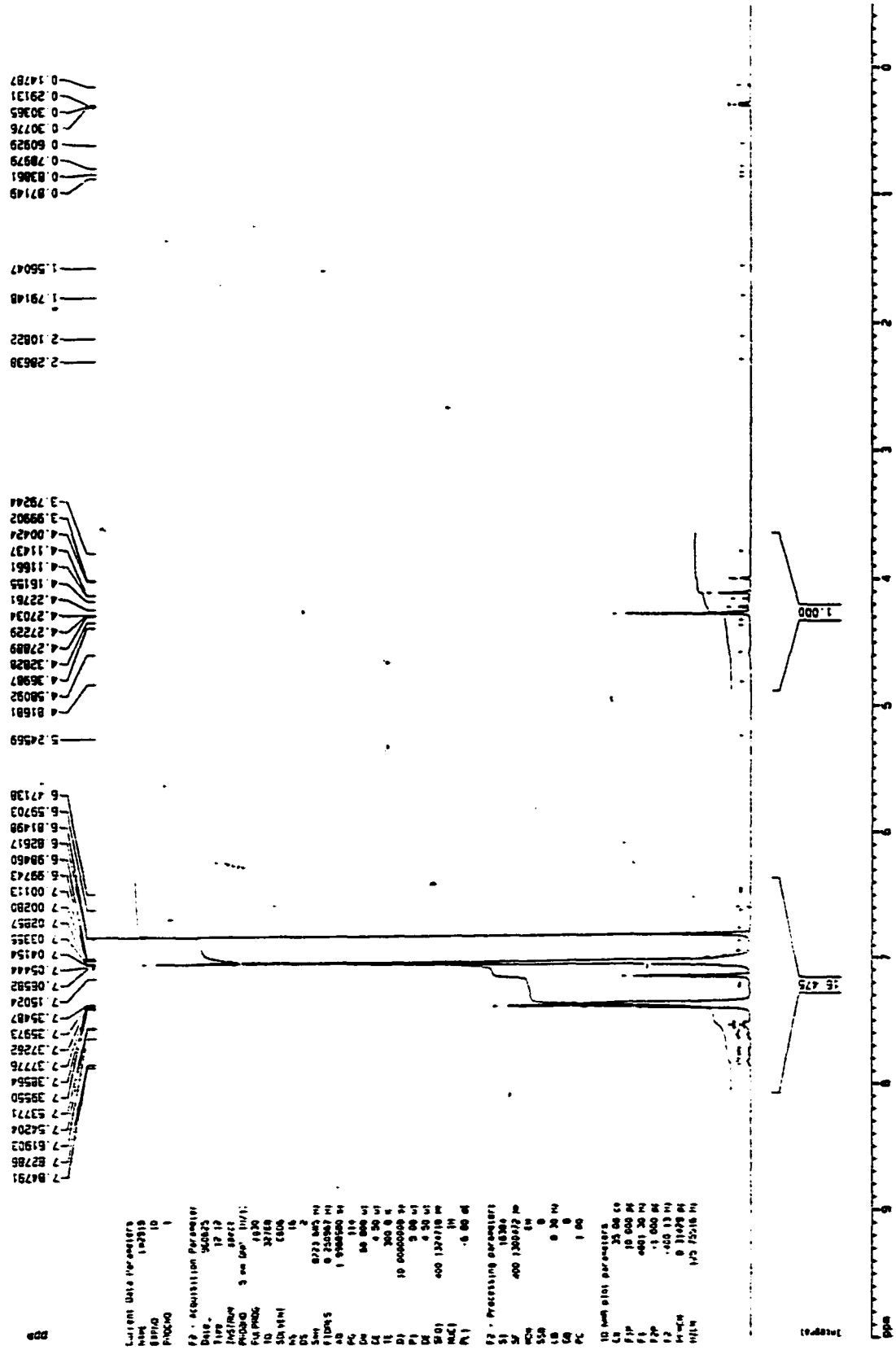

Figure 4-10. Reaction of (7) + PPh_3 (0.19 M) at 50 °C for 12 hours. ^1H NMR (C_6D_6)

Figure 4-11. Reaction of (7) + PPh_3 (0.19 M) at beginning, 20 °C. ^{31}P NMR (C_6D_6)

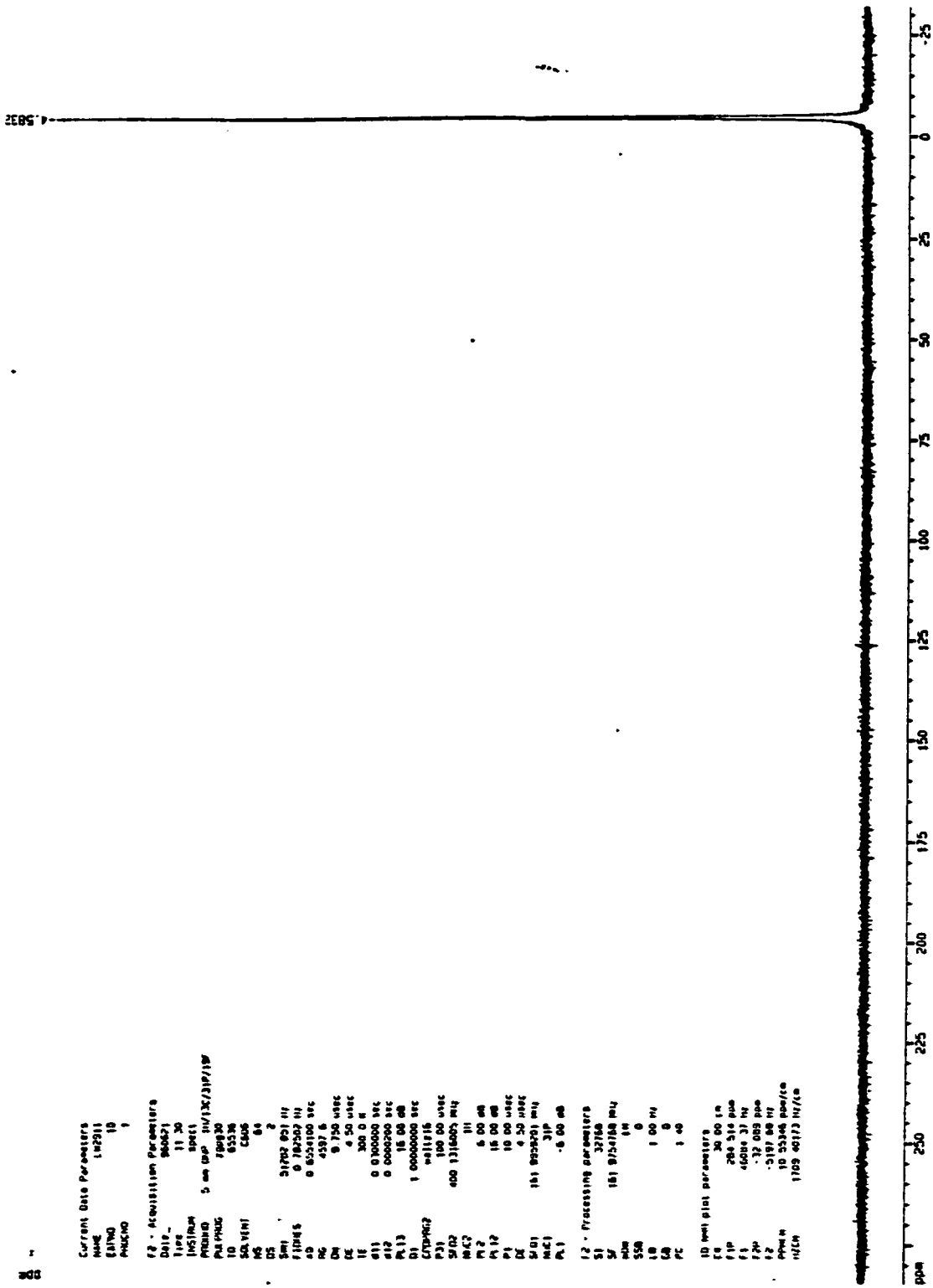

Figure 4-12. Reaction of (7) + PPh_3 (0.19 M) at 50 °C for 30 min. ^{31}P NMR (C_6D_6)

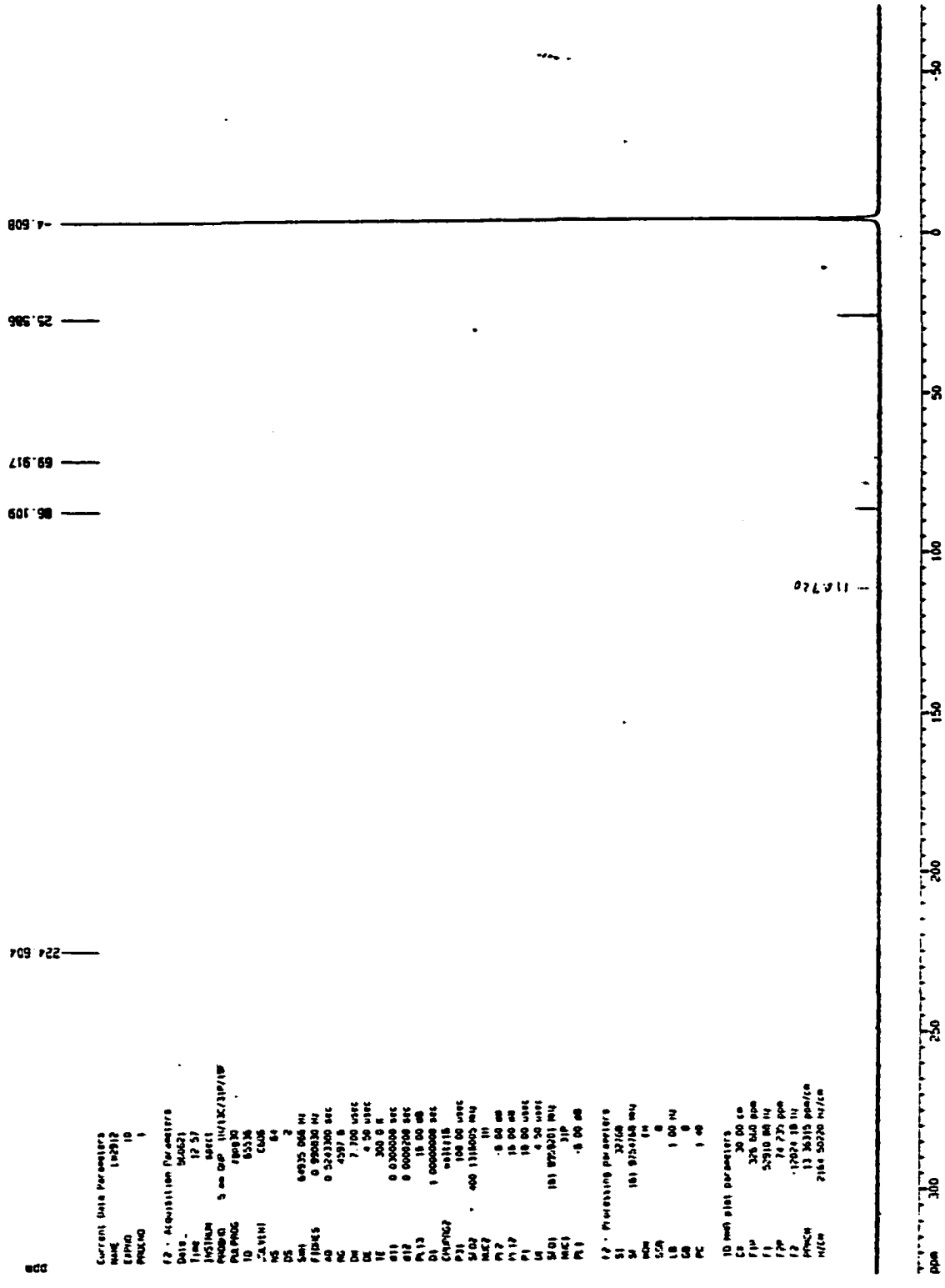

Figure 4-13. Reaction of (7) + PPh_3 (0.19 M) at 50 °C for 1 hour. ^{31}P NMR (C_6D_6)

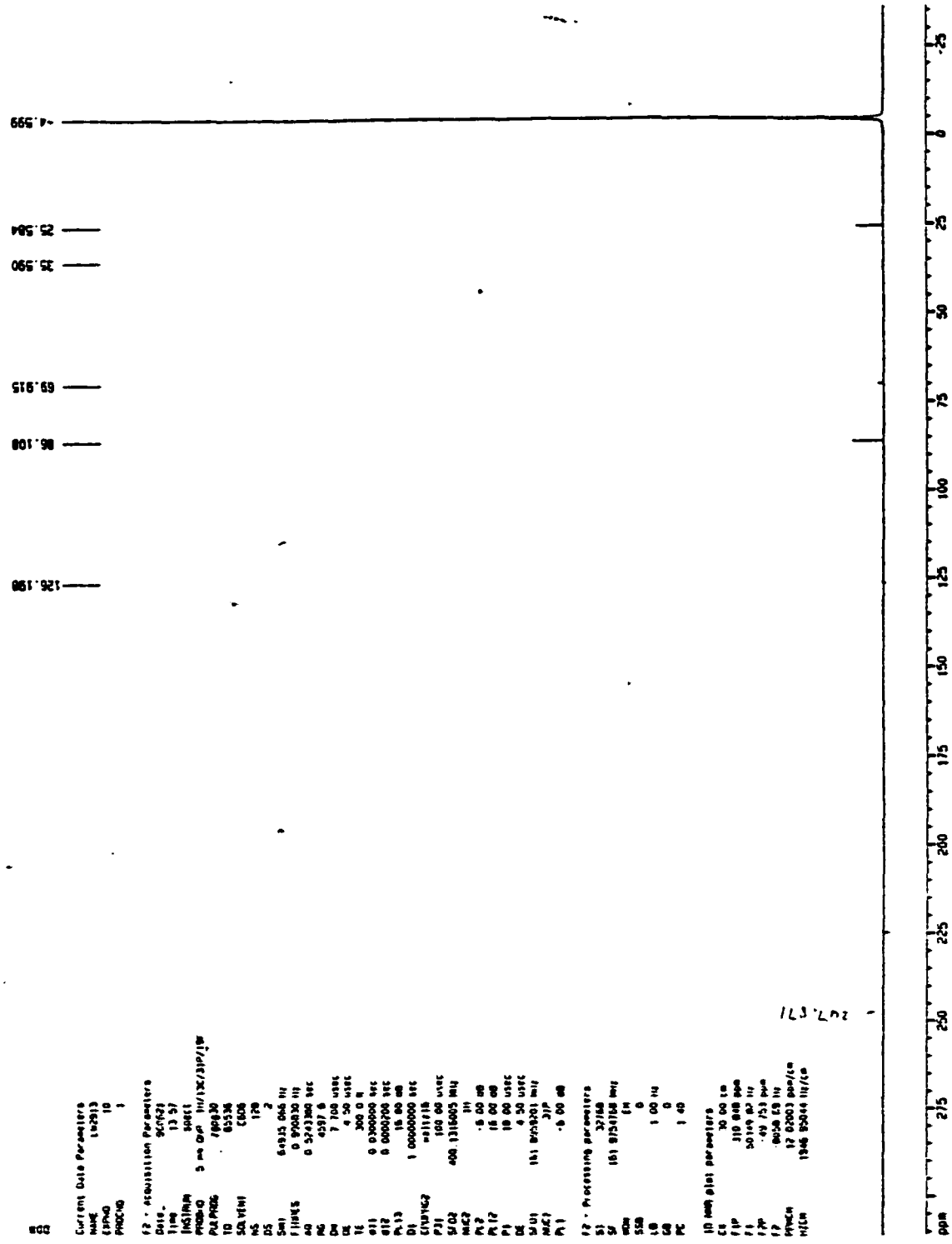

Figure 4-14. Reaction of (7) + PPh_3 (0.19 M)at 50 °C for 1.5 hour. ^{31}P NMR (C_6D_6)

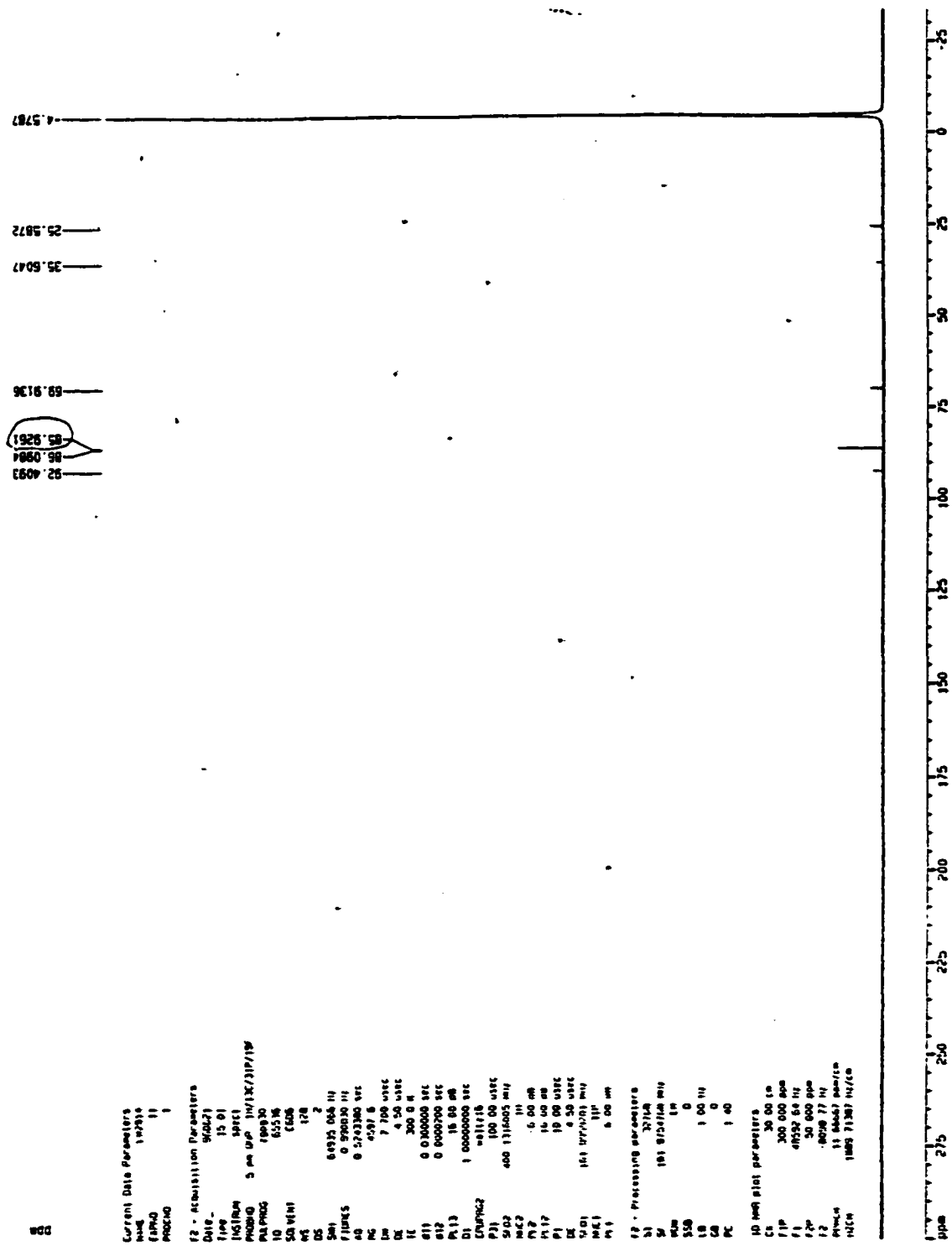

Figure 4-15. Reaction of (7) + PPh_3 (0.19 M) at 50 °C for 2 hours. ^{31}P NMR (C_6D_6)

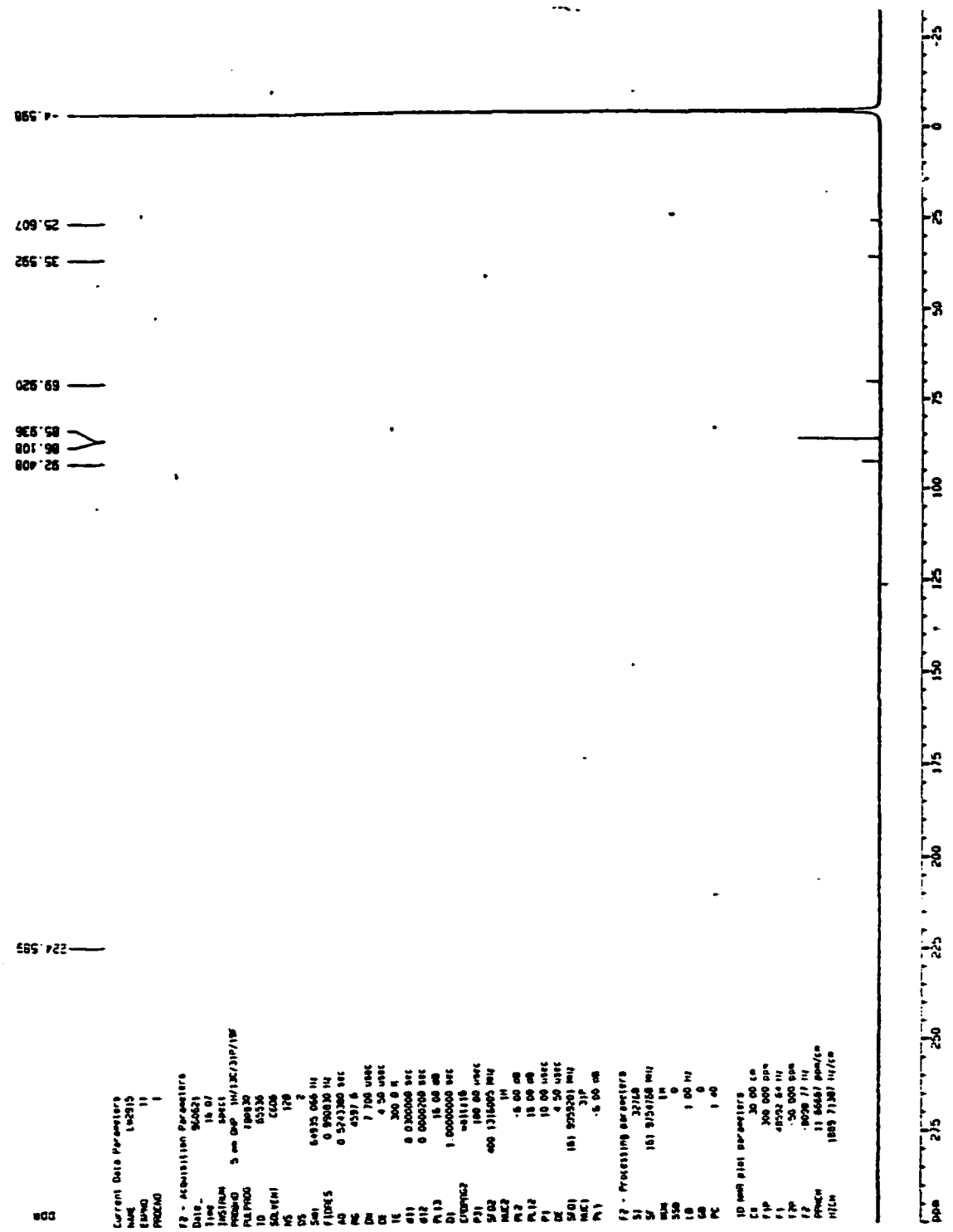

Figure 4-16. Reaction of (7) + PPh_3 (0.19 M) at 50 °C for 3 hours. ^{31}P NMR (C_6D_6)

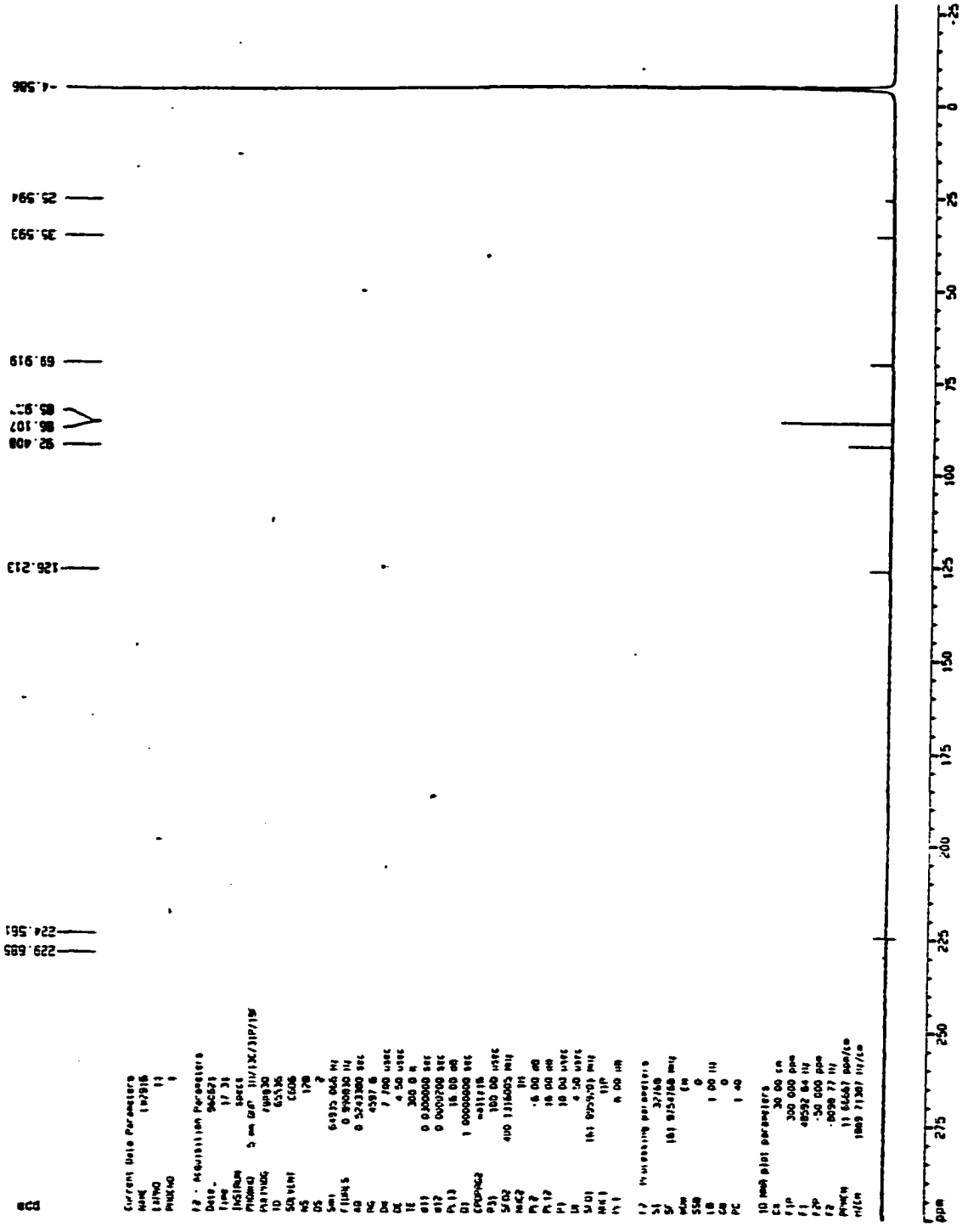

Figure 4-17. Reaction of (7) + PPh_3 (0.19 M) at 50 °C for 4 hours. ^{31}P NMR (C_6D_6)

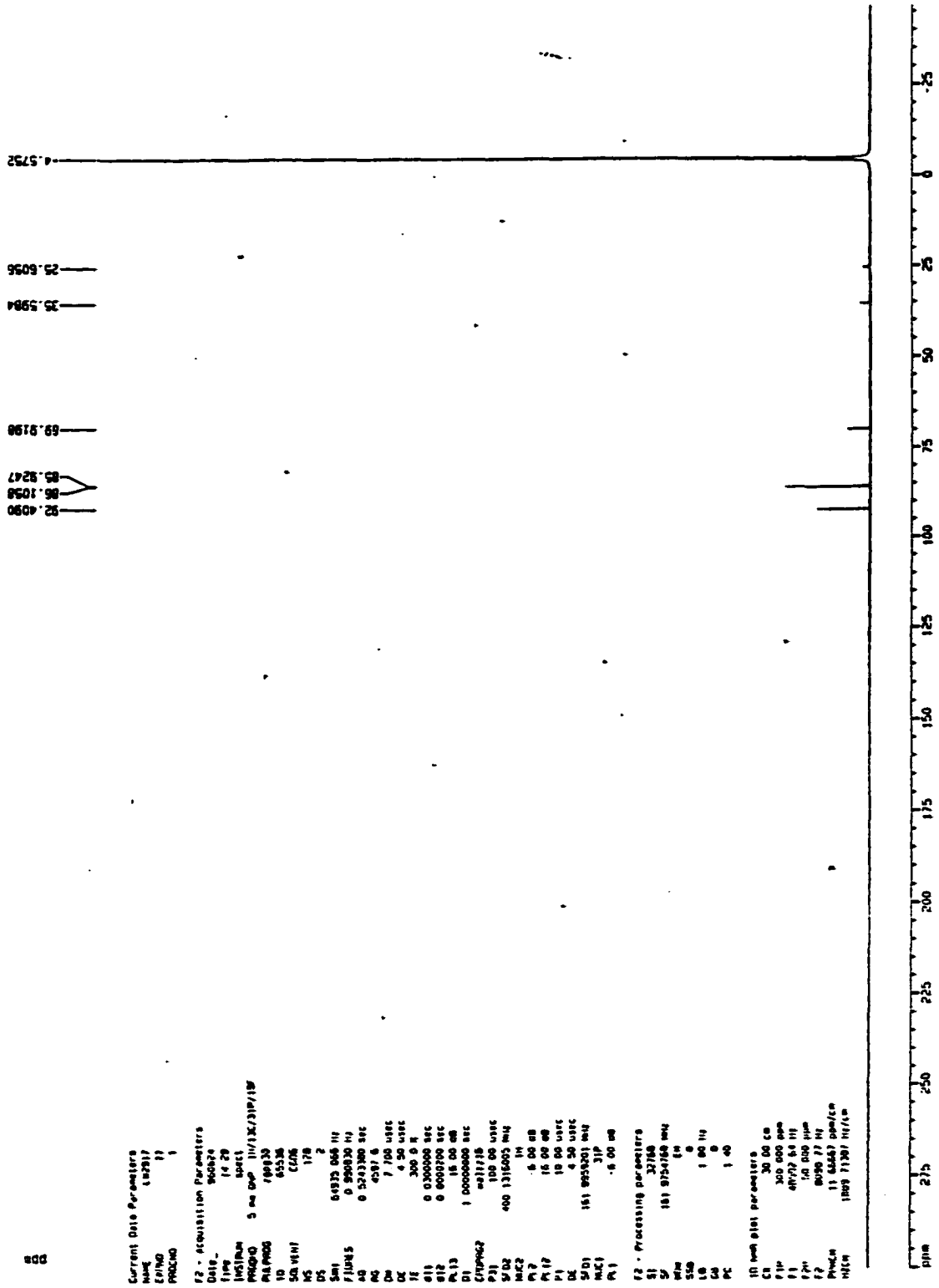

Figure 4-18. Reaction of (7) + PPh_3 (0.19 M) at 50 °C for 6 hours. ^{31}P NMR (C_6D_6)

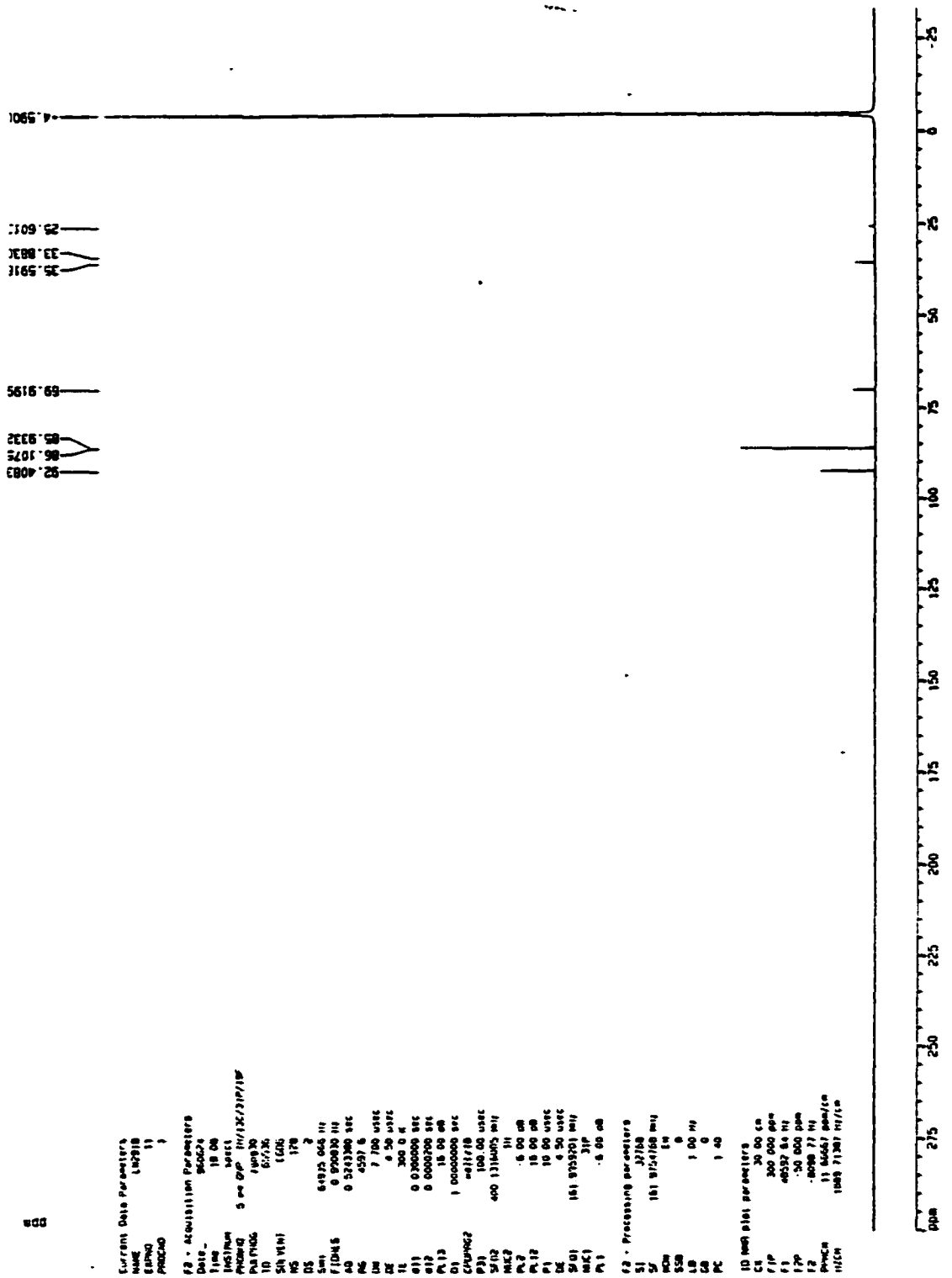

Figure 4-19. Reaction of (7) + PPh_3 (0.19 M) at 50 °C for 8 hours. ^{31}P NMR (C_6D_6)

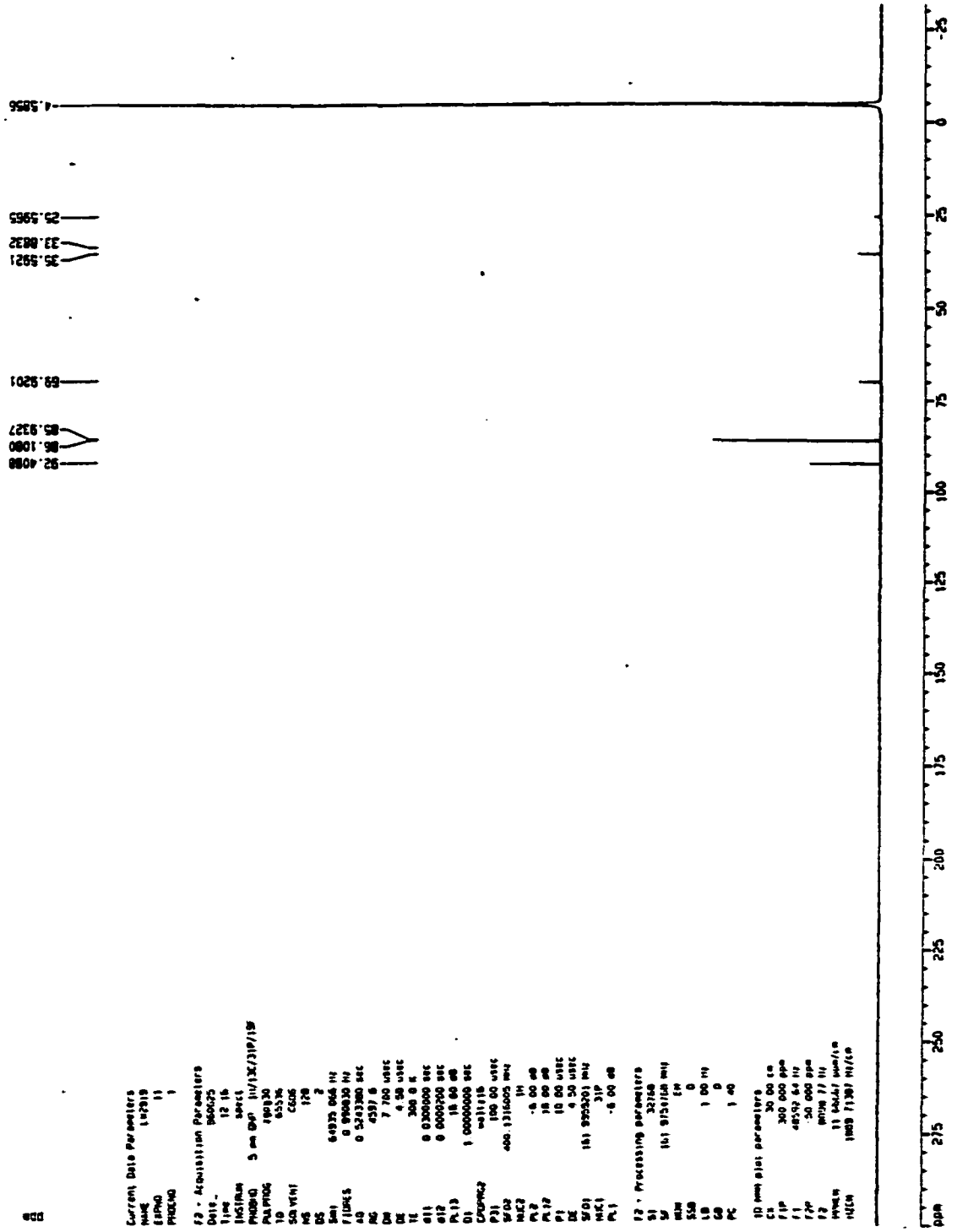

Figure 4-20. Reaction of (7) + PPh_3 (0.19 M) at 50 °C for 12 hours. ^{31}P NMR (C_6D_6)

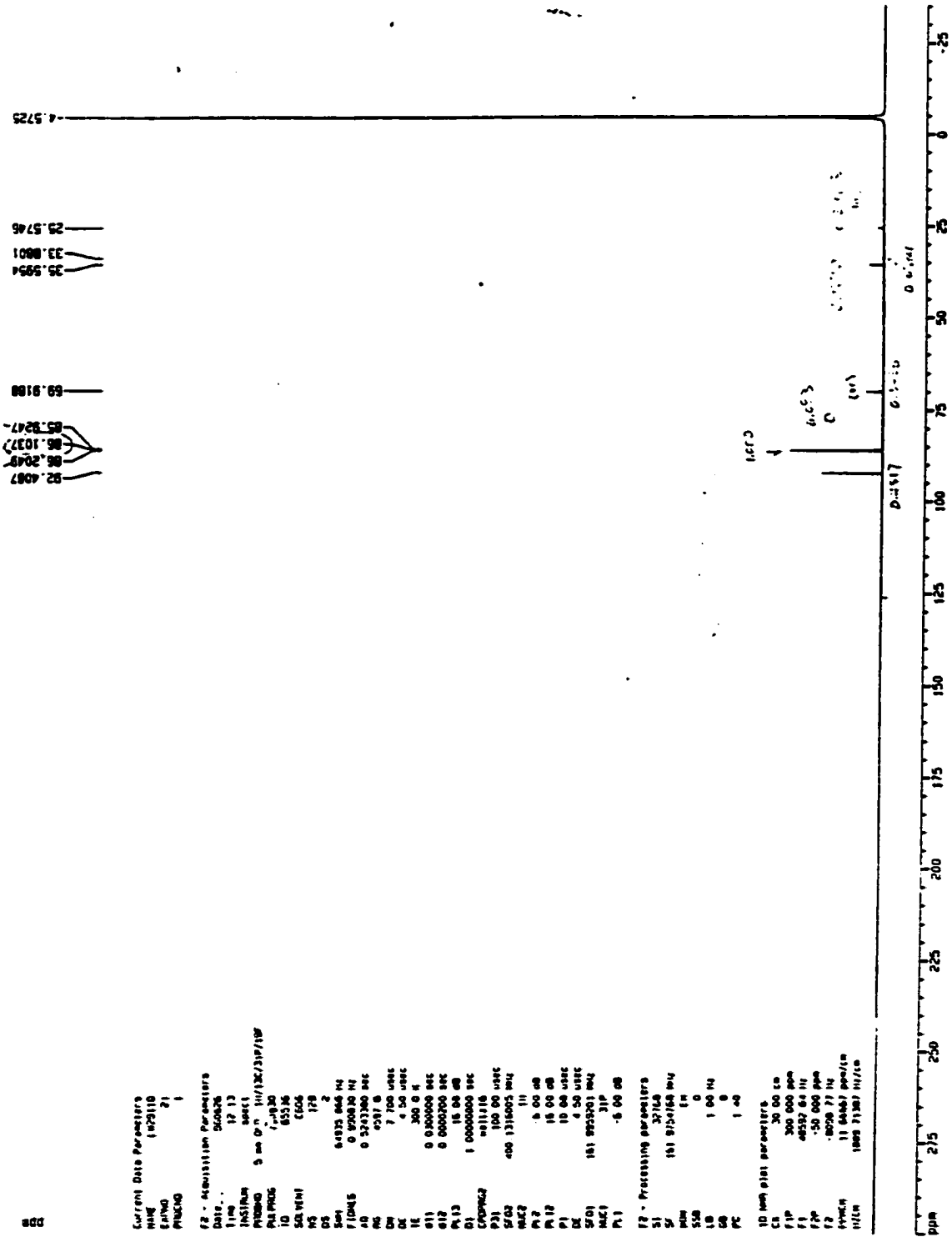

Figure 5-1. Mixture of $(C_6H_6)Cr(CO)_3$ + PPh_3 (0.40 M) at 50 °C for 14 hours. ^1H NMR (C_6D_6)

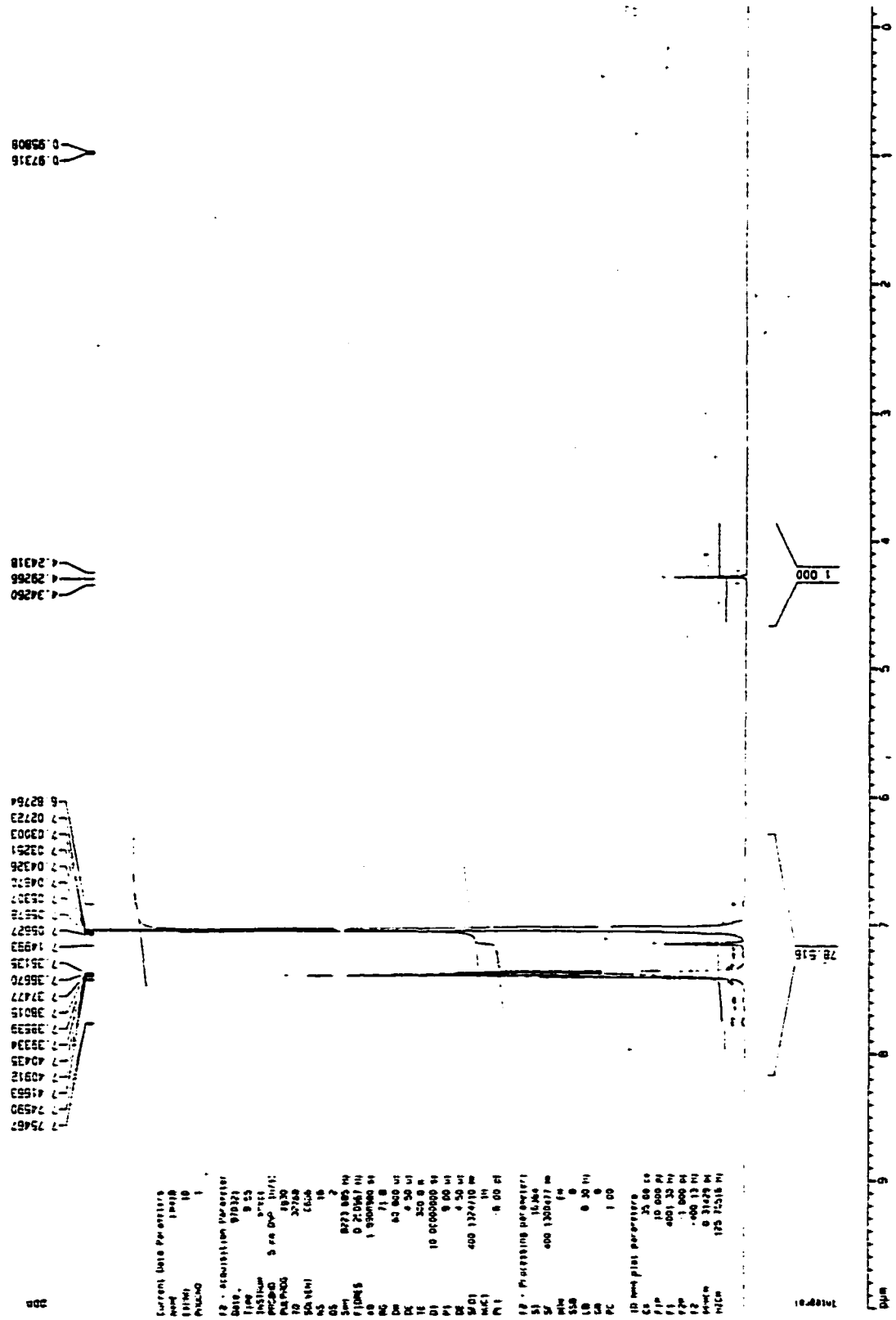

Figure 5-2. Mixture of $(C_6H_6)Cr(CO)_3$ + PPh_3 (0.40 M) at 50 °C for 14 hours. ^{31}P NMR (C_6D_6)

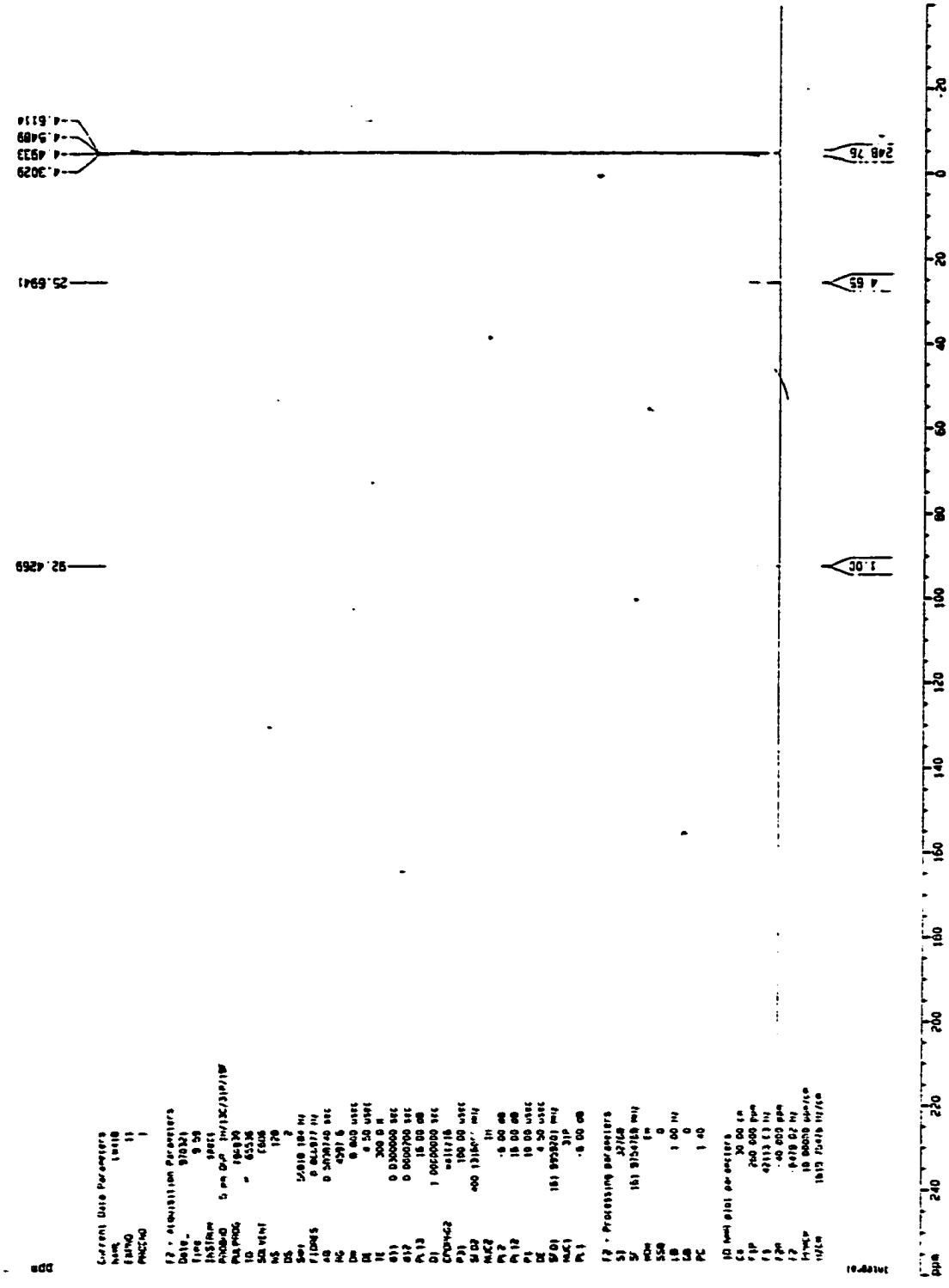

Figure 5-3. Mixture of $(C_6H_6)Cr(CO)_3$ + PPh_3 (0.40 M) at 50 °C for 14 hours. ^{13}C NMR (C_6D_6)

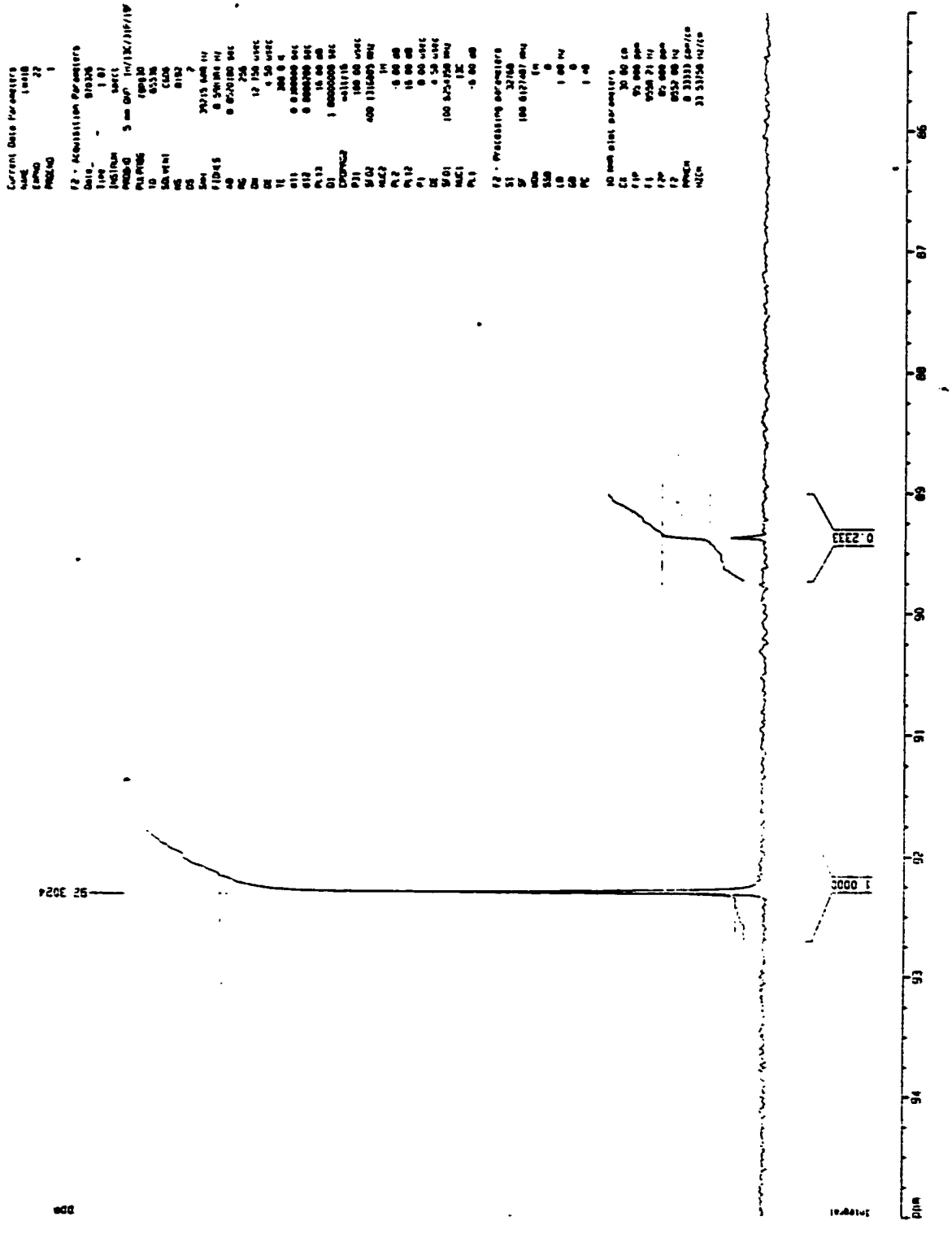

Part 2

Investigation of a New Class of Electron-withdrawing Phosphorus Ligands in Rhodium Catalyzed Hydroformylation

I. Introduction

Hydroformylation is one of the most important homogeneously catalyzed reactions in industry, producing annually over 5 million tons of linear aldehydes and alcohols (eq 1).[1]

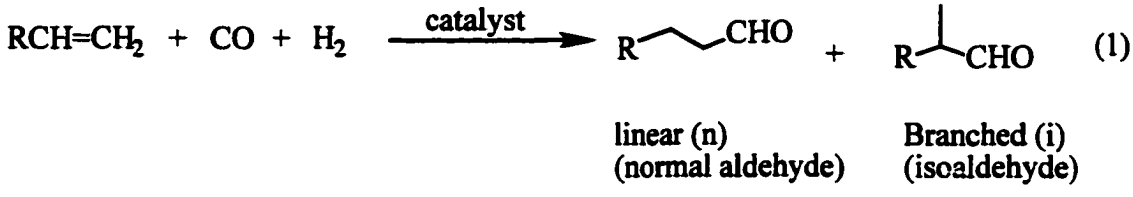

Major uses for these linear chemicals include industrial solvents and incorporation into plasticizers and detergents. Asymmetric hydroformylation holds equal interest, since the optically pure aldehydes can serve as starting materials for the synthesis of pharmaceuticals.[2] (eq 2)

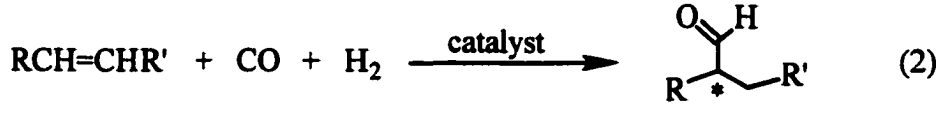

The catalyst systems involve transition metals such as Rh, Co, Pt[3] and Ru[4] and a variety of phosphine and phosphite ligands.[5] Among the metals, cobalt was used in industry but has now been replaced by rhodium; other metals are still in the research stage.

When industrial hydroformylation was first introduced in the 1940's cobalt catalysts were used initially. General conditions[6] were 150-180 °C

and 200-400 atm. $HCo(CO)_4$ was the actual catalytic species. The cobalt-catalyzed process was beset with several difficulties. The ratio of normal aldehyde to isoaldehyde (n/i; see eq 1) was low and only little control could be exercised over the regiochemistry. Cobalt hydrido tetracarbonyl was a volatile, unstable complex that was difficult to separate from the products and recycle into the system. The high temperatures promoted the formation of by-products such as alcohols and aldol condensation products. The alcohols formed acetals with the aldehydes and complicated the separation schemes.

These deficiencies have been greatly improved by the use of rhodium as a catalyst with phosphine ligands, such as PPh_3. For instance, a cobalt catalyst[6] (Scheme I) at 180 °C and 340 atm of CO/H_2 conditions gives an n/i ratio of 2.5. A rhodium catalyst without phosphine modifiers operates at 130 °C and much lower pressure, 14 atm, but favors the branched aldehyde. The rhodium catalyst with excess PPh_3 produces an n/i ratio of 15 under very mild conditions (110 °C and 7 atm). In addition, Rh is 1,000 to 10,000 times more reactive than Co[5], allowing much smaller amounts of Rh to be used. This is an important consideration, given the high cost of this metal. These features resulted in the adoption of modified rhodium catalysts in the

industry in 1976 by Union Carbide and now rhodium dominates in the commercial hydroformylation process. Due to the high cost of rhodium and

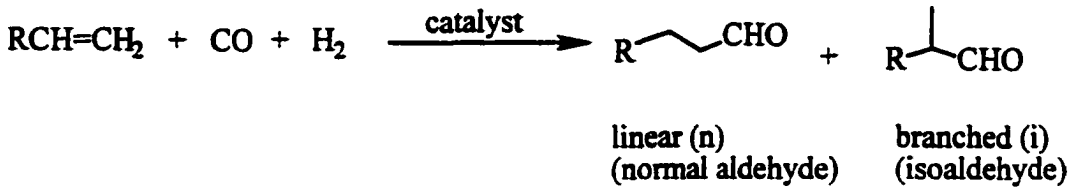

linear (n) (normal aldehyde) branched (i) (isoaldehyde)

Cobalt:	180 °C, 340 atm.	n/i = 2.5
Rhodium:	130 °C, 14 atm.	n/i = 1/3
Rh + PPh_3(1:100)	110 °C, 7 atm.	n/i = 15

Scheme I

a desire for perfect selectivity and even milder conditions, research on this process continued unabated in the nineties.

Early research focused on the steps of the catalytic cycle as well as the electronic and steric effects of the phosphorus ligands on rate and regioselectivity.[5,7] The generally accepted catalytic mechanism is that proposed by Wilkinson[8] 30 years ago.

The starting catalyst, **1**, in Scheme II is generated *in situ*. It loses one CO to form the 16-electron intermediate, **2**. Alkene coordination is followed by H migration (so-called "alkene insertion") to either one of the two sp^2 carbons of **3** to form the four-coordinate alkyl rhodium, **4** (linear insertion) and **4'** (branched insertion). Coordination of a CO ligand to **4** to give **5**,

followed by the migration of the alkyl group to CO gives a 16-electron acyl rhodium intermediate. Oxidative addition of H_2 produces a 6-coordinate rhodium species that undergoes reductive elimination of a hydrogen atom and acyl group to release the aldehyde and regenerate intermediate **2**.

In general stronger donor and bulkier monodentate ligands give slower rates and a smaller n/i ratio.[7] For instance, under one reported set of reaction conditions for hydroformylation of 1-octene, the acceptor ligand, $(n\text{-BuO})_3P$, was about four times faster than the donor ligand, PBu_3; the n/i ratios for $(n\text{-BuO})_3P$ and PBu_3 were 4.3 and 2.4, respectively. The $(p\text{-PhC}_6H_4)_3P$ ligand was 1.4 times faster than the bulkier ligand, $(o\text{-PhC}_6H_4)_3P$; the n/i ratios for $(p\text{-PhC}_6H_4)_3P$ and $(o\text{-PhC}_6H_4)_3P$ were 5.7 and 1.1, respectively.[7] However, addition of an excess of a monodentate ligand typically increases the rate and gives higher selectivity for the linear aldehyde.[7,9] It has been suggested that this arises as a result of keeping the Rh complexes in solution with two[9] or more[7] coordinated phosphine ligands [i.e., $HRh(CO)_2(PPh_3)_2$ or $HRh(CO)(PPh_3)_3$] under the reaction conditions.

However, bidentate phosphine ligands behave quite differently from the monodentate ligands. Stoichiometric amounts of chelating ligands are

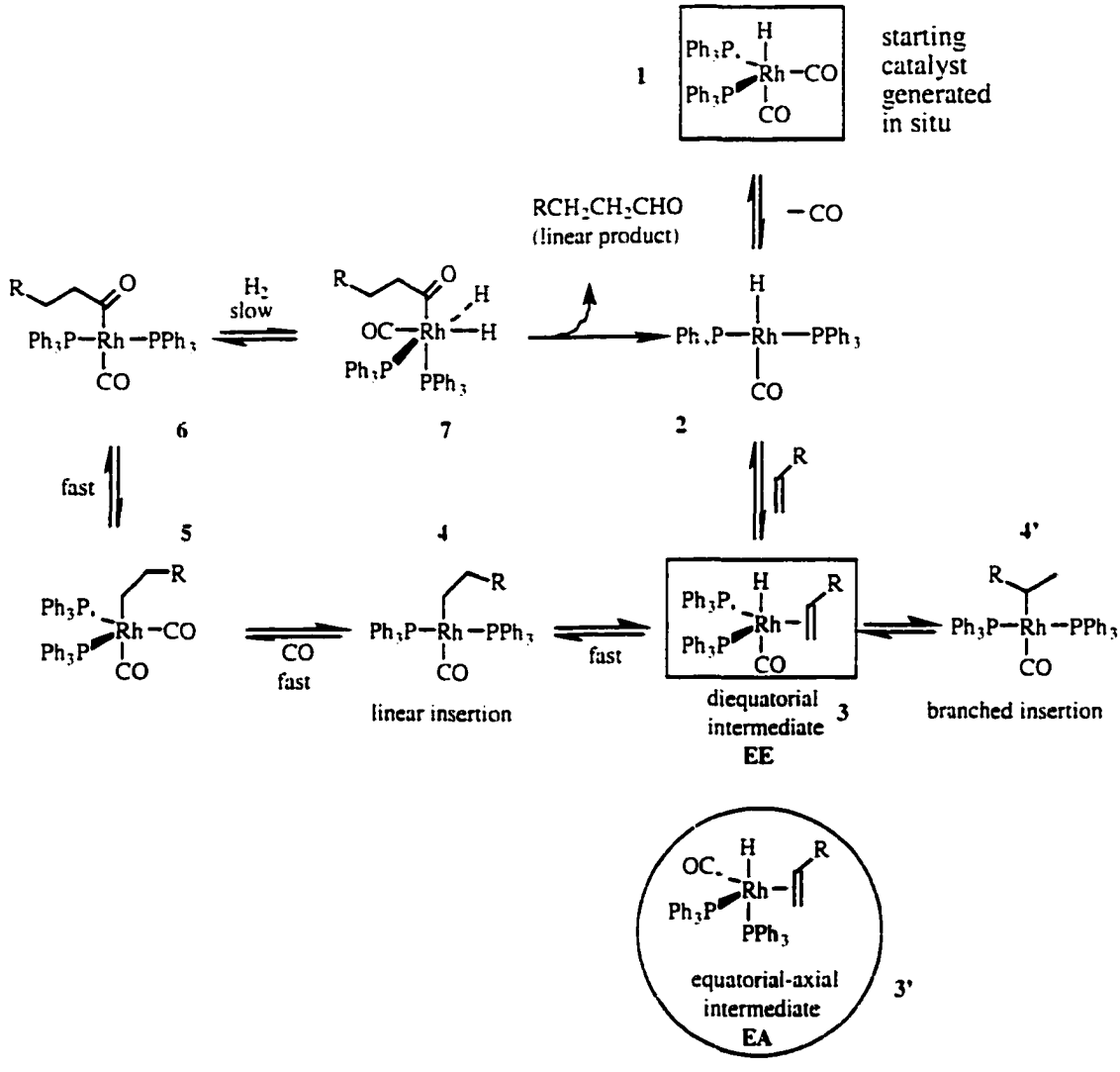

Scheme II

enough to achieve high selectivity for the linear aldehyde.[10] Recent results have revealed that a bulky chelating phosphite gives exceptionally high n/i ratios,[11,12] as can certain bidentate chelating phosphines (Scheme III).[13,14] The explanation for this high regioselectivity proposed by Casey[13] in 1992

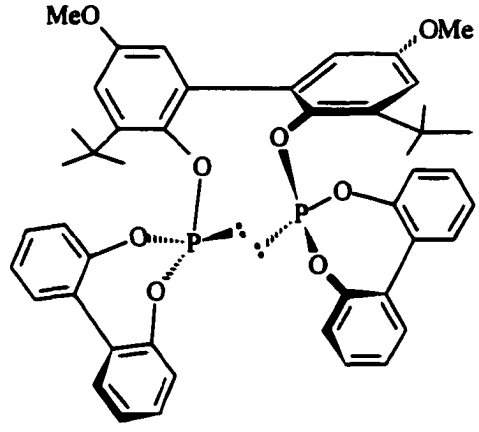

n/i > 40 for

References 11, 12.

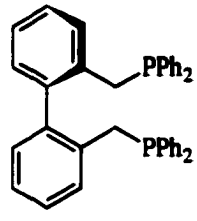

BISBI

n/i = 66.5 for 1-hexene

Reference 13

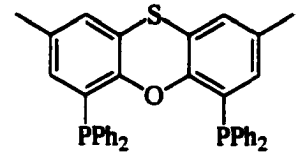

Thixantphos

n/i = 40.5 for 1-octene

Reference 14

Scheme III

involves the geometry of the intermediate **3** or **3'** where alkene insertion occurs to give the linear or branched product. As shown in Scheme II, the

two coordinated phosphorus atoms may occupy either the two equatorial sites (the **EE** intermediate **3**, ∠P-Rh-P = 120°) or the equatorial and axial sites (the **EA** intermediate **3'**, ∠P-Rh-P = 90°). Casey defined the "natural bite angle" as the preferred P-Rh-P chelation angle calculated using molecular mechanics and determined only by ligand backbone constraints and not by metal valence angles.[13] In a catalyst, the chelating ligand would prefer one geometry or the other because of its natural bite angle. Casey chose several bidentate phosphines to study, having similar electronic properties and natural bite angles from 112.6° to 84.5° (Scheme IV). It was

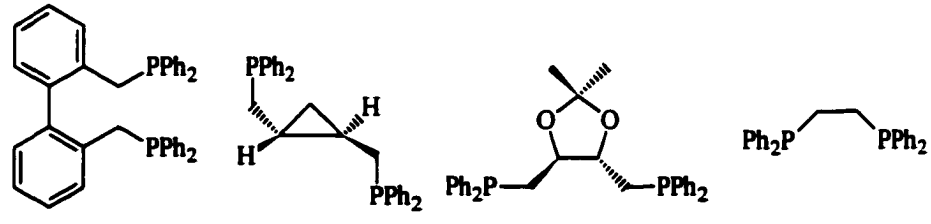

	BISBI	T-BDCP	DIOP	DIPHOS
Calculated bite angles:	112.6°	106.6°	102.2°	84.5°
n/i:	66.5	12	8.5	2.1

Scheme IV: Natural bite angle of some ligands

found that the large bite angle ligands favored the straight chain aldehydes, presumably via the **EE** intermediate.[13,14] The reasons for the increased regioselectivity of hydroformylation seen for chelates with large natural bite angles remain unknown. For instance, the working hypothesis can be that

the **EE** intermediate gives the linear aldehyde while the **EA** gives branched, but this is not strictly necessary since one intermediate could give different products depending on the nature of the chelating ligand bite angle. Of course, there is also no simple explanation for why the **EE** intermediate should give the linear aldehyde and the **EA** the branched.

In addition, when calculating the natural bite angle, other ligands on rhodium are ignored and the range of the angle, or flexibility of the ligand, is unusually large.[13] For example, while the published natural bite angle of BISBI listed in Scheme IV is 112.6°, in fact the angle can range from 92° to 155° with less than 3 kcal/mol of additional strain energy,[13] making the four significant figure precision doubtful at best. This range would overlap those of the other ligands listed in Scheme IV, and so there is no requirement that the **EE** intermediate forms exclusively for the "large" bite-angle ligand. Nonetheless, for the ligands described to date, a correlation of natural bite angle with n/i selectivity is apparent, and the bite angle idea, if not the precise value, represents a significant advance in understanding the hydroformylation reaction.

Given similar steric bulkiness, π-acceptor ligands are superior to σ-donors. Unruh and Christenson[15] studied the regioselectivity of rhodium catalyzed hydroformylation of 1-hexene using a series of 1,1'-

bis(diarylphosphino)ferrocene ligands, which were presumed to coordinate diequatorially. They found a strong correlation between selectivity for linear aldehyde formation and the electron withdrawing ability of the aryl substituents, with stronger π-acceptors giving higher n/i ratios. Casey's group[16,17] also found enhancement for the selectivity to the linear aldehyde when each phenyl group of the BISBI ligand in Scheme III was replaced with the electron-withdrawing arene group, [3,5-$(CF_3)C_6H_3$].

A class of phosphorus ligands that possess π-acceptor ability significantly greater than that of phosphites and approaching that of CO are fluoroalkyl phosphines, such as $(CF_3)_2P(CH_2)_nP(CF_3)_2$. However, the syntheses of these ligands are generally multistep and often involve $(Rf)_2PP(Rf)_2$ precursors (Rf = fluoroalkyl group) that are not readily available. Another approach was described recently by Moloy[18] (at that time from Union Carbide), which details synthetic work on the new electron-withdrawing ligands, $(pyrrolyl)_{3-x}PPh_x$ (x = 0-2), and their complexes with rhodium. However, he did not publish hydroformylation results while another research group[19] did for hydroformylation of 1-hexene using these ligands and found an n/i ratio of 31 at best using the $[P(NC_4H_4)_3]$ ligand with a molar ratio (P to Rh) of 4.1 at 40 °C.

At the same time as Moloy reported his (pyrrolyl)$_{3-x}$PPh$_x$ ligands, another type of electron-withdrawing ligand had been synthesized in our lab,[20] namely 2-phenyl-1,3-di-*p*-toluenesulfonyl-1,3,2-diazaphospholidine (**TosL**) and *N, N'*-bis(diphenylphosphino)-*N, N'*-di-*p*-toluenesulfonyl-1,2-ethanediamine (**diTosL**). The phosphorus atom is attached to one or two strongly electron-withdrawing sulfonamido groups. On the basis of IR studies of tungsten carbonyl complexes, they are comparable to phosphites in π-acidity but worse σ-donors than both phosphines and phosphites,[20] providing an interesting hydroformylation study.

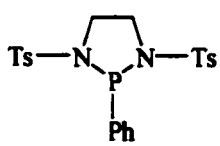

TosL

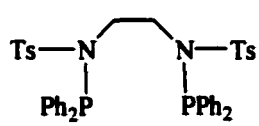

diTosL

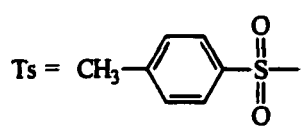

I will report in this thesis the results of hydroformylation using these ligands, as well as the syntheses of **diTosL** analogs and chelate analogs of **TosL** and their application to hydroformylation. These results will show that for these aminophosphines, (1) chelation is necessary for effective catalysis, (2) the electron-withdrawing sulfonyl moiety is far superior to an electron-donating methyl group on nitrogen, (3) the N(Ts)PPh$_2$ moiety is surprisingly bulky, making syntheses of chelating analogs of **diTosL**

exceedingly difficult, and (4) syntheses of chelating analogs of TosL can be carried out but the resultant ligands are insoluble in most organic solvents and unsuitable for hydroformylation.

II. Results and Discussion

A. Synthesis of analogs of TosL and diTosL.

The phosphorus atom in **diTosL** is attached to one sulfonamido group while in **TosL** it is attached to two sulfonamido groups. In order to compare the hydroformylation results, we designed three new ligands: *N*-diphenylphosphino-*N*-ethyl-*p*-toluenesulfonamide (**dpet**); *P,P'*-1,4-butanediylbis(1,3-di-*p*-toluenesulfonyl-1,3,2-diazaphospholidine) (**BTosL**); and *P,P'*-1,2-ethanediylbis(1,3-di-*p*-toluenesulfonyl-1,3,2-diazaphospholidine) (**ETosL**). **Dpet** is a monodentate analog of **diTosL**. Ligands **BTosL** and **ETosL** (with butane and ethane moieties linking the phosphorus atoms) are chelating analogs of **TosL**. **BTosL** has a larger bite angle than **ETosL** and the same chelate ring-size as **diTosL**, and would be expected to favor linear aldehydes more than **ETsoL**.

The synthetic methods are outlined in equations 3, 4 and 5. In all cases a sulfonamide reacts with a chlorophosphine, and Et_3N is used to tie up the HCl formed. Although the sulfonamide is a relatively acidic compound, the nitrogen is nucleophilic enough to displace chloride from phosphorus. Reaction of the sulfonamide TsN(H)Et[21] with PPh_2Cl affords **dpet** in 40% yield (eq 3). For reactions (4) and (5), one equivalent of the sulfonamide reacts at one P site to form one ring; the second sulfonamide reacts at the

other site to give the second ring in 75% and 67% yields, respectively. Elemental analysis of **dpet**, **BTosL** and **ETosL** supports their formulas.

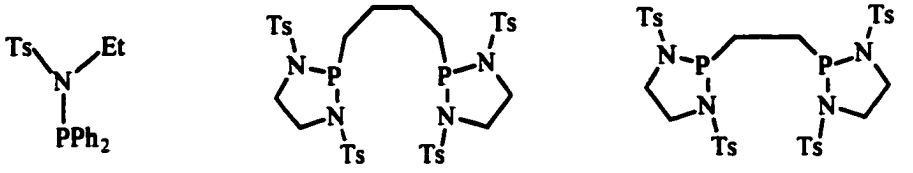

dpet **BTosL** **ETosL**

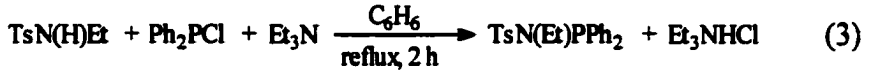

dpet

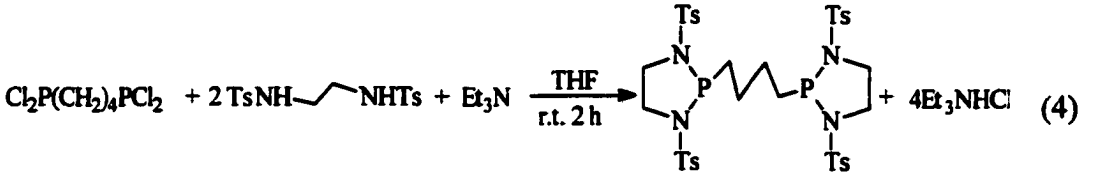

BTosL

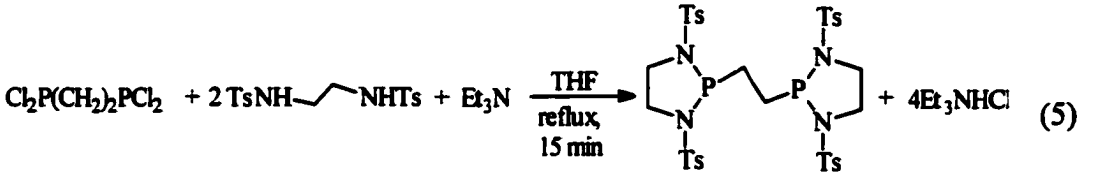

ETosL

Both **BTosL** and **ETosL** have peculiar solubility properties: they are insoluble in benzene, ether, THF, acetone, ethanol, or even nitromethane and acetonitrile, yet are slightly soluble in methylene chloride, DMF, and nitrobenzene, and less soluble in chloroform. When purified by

chromatography, they move very slowly on silica gel when eluted with methylene chloride by itself. Addition of a little acetonitrile or THF to methylene chloride, however, accelerates the movement dramatically, and results in separation from the sulfonamide.

While all of our evidence is consistent with the structure shown for **ETosL**, the alternative structure bicyclic **ETosL'** cannot be rejected. Both structures are symmetrical. While their NMR spectra would exhibit slightly different chemical shifts, the number of peaks and splitting patterns would

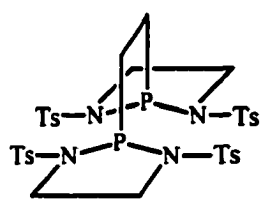

ETosL

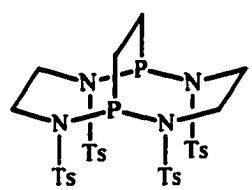

ETosL'

be the same. For instance, they both should have one ^{31}P signal, one ^{13}C signal for the four methylene groups bridging the nitrogen atoms and one ^{13}C signal exhibiting an AA'X pattern for the two methylene groups bridging both phosphorus atoms. Therefore, it is apparently impossible to tell which is which by NMR. Since **ETosL'** is not able to chelate a metal, it could be possible to distinguish them by reacting the product with a metal compound like *trans*-$BrW(CO)_4NO$[22,23] and/or with $(THF)W(CO)_5$[24] and testing the

NMR of the adduct. This characterization experiment remains untested. Nevertheless, we will assume for now that the **ETosL** structure is correct, since the cage structure of **ETosL'** makes its exclusive formation less likely.

During the synthesis of **BTosL**, another method was tested (eq 6) since a similar reaction was reported;[25] this would save one step since the tetrachloride in equation 4 is prepared from $(Et_2N)_2P(CH_2)_4P(NEt_2)_2$.

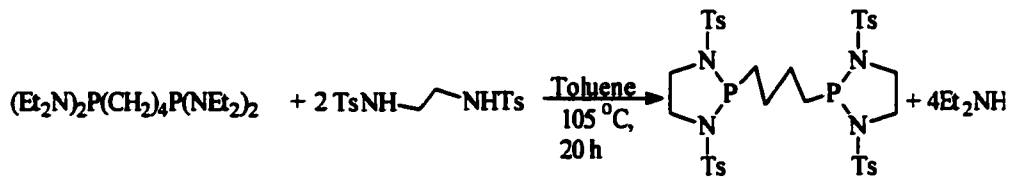

(6)

The sulfonamide and $(Et_2N)_2P(CH_2)_4P(NEt_2)_2$ in toluene were heated to 105 °C in a one-necked round-bottomed flask under nitrogen for 20 hours. It was found that about 25% of **BTosL** formed according to ^1H NMR, but the reaction was not clean enough to supercede the chloride displacement method.

B. Synthesis of 1,4-bis(dichlorophosphino)butane (BDB).

As mentioned before, **BDB** is used to prepare **BTosL**. The synthetic method for **BDB** is known, but since it involves several steps it is outlined in Scheme V.[26]

One starts with preparation of the di-Grignard reagent, $BrMg(CH_2)_4MgBr$, followed by addition of

bis(diethylamino)chlorophosphine, $(Et_2N)_2PCl$, at low temperature. Addition of 1,4-dioxane precipitates the salt and makes filtration much easier. The amino phosphine (**BBB**) is reacted with PCl_3 to afford 1,4-bis(dichlorophosphino)butane which is purified by vacuum distillation.

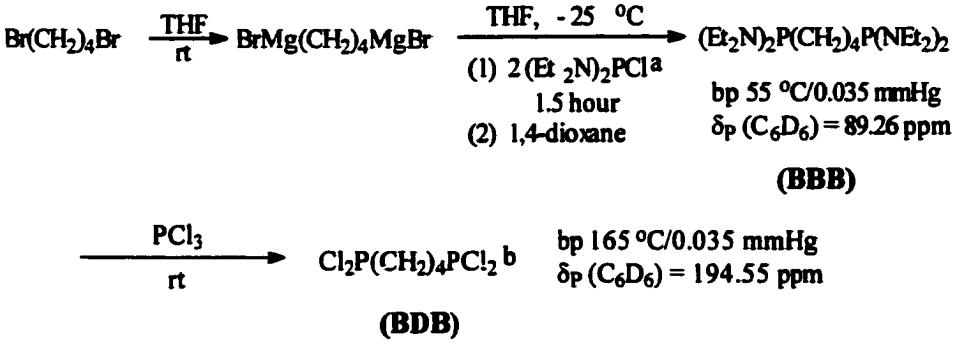

BBB: 1,4-Bis[bis(diethylamino)phosphino]butane

BDB: 1,4-Bis(dichlorophosphino)butane

a: [Chantrell, P.G.; Pearce, C.A.; Toyer, C.R.; Twaits, R. *J. Appl. Chem.* **1964**, 563]

b: [Diemert, K.; Kuchen, W.; Kutter, J. *Phosphorus and Sulfur* **1983**, 15, 155-164]

Scheme V

In order to shorten the synthesis of **BDB**, an alternative method involving direct incorporation of PCl_2 unit was tried (eq 7).

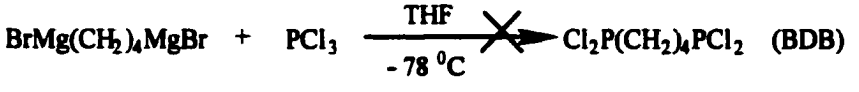

(7)

Under stirring, the di-Grignard reagent was added via a cannula (a long metal tube, like a long needle) to 20 equivalents of PCl_3 at -23 °C over a

one-hour period. Smoke formed during the addition of the di-Grignard reagent. After removing the cooling bath, the mixture was stirred for one more hour, and then fractionally distilled. However, nothing distilled over at 50 °C/0.05 torr and above, even when the flask was heated to 160 °C. It was thought that the reaction might take place too vigorously to form the desired compound. When the reaction was repeated once at - 78 °C, the same phenomenon was observed.

It was reported in literature[27] that the following reaction conditions worked for preparation of an alkyl dichlorophosphine (eq 8):

$$t\text{-BuMgCl} + PCl_3 \xrightarrow[\text{vigorous stirring}]{\text{ether, - 48 }^0\text{C, 2 h}} t\text{-BuPCl}_2 \qquad (8)$$

The filtered *t*-butylmagnesium chloride solution was added dropwise to a solution of 2.5 equivalents of PCl_3 in ether at - 48 °C for two hours. In the third trial, the filtered di-Grignard reagent solution was added to a solution of 5 equivalents of PCl_3 in THF at -78 °C for 2 hours. The mixture was warmed up to room temperature and the low boiling point components were removed in vacuo. The resultant liquid was tested by NMR in benzene-d_6. One minor peak at δ = 190 ppm was observed among tens of ^{31}P signals. That was not a clean reaction, and no further attempts were made.

C. Novel ^{13}C NMR Spectra of Diphosphorus Compounds.

It is interesting to look at the ^{13}C NMR spectra for **BTosL** and its starting materials, **BBB** and **BDB**, and for **ETosL** and its starting material, 1,2-bis(dichlorophosphino)ethane, $Cl_2PCH_2CH_2PCl_2$. The two middle carbons (C2 & C3 in the C4 linkers) that link both phosphorus atoms exhibit unusual NMR signals. For **BBB** and **BDB**, there are four lines in the spectrum. This results from an ABX spin system[28] (the two phosphorus atoms are A and B

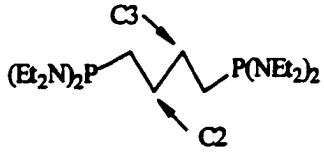

BBB

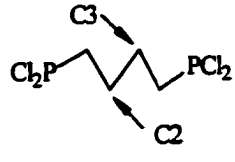

BDB

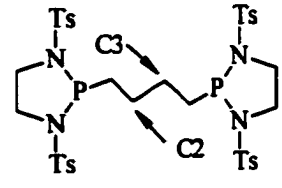

BTosL

nuclei and the carbon is X) since the two phosphorus atoms are chemically as well as magnetically nonequivalent due to the presence of only a single ^{13}C atom in the NMR-active isotopomer. That is, for instance, the NMR active **BDB**, $Cl_2PCH_2(^{13}CH_2)CH_2CH_2PCl_2$, is actually asymmetric, and so the P atoms are in different environment. The separation of lines one and four are equal to $^2J_{PC} + {}^3J_{PC}$ (that is, $J_{AX} + J_{BX}$ in the ABX system); $J_{PP'}$ is not equal to zero. With suitable parameters, the spectra (Figures 1, 2, 3) were calculated using the program, gNMR, and give excellent fits to the observed

spectra as seen. The calculated coupling constants are summarized in Table I.

There are three lines in the spectrum for **BTosL**. However, the middle line is broader than the other two. In **BBB** and **BDB**, the separation of the middle peaks is about equal to $\Delta\nu_{PP'}$, and as the $\Delta\nu_{PP'}$ value is decreased, the middle two lines as seen in **BBB** and **BDB** gradually coalesce, giving a three-line spectrum as seen in **BTosL**. In the above three cases, the small "wing" satellite peaks at ~ $\pm J_{PP'}$ were found to merge with the two observed outer peaks.

For the ethanediyl cases, four lines are also seen for the ^{13}C signal, but there is no clear evidence for ABX splitting. For $Cl_2PCH_2CH_2PCl_2$, a clean 1:1:1:1 doublet of doublets is most simply fit with $J_{PP'} = 0$, $J_{PC} = 50$ Hz and $J_{P'C} = 9$ Hz (Figure 4-1), although the 50 Hz coupling is admittedly unusual (Figures 4-2 and 4-3 are the ^{1}H and ^{31}P NMR spectra, respectively). For **ETosL**, the low-solubility has precluded our obtaining a high-quality ^{13}C NMR. The 4 lines that are clearly observed can be fit with $J_{PP'} = 0$, $J_{PC} = 41$ Hz and $J_{P'C} = 19$ Hz.

Table I. ^{13}C NMR data for diphosphines

Compound	δ (ppm)	Peak width (Hz)	$\Delta\nu_{PP'}$ (Hz)	$J_{PP'}$ (Hz)	$^2J_{PC}$ (Hz)	$^3J_{P'C}$ (Hz)
BBB	27.39	2.5	8.50	15.00	28.00	9.6
BDB	23.49	2.5	4.00	12.00	17.50	6.00
BTosL	23.93	2.5	1.65	14.50	22.00	7.00

Figure 1: Real and calculated ^{13}C NMR spectra for **BBB**.

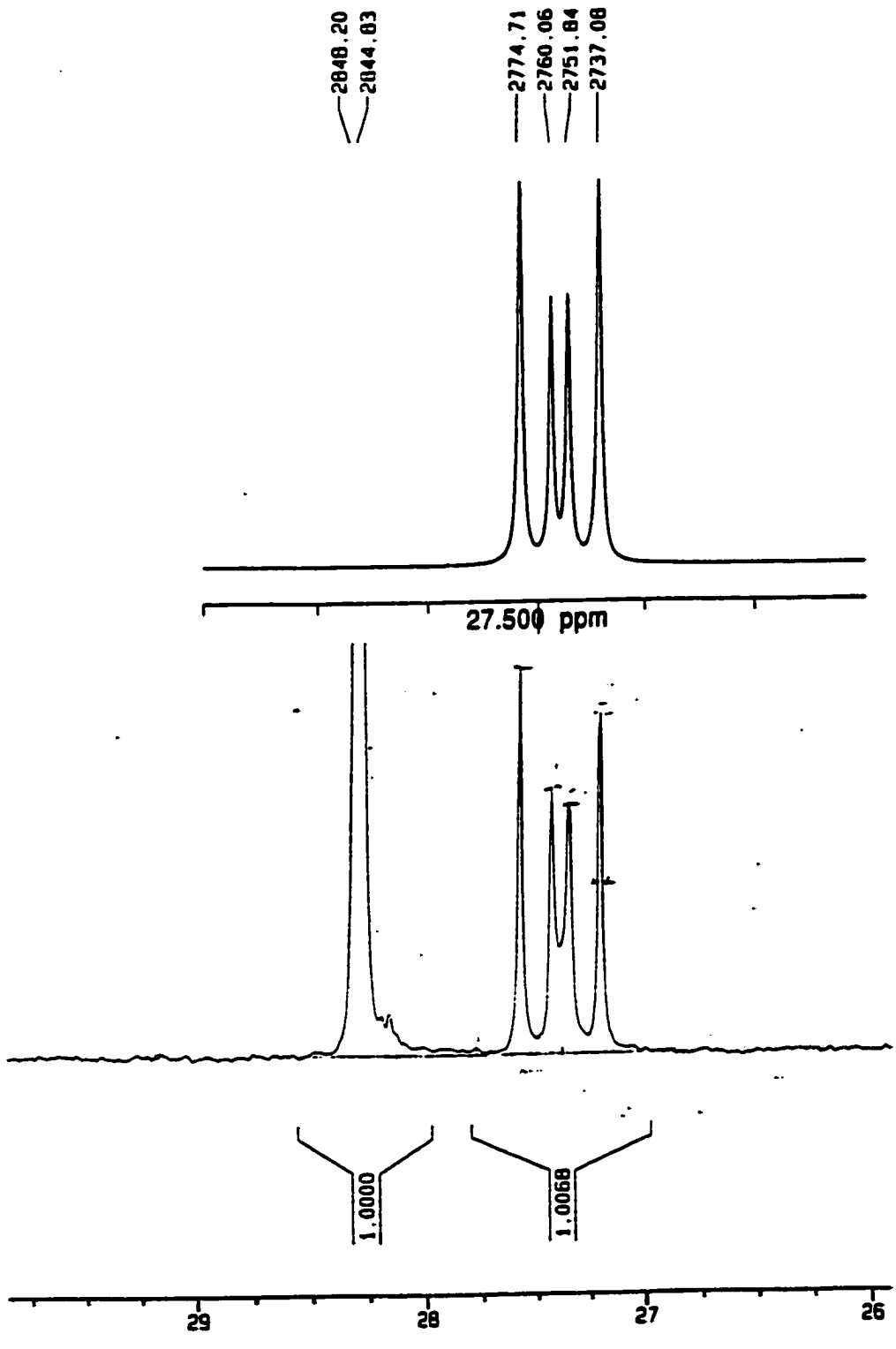

Figure 2: Real and calculated ^{13}C NMR spectra for **BDB**.

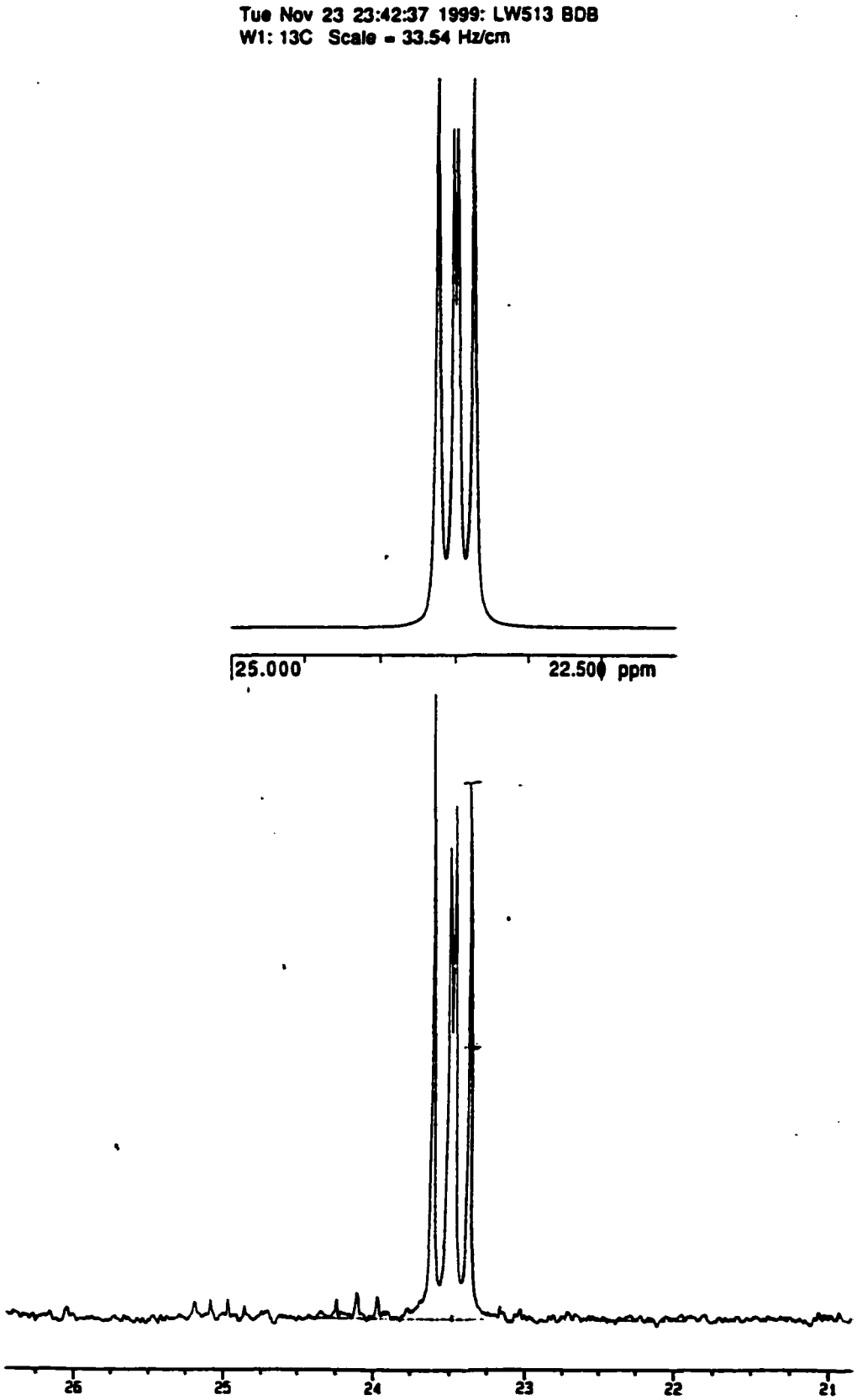

Figure 3: Real and calculated ^{13}C NMR spectra for **BTosL**.

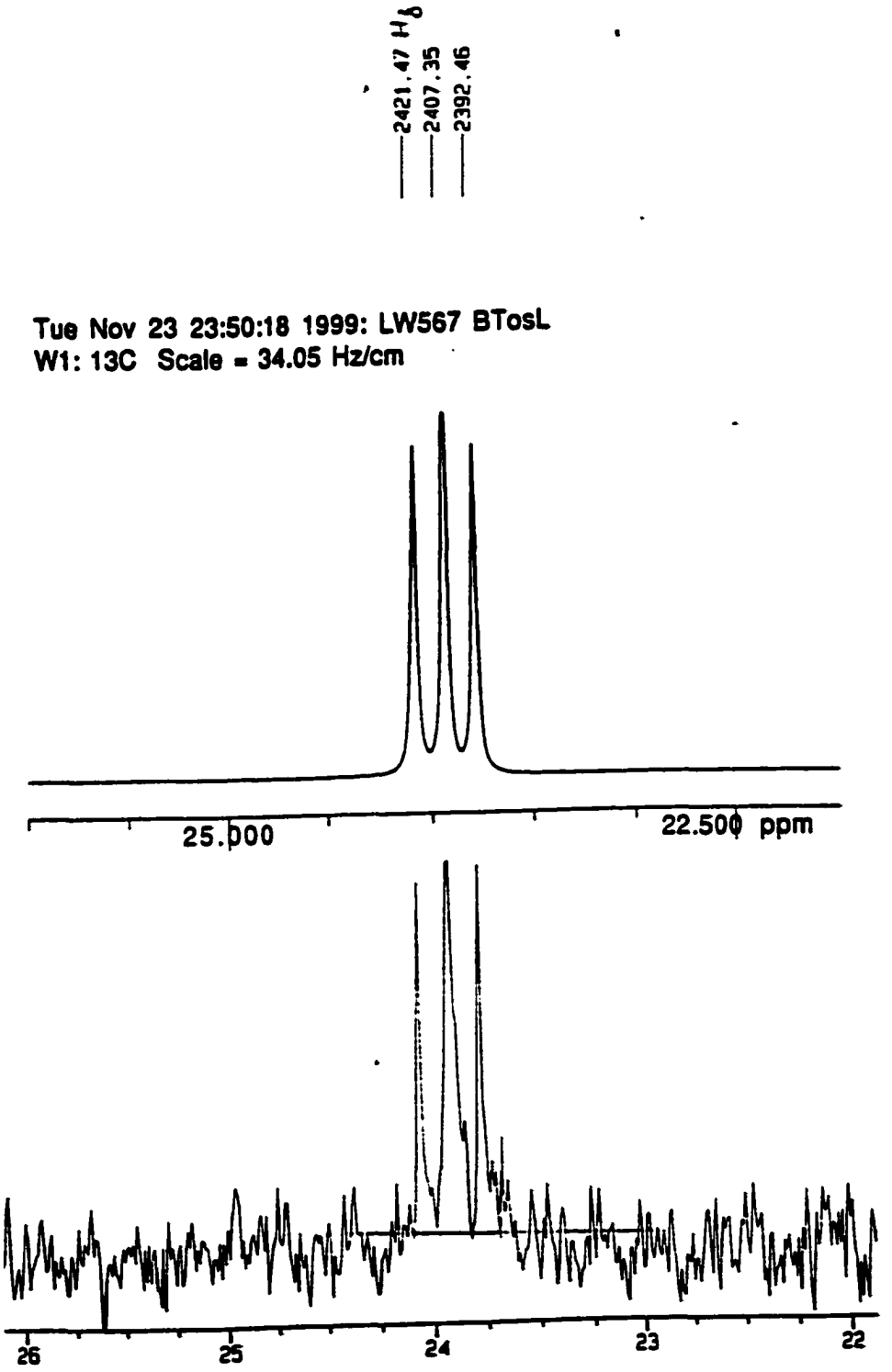

Figure 4-1: ^{13}C NMR spectrum ($CDCl_3$) of $Cl_2PCH_2CH_2PCl_2$.

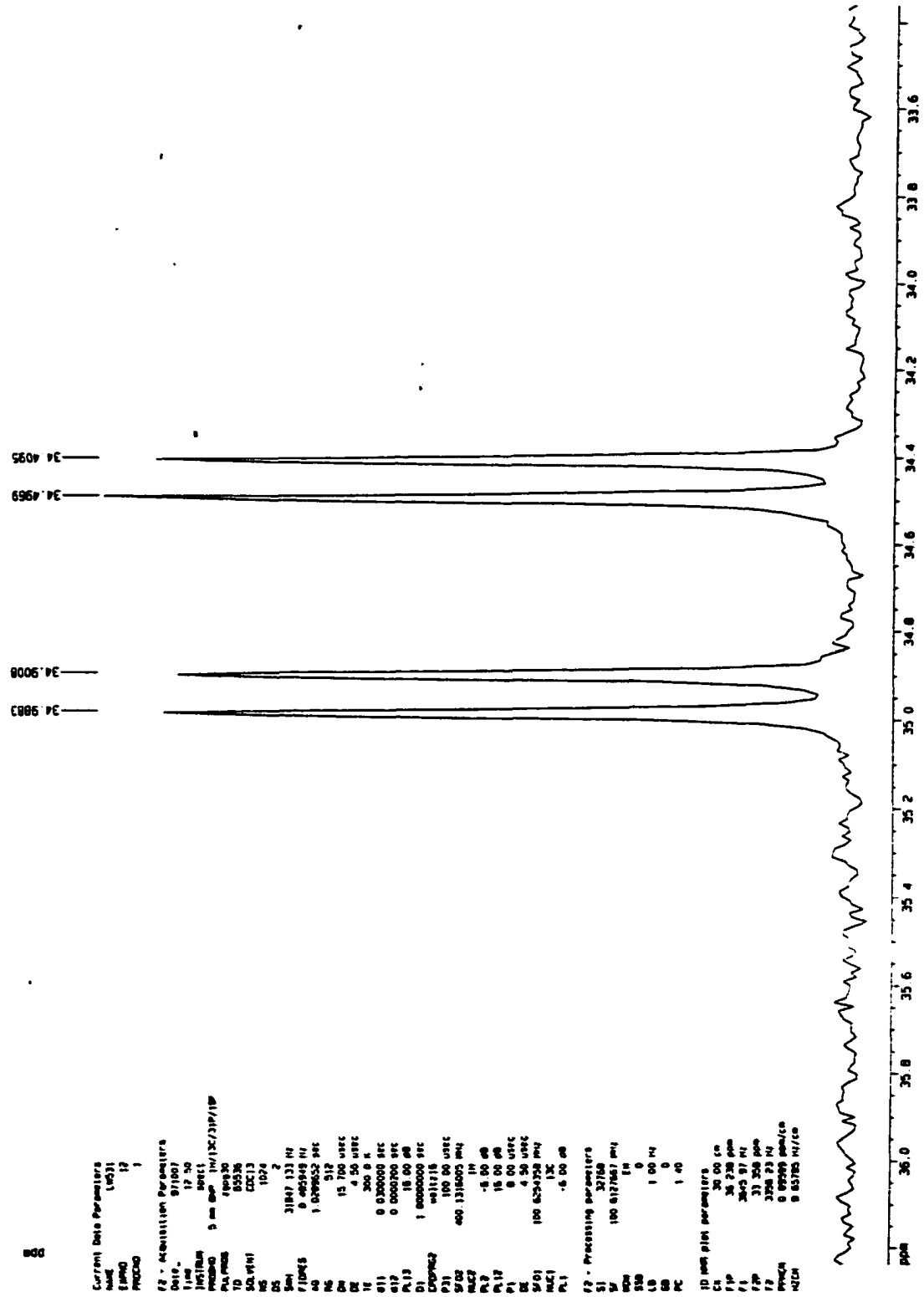

Figure 4-2: ^{1}H NMR spectrum ($CDCl_3$) of $Cl_2PCH_2CH_2PCl_2$.

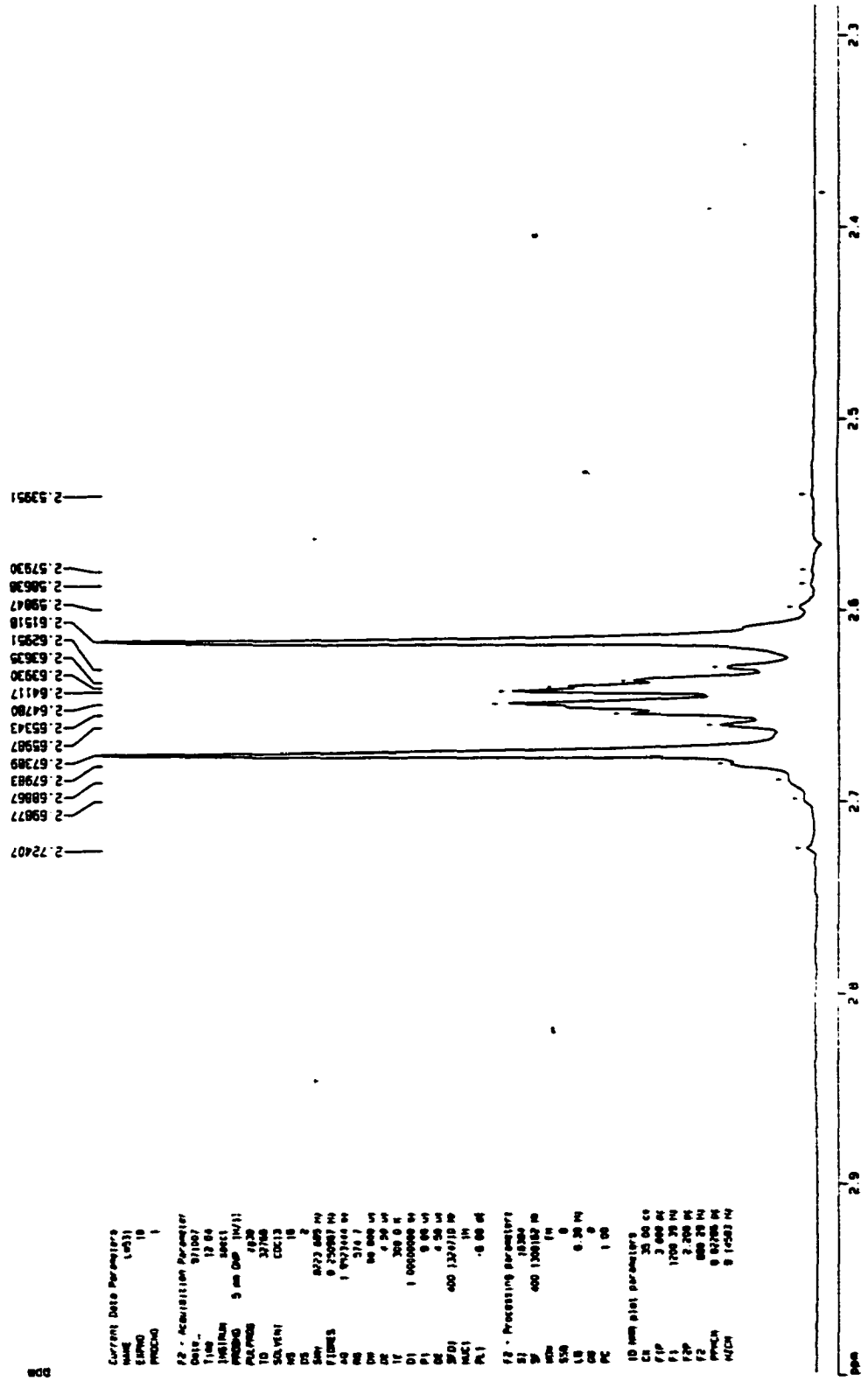

Figure 4-3: ^{31}P NMR spectrum ($CDCl_3$) of $Cl_2PCH_2CH_2PCl_2$.

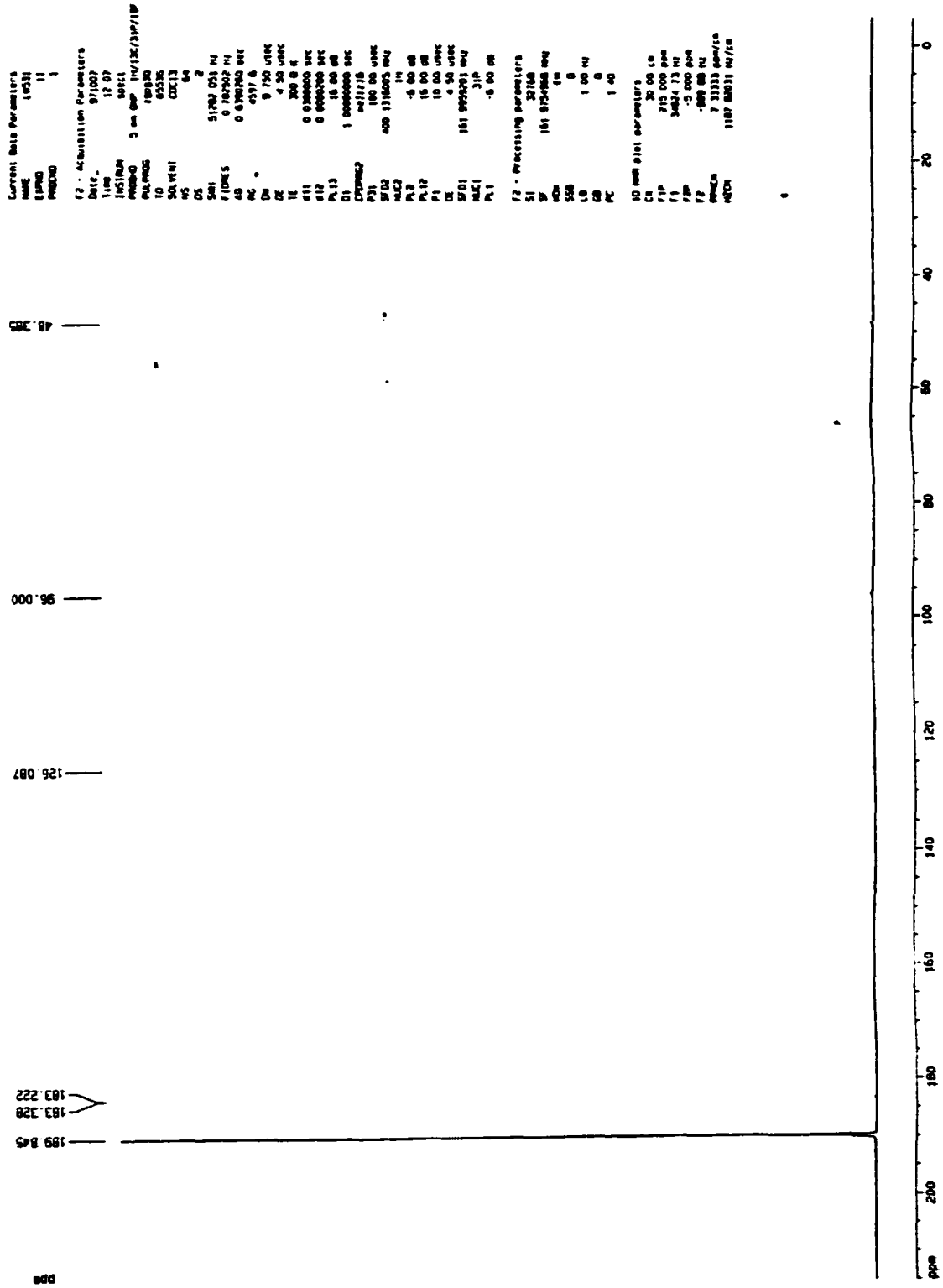

D. Synthesis of *N*-(Diphenylphosphino)-*N,N'*-1,2-phenylenebis-*p*-toluenesulfonamide (PPhyl).

Modifications of **diTosL** were sought in order to investigate the steric and electronic effects and to improve its regioselectivity for hydroformylation (vide infra). *N,N'*-bis(diphenylphosphino)-*N,N'*-ditosyl-*o*-phenylenediamine (**diPPhyl**) is an analog of **diTosL** that has a more rigid backbone. During the preparation of **diPPhyl**, however, its monophosphorus compound, **PPhyl**, was obtained unexpectedly, and **diPPhyl** itself could not be prepared.

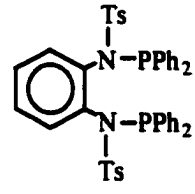

diPPhyl

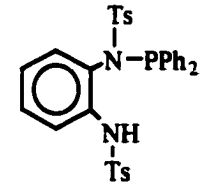

PPhyl

As usual, the standard method was initially used, in which the sulfonamide[29] was combined with 2 equivalents of PPh_2Cl in THF in the presence of triethylamine. P-31 NMR immediately showed a strong peak at 72 ppm and a weak peak at 75 ppm. This is a reasonable region for **PPhyl** and **diPPhyl** compared to **dpet** ($\delta_P = 55.12$ ppm) and **diTosL** ($\delta_P = 60.37$ ppm). The relative ratio did not change very much after 48-hour stirring at

room temperature and then 1-hour refluxing. Proton NMR exhibited two strong peaks with the same intensity at 2.40 and 2.32 ppm which are in the aromatic methyl region. Their relative ratio did not change with reaction time and temperature as well. When the NMR sample was spiked with a small amount of the sulfonamide starting material, a new methyl signal emerged between the 2.40 and 2.32 ppm signals, indicating that the starting sulfonamide had been used up. When one equivalent of Ph_2PCl was used (eq 9), the same ^1H and ^{31}P NMR spectra were obtained. These results

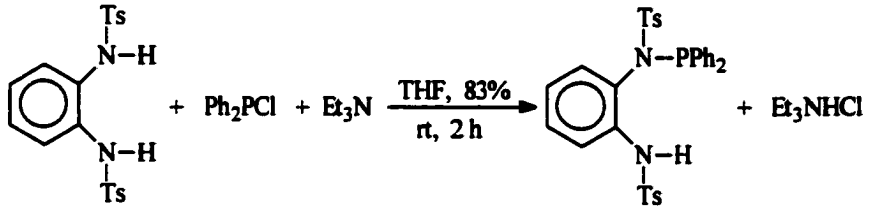

(9)

PPhyl

suggested that the product contained one phosphorus only, i.e. **PPhyl**. **PPhyl** was recrystallized from chloroform/ether (1:1 v/v) in 83% yield, and elemental analysis supported this formulation.

It is interesting to compare the proton NMR spectra of **PPhyl** and its starting materials (Figure 5). For *o*-phenylenediamine, the four aromatic proton signals appear at 6.68-6.69 ppm as an AA'BB' pattern. The shielded peaks, compared to benzene at 7.27 ppm, obviously result from electron donation of the two amino groups. After tosylation, they appear at 6.97-7.03

ppm, moving downfield as expected due to the electron-withdrawing tosyl groups. When one Ph_2P group is attached, the molecule loses symmetry. The four peaks are well separated and become a first order pattern. Two of them are shielded, moving upfield to 6.42 and 5.86 ppm. These ultra high chemical shifts might result from anisotropy due to the toluene group. A possible conformation generated by molecular modeling using the *Chem3D Plus* MM2 force field is shown in Figure 6. In this conformation, the two protons, H1 and H2 on the phenylenediamine moiety are above the edge of the benzene ring of the Ts moiety. The distance is 2.69 Å between H1 and the ring, and 4.51 Å between H2 and the ring. The coupling pattern identifies the 5.86 ppm proton as H1 or H4; on the basis of this conformation we therefore tentatively assign this peak to H1 due to shielding by the benzene ring. The benzene ring of the other Ts and one phenyl on phosphorus lie in a π-stacking arrangement. The distance is about 3.60 Å between the rings.

Figure 5: ^{1}H NMR ($CDCl_3$) of a) **PPhyl**; b) *N,N'-o*-phenylenebis(*p*-toluenesulfonamide)

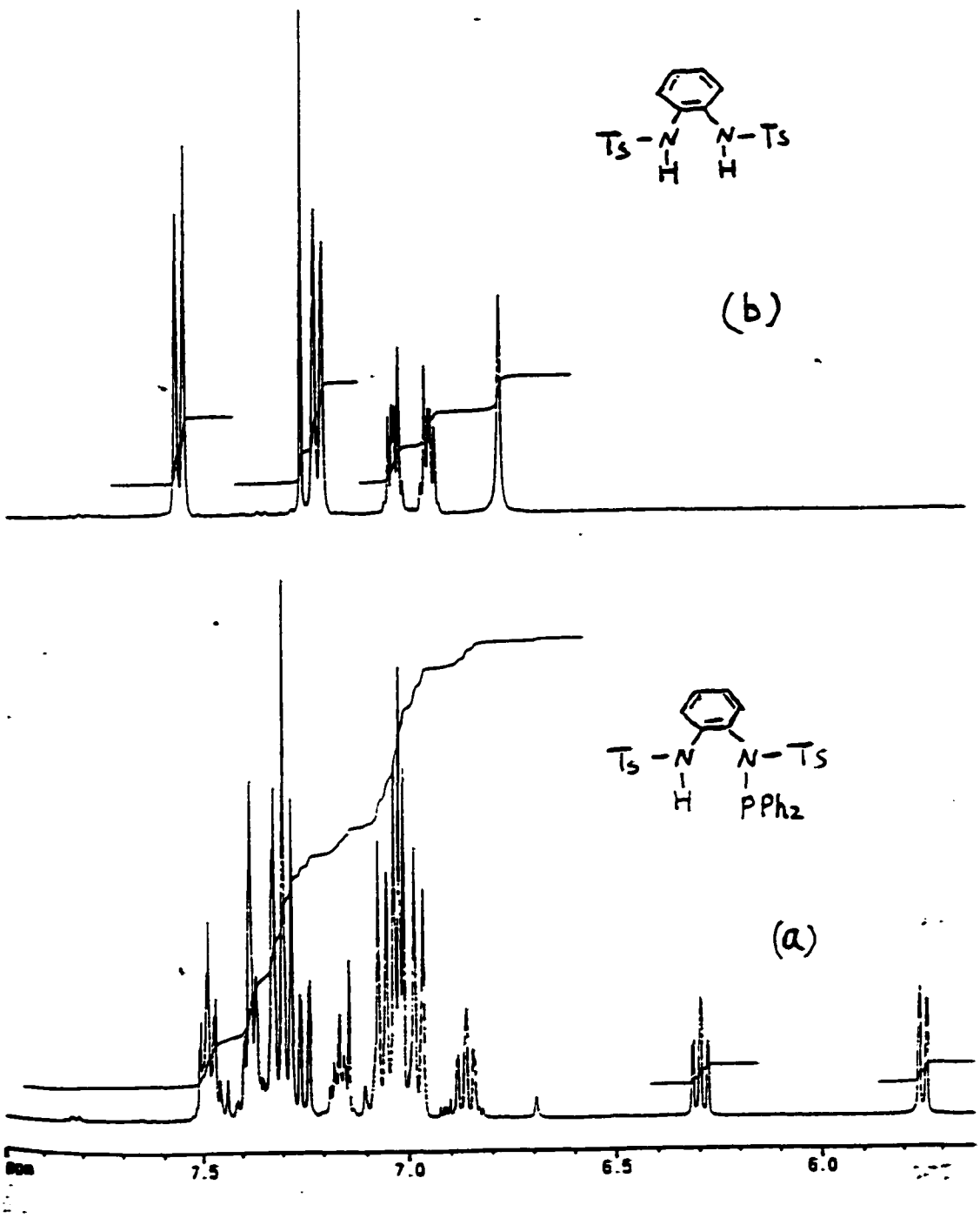

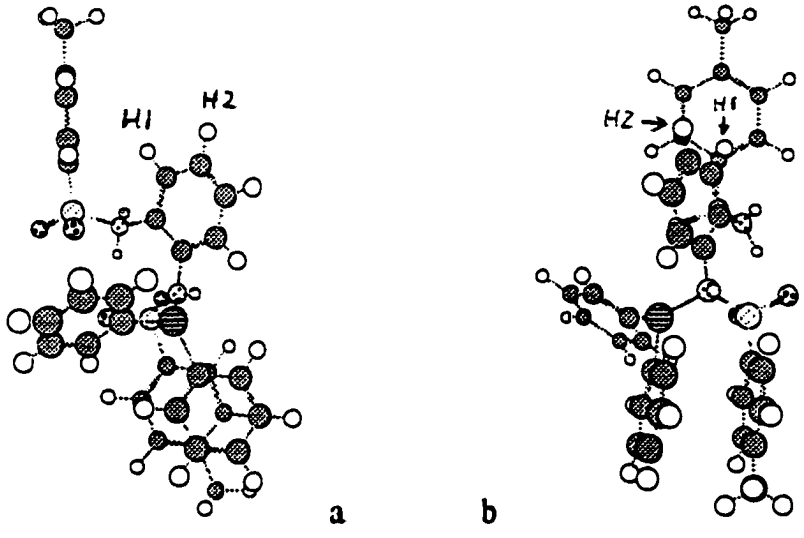

Figure 6: A possible conformation of **PPhyl** generated by *Chem3D Plus* program, showing that the two hydrogen atoms H1 and H2 are above the benzene ring. Rotate a 90° about z axis clockwise (top view) to give b.

E. Attempt to synthesize *N,N'*-bis(diphenylphosphino)-*N,N'*-ditosyl-*o*-phenylenediamine (diPPhyl) and *N,N'*-bis(diphenylphosphino)-*N,N'*-ditosyl-1,8-diaminonaphthalene (diPNAP).

The attraction of these ligands is that they have different bite angles and rigid backbone, allowing comparison to each other and to **diTosL**.

1) *N,N'*-bis(diphenylphosphino)-*N,N'*-ditosyl-*o*-phenylenediamine (diPPhyl).

As described above, **diPPhyl** could not be obtained by reacting the diamide with chlorodiphenylphosphine in the presence of triethylamine. Two factors were considered for the failure, steric hindrance and weak nucleophilicity. Unlike *N,N'*-1,2-ethanediylbis(toluenesulfonamide), the backbone of the sulfonamide is rigid. When one diphenylphosphino group is attached to one nitrogen atom, steric hindrance around the other nitrogen atom increases, resulting in a difficult approach for the other phosphino group. Since the nitrogen atom is attached to an aromatic ring, the nucleophilicity of the amide is lower than in the corresponding species leading to **diTosL**, making the reaction more difficult. Several modifications to the reaction conditions were tried, principally to attack the electronic effect.

(i) Activating the sulfonamide.

First trial:

In the glovebox, the diamide (a 40-mg scale) was treated with 2 equivalents of n-BuLi at -40 °C in THF for 5 minutes, followed by addition of 2 equivalents of Ph_2PCl. The clear solution was stirred for 10 minutes and THF was removed in vacuo. Methylene chloride was added to

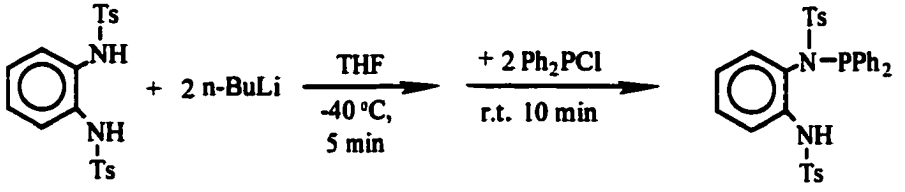

(10)

precipitate LiCl out. Filtration, followed by removal of methylene chloride gave a solid that contained, based on the ^{31}P NMR spectrum (Figure 7), 85% of Ph_2PCl and PPhyl in 1:1.1 ratio. The proton NMR showed complete reaction of sulfonamide. The results suggested that all of the sulfonamide reacted with one equivalent of Ph_2PCl only. Since no Ph_2PBu (δ_P = 17.1 ppm)[30] formed, all of the BuLi had apparently reacted by the time the Ph_2PCl was added, presumably forming the N anion of which one reacted with Ph_2PCl and the other picked up a hydrogen during workup. Hence, we conclude that the lithium dianion is not reactive enough to give two displacement reactions with PPh_2Cl under these conditions.

Figure 7: Reaction of sulfonamide with n-BuLi and then with PPh_2PCl (1:2:2) in THF. a) ^1H NMR; b) ^{31}P NMR. ($CDCl_3$)

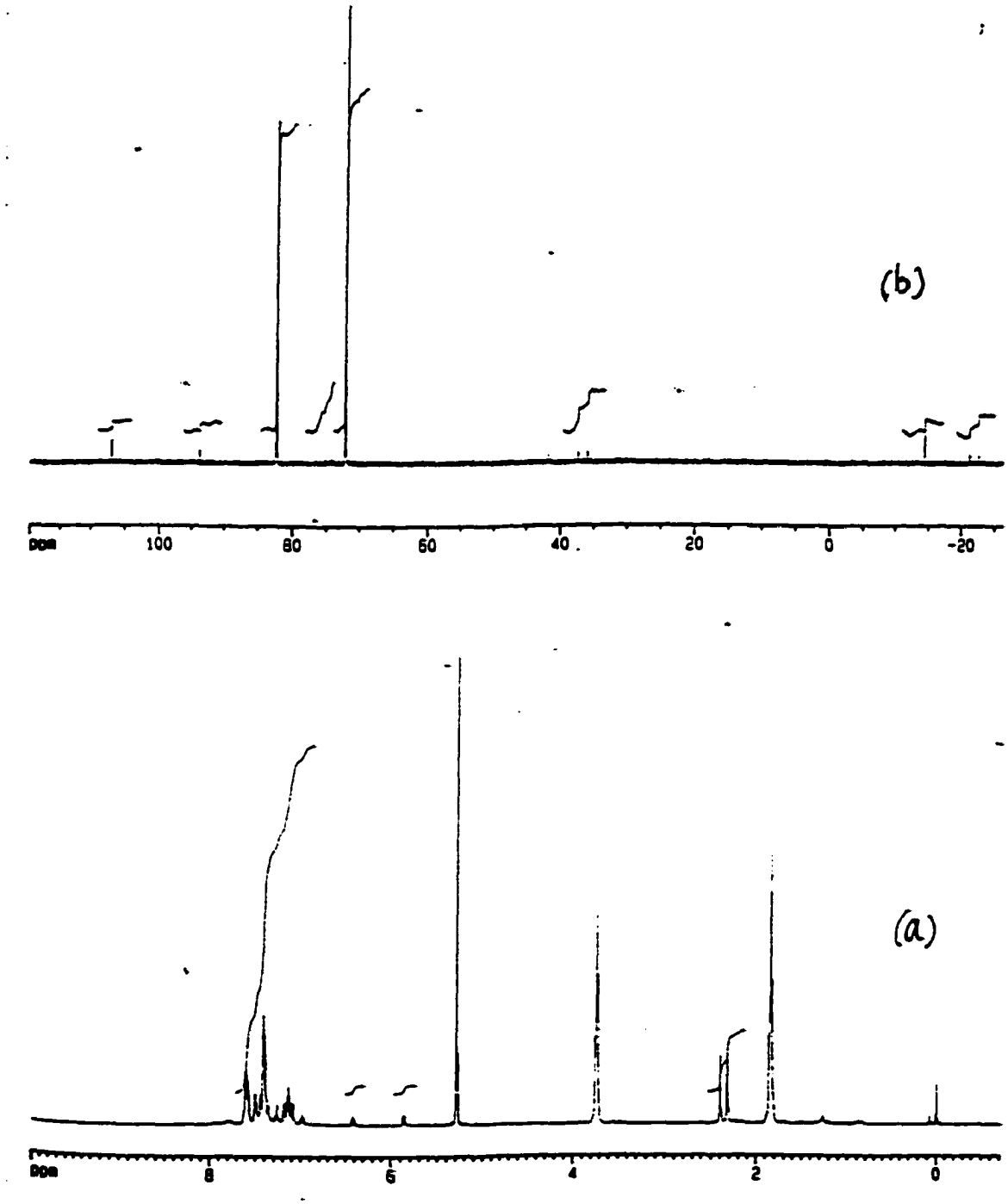

Second trial:

The reaction was carried out as described above, but instead of removing the solvent after 10 minutes, was allowed to stir for 24 hours. Interestingly, the clear solution after 10-minute reaction gave rise to a precipitate which appeared 30 minutes after the addition of Ph_2PCl.

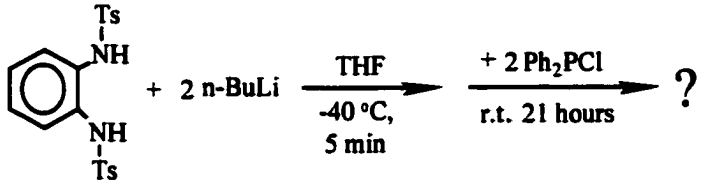

(11)

Filtration, followed by removal of THF gave a solid to test by NMR in chloroform-*d*. Iodomethane was used once before removal of THF to try to destroy any anions present. However, the NMR showed no difference between these two experiments.

Decomposition seemed to take place during purification of the reaction product. During recrystallization, it was observed that a clear filtrate turned cloudy and the white solid recovered from the filtrate turned light yellow. Chromatographic purification using a silica gel column was tried. An eluent containing CH_2Cl_2 and THF (1:1 v/v) was used to elute the mixture dissolved in methylene chloride. Only the yellow band contained the interesting component and the recovery was terribly low.

After making great efforts, a relatively pure solid product of the reaction was obtained from recrystallization from ether at -40 °C. Its ^{1}H NMR showed mainly 6 types of protons (Figure 8) at δ 7.83 (m, 4H), 7.47 (m, 2H), 7.42 (m, 4H), 7.30 (dd, 8.0 Hz, J_{PH} = 1.5 Hz, 2H), 6.97 (d, 8.0 Hz, 2H) (aryl), 2.23 (s, 3H, CH_3). The ratio of aromatic protons to methyl protons is 14:3, instead of 16:3 as expected from the formula of **diPPhyl**. In addition, ^{31}P NMR exhibited one major peak (Figure 8) at 41.78 ppm which is about 10 to 30 ppm to higher field than that of similar compounds (δ_P = 72.10 ppm for **PPhyl**; 72.2 ppm for **DBT** [see later result]; 55.12 ppm for **dpet**; and 60.37 ppm for **diTosL**). Based on the ratio of aromatic to methyl protons and the appearance of the phosphorus signal, one might think that the compound might not be **diPPhyl**. However, the observed ratio of 14:3 is ~15.65 : 3.35. If one assumes the presence of 19 hydrogen as in **diPPhyl**, it is still acceptable within experimental error. In addition, it had only one methyl signal as well as one ^{31}P signal, consistent with the symmetric molecule **diPPhyl**, while the phosphorus NMR signal is at surprisingly high

Figure 8: NMR spectra ($CDCl_3$) for the solid from reaction of sulfonamide with n-BuLi and then with Ph_2PCl in THF for 21 hours.
a) ^{1}H; b) ^{31}P; c) ^{13}C.

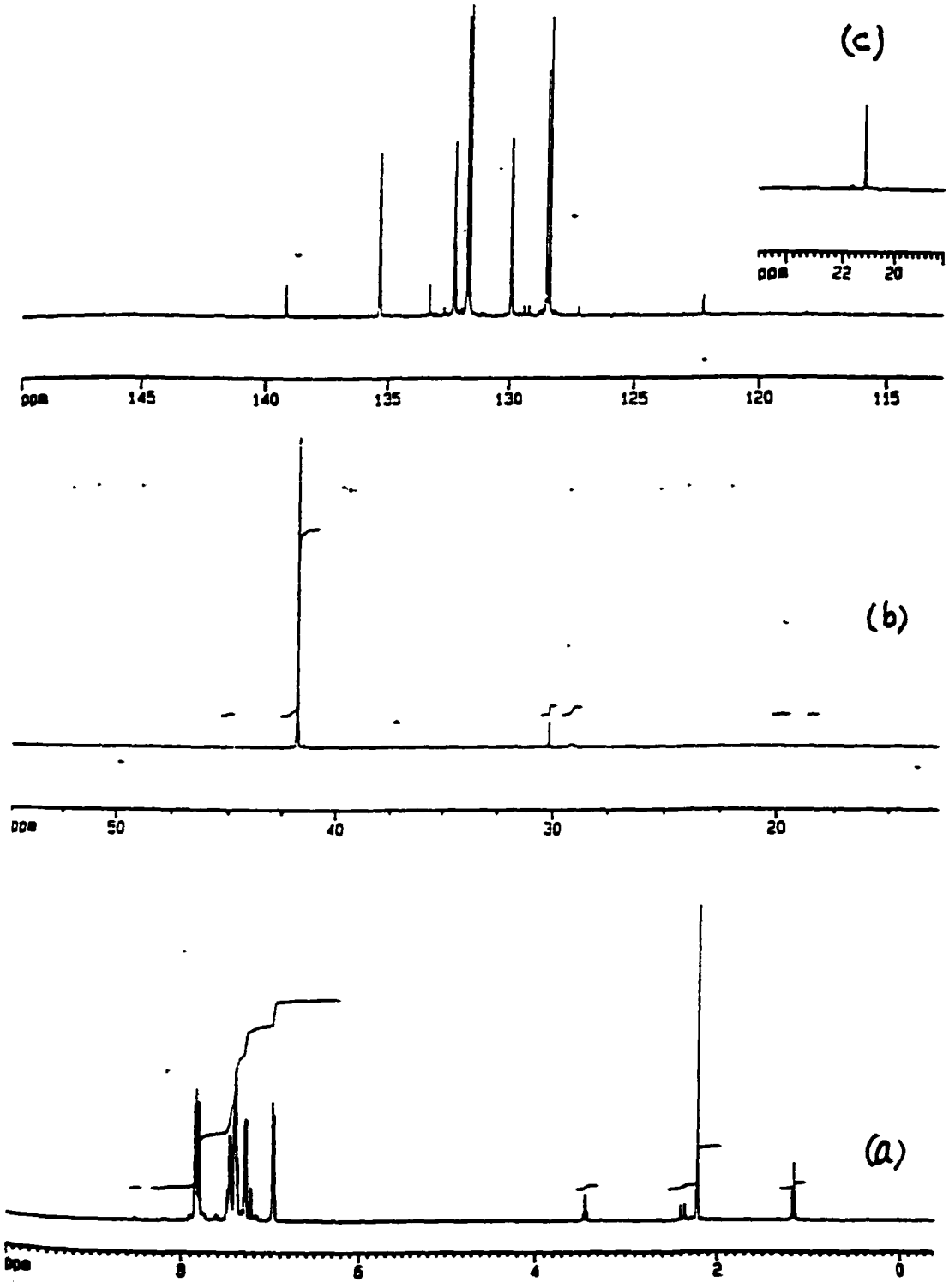

field compared to related compounds. **DiPPhyl** would be highly strained compared to **diTosL** due to the rigid backbone of **diPPhyl**, and compared to **PPhyl** due to one more hindered PPh_2 group in **diPPhyl**. Therefore, the electronic properties of **diPPhyl** could be different from **diTosL** and **PPhyl**, giving rise to the unusual NMR peak position. More investigation needs to be done in order to draw a conclusion.

Third trial:

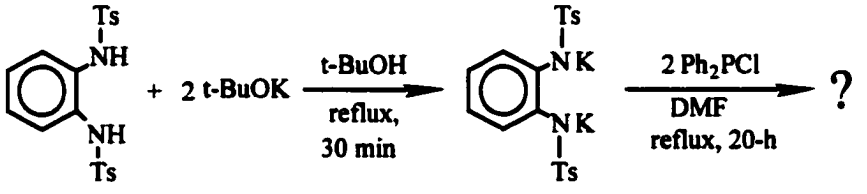

(12)

According to the literature,[31] the potassium salt of the dianion shown in eq 13 could be formed by refluxing the diamide with 2 equivalents of t-BuOK in t-BuOH for 30 minutes, followed by removal of the alcohol. In the glove-box, the potassium salt was dissolved in DMF and 2 equivalents of Ph_2PCl were added. The solution was refluxed for 20 hours. Filtration, followed by removal of DMF on a vacuum line, gave an oily material which had phosphorus NMR signals at 35.48 (d) and 28.12 (d) ppm. There is no evidence that this is the desired compound.

(ii) Activating chlorodiphenylphosphine.

$$Ph_2PCl + AgBF_4 \xrightarrow[10\ min]{CH_2Cl_2} \xrightarrow[2\ hours]{+\ Et_3N,\ o\text{-}TsNHC_6H_4N(PPh_2)Ts} ? \qquad (13)$$

The phosphenium cation, $Ph_2P^{\oplus}$, may be more reactive than Ph_2PCl itself with the sulfonamide. We are not aware of any reports of this material, although metal complexes of PPh_2[32] and other phosphenium cations are known,[33] but by analogy to trityl cation, Ph_3C^+, it might be obtainable by halide abstraction. Therefore, 1.1 equivalent of Ph_2PCl was added at room temperature to a suspension of 1.1 equivalent of $AgBF_4$ in methylene chloride. The mixture was stirred for 10 minutes and filtered through Celite to remove the resultant white AgCl precipitate. Triethylamine (2.4 equivalents) was added to the clear filtrate, followed by addition of a solution of 1 equivalent of **PPhyl** in methylene chloride. Two hours later, the solvent was removed and CD_2Cl_2 was added to the residue to test with NMR. The NMR showed that the residue was still **PPhyl** itself (δ_P = 72.36 ppm and δ_H = 2.41, 2.34 ppm for two methyl groups). No **diPPhyl** formed.

However, the ^{31}P NMR spectrum showed something interesting. There are two strong, sharp peaks at low field, 165.40 and 159.93 ppm. They were separated by 886 Hz, and have the same intensity (Figure 9). It was thought

that Ph_2PF [NMR data:[34] δ_P (H_3PO_4) 168 ppm; δ_F ($CFCl_3$) -202 ppm; J_{PF} = 905 Hz] might form via the abstraction of one fluorine from BF_4^- by a phosphorus cation. In order to look at this reaction more clearly, Ph_2PCl was reacted with $AgBF_4$ in CD_2Cl_2 without adding Et_3N and **PPhyl** (eq 14). Two signals at 161 and 155 ppm, separated by 913 Hz, were observed

$$Ph_2PCl + AgBF_4 \xrightarrow[1\ hour]{CD_2Cl_2} Ph_2P^{\oplus}\ FBF_3^{\ominus} \longrightarrow Ph_2PF \qquad (14)$$

(Figure 10), yet were much weaker and very broad. In the ^{19}F NMR (Figure 10), there were also two broad signals at -169.6 and -172.0 ppm relative to $CFCl_3$ (chemical shifts not calibrated), separated by 922 Hz. The broad peaks in both spectra might result from an equilibrium (eq 15) in which the

$$Ph_2P^{\oplus}\ FBF_3^{\ominus} \rightleftharpoons Ph_2PF + BF_3 \qquad (15)$$

fluorine atom comes on and off the phosphorus atom. In the presence of NEt_3, Et_3N-BF_3 would be expected to form so sharp lines for the Ph_2PF would be reasonable.

Figure 9: Reaction of $Ph_2P^+BF4^-$ with **PPhyl** in the presence of Et_3N.
a) ^1H NMR; b) ^{31}P NMR. (CD_2Cl_2)

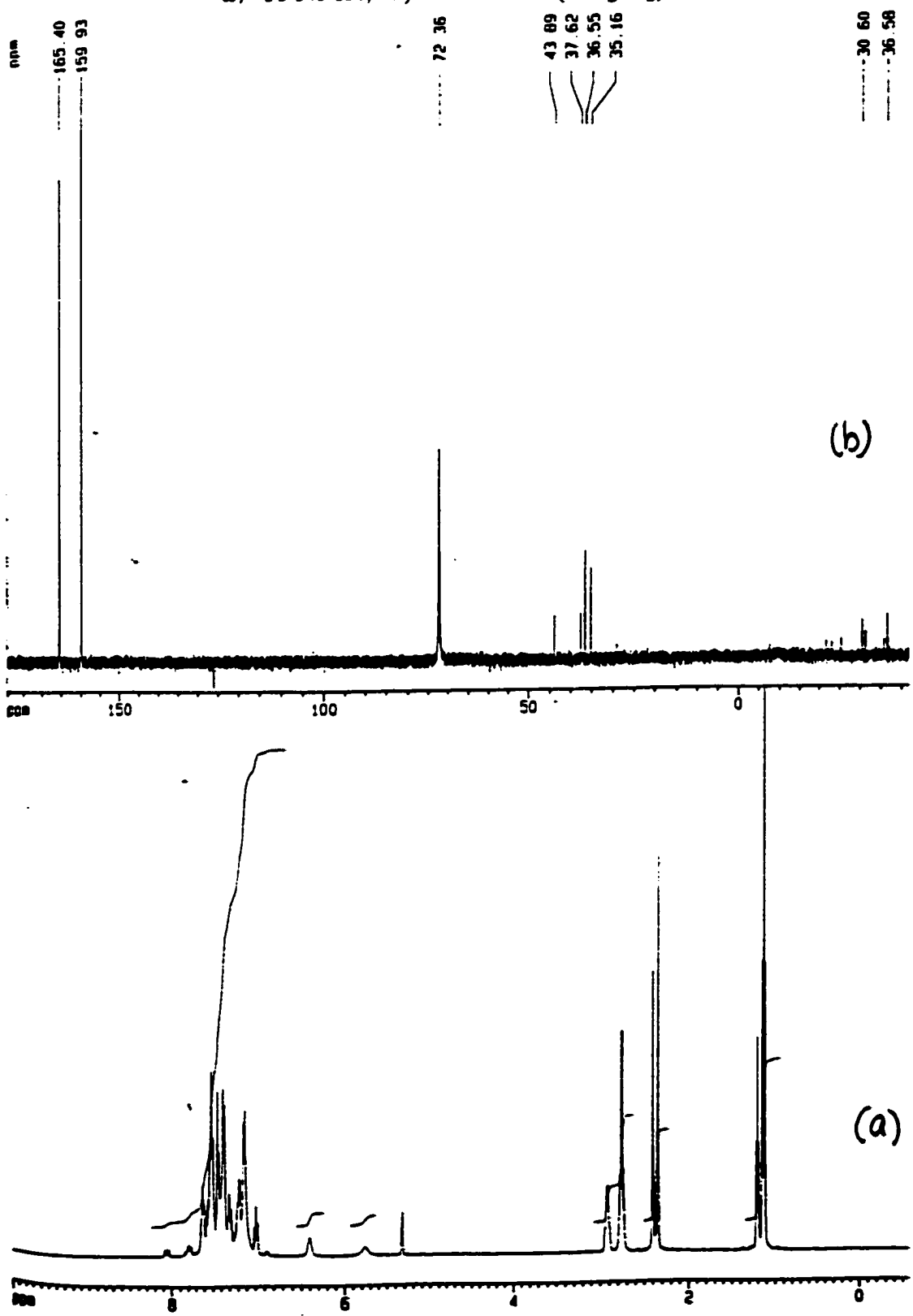

Figure 10: Reaction of Ph_2PCl with $AgBF_4$. a) ^{31}P NMR; b) ^{19}F NMR (CD_2Cl_2)

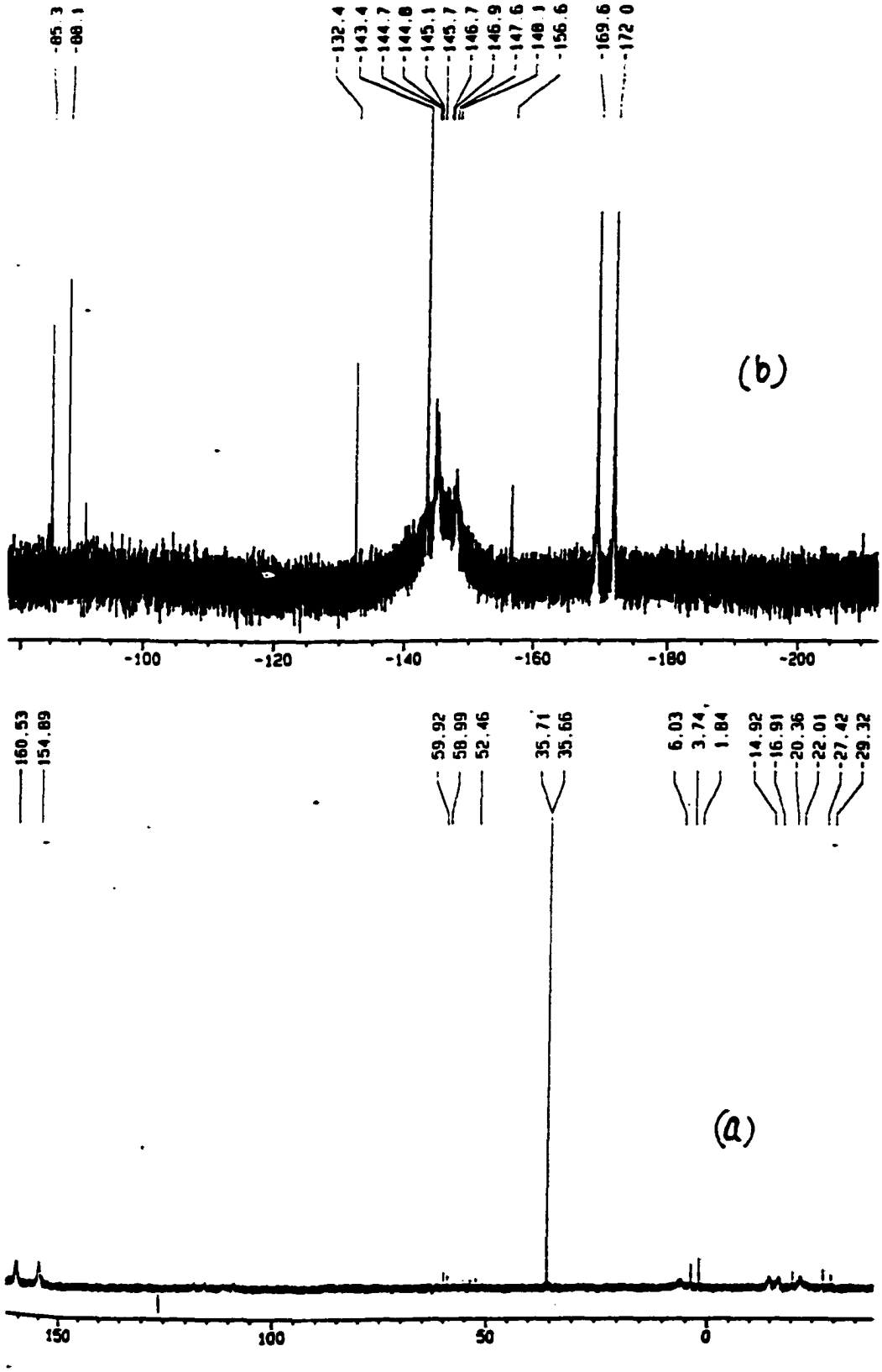

Another reaction was carried out at the same time for comparison (eq 16). One equivalent of Ph_2PCl was reacted with one equivalent of $AgSbF_6$

$$Ph_2PCl + AgSbF_6 \xrightarrow[1\ hour]{CH_2Cl_2} ? \qquad (16)$$

in CH_2Cl_2 at room temperature for one hour. ^{31}P NMR of the mixture showed that, among about ten peaks, there were no bands at about 160 ppm observed, indicating that either Ph_2PF did not form or the peaks were too broad to be seen. No clear evidence for formation of Ph_2P^+ was obtained, and no further investigation was carried out.

2) *N,N'*-bis(diphenylphosphino)-*N,N'*-ditosyl-1,8-diaminonaphthalene (diPNAP).

Two equivalents of Ph_2PCl were combined with one equivalent of *N,N'*-ditosyl-1,8-diaminonaphthalene[29] (TNAP) at room temperature in THF containing about 2.5 equivalents of triethylamine (eq 17). After 1 hour, the ^{31}P NMR spectrum showed two major phosphorus-containing compounds, of which one (δ_P = 82.36 ppm) was the starting material, Ph_2PCl, while the other (δ_P = 70.66 ppm) was the product. The question was did the product contain one phosphorus atom or two equivalent phosphorus atoms. In the ^1H NMR, there were three methyl signals. Addition of a little TNAP resulted in

enhancement of the most intense peak at 2.30 ppm, indicating that this methyl was due to the starting material. The other two peaks at 2.50 and 2.29 ppm were apparently due to an asymmetric product. In other words,

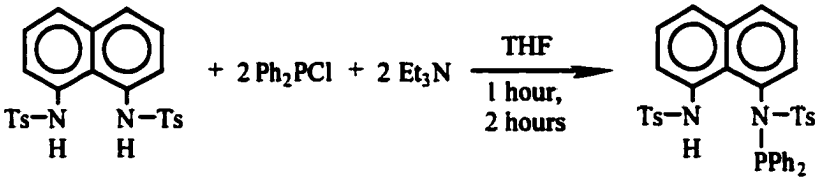

(17)

the product was *N*-diphenylphosphino-*N,N'*-ditosyl-1,8-diaminonaphthalene (**PNAP**) instead of **diPNAP**. Another characteristic of this asymmetric molecule was the anisotropy effect as seen in **PPhyl**. One aromatic proton was highly shielded so that the chemical shift moved up to 6.34 ppm. About 33% of the **TNAP** was converted into **PNAP**, according to the methyl proton integration (the integration of the three methyl peaks added up to 100%). When the mixture was stirred for 19 hours or refluxed for 3 hours, more decomposition was observed based on ^{31}P NMR. Purification of **PNAP** was not carried out.

We also tried to use n-BuLi (one or two equivalents) to react with one equivalent of **TNAP** in THF at room temperature, followed by addition of one (or two) equivalents of Ph_2PCl. Only a small amount of **PNAP** formed as well.

F. Attempt to synthesize *N*-diphenylphosphino-*N,N'*-(1,1'-biphenyl)-2,2'-diylbis(*p*-toluenesulfonamide) (DBT) and *N,N'*-(1,1'-biphenyl)-2,2'-diylbis(*N*-diphenylphosphino-*p*-toluenesulfonamide) (BBT)

Compared to *N,N'*-1,2-phenylenebis(*p*-toluenesulfonamide) and 1,8-di-*p*-toluenesulfonamidonaphthalene, the key difference in the backbone of biphenyl sulfonamide, **BDT** [*o*-$TsNHC_6H_4C_6H_4NHTs$], is that the two rings will not lie in the same plane. Instead, with or without the attachment of the bulky sulfonamido group at the ortho position, they twist at an angle. This twisting will have two effects. First, the aromatic properties of the two rings are relatively independent of each other. For *N,N'*-1,2-phenylenebis(*p*-toluenesulfonamide) and 1,8-di-*p*-toluenesulfonamidonaphthalene, when one phosphino group is attached to one N atom, the nucleophilicity at the other N atom will be affected through the aromatic ring. In the case of biphenyl, however, this effect is expected to be reduced greatly since the twisting of the two rings can result in negligible overlap of the *p*-orbitals at either end of the C-C σ-bond. Second, the twisting should reduce the repulsive steric interaction between the bulky $N(Ts)PPh_2$ groups. Therefore, reaction (18) should produce compound **BBT** more easily than that for the phenylene and naphthalene sulfonamides.

At 15 °C, when one mole of biphenyl sulfonamide was reacted with 2 moles of PPh_2Cl for one hour in the presence of Et_3N (eq 18), the product

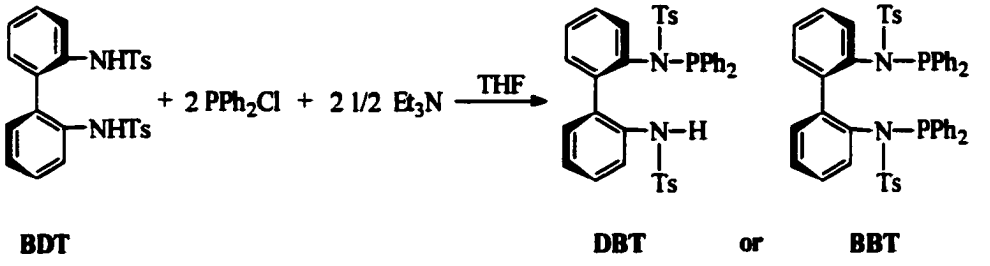

(18)

BDT **DBT** or **BBT**

showed two major ^{31}P NMR ($CDCl_3$) signals at 74.1 and 72.2 ppm in a ratio of ~1:1.7 in peak height. The sulfonamide starting material had been used up while there was still some PPh_2Cl left. It was thought that one signal resulted from compound **DBT** and the other belonged to **BBT**. However, the ratio did not vary much (between 1.5 and 1.8) as the reaction conditions changed, such as stirring at ambient temperature for 6 days, staying at – 40 °C for one hour, refluxing for 17 hours, or even 1 or 6 equivalents of PPh_2Cl used. After recrystallization from a mixture of chloroform and hexane solvents (1:2 volume : volume), the ^1H NMR ($CDCl_3$) exhibited a ratio of 2 to 9 for methyl protons to aromatic protons. This ratio fit the structure for **DBT** (expected ratio: methyl-H : aromatic-H (including the one attached to N atom) = 2:9) but not **BBT** (expected ratio: methyl-H : aromatic-H = 1:6). However, there were 4 methyl signals at 2.44(s), 2.38(s), 2.37(s) and 2.36(s)

ppm. The ratio of peaks at 2.44 and 2.37 was 1:1 and the ratio of the other two was also 1:1; the ratio of the 2.44/2.37 : 2.38/2.36 sets was about 2:1. These two sets of methyl groups, along with two types of phosphorus, could arise from two conformations of structure **DBT**.

When the above reaction was carried out, a third phosphorus NMR signal was observed at 70.7 ppm. It was broader than the other two peaks. Its intensity varied with reaction conditions. For instance, under the conditions of –40 °C for one hour, the peak reached its highest level, 20% of the peak height at 74.1 ppm. Under the condition of refluxing for 17 hours, its amount was negligible. However, when a strong base was used, such as BuLi, it became the major component in the mixture.

The biphenyl sulfonamide was treated with 2 equivalents of BuLi in THF at –40 °C for an hour, followed by addition of PPh_2Cl (eq 19). The contents

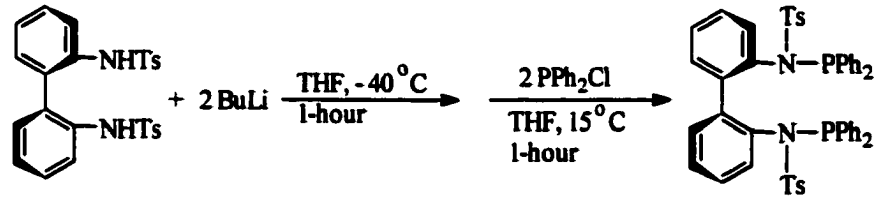

(19)

BBT

were stirred at 15 °C for another hour; a large amount of precipitate appeared in 30 minutes. After filtration, some methylene chloride was added to quench the reaction. (If ethanol was used to quench, the compound

we were interested in decomposed since no peaks appeared in the region of 50~100 ppm. The main phosphorus compound had an intense signal at δ_P 111.50 ppm. This could be Ph_2POEt as compared to δ_P 116 ppm of Ph_2POMe.[35] This compound could result from attack of the oxygen atom in ethanol on the phosphorus atom.) The solvent was removed in vacuo. The resultant solid showed 3 major phosphorus signals in the ^{31}P NMR ($CDCl_3$) at 74.1, 72.2 and 70.7 ppm in a ratio of 1:1.5:4 in peak height. A new major methyl proton peak at 2.35 ppm was also observed in ^1H NMR spectrum. The ratio of methyl protons to aromatic protons was about 1:6, consistent with that in compound **BBT**. Therefore, it is possible that the δ 70.7 ppm compound is the desired compound **BBT**. Further investigation of this compound, including purification and elemental analysis, needs to be done.

G. Attempt to synthesize TosL analog A and diTosL analog BDC.

Under stirring at – 40 °C, 15 μL (20 mg, 0.11 mmol) of $PPhCl_2$ was added via a micro syringe to a suspension of 46 mg (0.11 mmol) *trans*-1,2-di-*p*-toluenesulfonamidocyclohexane (racemic) in 38 μL (28 mg, 0.27 mmol) of Et_3N and 3 mL of diethyl ether (eq 20). The contents were stirred at 15 °C for 2 hours, yielding a large amount of white powder. The precipitate, according to the NMR spectrum, contained mainly Et_3NHCl salt and unreacted sulfonamide, and was filtered off. The solvent in the filtrate

was removed. The resultant white powder was contaminated by Et_3NHCl salt. It contained one ^{31}P NMR ($CDCl_3$) signal at 94.55 ppm, comparable to

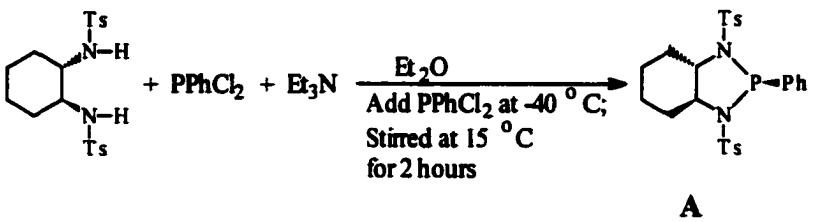

(20)

A

TosL at 91.28 ppm. ^1H NMR showed two strong methyl signals with the same intensity at 2.56 and 2.38 ppm and the ratio of methyl hydrogen to the aromatic hydrogen was about 6:13. There were also 8 aliphatic carbons observed in ^{13}C NMR. These data indicated the formation of compound **A**. Due to the new ring with the Ph group out of the plane, compound **A** no longer has the C_2 symmetry axis present in the trans starting material, so all carbons and hydrogen atoms are chemically non-equivalent. Therefore, 8 aliphatic carbon signals are expected in the ^{13}C NMR. When the NMR solution was exposed to air for 3 days, the ^1H and ^{31}P NMR spectra did not change significantly.

However, the reaction of the same sulfonamide with PPh_2Cl to produce *trans*-1,2-bis(*N*-diphenylphosphino-*p*-toluenesulfonamido)cyclohexane (**BDC**) was not observed. When one equivalent of the sulfonamide was mixed with 2 equivalents of PPh_2Cl in benzene or in THF for 3 hours at room temperature in the presence of 2.5 equivalents of triethylamine, there

was no phosphorus NMR signal at ~ 60 ppm (δ_P 60.37 for **diTosL**). ^1H NMR exhibited mainly the unreacted sulfonamide. When the same solutions were refluxed for 15 to 20 hours (eq 21), the ^{31}P signal was still not observed.

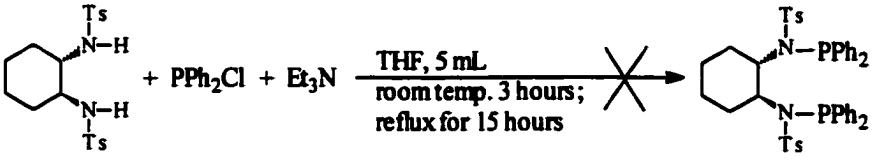

(21)

BDC

H. Hydroformylation of 1-octene or 1-hexene.

The hydroformylation reaction is carried out in a 90-mL, thick-wall glass vessel (called a Fisher-Porter bottle) equipped with a magnetic stirrer. The recipe includes $Rh(acac)(CO)_2$ (the precursor of the catalyst), decane (an internal standard), the ligand, the alkene and the solvent. They are mixed in the vessel. The vessel is quickly flushed with synthesis gas (1:1 of $CO:H_2$) at 84 psi three times and then pressurized to 84 psi. The solution is heated to the desired temperature in an oil bath for a period of time. The pressure was kept constant throughout the reaction (see Experimental for method). The n/i ratios and yields are determined by GC. In order to make sure we can reproduce the literature results, we chose PPh_3 for comparison because it is used industrially. Typical literature conditions[7] are 5% Rh/C (rhodium on

carbon) as the precursor of the catalyst, a ratio of PPh_3 to Rh of 10:1, and heating at 90 °C in toluene as solvent for 35 min under a pressure of 80-100 psi, giving an n/i ratio of 4 as shown in Table II. Under similar conditions using $Rh(acac)(CO)_2$ as the catalyst precursor, we obtained an n/i ratio of 3.2, close enough to 4. Without PPh_3, both selectivity (1.4 vs 3.2) and yield (9.2% vs 76%) are very poor in our hands. Since this is a catalytic reaction, turnover frequency (TOF) is a useful measure of reactivity (TOF = moles of aldehydes formed/unit time/moles catalyst). That is, in principle, the yield of the catalytic reaction can be the same in the presence and absence of the PPh_3 addition if one waits long enough. However, the longer reaction time will lead to a low TOF value, and properly indicate the lower catalytic reactivity in the absence of PPh_3. Because **TosL** is insoluble in benzene or toluene, which are the usual hydroformylation solvents, we chose THF as the reaction solvent and for safety reasons, we lowered the reaction temperature to 60 °C. However, for PPh_3, the same n/i ratio and similar yields in THF as in toluene are observed (see Table II).

Initial results are shown in Table III. From these data, we can see that the monodentate ligand **TosL** gave an n/i ratio of 1.7 while the chelating

Table II. Hydroformylation Results in THF and Toluene*

L (equiv)	Precursor [Rh] = 0.004 M	alkene (equiv)	time (h)	Solvent	T (°C)	n/i	yield (%)	TOF[a]
PPh_3 (10)[b]	5% Rh/C	1-octene (200)	35 min	toluene	90	4	--	--
PPh_3 (10)[c]	$Rh(acac)(CO)_2$	1-octene (200)	0.5	toluene	90	3.2	76	300
--[d]	$Rh(acac)(CO)_2$	1-octene (170)	1	toluene	90	1.4	9.2	15
PPh_3 (10)[e]	$Rh(acac)(CO)_2$	1-octene (200)	4	THF	60	3.2	84	42

* -- in all cases, $CO:H_2 = 1:1$.

a -- turnover frequency, mol of aldehydes/(hour x mol of Rh)

b -- Conditions: 90 °C, 80-100 psi in toluene. 5% Rh/C as the precursor of catalyst. [(7) Pruett, R.L; Smith, J.A. *J. Org. Chem.* **1969**, 34, 327-330]

c -- Conditions: 90 °C, 84 psi (6 atm) in toluene. $Rh(acac)(CO)_2$ as the precursor of catalyst.

d -- Conditions: 90 °C, 84 psi (6 atm) in toluene. $Rh(acac)(CO)_2$ as the precursor of catalyst. No PPh_3 ligand added.

e -- Conditions: 60 °C, 84 psi (6 atm) in THF. $Rh(acac)(CO)_2$ as the precursor of catalyst.

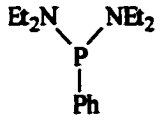

Bis(diethylamino)phenylphosphine **[BDPP]**

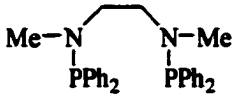

N,N'-1,2-Ethanediylbis(*N*-methyl-*P,P*-diphenylphosphinous amide) **[EMPA]**

Table III. Hydroformylation Results[a]

L (equivalents)	alkene (equiv)	time (hour)	T (°C)	n/i	yield (%)	TOF[b]
TosL (10)	1-octene (200)	5.5	60	1.7	57	21
diTosL (5)	1-octene (200)	5	60	10	62	35
PPh_3 (10)	1-octene (200)	4	60	3.2	84	42
BDPP[c]	1-hexene(1000)	15	80	1.97	42	30
EMPA[c]	1-hexene(1000)	15	80	2.3	80	56

a -- Conditions: 60 °C, 84 psi (6 atm) in THF. $Rh(acac)(CO)_2$ as the precursor of catalyst. [Rh] = 0.004 M

b -- turnover frequency, mol of aldehydes/(hour x mol of Rh)

c -- Conditions: 80 °C, 25 atm, 15 hours, [1-hexene]/[Rh] = 1000 in benzene. $RhCl(CO)L_2$ as the precursor of the catalyst

[(36) Grimblot, J.; Bonnelle, J. P.; Mortreux, A.; Petit, F. *Inorg. Chim. Acta* **1979**, *34*, 29-36.]

ligand **diTosL** strongly favored the linear product. The ratio is 10, greater than 3.2 for PPh_3; and its yield, 62%, is comparable to that of PPh_3. Comparing to the known alkyl amino phosphines[36], one can see that **TosL** gives a similar n/i ratio (1.7) as **BDPP** does (1.97), while **diTosL** is superior to its methyl analog **EMPA** (10 vs 2.3), indicating that the Ts moiety plays a role in regioselectivity.

Table IV contains hydroformylation results for **dpet** and **diTosL**. From here one can see that the chelating ligand, **diTosL**, produces much higher n/i ratios than its monodentate analog, **dpet**. Using 1 and 2 equivalents of **diTosL** gives rise to n/i ratios of 8.9 and 10, yields of 83%, and TOF of 48 and 45, while an n/i ratio of only 2.5 is obtained for **dpet** (2-10 equivalents), in yields from 45 to 82% and with TOF from 20 to 39. Thus, while addition of excess **dpet** allows the yield to be pushed up to the levels obtained with only 1 equivalent of **diTosL**, the n/i ratio cannot be raised. Clearly, chelation favors formation of linear product.

Since **BTosL** and **ETosL** do not dissolve in THF (or most other solvents), DMF was chosen as the solvent for the reaction. Temperature,

Table IV. Hydroformylation Results for monodentate **dpet** and chelating **diTosL** ligands

L (equivalents)	alkene (equiv)	time (hour)	n/i	yield (%)	TOF
dpet (2)	1-hexene (200)	4.5	2.5	45	20
dpet (5)	1-hexene (200)	4	2.5	71	36
dpet (10)	1-hexene (200)	4	2.5	82	39
diTsoL (1)	1-hexene (200)	4	8.9	83	48
diTosL (2)	1-hexene (200)	4	10.	83	45

Conditions: 60 °C, 84 psi (6 atm) in THF. $Rh(acac)(CO)_2$ as the precursor of catalyst. [Rh] = 0.004 M

pressure and reaction time were held the same. The PPh_3 ligand was again used for comparison, and it gave the same n/i ratio as in THF and the yields were similar. However, DMF seems to affect **diTosL** dramatically (Table V). The n/i ratio for **diTosL** dropped to 5.4 in DMF from 8.9 in THF and the yield dropped to 0.7% from 83%, while **BTosL** did not catalyze the reaction at all. We conclude that the more strongly coordinating solvent prevents the weakly coordinating phosphinamide ligands from binding to Rh, and so the additives have no effect on the reaction.

PPhyl acts like the monodentate ligand. Similar to **dpet** and **TosL**, **PPhyl** gave a low n/i ratio of 1.6. The yield, however, was much lower (Table VI). One reason for the low yield could be a steric effect. That is, the **PPhyl** N atom connected to the PPh_2 group is attached the bulky *o*-$TsN(H)C_6H_4$ group, compared to the much smaller ethyl group in **dpet**. There is no direct comparison to **TosL** since it is electronically different, but the cyclic structure ties back the bulky tosyl groups unlike **PPhyl**. We suggest that the steric bulk results in the slower rate and lower selectivity for the linear aldehyde, and there is no evidence for chelation by the *o*-N(H)Ts group.[7]

Table V. Hydroformylation Results in DMF

L (equivalents)	alkene (equiv)	time (hour)	n/i	yield (%)	TOF
PPh_3 (10)[a]	1-octene (200)	4	3.2	84	42
PPh_3 (10)	1-hexene (674)	4	3.1	62	105
diTosL (1)	1-hexene (674)	4	5.4	0.7	1.1
BTosL (1)	1-hexene (674)	4	no reaction	--	--

Conditions: 60 °C, 84 psi (6 atm) in DMF. $Rh(acac)(CO)_2$ as the precursor of catalyst. [Rh] = 0.004 M

a -- Conditions: 60 °C, 84 psi (6 atm) in THF. $Rh(acac)(CO)_2$ as the precursor of catalyst.

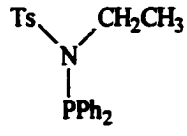

dpet

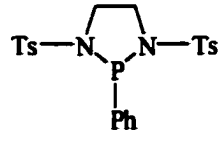

TosL

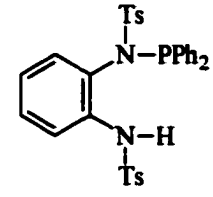

PPhyl

Table VI. Hydroformylation Results for **PPhyl**

L (equivalents)	alkene (equiv)	time (hour)	n/i	yield (%)	TOF
dpet (10)	1-hexene (200)	4	2.5	82	39
TosL (10)	1-octene (200)	5.5	1.7	57	21
PPhyl (5)	1-octene (200)	4	1.6	2.6	1.4

Conditions: 60 °C, 84 psi (6 atm) in THF. $Rh(acac)(CO)_2$ as the precursor of catalyst. [Rh] = 0.004 M

Styrene is quite reactive in hydroformylation and turns out to give rise to predominantly the branched aldehyde, so it is generally the substrate of choice for asymmetric hydroformylation, besides being a natural entry point for chiral naproxen analogs, for instance.[2] The data for the hydroformylation of styrene for PPh_3 and **diTosL** is given in Table VII. In this case the branched aldehyde is desired. It is seen from the data that PPh_3 gives an n/i ratio of 0.19 and 88% yield of total aldehydes. **DiTosL** gives an n/i ratio of 0.67 (2 equivalents used) to 0.71 (10 equivalents used) and 85% to 66% yield. Its selectivity for the branched aldehyde is not as good as that for PPh_3, although the yield is comparable.

Table VII. Hydroformylation Results of Styrene in THF

L (equivalents)	alkene (equiv)	time (hour)	n/i	yield (%)	TOF
PPh_3 (10)	styrene (674)	4	0.19	88	140
diTosL (2)	styrene (674)	4	0.67	85	140
diTosL (10)	styrene (674)	4	0.71	66	110

Conditions: 60 °C, 84 psi (6 atm) in THF. $Rh(acac)(CO)_2$ as the precursor of catalyst. [Rh] = 0.002 M

I. Comparison of hydroformylation results

TosL and **diTosL** are the first two *N*-sulfonyl ligands synthesized in our lab. Since this is a new class of trivalent phosphorus ligands, the electronic,

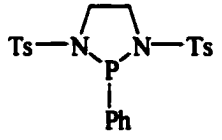

TosL

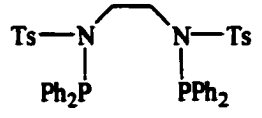

diTosL

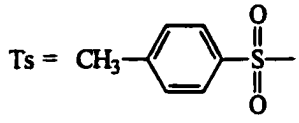

steric and geometric properties warrant investigation. The preliminary hydroformylation results (Table IV) showed that the chelate ligand, **diTosL**, favored the formation of linear aldehydes more than the monodentate ligand, **TosL**, so we focused on chelate ligands and their geometric properties. The following ligands were designed:

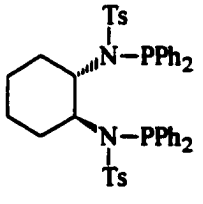

BDC

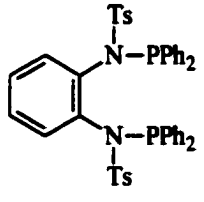

diPPhyl

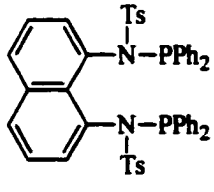

diPNAP

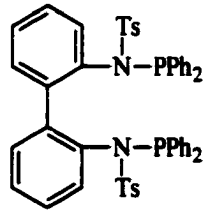

BBT

Ligands **BDC** and **diPPhyl** each would give a 7-member chelate ring with rhodium, the same as **diTosL**, but their backbones are more rigid than **diTosL**. Furthermore, these two ligands allow one to compare the

difference between an aliphatic linkage and an aromatic backbone. Ligands **diPNAP** and **BBT** would give 8- and 9-member chelate rings, respectively. The backbone of **BBT** is a little more flexible than **BDC**, **diPPhyl** and **diPNAP** since the two benzene rings of biphenyl are able to rotate around the C-C single bond. In addition, **BBT** is an analog of Casey's **BISBI** ligand (Schemes III, IV). They both have the same chelate ring size, but **BBT** would be a poor donor ligand because the Ts(Ar)N group would be attached to the diphenylphosphino group, while the **BISBI** ligand is relatively electron-donating because the $ArCH_2$ group is attached to the diphenylphosphino group.

During the synthesis of these ligands, however, none of them could be prepared using the procedure that was suitable for **diTosL**,[20] that is, reacting the corresponding sulfonamide with PPh_2Cl in THF or benzene in the presence of triethylamine. Even when BuLi, a much stronger base than Et_3N, was used, **diPPhyl** and **diPNAP** were still not formed. In **diTosL**, the two carbons linking both N atoms could rotate around the C-C single bond and the most stable conformation around the two carbons was expected to be anti staggered (Scheme VI). In the case of the starting material of **BDC**, on the other hand, both sulfonamido groups occupy equatorial sites. The preferred conformation is gauche. For the starting materials of **diPPhyl** and

diPNAP, the two N atoms lie in the plane of the backbone, and unlike in **diTosL**, the sulfonamido groups in the starting materials must be eclipsed;

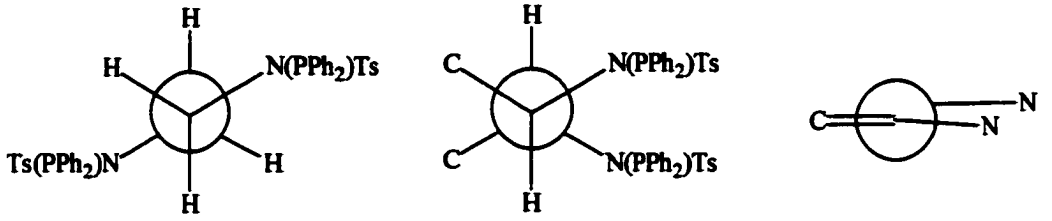

diTosL (anti staggered) **BDC** (gauche) **diPPhyl & diPNAP** (syn coplanar)

Scheme VI

that is, they are syn coplanar. These conformations would create high steric hindrance around the N atoms, especially after one diphenylphosphino group had been attached to one N atom, resulting in the difficulty for the second phosphorus atom in approaching the second N atom.

In the case of the precursor to **BBT**, although the carbon linkage was two carbons longer than that of **diTosL** and there was flexibility on the backbone, the **diTosL** procedure still failed to produce **BBT**. However, **BBT** might form when a strong base, BuLi, was used. The reason could be that the nucleophilicity of the N atom was weakened when it was attached to an aromatic ring, instead of an aliphatic carbon.

We also designed ligands **BTosL** and **ETosL**, chelating analogs of **TosL**. Unfortunately, these two ligands are not soluble in common

hydroformylation solvents, such as benzene, toluene, or THF. In DMF, **BTosL** showed no catalytic ability for the hydroformylation reaction (Table V), indicating that these ligands are not suitable to catalyze hydroformylation reactions.

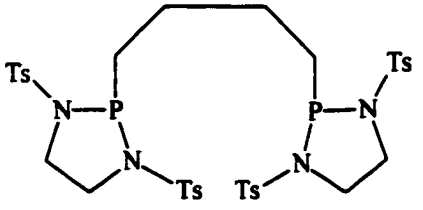

BTosL

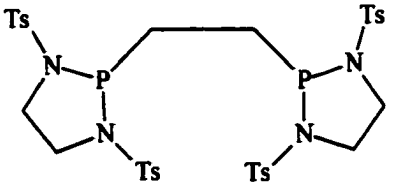

ETosL

Due to difficulty in synthesis of **diTosL** analogs designed here, for continuing study, it may be necessary to reduce steric hindrance of the target ligands, such as replacing the *p*-toluenesulfonyl group with the methanesulfonyl group. For instance, the sulfonamide precursor, $MsNHC_6H_4C_6H_4NHMs$, [**BBMs**] has been prepared (see Experimental Section). It can be used to synthesize the **diTosL** analog ligand.

III. Conclusion

The electron-withdrawing chelating ligand **diTosL** strongly favors the formation of linear aldehyde in hydroformylation of 1-hexene. Two reasons should be taken into account: π-acceptor ability of the phosphorus donor ligand due to the electron-withdrawing sulfonamide group, and chelation. The known chelating ligand **EMPA** has a methyl group in place of the tosyl group of **diTosL** and therefore is relatively electron-donating. It gives an n/i ratio of 2.3 for hydroformylation of 1-hexene while **diTosL** produces a value of 10. On the other hand, the ligand **dpet**, the monodentate analog of **diTosL**, also gives lower selectivity for the linear aldehyde, showing that, chelation in addition to the sulfonamide group is required for high selectivity. As the amount of **dpet** increases, the rate increases and the yield can be pushed up to the levels obtained with only one equivalent of **diTosL**, but the n/i ratio remains the same.

In order to investigate the steric and electronic effects and to improve its regioselectivity for the linear aldehyde, modifications of **diTosL** were sought and the chelating ligands **BDC**, **diPPhyl**, **diPNAP**, and **BBT** were designed. However, none of them could be prepared using the procedure that was suitable for **diTosL**. The common feature of these designed ligands is that the backbone is rigid. The two bulky groups, $Ts(PPh_2)N$, are much

closer to each other than in **diTosL**, and the high degree of steric hindrance around the N atoms evidently precludes attachment of both diphenylphosphino groups.

Since both chelation and a single sulfonamide group attached to the phosphorus donor atom lead to high selectivity, synthesis of a chelating analog of TosL, having two sulfonamide groups attached to phosphorus, was desired. **BTosL** and **EtosL**, two chelating analogues of **TosL**, were prepared. Unfortunately, **BTosL** and **ETosL** were not soluble in common hydroformylation solvents such as benzene, toluene and THF. In DMF, **BTosL** showed no catalytic ability for the reaction. The selectivity and rate for **diTosL** were also lowered in DMF, while the selectivity for PPh_3 did not change. This suggests that the more strongly coordinating solvent DMF prevents the weakly coordinating phosphinamide ligands from binding to Rh, and so the additives can have no effect on the reaction. The better donor PPh_3 is not affected simply because it still binds rhodium in DMF.

For continuing study, it may be necessary to reduce the steric hindrance of the target ligands, perhaps by replacing the *p*-toluenesulfonyl group with the methanesulfonyl group or with longer alkyl chain sulfonyl groups. This change may also be helpful in improving the solubility of **TosL** chelating analogues.

IV. Experimental Section

General Considerations. Manipulations of air-sensitive compounds were carried out in a Vacuum Atmospheres inert-atmosphere drybox under recirculating nitrogen gas. Solvents stored in the box were purified under nitrogen. Acetonitrile was purified by sequential distillation from calcium hydride and then phosphorus pentoxide. Benzene, ether and THF were distilled from sodium benzophenone ketyl. Hexane (containing alkene impurities) was purified by washing successively with the following solutions and water: 5% of concentrated nitric acid in concentrated sulfuric acid, water, sodium bicarbonate solution, and water. The washed hexane was then dried over calcium chloride and distilled from *n*-butyllithium in hexane. Methylene chloride and chloroform were distilled from phosphorus pentoxide. Triethylamine was distilled from calcium hydride. DMF was shaken with potassium hydroxide and distilled from calcium oxide. 1,4-Dioxane was treated with calcium hydride until no bubbles appeared and then distilled. *t*-Butyl alcohol was distilled from calcium oxide. Pyridine was dried over potassium hydroxide pellets and distilled over BaO. 1,4-Dibromobutane (Aldrich) and diethylamine were distilled before use.

CD_2Cl_2 and $CDCl_3$ were vacuum-transferred from phosphorus pentoxide while C_6D_6 was vacuum-transferred from sodium benzophenone ketyl.

NMR spectra were recorded on a Bruker DPX-400 spectrometer; chemical shifts are reported relative to hydrogen in C_6D_6 (δ 7.15), $CDCl_3$ (δ 7.24), or CD_2Cl_2 (δ 5.32) ^1H NMR; and to carbon-13 in C_6D_6 at 128.0 ppm, $CDCl_3$ at 77.0 ppm or CD_2Cl_2 at 53.8 ppm for ^{13}C NMR. Gas Chromatography was carried out on a Perkin-Elmer GC, model 8500, using a carbowax-20M capillary column (25m x 0.32mm), a split injector and an FID detector. The retention time of n-heptanal was determined using an authentic sample purchased from Aldrich. Elemental analysis was done by Desert Analytics, Tucson, AZ.

The following chemicals were used as received: acetylacetone (Aldrich), 1,2-bis(dichlorophosphino)ethane ($Cl_2PCH_2CH_2PCl_2$, Strem Chemicals), butyllithium hexane solution (Aldrich), chlorodiphenylphosphine (Ph_2PCl, Aldrich), *trans*-1,2-diaminocyclohexane (Aldrich), 1,8-diaminonaphthalene (Aldrich), dichlorophenylphosphine ($PPhCl_2$, Aldrich), 2,2'-dinitrobiphenyl (Aldrich), ethylamine 70% aqueous solution (Aldrich), granular tin (Fisher Scientific), methanesulfonyl chloride (Aldrich), 1,2-phenylenediamine (Kodak), *p*-toluenesulfonyl chloride (Aldrich), $AgBF_4$ (Pennwalt), $AgSbF_6$ (Aldrich), *t*-BuOK (ACROS), and $RhCl_3 \cdot H_2O$ (Fisher Scientific).

Bis(diethylamino)chlorophosphine.[25a] **[$(Et_2N)_2PCl$] (1)** This compound is known. The preparation procedure described in reference 25a was modified as follows. A dropping funnel and a 3-necked round-bottom flask equipped with a magnetic stirrer (although a mechanical stirrer should be used in the future) were set up in the box, stoppered with septa and then brought outside. Hexane (rather than light petroleum, 200 mL) and PCl_3 (8.7 mL, 0.1 mol) were transferred to the flask via a syringe, and 41.4 mL (0.4 mol) of Et_2NH and 40 mL of hexane were transferred to the dropping funnel via a cannula. The flask was cooled in an EtOH/dry ice bath (-70 °C) and the Et_2NH solution was added dropwise to the PCl_3 solution over 1.5 hour under nitrogen gas. The contents were allowed to warm to room temperature and then filtered through a coarse frit carefully while nitrogen gas was blowing on the top of the funnel. The solid was quickly washed with two portions of hexane. The combined filtrate was distilled at 1 atmosphere until no more low boiling point distillates appeared, and then at reduced pressure. The fraction distilling at 55 °C/0.035 mmHg was collected (12.7 g, 60% yield), giving a colorless liquid. ^1H NMR ($CDCl_3$) δ 3.13 (b, 2H), 1.10 (t, 7.1 Hz, 3H); $^{13}C\{^1H\}$ NMR ($CDCl_3$) δ 41.10 (d, 18 Hz, CH_2), 13.79 (d, 4.7 Hz, CH_3); $^{31}P\{^1H\}$ NMR ($CDCl_3$) δ 160.73.

1,4-Bis[bis(diethylamino)phosphino]butane (BBB).[25b]

$[(Et_2N)_2P(CH_2)_4P(NEt_2)_2]$ (2) This compound is known. The following preparation procedure gives more details than are described in reference 25b. In the box, 1.54 g (63.2 mmol) of Mg turnings were added to 35 mL of THF in a round-bottom flask equipped with a magnetic stirrer, and a solution of 6.82 g (3.81 mL, 31.6 mmol) of 1,4-dibromobutane in 35 mL of THF was added to the dropping funnel. The dropping funnel was then capped with a rubber septum and the setup was then brought outside the box and, under the protection of nitrogen gas, the dibromobutane solution was slowly added over a period of 2 hours. After completion of addition, 30 mL of THF was added through the dropping funnel and the suspension was stirred until little Mg was left. Then the flask was cooled in a CCl_4/dry ice bath (- 23 °C) and a solution of 12.69 g (60.2 mmol) of bis(diethylamino)chlorophosphine in 35 mL of THF was added dropwise to the suspension through the same funnel over a period of 1 hour. The cooling bath was removed and stirring continued for an hour. At this point, 30 mL of 1,4-dioxane was added in one portion, giving copious amounts of magnesium salts as a white precipitate. The solid was filtered off through a coarse frit carefully while nitrogen gas was blowing on the top of the funnel, and then washed with two portions of THF. The filtrate was subject to fractional distillation and the product

distilled at 120-165 °C/0.035 mmHg, giving 2.7 g (22% yield) of a colorless liquid. This product is unstable in chloroform. ^{1}H NMR (C_6D_6) δ 2.96 (m, 16H, ethyl CH_2), 1.67 (b, 8H, chain CH_2), 0.98 (t, 7 Hz, 24 H); $^{13}C\{^{1}H\}$ NMR (C_6D_6) δ 42.82 (d, 15.5 Hz, ethyl CH_2), 28.29 (d, $^{1}J_{PC}$ = 3.4 Hz, chain CH_2), 27.39 (ABX pattern, 4 lines, chain CH_2, $^{2}J_{PC}$ = 28.00 Hz, $^{3}J_{P'C}$ = 9.60 Hz, $J_{PP'}$ = 15.00 Hz, $\Delta\nu_{PP'}$ =8.50 Hz), 15.24 (d, 2.8 Hz, CH_3); $^{31}P\{^{1}H\}$ NMR (C_6D_6) δ 89.26. Lit.[25b] δp (33% in toluene) 87.9.

1,4-Bis(dichlorophosphino)butane (BDB).[25b] $[Cl_2P(CH_2)_4PCl_2]$ (3) This compound is also described in reference 25b. The following preparation procedure gives more details. In the box, 1.7 g (4.2 mmol) of **BBB** was added dropwise to 2 mL (23 mmol) of PCl_3 over 30 min. Stirring was continued for one hour. The yellow suspension was subject to fractional distillation and the product distilled at 83 °C/0.07 mmHg, giving 0.80 g (75% yield) of a colorless liquid. ^{1}H NMR (C_6D_6) δ 1.44 (m, 4H), 1.08 (m, 4H); $^{13}C\{^{1}H\}$ NMR (C_6D_6) δ 41.86 (d, 45.0 Hz), 23.49 (ABX pattern, 4 lines, $^{2}J_{PC}$ = 17.50 Hz, $^{3}J_{P'C}$ = 6.00 Hz, $J_{PP'}$ = 12.00 Hz, $\Delta\nu_{PP'}$ =4.00 Hz); $^{31}P\{^{1}H\}$ NMR (C_6D_6) δ 194.45. Lit.[25b] δp (pure) 192±1 ppm.

***N*-Ethyl-*p*-toluenesulfonamide (4).[21]** This is a known compound. The following modified procedure is based on that described in reference 21. To

a solution of 5.44 g (0.14 mol) of NaOH in 150 mL of water in a 500-mL round-bottom flask was added 5 mL of an aqueous ethylamine solution (70% by mass, Aldrich) containing 2.8 g (0.06 mol) of $EtNH_2$. Under stirring, 12.96 g of *p*-toluenesulfonyl chloride (TsCl) was added. The contents were stirred for an hour, the suspension was filtered (and 4.59 g of TsCl was recovered), and then the clear filtrate was poured onto 12 mL of concentrated HCl in 10 g of ice in a 400-mL beaker with vigorous stirring. After 5 minutes of stirring, the suspension was filtered. The solid was washed with water three times and dried under vacuum overnight to give 3.96 g (45% yield based on TsCl) of white crystalline product. mp: 63-5 °C. Solubility: very soluble in ethanol, diethyl ether, chloroform and benzene; insoluble in hexane. ^1H NMR ($CDCl_3$) δ 7.76 (d, 2H, 8.2 Hz), 7.31 (d, 2H, 8.2 Hz), 4.43 (br, 1H), 3.00 (m, 2H), 1.10 (t, 3H, 7.2 Hz); $^{13}C\{^1H\}$ NMR ($CDCl_3$) δ 143.39, 136.95, 129.71, 127.13, 38.24, 21.53, 15.08.

***N*-Diphenylphosphino-*N*-ethyl-*p*-toluenesulfonamide (5, dpet).** In the dry box, 1.9 mL (2.3 g, 0.010 mol) of Ph_2PCl was added in 3 portions to a stirred solution of 2.00 g (0.010 mol) of TsNHEt and 1.7 mL (1.2 g, 0.012 mol) of Et_3N in 50 mL of benzene. The mixture was refluxed outside the box for 2 hours. The solvent was then removed on the vacuum line and the solid was brought into the box. Benzene (20 mL) was added to extract the

product from the $Et_3NH^+Cl^-$, which was filtered through Celite and the solvent in the filtrate was removed in vacuo again. The resultant solid was dissolved in 50 mL of anhydrous diethyl ether in air at ambient temperature (slow process) and recrystallized at –20 °C in the freezer outside the box for two days to give 1.3 g of $TsN(PPh_2)Et$ (yield 40%). mp 119-120 °C. ^1H NMR ($CDCl_3$) δ 7.80 (d, 8.2 Hz, 2H), 7.28 (d, 8.2 Hz, 2H), 7.33-7.18 (m, 10H), 3.42 (qd, $^3J_{HH}$=7.0 Hz, $^3J_{PH}$=2.2 Hz, 2H), 2.44 (s, 3H), 0.63 (t, $^3J_{HH}$=7.0 Hz, 3H); $^{31}P\{^1H\}$ NMR ($CDCl_3$) δ 55.12; $^{13}C\{^1H\}$ NMR ($CDCl_3$) (assignments made based on diTosL data[20]) δ 143.25 (C5), 138.88 (C8), 135.21 (d, $^1J_{PC}$ = 17.2 Hz, C1), 132.33 (d, $^2J_{PC}$ = 21.3 Hz, C2), 129.62 and 129.44 (C6 and C7), 128.55 (d, $^3J_{PC}$ = 6.0 Hz,

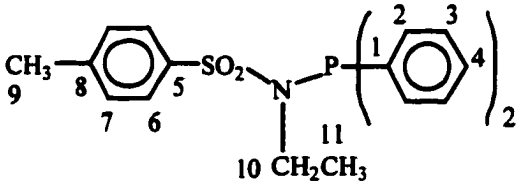

dpet

C3), 127.42 (d, $^4J_{PC}$ = 3.0 Hz, C4)(aryl), 44.14 (d, $^2J_{PC}$ = 2.4 Hz, C10), 21.56 (C9), 15.36 (C11). Anal. Calcd for $C_{21}H_{22}NO_2PS$: C, 65.78; H, 5.78; N, 3.65. Found: C, 65.80; H, 5.84; N, 3.53.

***P,P'*-1,4-Butanediylbis(1,3-di-*p*-toluenesulfonyl-1,3,2-diazaphospholidine) (6, BTosL).** In the box, a solution of 0.22 g (0.85

mmol) of 1,4-bis(dichlorophosphino)butane in 4 mL of THF was added dropwise to a suspension of 0.64 g (1.7 mmol) of $TsNHCH_2CH_2NHTs$ in 10 mL of THF in the presence of 0.71 mL (5.1 mmol) of triethylamine. The mixture was stirred for two hours, and then removed from the box and filtered. The solid was washed two times with a small amount of THF and dried under vacuum. The resultant solid was dissolved in 140 mL of chloroform at 50 °C in air and recrystallized at –20 °C for two hours to give 0.54 g (75% yield) of desired compound as a white, air-stable solid. ^1H NMR (CD_2Cl_2) δ 7.54 (d, 8.2 Hz, 8H), 7.16 (d, 8.2 Hz, 8H), 3.65 (m, 4H, C(Ha)Hb, ring), 3.05 (m, 4H, C(Ha)Hb, ring), 2.43 (s, 12H, CH_3), 1.88 (m, 4H, chain CH_2), 1.75 (m, 4H, chain CH_2); $^{31}P\{^1H\}$ NMR (CD_2Cl_2) δ 111.09; $^{13}C\{^1H\}$ NMR (CD_2Cl_2) δ 144.28 (ipso), 135.94 (ipso), 130.05 and 127.44 (d, J_{PC} = 1.9 Hz)(aryl), 48.18 (d, 5.8 Hz, ring CH_2), 36.18 (d, $^1J_{PC}$ = 32.1 Hz, chain CH_2), 23.91 (ABX pattern, 3 lines, chain CH_2, $^2J_{PC}$ = 22.00 Hz, $^3J_{PC}$ = 7.00 Hz, $J_{PP'}$ = 14.00 Hz, $\Delta\nu_{PP'}$ =1.65 Hz), 21.73 (CH_3). Anal. Calcd for $C_{36}H_{44}N_4O_8P_2S_4$: C, 50.81; H, 5.21; N, 6.58; Found: C, 51.07; H, 4.83; N, 6.50.

***P,P'*-1,2-Ethanediylbis(1,3-di-*p*-toluenesulfonyl-1,3,2-diazaphospholidine) (7, ETosL).** In the box, a solution of 0.54 g (2.3 mmol) of 1,2-bis(dichlorophosphino)ethane in 6 mL of THF was added

dropwise to a suspension of 1.7 g (4.6 mmol) of $TsNHCH_2CH_2NHTs$ in 30 mL of THF in the presence of 1.6 mL (11.5 mmol) of triethylamine. The mixture was refluxed for 15 min outside the box under nitrogen, and then filtered in air through a frit. The solid was washed two times with a small amount of THF and then dried in vacuo for one hour. Since Et_3NHCl dissolves much faster in methylene chloride than **ETosL**, Et_3NHCl was removed by washing the powder with 40 mL of methylene chloride yielding 1.27 g (67% yield) of spectroscopically pure product as a white, air-stable solid. Recrystallization from methylene chloride (0.26 g dissolved in 20 mL of boiling CH_2Cl_2 in air and then stored at –20 °C for six hours) gave analytically pure material (54% recovery). ^1H NMR (CD_2Cl_2) δ 7.55 (d, 8.2 Hz, 8H), 7.18 (d, 8.2 Hz, 8H), 3.70 (m, 4H, C(Ha)Hb), 3.08 (m, 4H, C(Ha)Hb), 2.43 (s, 12H, CH_3), 2.01 (t, J_{PH}=7.5 Hz, 4H, chain CH_2); $^{31}P\{^1H\}$ NMR (CD_2Cl_2) δ 107.68; $^{13}C\{^1H\}$ NMR (CD_2Cl_2) δ 144.45 (ipso), 135.82 (ipso), 130.12 and 127.45 for four aromatic carbons; three aliphatic carbons: 48.22 (ring CH_2), 28.15 (dd, $J_{PC} = 41$ Hz, $J_{PC'} = 19$ Hz, $J_{PP'} = 0$), 21.74 (CH_3). Anal. Calcd for $C_{34}H_{40}N_4O_8P_2S_4$: C, 49.63; H, 4.90; N, 6.81. Found: C, 49.32; H, 4.91; N, 6.59.

***N,N'*-1,2-Phenylenebis(*p*-toluenesulfonamide).[29] [*o*-$TsNHC_6H_4NHTs$] (8)** This compound was prepared according to the procedure described in

reference 29. A solution of 34.9 g (0.183 mol) of TsCl in 33 mL of HPLC grade pyridine was added dropwise to a solution of 7.57 g (0.070 mol) of 1,2-phenylenediamine in 17 mL of pyridine over a period of 2.5 hours with vigorous stirring. The rate of addition was adjusted to keep the temperature of the mixture below 60 °C without external cooling. After stirring overnight, the contents were poured with stirring in portions into 250 mL of 15% HCl solution. After three hours of stirring, the initially oily product completely solidified. The solid was collected on a coarse frit, dried, and recrystallized from boiling glacial acetic acid to give 20.3 g (70% yield) of product as a beige solid. Solubility data: very soluble in acetone and THF; 2.5 mg/mL benzene; 15 mg/mL methylene chloride; 10 mg/mL chloroform; insoluble in ether even in the presence of triethylamine. ^{1}H NMR ($CDCl_3$) δ 7.57 (d, 8.2 Hz, 4H), 7.22 (d, 8.2 Hz, 4H), 7.03 (m, 2H), 6.97 (m, 2H), 6.81 (b, 2H), 2.39 (s, 6H); $^{13}C\{^1H\}$ NMR ($CDCl_3$) δ 144.21, 135.42, 130.85, 129.63, 127.55, 127.40, 126.27, 21.62.

***N*-(Diphenylphosphino)-*N,N'*-1,2-phenylenebis-*p*-toluenesulfonamide (9, PPhyl).** In the box, 0.54 g (2.4 mmol) of Ph_2PCl was added to a solution of 1.0 g (2.4 mmol) of *N,N'*-ditosyl-*o*-phenylenediamine and 0.49 g (4.8 mmol) of triethylamine in 17 mL of THF. After stirring for 2 hours, the mixture was filtered through Celite to remove Et_3NHCl, washed twice with a

small amount of THF, and the solvent removed in vacuo. The resultant solid was recrystallized from about 10 mL of $CHCl_3$/ether (1:1 v/v) at – 40 °C overnight to give 1.2 g (83% yield) of **PPhyl** as a white solid. ^1H NMR ($CDCl_3$) δ 7.14-7.61 (m, 20H), 6.98 (m, H2), 6.42 (td, 7.7Hz, 1.4Hz, H3), 5.86 (dd, 8.0Hz, 1.4Hz, H1), 2.41 (s, 3H), 2.32 (s. 3H); $^{31}P\{^1H\}$ NMR ($CDCl_3$) δ 72.10 ppm; $^{13}C\{^1H\}$ NMR ($CDCl_3$) δ 144.41, 143.66, 136.92, 136.40, 135.72, 134.75 (d, 17.3Hz), 134.20 (d, 25.2 Hz), 133.06 (d, 21.5Hz), 132.10, 130.27, 129.43, 129.04 (d, 1.6Hz), 128.97, 128.34 (t, 2.7Hz), 128.24, 127.53, 122.53, 117.49 (aryl), 21.66, 21.53. Anal. Calcd for

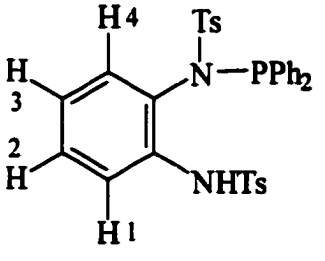

$C_{32}H_{29}N_2O_4PS_2$: C, 63.99; H, 4.87; N, 4.66. Found: C, 64.03; H, 4.86; N, 4.72.

1,8-Di-*p*-toluenesulfonamidonaphthalene.[29] [1,8-TsNHC$_{10}$H$_6$NHTs] (10) This compound was prepared according to the procedure described in reference 29 except for the recrystallization solvent. A solution of 28.0 g (0.147 mol) of TsCl in 53 mL of HPLC grade pyridine was added dropwise to a solution of 11.1 g (0.070 mol) of 1,8-diaminonaphthalene in 20 mL of

pyridine over a period of 2.5 hours with vigorous stirring. The rate of addition was adjusted to keep the temperature of the mixture below 60 °C without external cooling. After stirring overnight, the contents were poured with stirring in portions into 250 mL of 15% HCl solution. After three hours of stirring, the initially oily product completely solidified. The solid was collected on a frit, dried and recrystallized from methylene chloride to give 24.4 g (56% yield) of product as a beige solid. mp: 206-7 °C (Lit.[29] 208 °C). Solubility data: 18 mg/mL methylene chloride; 17 mg/mL THF; insoluble in ether. ^{1}H NMR ($CDCl_3$) δ 8.34 (b, 2H), 7.68 (d, 8.2 Hz, 4H), 7.65 (dd, 8.4 Hz, 0.8 Hz, 2H), 7.23 (m, 6H), 7.04 (dd, 7.5 Hz, 0.8 Hz, 2H), 2.38 (s, 6H); ^{13}C{^{1}H} NMR ($CDCl_3$) δ 144.26, 136.22, 135.26, 131.28, 129.62, 128.14, 127.71, 125.59, 123.94, 123.48, 21.60.

2,2'-Diaminobiphenyl.[37] (11) This compound was prepared using a modification of the procedure described in reference 37. Granular tin (17.09 g, 0.144 mol) was added to a suspension of 8.79 g (0.0360 mol) of 2,2'-dinitrobiphenyl and 72 mL of concentrated HCl in 180 mL of absolute ethanol. The mixture was refluxed for 30 minutes, cooled to room temperature, and then poured onto about 300 g of ice. The ice-cold solution was made basic with 10% NaOH yielding a suspension, which was extracted three times with ether. The combined ether extracts were washed with water

three times and dried over anhydrous Na_2SO_4 overnight. Filtration followed by removal of ether from the filtrate gave a yellow-orange solid which was washed with hexane three times and then recrystallized from absolute ethanol to give 4.02 g (61% yield) of product as white crystals. Under UV light, it shows a purple spot on a silica TLC plate at Rf = 0.38 (benzene : ethyl acetate = 20:1).

***N,N'*-[1,1'-biphenyl]-2,2'-diylbis(*p*-toluenesulfonamide) (BDT).[38] (12)** [$TsNHC_6H_4C_6H_4NHTs$] This compound was prepared according to the procedure described in the reference 38 except for the recrystallization solvent. A solution of 10.82 g (56.7 mmol) of *p*-toluenesulfonyl chloride (TsCl) in 16 mL of pyridine was added dropwise to a solution of 4.02 g (21.8 mmol) of 2,2'-diaminobiphenyl in 10 mL of pyridine. The mixture was stirred overnight and then poured into a mixture of 65 mL of concentrated HCl and 105 g of ice. The mixture was stirred for one more hour, the suspension was filtered, and the solid was washed with water until the filtrate was neutral. Drying under vacuum overnight gave 10.9 g of crude product. Recrystallization from boiling glacial acetic acid gave 8.94 g (83% yield) of a white crystalline product. Solubility: soluble in benzene, ethyl acetate, chloroform, methylene chloride and acetone; insoluble in ether. ^1H NMR ($CDCl_3$) δ 7.67 (d, 8.1 Hz, 2H), 7.49 (d, 8.2 Hz, 4H), 7.35

(td, 7.5 Hz, 1.3 Hz, 2H), 7.24 (d, 8.2 Hz, 4H), 7.04 (td, 7.5 Hz, 0.8 Hz, 2H), 6.49 (dd, 7.6 Hz, 1.3 Hz, 2H), 5.88 (s, 2H), 2.42 (s, 6H); $^{13}C\{^{1}H\}$ NMR ($CDCl_3$) δ 144.57, 135.85, 134.87, 130.26, 129.99, 129.89, 127.44, 127.09, 125.14, 121.29, 21.63.

***N*-Diphenylphosphino-*N,N'*-[1,1'-biphenyl]-2,2'-diylbis(*p*-toluenesulfonamide) (DBT) [Ts(Ph_2P)$NC_6H_4C_6H_4$NHTs] (13)** In the box, a solution of 0.89 g (4.1 mmol) of Ph_2PCl in 6 mL of THF at 15 °C was added dropwise through a dropping funnel to a solution of 1.0 g (2.0 mmol) of *N,N'*-[1,1'-biphenyl]-2,2'-diylbis(*p*-toluenesulfonamide) (**BDT**) and 0.53 g (5.2 mmol) of triethylamine in 14 mL of THF. A white precipitate appeared immediately. The mixture was stirred for one hour, filtered, and the solvent removed in vacuo. The resultant solid was dispersed in toluene, in which it was largely insoluble, and stirred for one hour, filtered and washed with hexane 3 times, giving 1.21 g (88% yield) of crude product. This product is not stable on silica gel. When TLC was performed on a silica gel plate, it decomposed back to the biphenyl starting material. However, the powder is stable in the glove box at room temperature for at least 5 months. Recrystallization of 0.131 g of the crude product in 0.8 mL of chloroform and 1.5 mL hexane in the freezer overnight gave 0.080 g (61% yield) of product still containing 6% by mass of triethylamine hydrochloride salt. The

powder is stable in air for at least 3 days. ^{1}H NMR ($CDCl_3$) δ 7.78~6.23 (m, 27H), 2.44(s), 2.38(s), 2.37(s) and 2.36(s) ppm (total of 6H for 4 methyl groups); the four methyl signals formed 2 sets: 2.44 and 2.37 (1:1 ratio) ppm, 2.38 and 2.36 (1:1 ratio) ppm. $^{31}P\{^{1}H\}$ NMR ($CDCl_3$) δ 74.11 and 72.24 ppm in a ratio of 1:1.7 in peak height. The ^{13}C NMR spectrum was not obtained satisfactorily due to weak signals resulting from the dilute solution.

Synthesis of *N,N'*-[1,1'-biphenyl]-2,2'-diylbismethanesulfonamide [BBMs][39] [$MsNHC_6H_4C_6H_4NHMs$] (14) This compound was prepared using a modification of the procedure described in reference 39. To a 50-mL round-bottom flask containing a magnetic stirring bar was added a yellowish solution of 2.0 g (10.9 mmol) of 2,2'-diaminobiphenyl in 6 mL of pyridine. A 10-mL pressure-equalizing dropping funnel connected to a nitrogen bubbler was attached to the flask. The system was purged with nitrogen several times. A red solution of 2.1 mL (3.1 g, 27.1 mmol) of methanesulfonyl (mesyl) chloride in 5 mL of pyridine was transferred to the funnel via a cannula. The mesyl chloride solution was added to the aminobiphenyl solution over a period of 35 minutes. The addition was slow enough to keep the reaction solution below 60 °C without external cooling. A precipitate appeared in 25 minutes. The mixture was stirred overnight,

then poured into a 250-mL beaker containing 30 mL of concentrated HCl and 55 g of ice (15% HCl). After stirring for two more hours, the mixture was filtered and the solid was washed with water until the filtrate was neutral. Drying under vacuum overnight gave 3.85 g of crude beige product that was contaminated with *N,N,N'*-[1,1'-biphenyl]-2,2'-diyltrismethanesulfonamide [$Ms_2NC_6H_4C_6H_4NHMs$] (~10%) as judged by ^1H NMR. Hydrolysis of this by-product in 100 mg of the crude product was carried out using 3.3 ml of 10% NaOH solution at 50 °C for 5 hours.[34b] The suspension was then cooled in an ice-water bath and acidified slowly with 1 mL of concentrated HCl. The mixture was stirred for 1 hour, the contents were filtered, and the solid was washed with water until the filtrate was neutral. Drying in air gave the desired product. ^1H NMR ($CDCl_3$) δ 7.66 (d, 8.2 Hz, 2H), 7.49 (m, 2H), 7.27 (m, 2H), 7.22 (m, 2H), 6.15 (b, 2H), 3.02 (s, 6H); $^{13}C\{^1H\}$ NMR ($CDCl_3$) δ 135.27, 131.14, 130.55, 125.89, 125.37, 119.96, 40.58.

***Trans*-1,2-Di(*p*-toluenesulfonamido)cyclohexane (DTC).[40] [*Trans*-1,2-(*p*-TsNH)$_2$C$_6$H$_{10}$] (15)** The following procedure is a modification of the procedure described in reference 50. With stirring, preferably mechanical, 8.35 g (43.8 mmol) of TsCl was added to a solution of 5.03 g (43.8 mmol) of trans-1,2-diaminocylohexane in 40 mL of water maintained at 60 °C to less

than 70 °C with an oil bath. A solution of 3.54 g of NaOH in 5 mL of water was added in portions, followed by addition of the second portion of 8.35 g of TsCl. The contents were then stirred at 100 °C for one hour. After cooling to room temperature, the suspension was poured into 6 mL of concentrated HCl in 30 g of ice. The suspension was stirred and then filtered. The solid was washed with water until the filtrate was neutral and then dried. Recrystallization from absolute ethanol gave 16 g of product as white crystalline needles (95% recovery and overall 86% yield). Solubility: soluble in acetone, THF and CH_2Cl_2; slowly soluble in $CHCl_3$ and ethyl acetate; slightly soluble in ethanol and benzene; insoluble in ether and hexane. ^1H NMR ($CDCl_3$) δ 7.76 (d, 8.2 Hz, 4H), 7.31 (d, 8.2 Hz, 4H), 4.85 (b, 2H), 2.74 (b, 2H), 2.43 (s, 6H, CH_3), 1.85 (b, 2H), 1.55 (b, 2H), 1.10 (b, 4H); $^{13}C\{^1H\}$ NMR ($CDCl_3$) δ 143.59, 137.02, 129.78, 127.26, 56.61, 33.38, 24.23, 21.58.

(Acetylacetonato)dicarbonylrhodium(I).[41] **[Rh(acac)(CO)$_2$] (16)** This compound was prepared using the procedure described in the reference 41. Four mL (3.9 g, 39 mmol) of acetylacetone was added to a red solution of 1.0 g (3.8 mmol) of $RhCl_3 \cdot 3H_2O$ in 20 mL of DMF. The solution was boiled in the air while stirring in an Erlenmeyer flask covered with a watch glass. After 7 min, the solution became orange-yellow. After 30 min, the

solution was cooled to room temperature and diluted with 50 mL of water to give an immediate voluminous crimson precipitate, which was filtered off through a coarse frit, and washed with small amounts of ethanol and ether yielding 1.02 g of crude product. Recrystallization from hexane gave 0.48 g of pure product as long green needles. IR (hexane): 2082 (s), 2067 (w), 2014 (s), 1983 (w) cm^{-1}. ^1H NMR ($CDCl_3$) δ 5.61 (s, 1H), 2.07 (s, 6H); $^{13}C\{^1H\}$ NMR ($CDCl_3$) δ 187.22, 183.67 (d, 72 Hz), 101.63 (d, 2 Hz), 26.97.

Attempt to synthesize *N,N'*-bis(diphenylphosphino)-*N,N'*-ditosyl-1,8-diaminonaphthalene (diPNAP). (17)

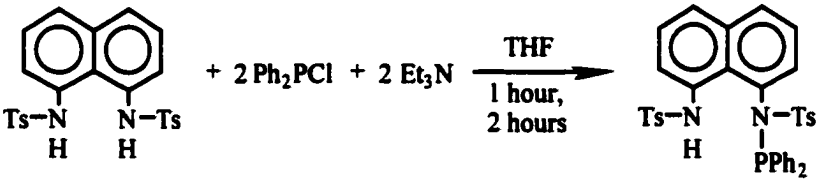

(17)

In the box, 0.95 g (4.3 mmol) of Ph_2PCl was added to a solution of 1 g (2.1 mmol) of *N,N'*-ditosyl-1,8-diaminonaphthalene[29] (TNAP) in 17 mL of THF containing 0.78 mL (5.6 mmol) of triethylamine. The solution was stirred at room temperature, and after one hour, a few mL of liquid were taken from the solution. After removal of most solvent in vacuo, $CDCl_3$ was added and the NMR spectrum of the solution recorded. Major NMR data

($CDCl_3$): δ_P 82.36 ppm (Ph_2PCl), 70.66 ppm (**PNAP**); δ_H 2.30 ppm (s, CH_3 of **TNAP**), 2.50 (s) and 2.29 (s) (CH_3 of **PNAP**). Relatively, about 33% of the **TNAP** was converted into **PNAP**, according to the methyl proton integration. Purification of **PNAP** was not carried out.

Attempt to synthesize *N,N'*-(1,1'-biphenyl)-2,2'-diylbis(*N*-diphenylphosphino-*p*-toluenesulfonamide). (BBT) (18)

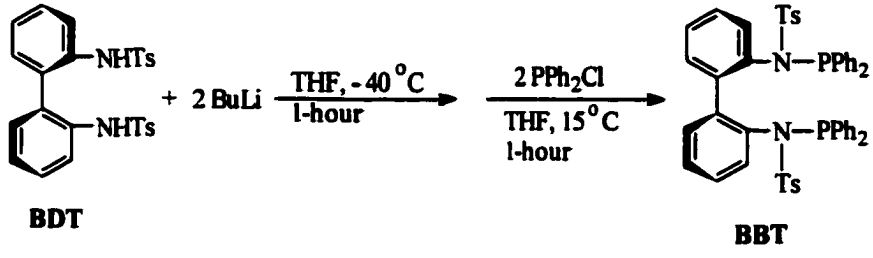

BDT **BBT** (19)

In the box, 124 μL of 1.6 M BuLi hexane solution (0.2 mmol BuLi) was added to a –40 °C solution of 48.7 mg (0.1 mmol) of **BDT** in 0.5 mL of THF. The mixture was stored in the freezer for an hour, followed by addition of 36 μL (0.2 mmol) of PPh_2Cl at 15 °C. After a few minutes of stirring a precipitate formed. Thirty minutes later, the suspension was filtered through Celite. A little methylene chloride was added to quench the reaction. After removing the methylene chloride, some $CDCl_3$ solvent was added for NMR test. The NMR solution was filtered through Celite before the spectrum was taken. The spectra indicated a mixture of a couple of

products and unreacted phosphine. Major NMR data: δ_P 74.1, 72.2, 70.7 (most intense) ppm. δ_H 2.35 (most intense CH_3) ppm.

Attempt to synthesize TosL analog A. (19) Under stirring at – 40 °C, 15 μL (20 mg, 0.11 mmol) of $PPhCl_2$ was added via a micro syringe to a suspension of 46 mg (0.11 mmol) *trans*-1,2-di-*p*-toluenesulfonamidocyclohexane in 38 μL (28 mg, 0.27 mmol) of Et_3N and 3 mL of diethyl ether. The contents were stirred at 15 °C for 2 hours, yielding

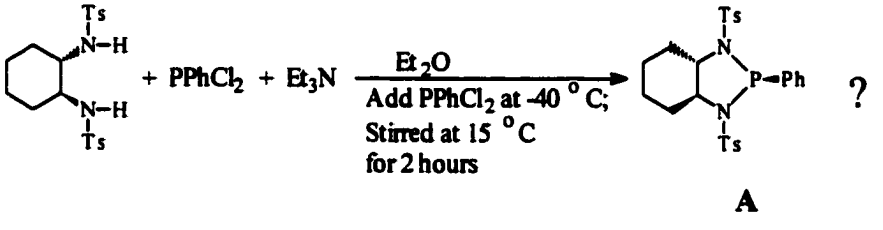

A (20)

a large amount of white powder. The precipitate, on the basis of the NMR spectrum, contained mainly Et_3NHCl salt and unreacted sulfonamide, and was filtered off. The solvent in the filtrate was removed. The resultant white powder was contaminated by the Et_3NHCl salt. Major NMR ($CDCl_3$) data: δ_H 7.9-7.8 (m, 4H), 7.5-7.4 (m, 5H), 7.3-7.2 (m, 2H), 7.00 (d, J = 8.1 Hz, 2H), 2.68 (d, J = 8.1 Hz, 1H), 2.55 (s, 3H), 2.47 (td, 1H), 2.37 (s, 3H), 2.29 (d, J = 13.4 Hz, 1H), 1.68 (b, 1H), 1.59 (b, 1H), 1.0-0.9 (m, 4H) ppm. δ_P 94.55 ppm. δ_C 144.1-126.6 (aromatic carbons), 67.23 (d, $^2J_{PC}$ = 3.7 Hz), 64.63 (d, $^2J_{PC}$ = 5.7 Hz), 31.91, 27.91, 23.96, 23.75, 21.76, and 21.59 ppm.

When the NMR solution exposed to air for 3 days, the ^{1}H and ^{31}P NMR spectra did not change significantly.

Attempt to synthesize diPPhyl. (20) In the box at –40 °C, 3 mL (1.6 M, 4.8 mmol) of BuLi hexane solution was added to a solution of 1.0 g (2.4 mmol) of *N,N'*-1,2-Phenylenebis(*p*-toluenesulfonamide) (**8**) in 25 mL of THF. The mixture was kept at –40 °C for 30 min, and then 880 μL (4.9 mmol) of PPh_2Cl at 20 °C was added with stirring. The mixture immediately turned orange and a precipitate appeared 30 minutes later. The contents were stirred for 24 hours. Iodomethane (0.3 mL, 4.8 mmol) was added to quench the reaction, followed by filtration on Celite. The solvent in the clear filtrate was removed under vacuum. The resultant orange solid was dried in vacuo for an hour (0.83 g of solid obtained), and then taken up in 7 mL of ether for 10 minutes. The turbid solution was filtered through Celite and the Celite was washed with a little amount of ether. The filtrate had to be filtered again until a clear filtrate was obtained. The filtrate was concentrated to ~ 6 mL and then stored at –40 °C for recrystallization for 7 days. The light yellow crystals formed were filtered, washed with small amount of ether three times, dried in vacuo for an hour, giving 49 mg of light yellow solid. Major NMR ($CDCl_3$) data: δ_H 7.83 (m, 4H), 7.47 (m, 2H), 7.42 (m, 4H), 7.30 (dd, 8.0 Hz, J_{PH} = 1.5 Hz, 2H), 6.97 (d, 8.0 Hz, 2H)

(aryl), 2.23 (s, 3H, CH_3); δ_P 41.78; δ_C 139.15 (d, 2.8 Hz), 135.34 (d, 3.4 Hz), 133.24 (s), 132.22 (d, 3.2 Hz), 131.65 (d, 10.3 Hz), 129.96 (b), 128.49 (d, 12.9 Hz), 122.28 (d, 4.6 Hz) and 21.15.

Hydroformylation of 1-hexene (one typical run). Reaction was carried out in a 90-mL Fisher-Porter vessel (Andrews Glass Co.) equipped with a magnetic stirrer and a single inlet, to which was attached a 4-way brass adapter equipped with a pressure gauge, gas inlet, and gas outlet. $Rh(acac)(CO)_2$ (6.71 mg, 0.0260 mmol) was weighed and then brought into the box. In the box, $Rh(acac)(CO)_2$, 39.3 mg (0.0533 mmol) of diTosL, 0.4734 g (5.62 mmol, 0.70 mL) of 1-hexene and 0.1465 g (0.24 mL) of decane (internal standard) were mixed in 5.0 mL of THF in the reaction vessel. The vessel was covered with parafilm, brought out of the box, and then quickly attached to the 4-way brass adapter installed in a well-ventilated fume hood. A shield was placed in front of the vessel. The vessel was flushed with 1:1 CO/H_2 synthesis gas at 84 psi three times and pressurized to 84 psi. Then the solution was heated to 60 °C in an oil bath for 4 hours. A small but sufficient reservoir of high-pressure syn gas feeds into the pressure regulator with the main tank shut off, so that the consumption of gas could be monitored while the reaction was maintained at constant pressure as described below. After cooling the reaction mixture,

the pressure of the system was released. The resultant solution was analyzed by GC. 0.483 g (4.23 mmol) of linear heptanal and 0.047 g (0.41 mmol) of isoheptanal were obtained, giving 83% yield (total amounts of aldehydes) and TOF of 45.

Before heating, the solution was light yellow. For the PPh_3 ligand, the solution remained yellowish throughout the experiment. For the other ligands used here, the solution turned color gradually from light yellow to orange or brown within 5 minutes of heating.

Precision of GC data and comparison of n/i ratio between GC and NMR instruments. The yields of aldehydes were determined by GC using an internal standard, and in addition NMR was used to provide an independent determination of the n/i ratio. Therefore, it is necessary to find out how precise the numbers can actually be. In addition, when a sample is withdrawn from reaction solution, do the results change if the products are separated from the catalyst? In order to test the accuracy of our analytical methods, 11 samples were tested. The results are summarized in Table VIII.

Table VIII: Precision of GC data and comparison to NMR results

Entry		Average w (g)		s		n/i		n/i
		3 runs	all runs	3 runs	all runs	3 runs	all runs	(NMR)
1-1	n	0.4650	0.4554	0.0214	0.0184	3.6	3.5	3.7
[k=6]	i	0.1306	0.1292	0.0096	0.0077	(±0.3)		(±0.7)
1-2	n	0.4078	0.4034	0.0209	0.0160	3.7	3.6	3.7
[k=5]	i	0.1109	0.1104	0.0046	0.0033	(±0.3)		(±0.7)
2-1	n	0.5109	0.5137	0.0278	0.0234	8.9	8.9	9
[k=4]	i	0.0574	0.0577	0.0041	0.0034	(±0.8)		(±3)
2-2	n	0.5168	0.5175	0.0292	0.0207	8.8	8.8	9
[k=5]	i	0.0590	0.0588	0.0034	0.0024	(±0.7)		(±3)
3-1	n	0.4781	0.4828	0.0206	0.0173	10.	10.	11
[k=5]	i	0.0465	0.0473	0.0040	0.0035	(±1)		(±4)
3-2	n	0.4788	0.4885	0.0143	0.0179	10.	10.	10
[k=5]	i	0.0479	0.0473	0.0022	0.0018	(±1)		(±4)
4-1	n	0.3194	0.3112	0.0134	0.0162	2.5	2.5	N/A
[k=5]	i	0.1304	0.1269	0.0017	0.0050	(±0.2)		
4-2	n	0.3157	0.3100	0.0044	0.0136	2.3	2.4	2.3
[k=7]	i	0.1389	0.1278	0.0116	0.0127	(±0.2)		(±0.5)
4-3	n	0.2840	--	0.0118	--	2.6	--	2.7
[k=3]	i	0.1083	--	0.0061	--	(±0.2)		(±0.5)
5	n	0.3268	0.3123	0.0119	0.0215	2.5	2.5	2.4
[k=5]	i	0.1330	0.1261	0.0055	0.0105	(±0.2)		(±0.5)
6	n	0.1935	0.1832	0.0195	0.0203	2.5	2.5	2.2
[k=5]	i	0.0770	0.0738	0.0045	0.0058	(±0.2)		(±0.5)

w -- mass; s -- standard deviation; k -- total number of runs.

Entries 1-1, 2-1, 3-1, 4-1, 5 and 6 were the solutions tested before vacuum transfer. Entries 1-2, 2-2, 3-2 and 4-2 were the solutions separated from the catalyst via vacuum transfer. Solutions 1-1 and 1-2 were from the same reaction and 1-1 was before vacuum transfer while 1-2 was after. Therefore, the n/i ratios for these two solutions should be the same or close. The other three pairs, 2-1 and 2-2, 3-1 and 3-2, 4-1 and 4-2, had the same relationship as 1-1 and 1-2. Solution 4-2 was further distilled to remove the low boiling-point solvent to give solution 4-3.

Three to seven runs were performed for each sample. The values of the n/i ratios between the first "3 runs" and "all runs" agree with each other. For entry 4-2 for instance, the difference in n/i ratio between "3 runs" (2.3) and "all runs" (2.4) is about 4%, suggesting that measuring up to 7 times is no better than 3 times. The errors of the n/i ratio fall into a range of 8% - 10% and are independent of how large the n/i value is.

The values of n/i ratio from NMR fairly agree with those from GC. The n/i ratio is determined by the ratio of integration of normal to branched aldehyde protons. Since the integration of aldehyde proton is small in the full spectrum, a larger error is expected than from the GC determination; furthermore, the greater the ratio, the larger the error.

When a sample is withdrawn from the reaction solution, it can be analyzed directly[13] or first quenched to deactivate the catalyst[14] or vacuum-transferred from the catalyst.[42] Comparison data before and after vacuum transfer (entries 1-1 and 1-2 to 4-1 and 4-2) are provided in the table. Based on these four pairs of n/i ratios, one can see that the mass of n-aldehyde drops on average 3.1% while the mass of iso-aldehyde drops 0.7%. This difference does not result in a significant change in n/i ratio.

Calculation of moles of syn gas used. In addition to the GC method, the consumption of syn gas could be used to estimate the yield of hydroformylation. In order to do so, it is necessary to find out the reservoir volume, V, between the tank pressure gauge on the regulator and the syn gas tank (see the picture below).

1. The volume, V1, of the ¼" copper tubing between the pressure gauge and the reaction bottle: (L – length of the tubing)

$V1 = \pi(d^2/4)L = 3.14 \times 0.46^2/4 \times 630 = 105$ (cm^3, or mL)

2. The syn gas volume, Vg, in the tubing and the reaction bottle:

Vg = 105 mL (V1) + 90 mL (the bottle volume) – 5 mL (reaction solution volume) = 190 mL

3. At normal pressure, the reaction bottle filled with 5 mL of water was attached to the tubing. The syn gas tank was closed and the reservoir

was filled with the gas. The pressure (high side) was noted, and then the regulator valve was opened to fill up the tubing and the bottle up

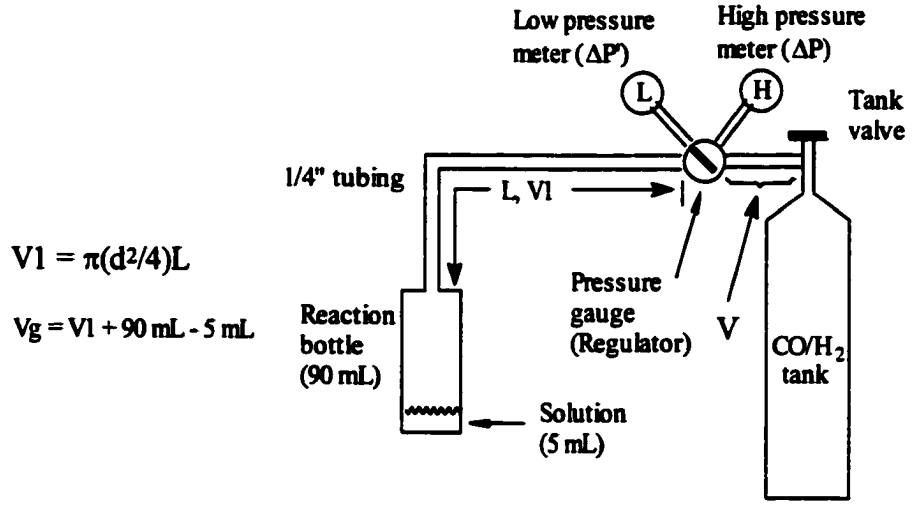

to 14 psi. The high change was 390 psi. Assuming constant temperature (T = 297 K), then:

$(\Delta P')Vg = (\Delta P)V$

$(\Delta P')Vg = (14/14.696) \times 190$ and $(\Delta P)V = (390/14.696)V$

where

Δn : millimoles of syn gas used

14.696: 1 atm = 14.696 psi

$\Delta P'$: Pressure change in psi read-out of the low pressure meter

ΔP : Pressure change in psi read-out of the high pressure meter

$V = (14/14.696) \times 190/(390/14.696) = 6.82$ mL

Once te reservoir volume between the tank pressure gauge on the regulator and the syn gas tank has been calculated, then the read-out of the pressure change, ΔP, of the reservoir for each hydroformylation run allows Δn for the hydroformylation reaction to be calculated as follow:

$\Delta n = (\Delta PV)/(RT) = (\Delta P/14.696) \times 6.8/(82.1T) \times (1000 \text{ mmol/mol}) =$

$5.64(\Delta P/T)$ (in mmol)

$n_{CO} = n_{H2} = \Delta n/2$

The yield calculated in this manner is usually lower than that from the GC method. For example, when two equivalents of **diTosL** to Rh were used for hydroformylation of 1-hexene, a 67% yield was calculated using this method while an 83% yield was obtained by GC. Errors in the pressure gauges and in the volume of the copper tubing most likely account for the difference.

GC parameters:

Instrument: Perkin-Elmer 8500 GC with a FID detector, a split/splitless injector, and a temperature-programmable oven, nitrogen carrier gas, and injection of 1 μL of sample at a split ratio of ~200 :1 on a carbowax-20M capillary column (length: 25 meter; Inner diameter: 0.32 mm; Film thickness: 0.25 micron).

Method for 1-hexene starting material (Sections 1-3 refers to the GC computer automation program):

Section 1 GC Control

	1	2
Oven temperature (°C):	40	110
Iso time (min)	3.5	3.5
Ramp rate (°C/min)	10.0	

Equilibration time: 0.2 min Total run time: 14 min

Head pressure: 10 psi Carrier gas tank pressure: 105 psi

Injector: 250 °C; Detector: 350 °C; FID sensitivity: low

Section 2 Timed events: after 1.00 min, relay 2 turned off.

Section 3 Data Handling (Acquisition):

DET 2 AREA SENS	<200 after performing SENS RUN
DET 2 BASE SENS	6
WIDTH	5
SKIM SENS	0
BASELINE CORR	B-B

Component	Retention Time(RT) (min)	Response Factor (RF)*
1-Hexene	1.80	0.7678
THF (solvent)	2.17†	1.0 (as unknown)
n-Decane	3.07†	1.0 (internal standard)
Isoheptanal	4.41	1.3200
Heptanal	5.96	1.3200

* RF was determined by injecting known amounts of authentic samples except for isoheptanal. The RF of isoheptanal was assumed to be the same as that of heptanal. Isoheptanal was identified by comparison of the ratio of its area to that of heptanal in the chromatogram to the ratio of isoheptanal to heptanal in the ^{1}H NMR spectrum.

† By the time hexene was used, the column was cut shorter. Compared to octene method, therefore, THF and n-decane have shorter retention times in hexene method.

Method for 1-octene starting material:

Section 1 GC Control

	1	2	
Oven temperature (°C):	40	180	
Iso time (min)	3.5	7.5	
Ramp rate (°C/min)	10.0		
Equilibration time:	0.2 min		Total run time: 25 min

Other conditions including those in Sections 2 and 3 are the same as those for 1-hexene.

Component	Retention Time(RT) (min)	Response Factor (RF)*
n-Octane	2.37	0.7756
1-Octene	2.54	0.8467
THF (solvent)	2.62†	0.8857
cis-2-Octene	2.67	0.7482
n-Decane	4.19†	1.0 (internal standard)
Isononanal	9.47	1.53
Nonanal	10.95	1.5296

* See above; isomonanal/nonanal ratios determined as described for heptanal.

† See above; retention times are longer here than in hexene method.

V. References

(1) Broussard, M. E.; Juma, B.; Train, S. G.; Peng, W. J.; Laneman, S. A.; Stanley, G. G. *Science* **1993**, *260*, 1784-1788.

(2) Nugent, W. A.; Rajanbabu, T. V.; Burk, M. J. *Science* **1993**, *259*, 479-483.

(3) Stille, J. K.; Su, H.; Brechot, P.; Parrinello, G.; Hegedus, L. S. *Organometallics* **1991**, *10*, 1183-1189.

(4) Sanchezdelgado, R. A.; Rosales, M.; Andriollo, A. *Inorg. Chem.* **1991**, *30*, 1170-1173.

(5) Pruett, R. L. "Hydroformylation," In *Adv. Organometallic Chem.*; F. G. A. Stone and R. West, Ed.; 1979; Vol. 17; pp 1-60.

(6) Pruett, R. L. "Industrial Organic Chemicals Through Utilization of Synthesis Gas," *Ann N Y Acad Sci* **1977**, *295*, 239-248.

(7) Pruett, R. L.; Smith, J. A. *J. Org. Chem.* **1969**, *34*, 327-330.

(8) Evans, D.; Osborn, J. A.; Wilkinson, G. *J Chem Soc A* **1968**, 3133.

(9) Brown, C. K.; Wilkinson, G. *J. Chem. Soc. A* **1970**, 2753.

(10) Hughes, O. R. Unruh, J. D. *J. Mol. Catal.* **1981**, *12*, 71.

(11) Cuny, G. D.; Buchwald, S. L. *J. Am. Chem. Soc.* **1993**, *115*, 2066-2068.

(12) Moasser, B.; Gladfelter, W. L.; Roe, D. C. *Organometallics* **1995**, *14*, 3832-3838.

(13) Casey, C. P.; Whiteker, G. T.; Melville, M. G.; Petrovich, L. M.; Gavney, J. A.; Powell, D. R. *J. Am. Chem. Soc.* **1992**, *114*, 5535-5543.

(14) Kranenburg, M.; Vanderburgt, Y. E. M.; Kamer, P. C. J.; Vanleeuwen, P. W. N. M.; Goubitz, K.; Fraanje, J. *Organometallics* **1995**, *14*, 3081-3089.

(15) Unruh, , J. D.; Christenson, J. R. *J. Mol. Catal.* **1982**, *14*, 19-34.

(16) Casey, C. P.; Paulsen, E. L.; Beuttenmueller, E. W.; Proft, B. R.; Petrovich, L. M.; Matter, B. A.; Powell, D. R. *J. Am. Chem. Soc.* **1997**, *119*, 11817-11825.

(17) Casey, C. P.; Paulsen, E. L.; Beuttenmueller, E. W.; Proft, B. R.; Matter, B. A.; Powell, D. R. *J. Am. Chem. Soc.* **1999**, *121*, 63-70.

(18) Moloy, K. G.; Petersen, J. L. *J. Am. Chem. Soc.* **1995**, *117*, 7696-7710.

(19) Trzeciak, A. M.; Glowiak, T.; Grzybek, R.; Ziolkowski, J. J. *J. Chem. Soc., Dalton Trans.* **1997**, 1831-1837.

(20) Hersh, W. H.; Xu, P.; Wang, B.; Yom, J. W.; Simpson, C. K. *Inorg. Chem.* **1996**, *35*, 5453-5459.

(21) Berkowitz, W. F. "Acid Hydrolysis of Nylon 66," *J. Chem. Educ.* **1970**, *47*, 536.

(22) Cloton, R.; Commons, C. J. *Aust J Chem* **1973**, *26*, 1493-1500.

(23) Bonnesen, P. V.; Puckett, C. L.; Honeychuck, R. V.; Hersh, W. H. *J. Am. Chem. Soc.* **1989**, *111*, 6070-6081.

(24) Strohmeier, W.; Müller, F. J. *Chem. Ber.* **1969**, *102*, 3608-3612.

(25) Juge, S.; Stephan, M.; Laffitte, J. A.; Genet, J. P. *Tetrahedron Lett.* **1990**, *31*, 6357-6360.

(26) a: Chantrell, P.G.; Pearce, C.A.; Toyer, C.R.; Twaits, R. *J. Appl. Chem.* **1964**, 563. b: Diemert, K.; Kuchen, W.; Kutter, J. *Phosphorus and Sulfur* **1983**, *15*, 155-164.

(27) Metzger, S. H.; Basedow, O. H.; Isbell, A. F. *J. Org. Chem.* **1964**, *29*, 627-630.

(28) Hersh, W. H. *J. Chem. Educ.* **1997**, *74(12)*, 1485-9.

(29) Stetter, H. *Chem. Ber.* **1953**, *86*, 161-7.

(30) Grim, S. O.; McFarlane, W. *Nature,* **1965,** *208,* 995.

(31) Mikiciuk-Olasik, E.; Kotelko, B. *Polish J Chem* **1984,** *58,* 1211-4.

(32) Cowley, A. H.; Kemp, R. A.; Wilburn, J. C. *Inorg. Chem.* **1981,** *20,* 4289-4293.

(33) Malisch, W.; Pfister, H. *Organometallics* **1995,** *14,* 4443-4445.

(34) Brown, C.; Murray, M. Schmutzler, R. *J. Chem. Soc.* (C), **1970,** 878.

(35) Gordon, Arnold J.; Ford, Richard A. in *The Chemist's Companion: A Handbook of Practical Data, Techniques, and References.* John Wiley & Sons, Inc. New York **1972,** p295.

(36) Grimblot, J.; Bonnelle, J. P.; Mortreux, A.; Petit, F. *Inorg. Chim. Acta* **1979,** *34,* 29-36.

(37) Tashiro, M.; Yamato, T. *J. Org. Chem.* **1979,** *44(17),* 3037-41.

(38) Stetter, H. *Chem. Ber.* **1953,** *86,* 380-3.

(39) a: Jacob, P.; Richter, W.; Ugi, I. *Liebigs Ann. Chem.* **1991,** 519-522. b: Hunsch, S.; Richter, W.; Ugi, I.; Chattopadhyaya, J. *Liebigs Ann. Chem.* **1994,** 269-275.

(40) Heyns, K.; Heins, A. *Justus Liebigs Ann. Chem.* **1960,** *634,* 29-49.

(41) Varshavskii, T. S.; Cherkasova, T. G. *Russan J. Inorg. Chem.* **1967,** *12(6),* 899.

(42) Stille, J. K.; Su, H.; Brechot, P.; Parrinello, G. and Hegedus, L. S. *Organometallics,* **1991,** *10,* 1183-9.

Figure 11-1. ^{1}H NMR ($CDCl_3$) of $(Et_2N)_2PCl$ (1)

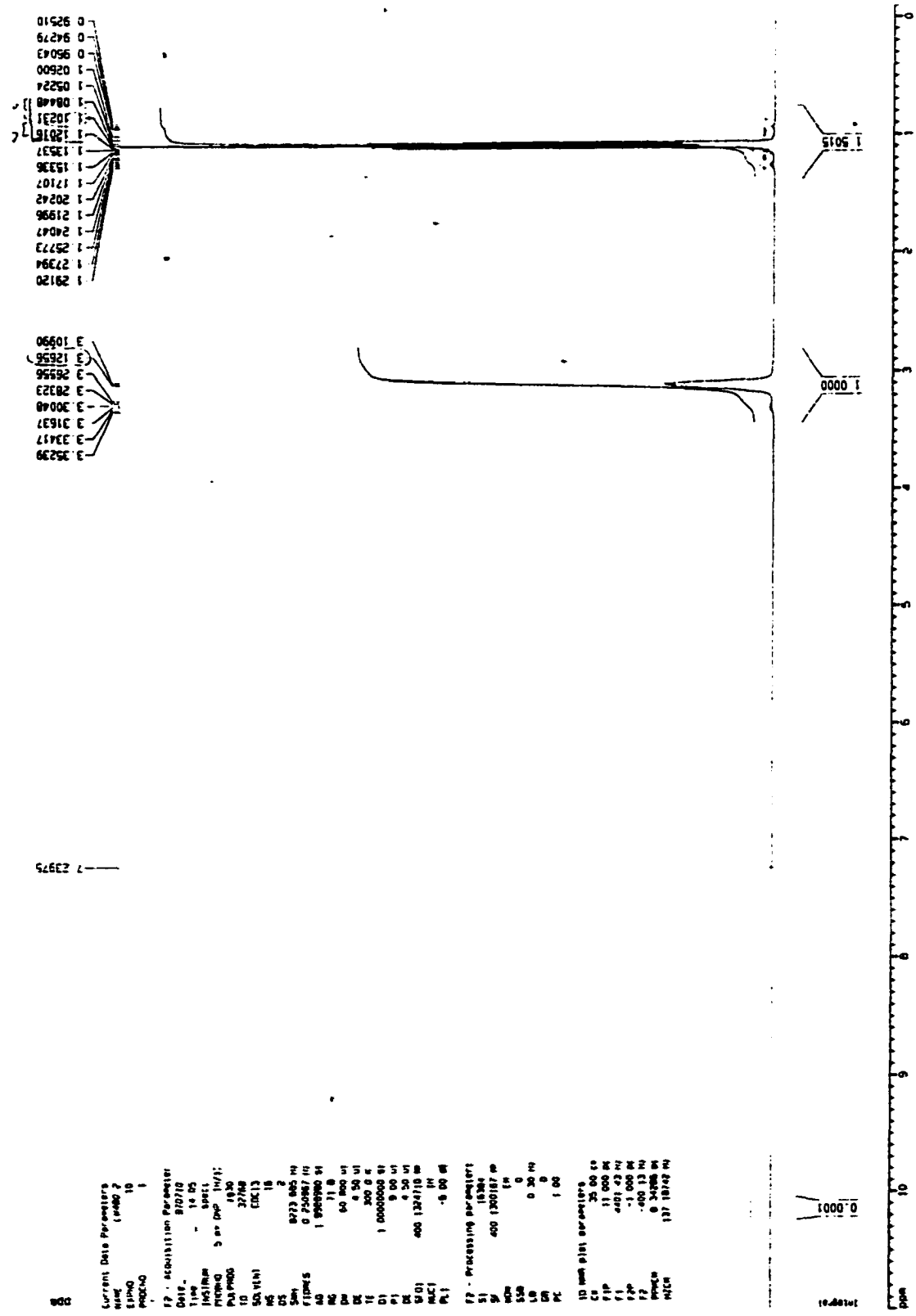

Figure 11-2. ^{31}P NMR ($CDCl_3$) of $(Et_2N)_2PCl$ (1)

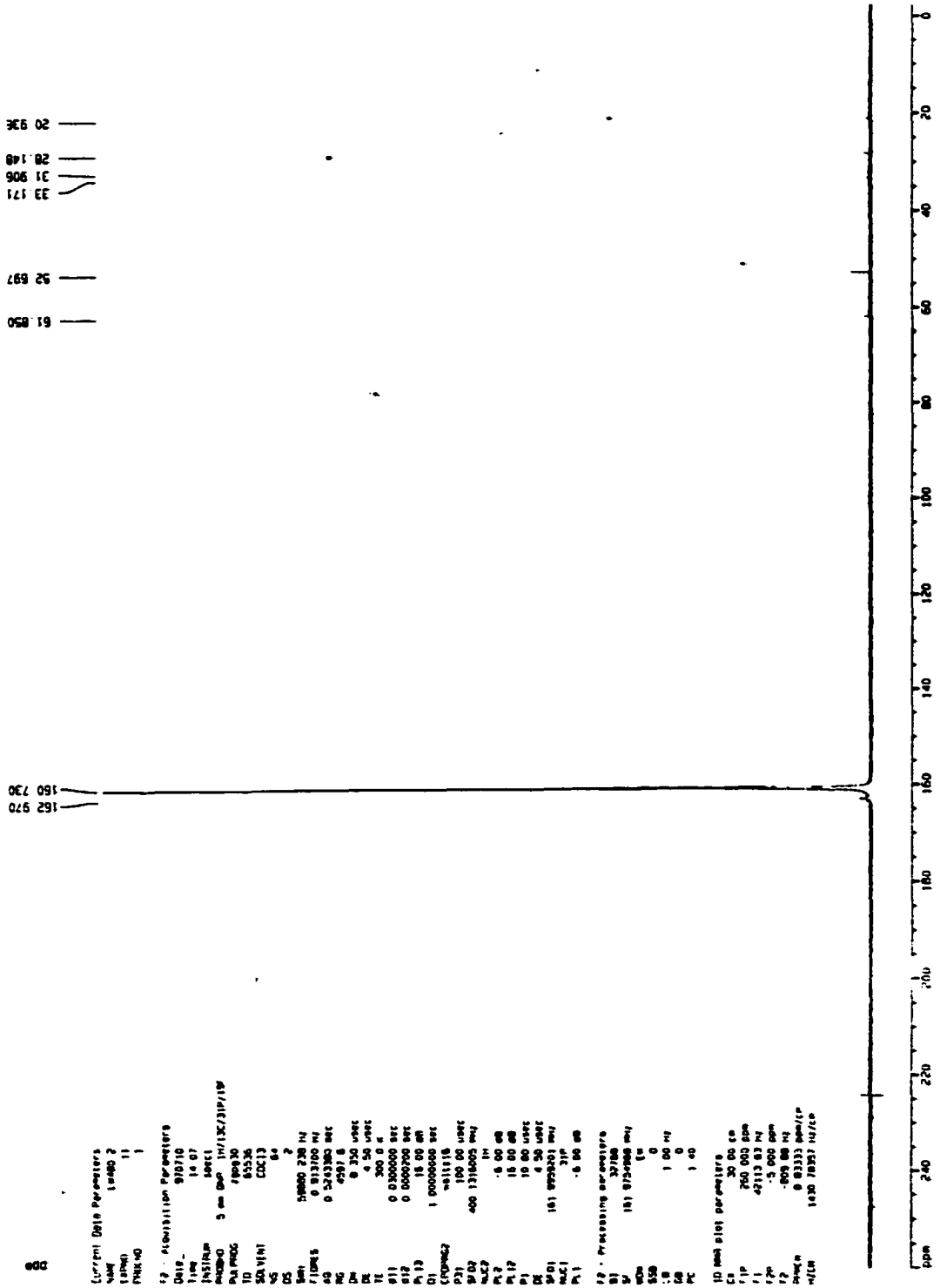

Figure 11-3. ^{13}C NMR ($CDCl_3$) of $(Et_2N)_2PCl$ (1)

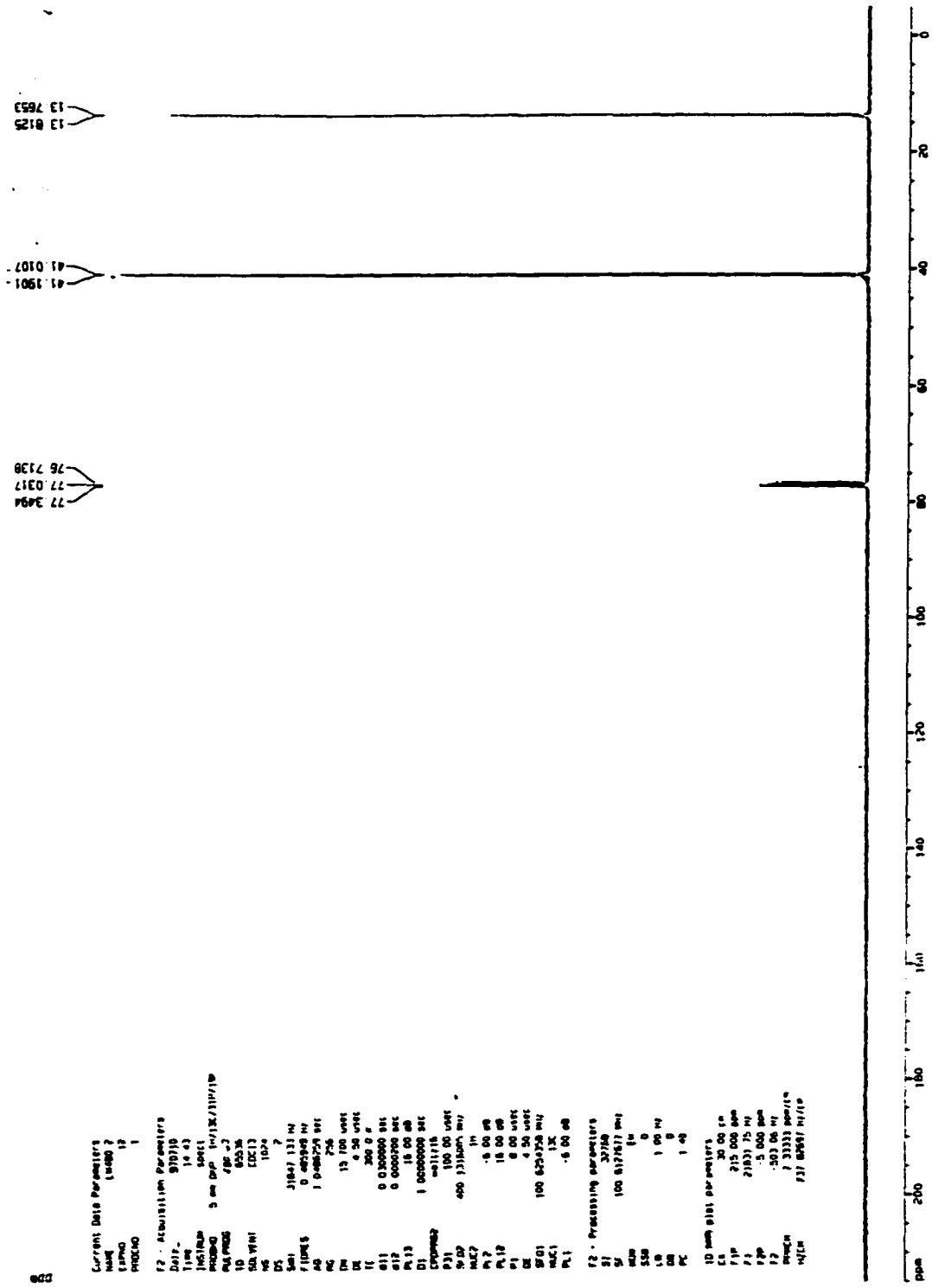

Figure 12-1. ^{1}H NMR (C_6D_6) of $(Et_2N)_2P(CH_2)_4P(NEt_2)_2$ (2, BBB)

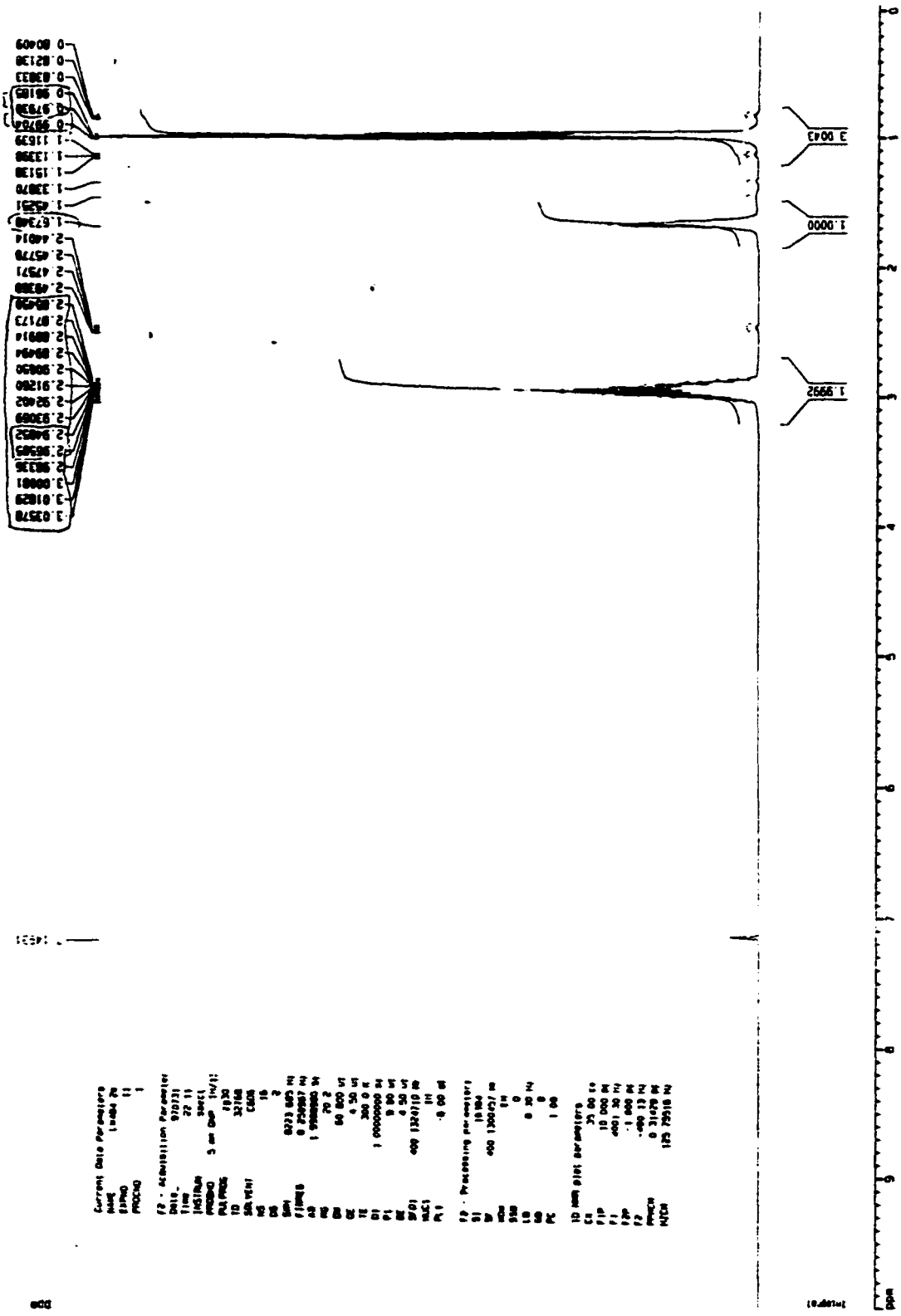

Figure 12-2. ^{31}P NMR (C_6D_6) of $(Et_2N)_2P(CH_2)_4P(NEt_2)_2$ (2, BBB)

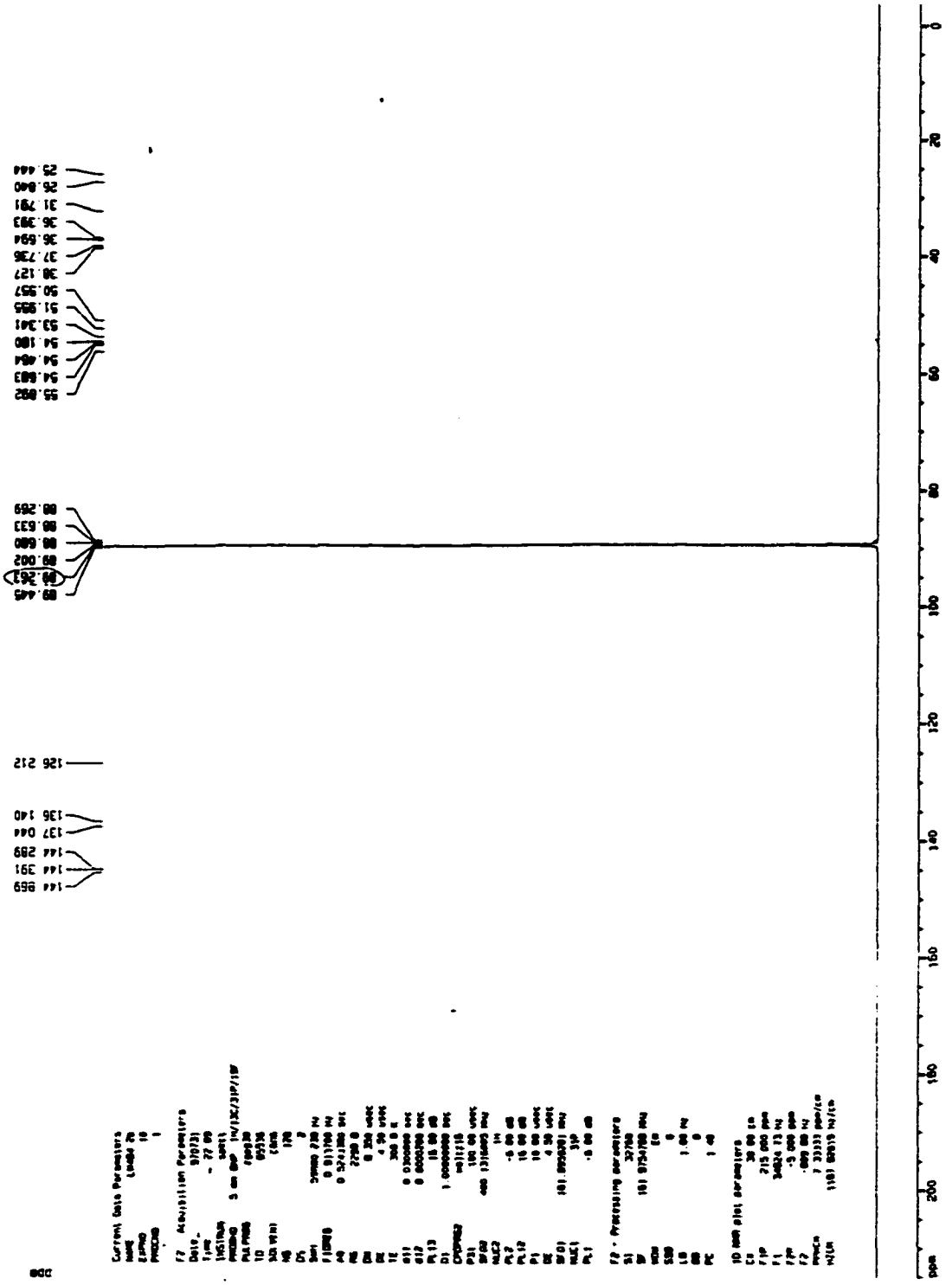

Figure 12-3. ^{13}C NMR (C_6D_6) of $(Et_2N)_2P(CH_2)_4P(NEt_2)_2$ (**2, BBB**)

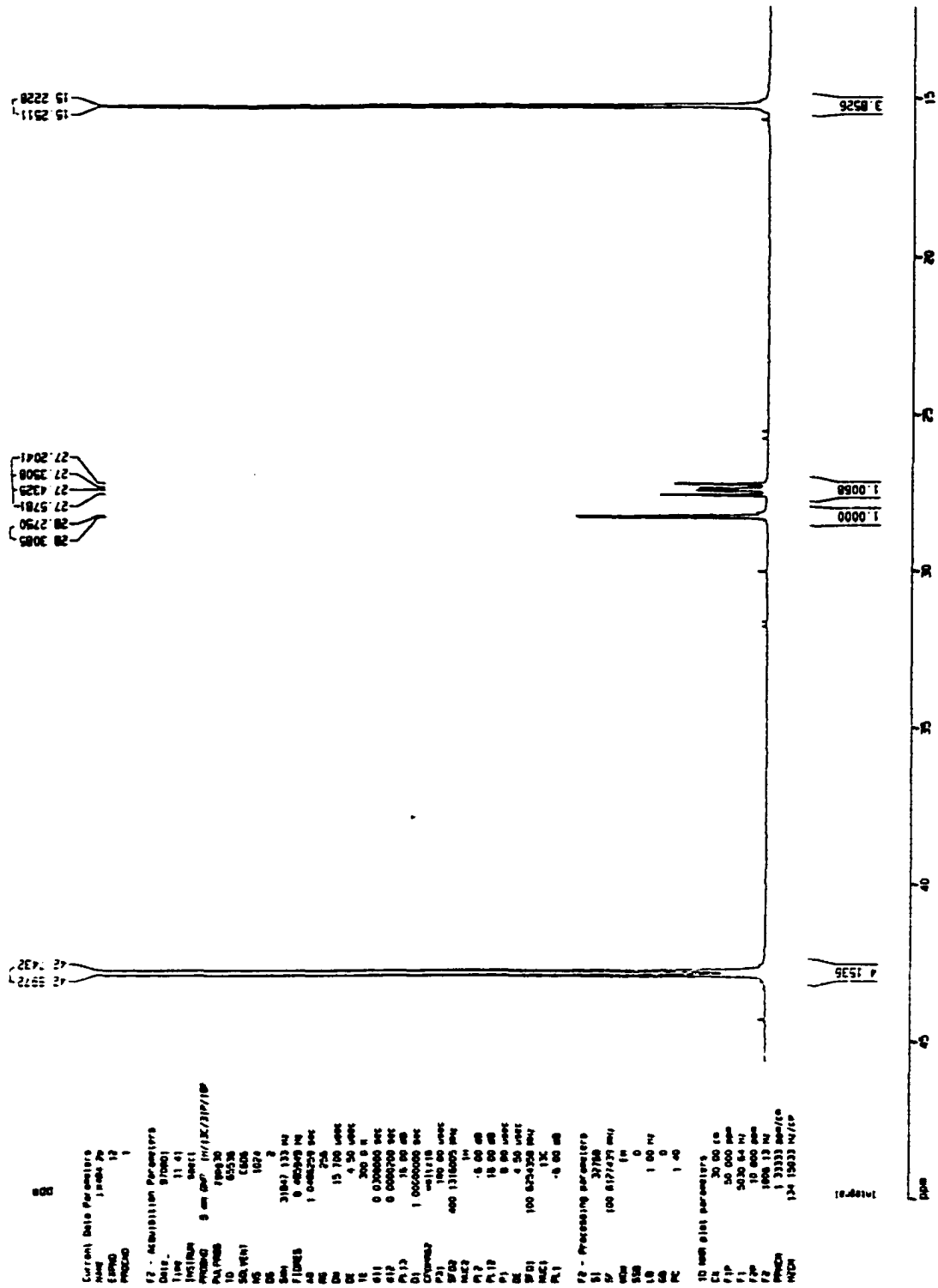

Figure 13-1. ^{1}H NMR (C_6D_6) of $(Et_2N)_2P(CH_2)_4P(NEt_2)_2$ (3, BDB)

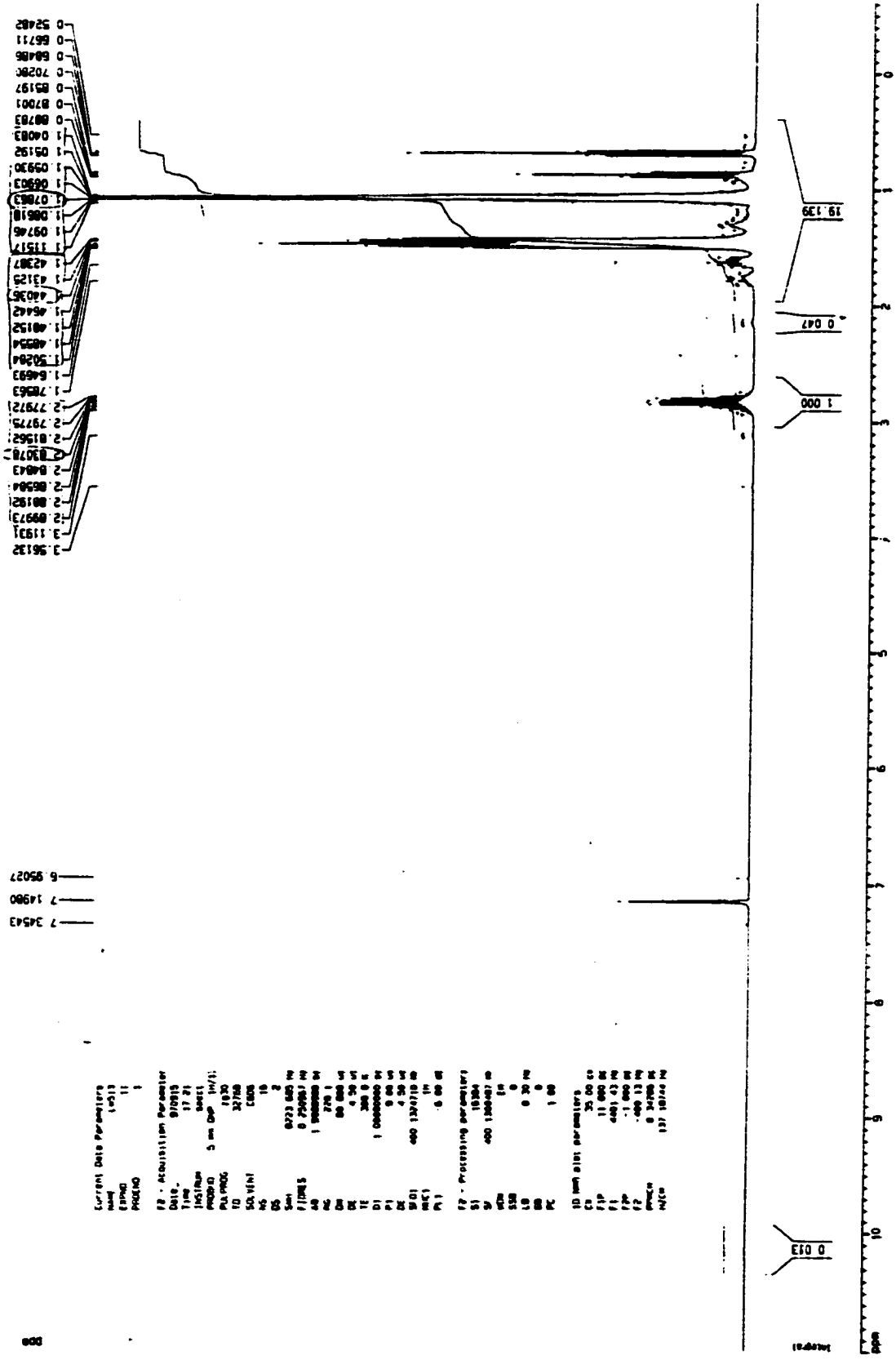

Figure 13-2. ^{31}P NMR (C_6D_6) of $(Et_2N)_2P(CH_2)_4P(NEt_2)_2$ (3, BDB)

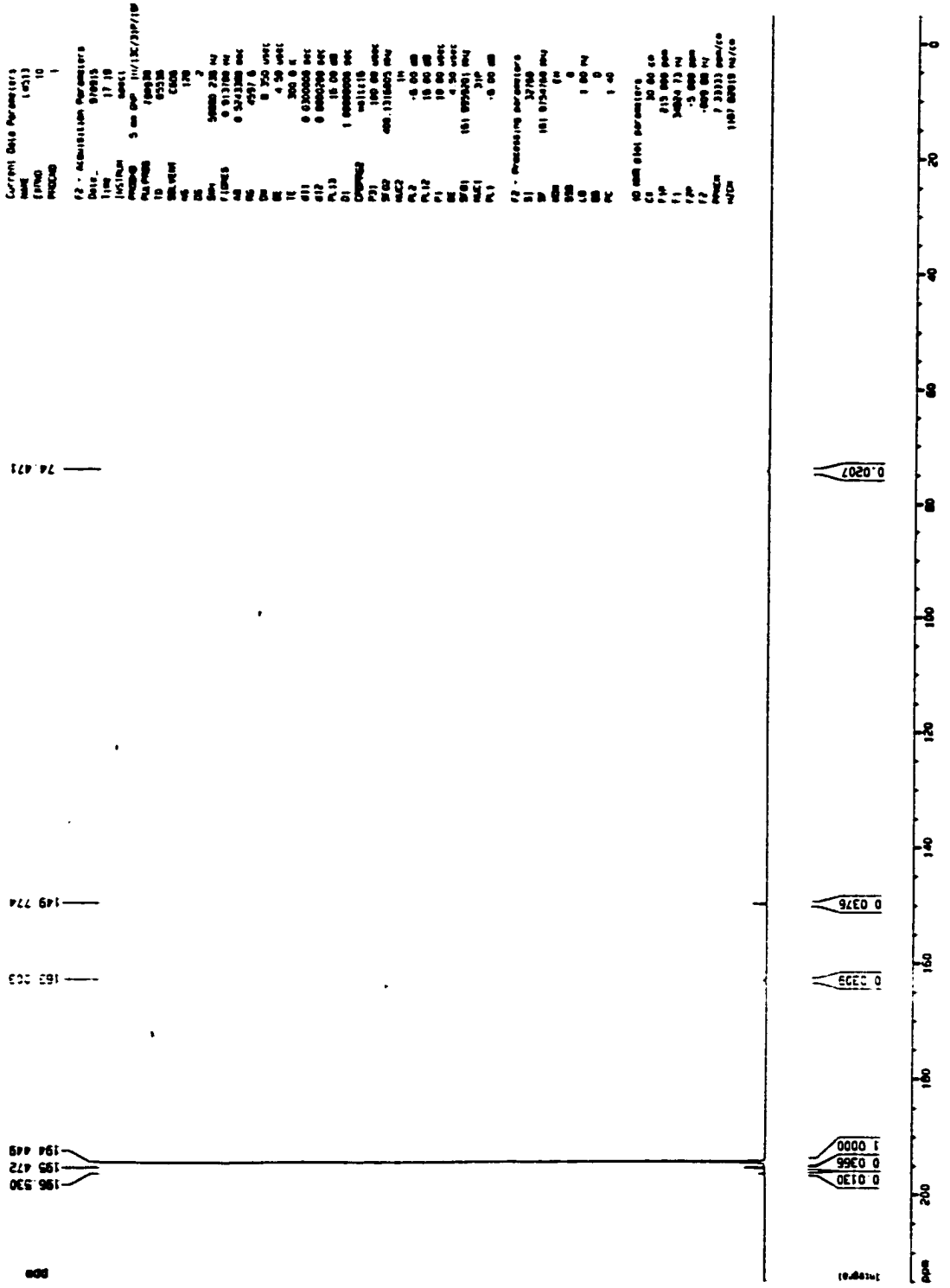

Figure 13-3. ^{13}C NMR (C_6D_6) of $(Et_2N)_2P(CH_2)_4P(NEt_2)_2$ (3, BDB)

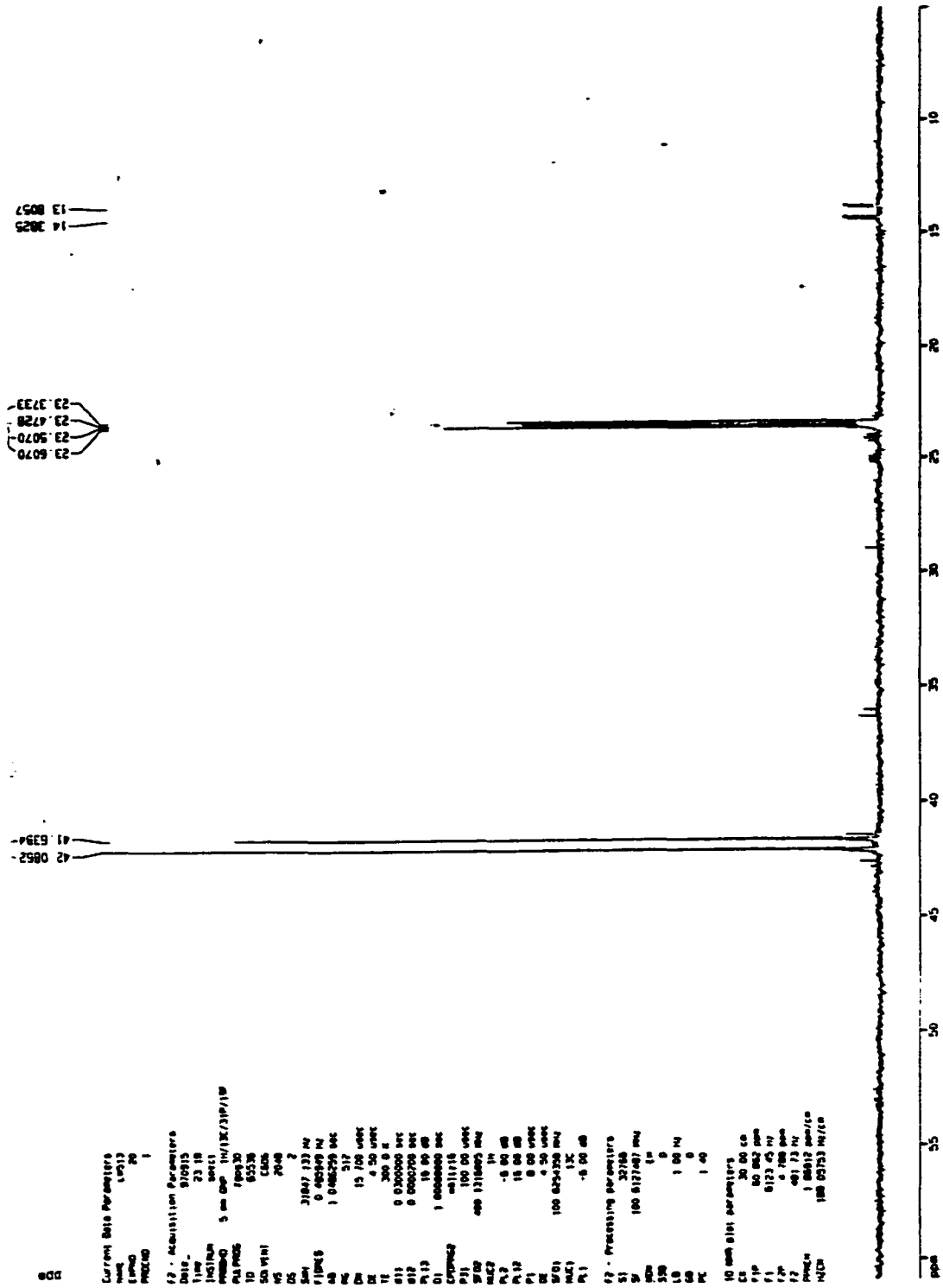

Figure 14-1. ^{1}H NMR ($CDCl_3$) of TsN(H)Et (4)

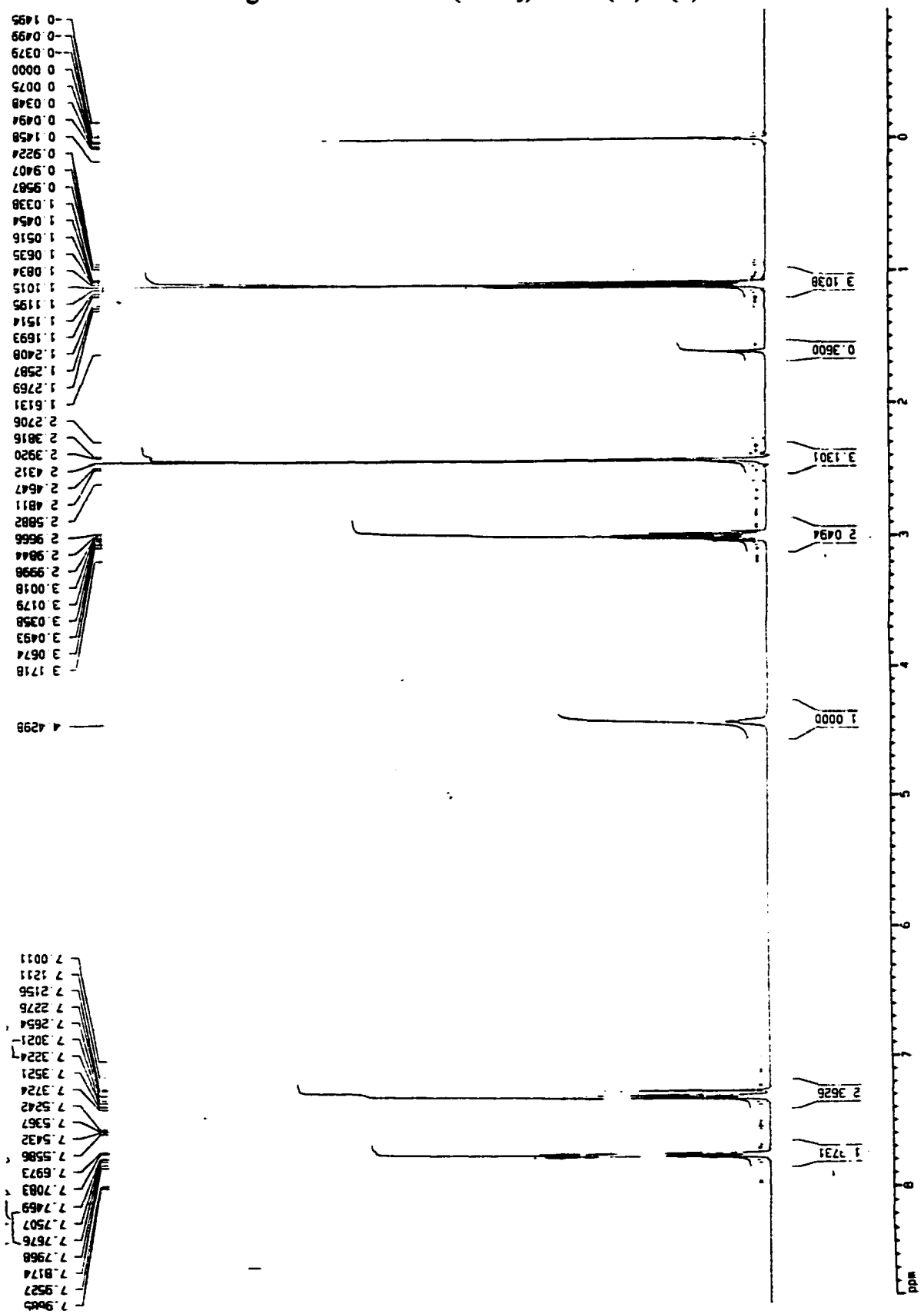

Figure 14-2. ^{13}C NMR ($CDCl_3$) of TsN(H)Et (4)

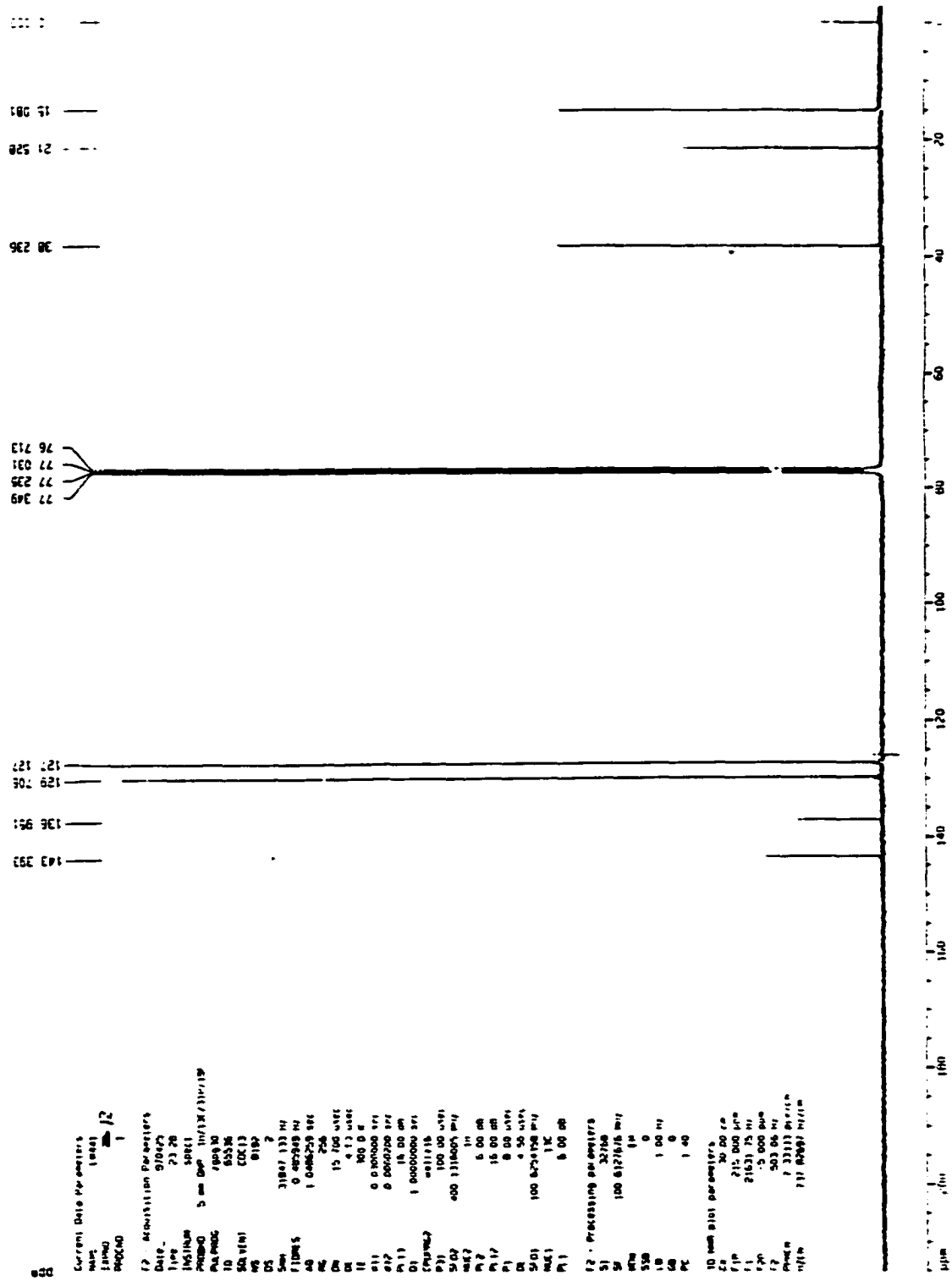

Figure 15-1. ^{1}H NMR ($CDCl_3$) of dpet (5)

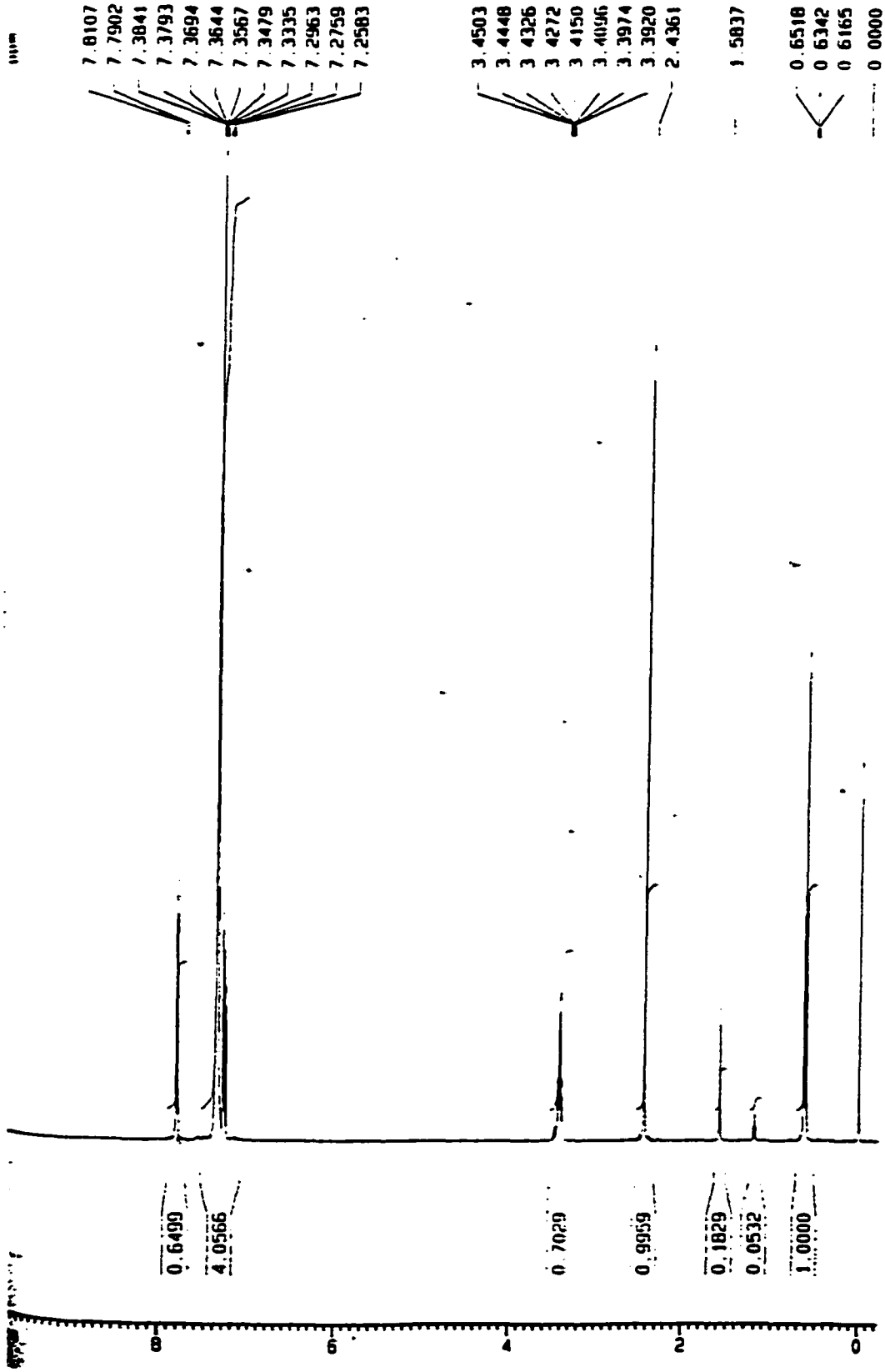

Figure 15-2. ^{31}P NMR ($CDCl_3$) of **dpet (5)**

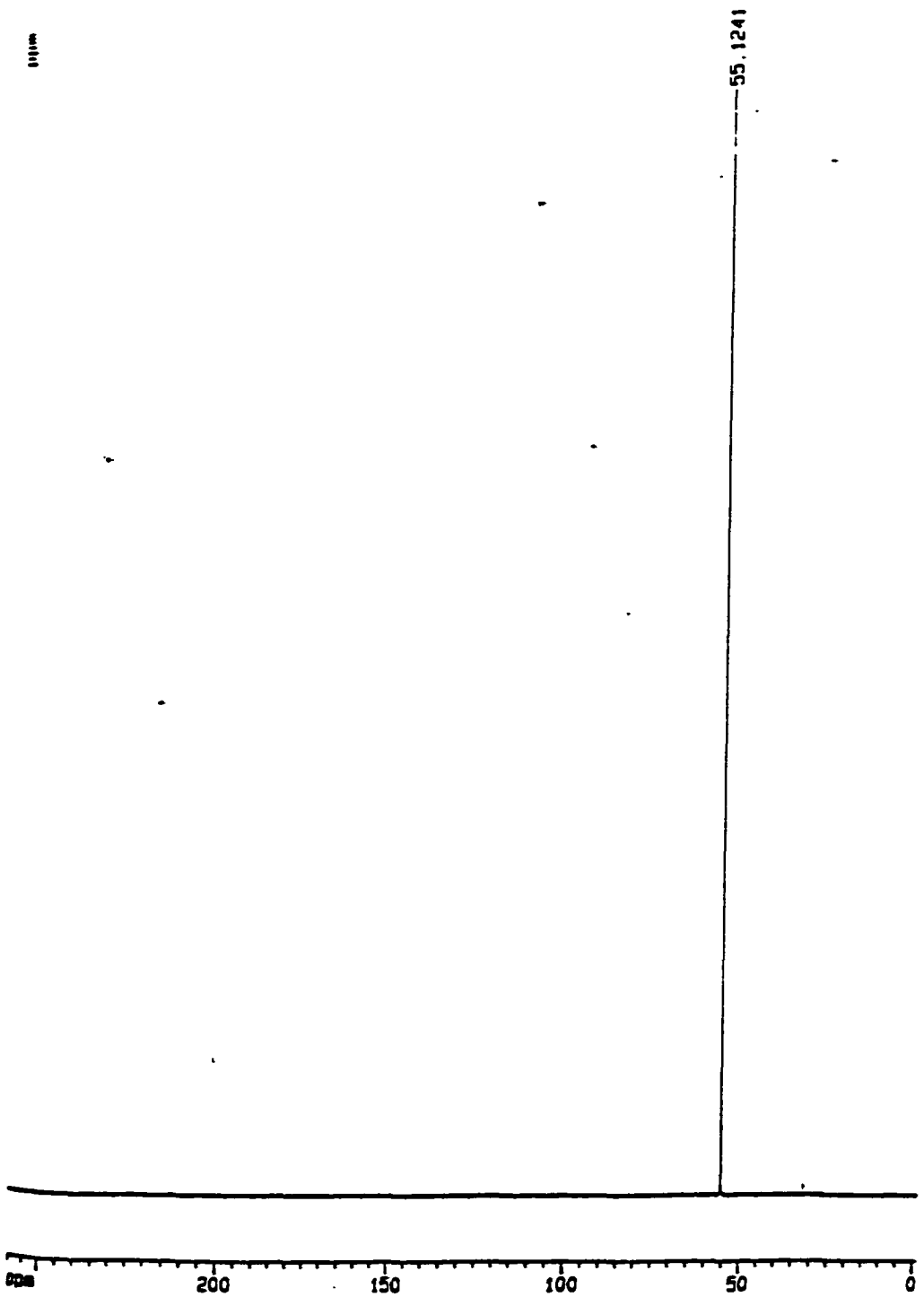

Figure 15-3. ^{13}C NMR ($CDCl_3$) of dpet (5)

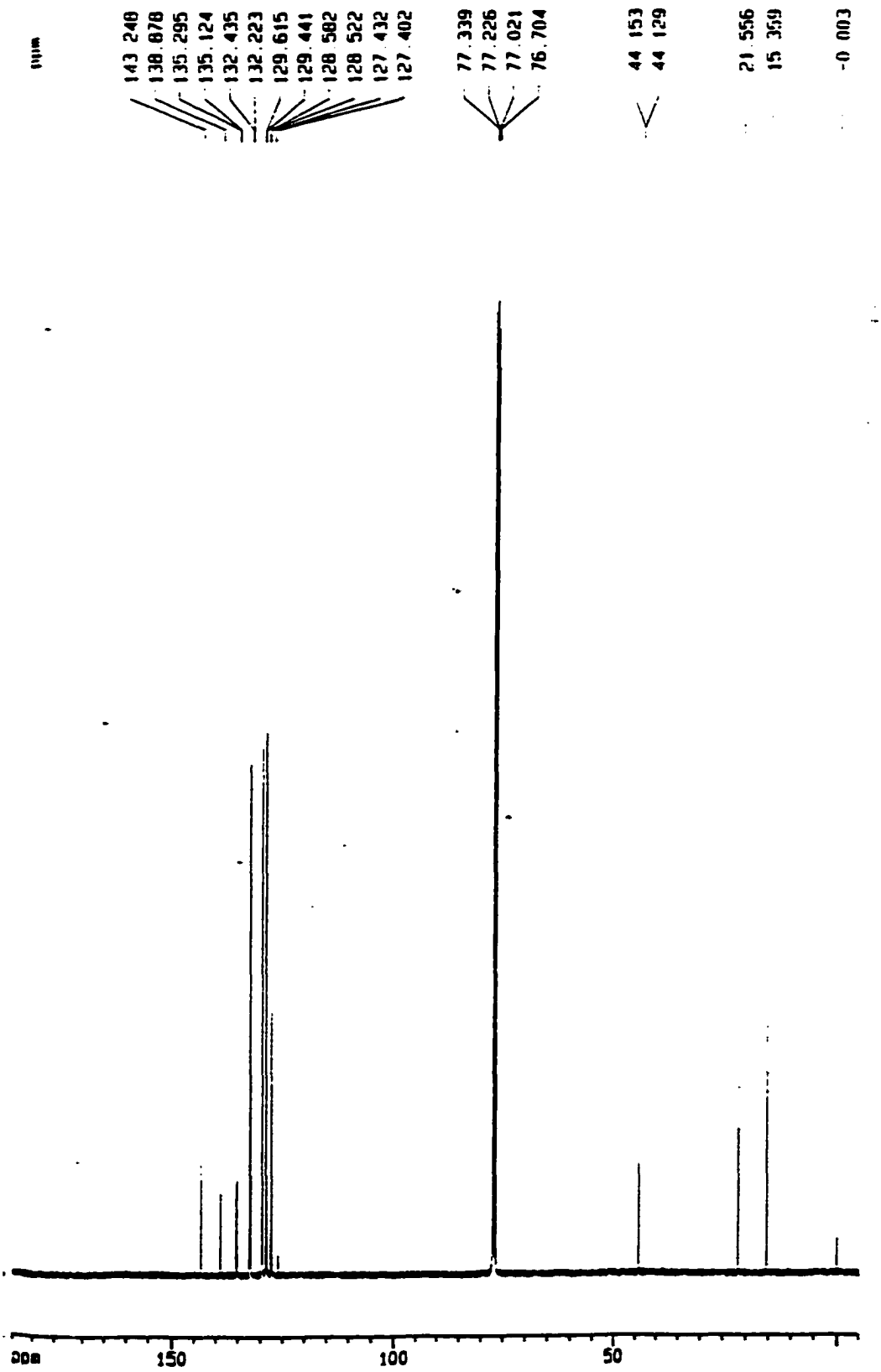

Figure 16-1. ^{1}H NMR (CD_2Cl_2) of **BTosL (6)**

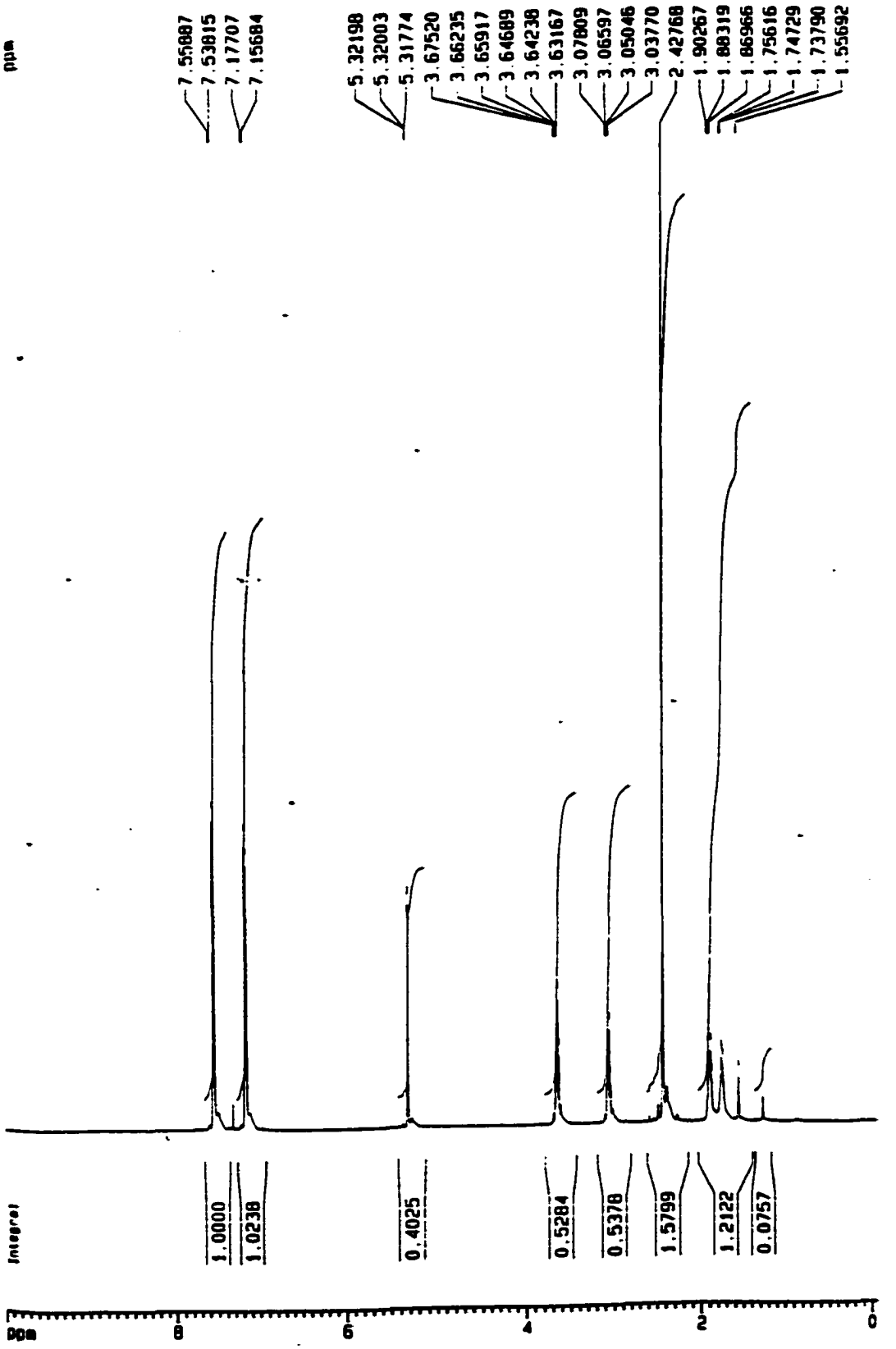

Figure 16-2. ^{31}P NMR (CD_2Cl_2) of **BTosL (6)**

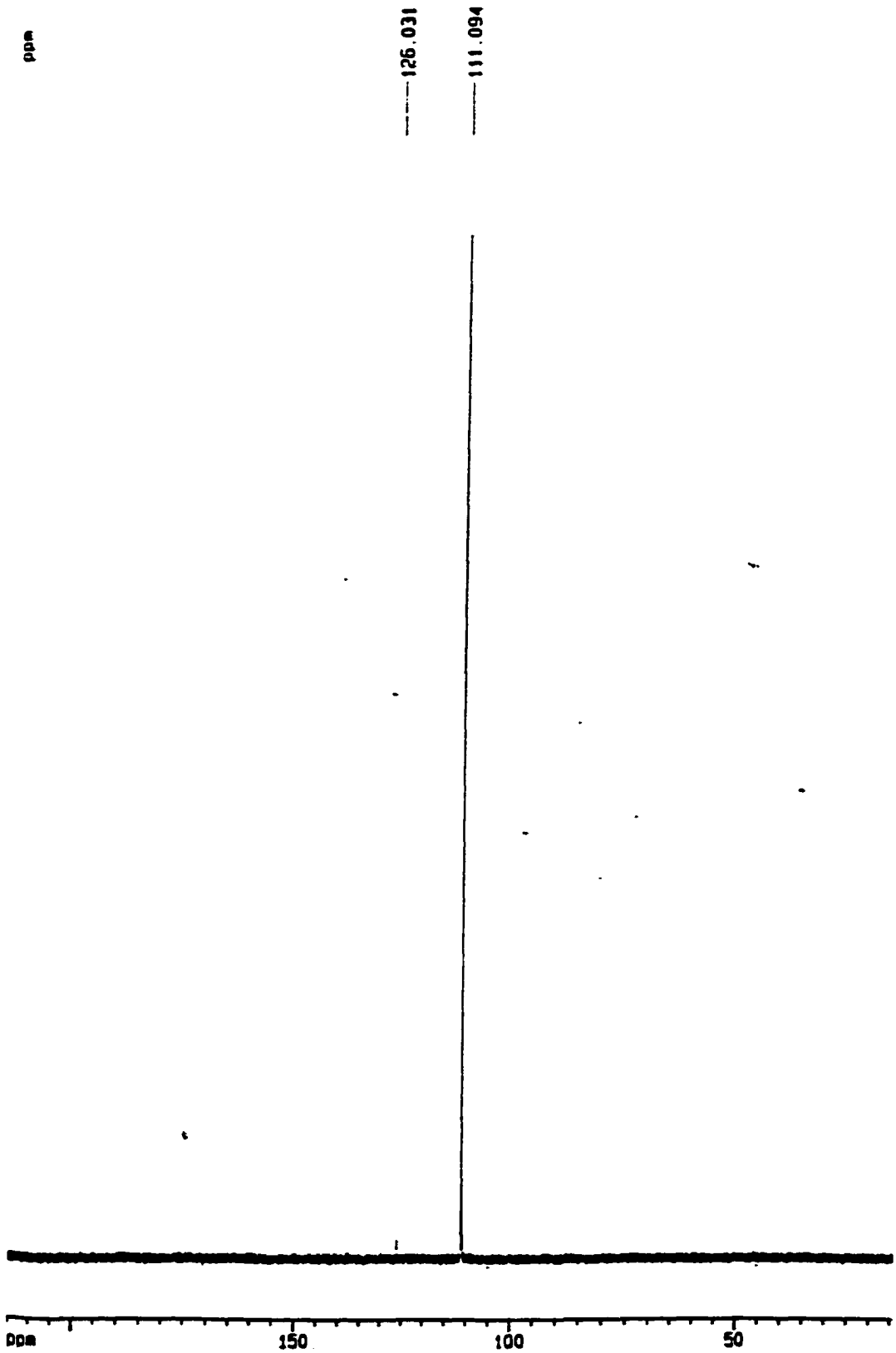

Figure 16-3. ^{13}C NMR (CD_2Cl_2) of **BTosL (6)**

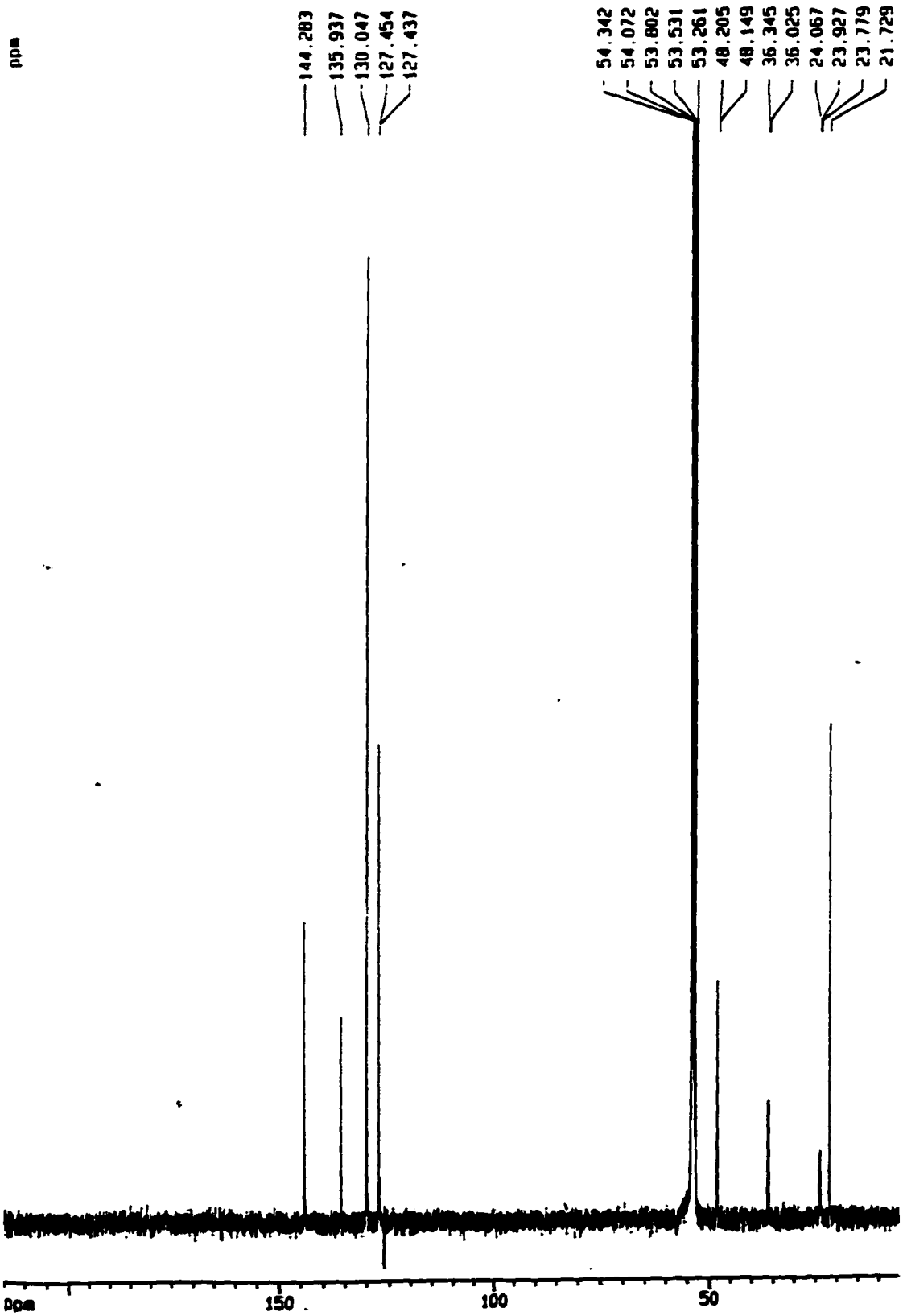

Figure 17-1. ^{1}H NMR (CD_2Cl_2) of **ETosL** (7)

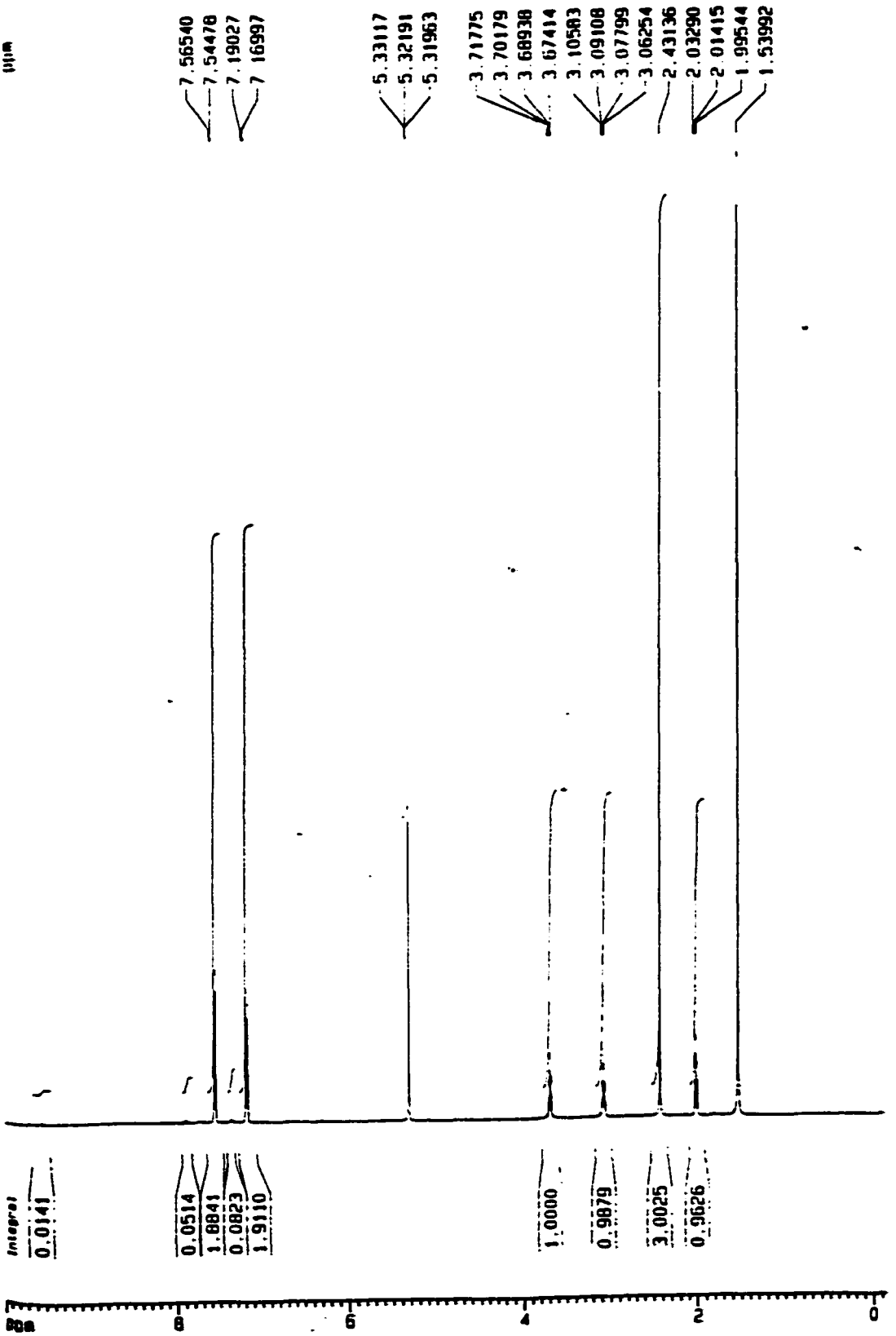

Figure 17-2. ^{31}P NMR (CD_2Cl_2) of **ETosL** (7)

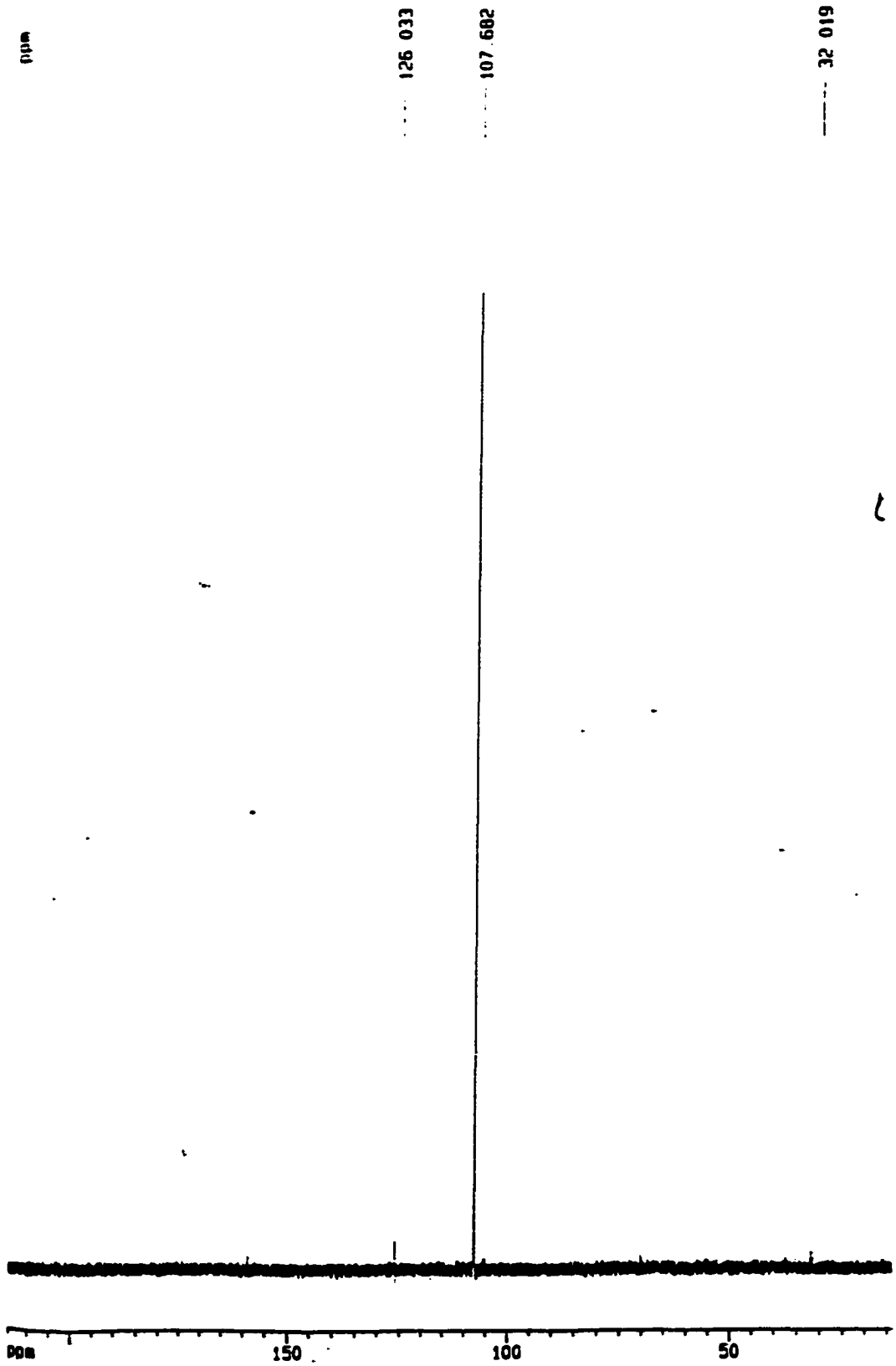

Figure 17-3. ^{13}C NMR (CD_2Cl_2) of ETosL (7)

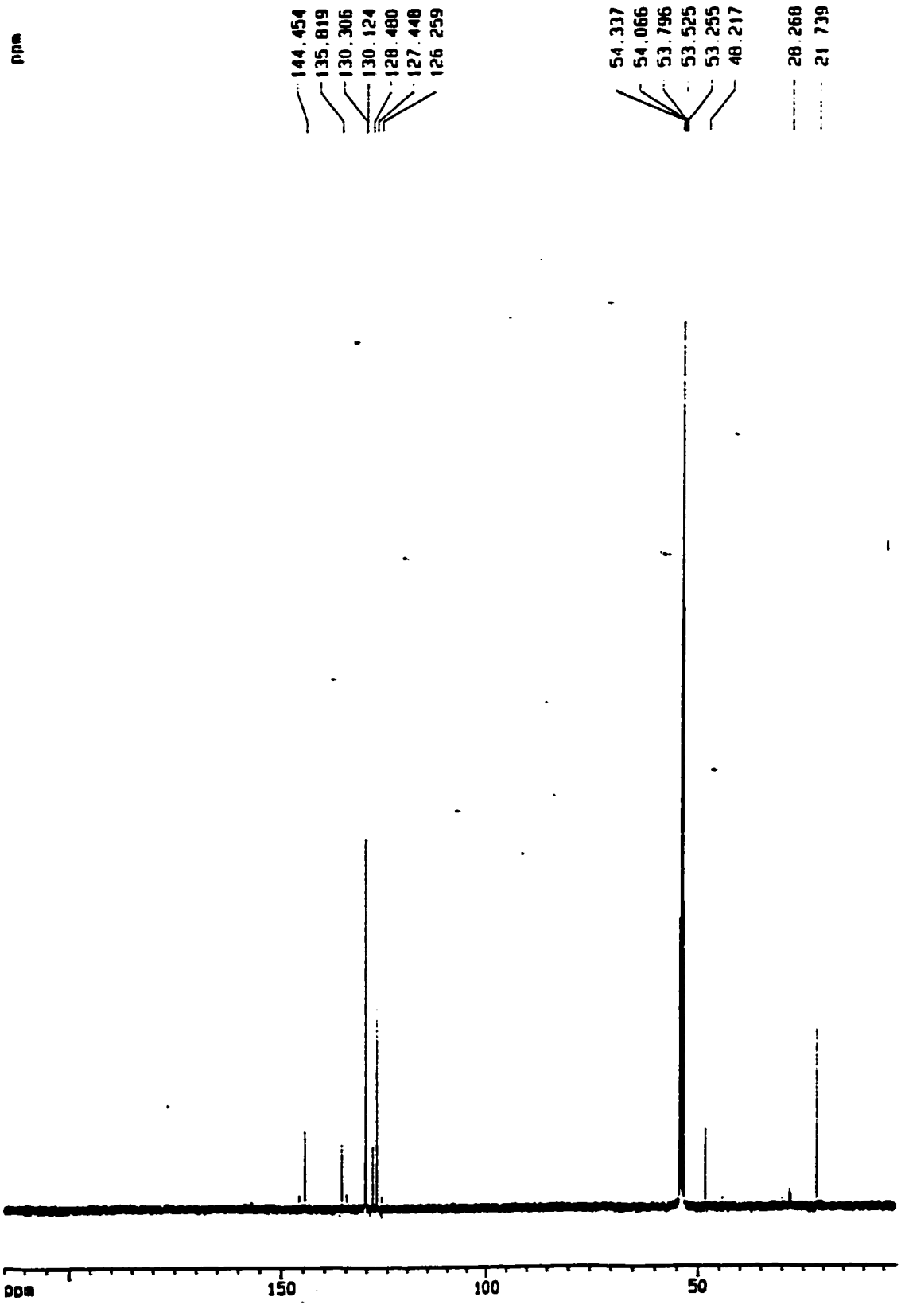

Figure 18-1. ^{1}H NMR ($CDCl_3$) of *o*-$TsNHC_6H_4NHTs$ (8)

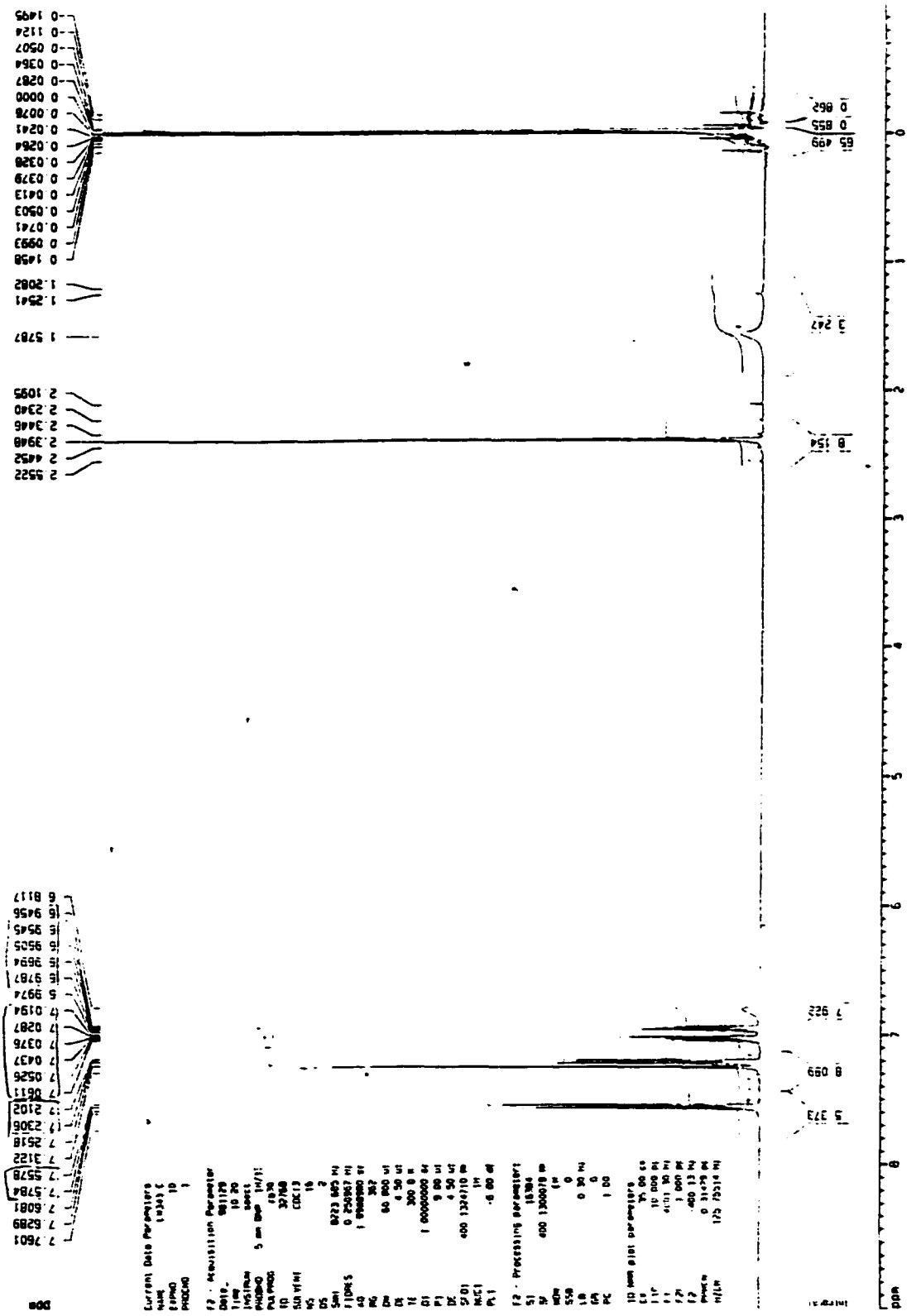

Figure 18-2. ^{13}C NMR ($CDCl_3$) of *o*-$TsNHC_6H_4NHTs$ (**8**)

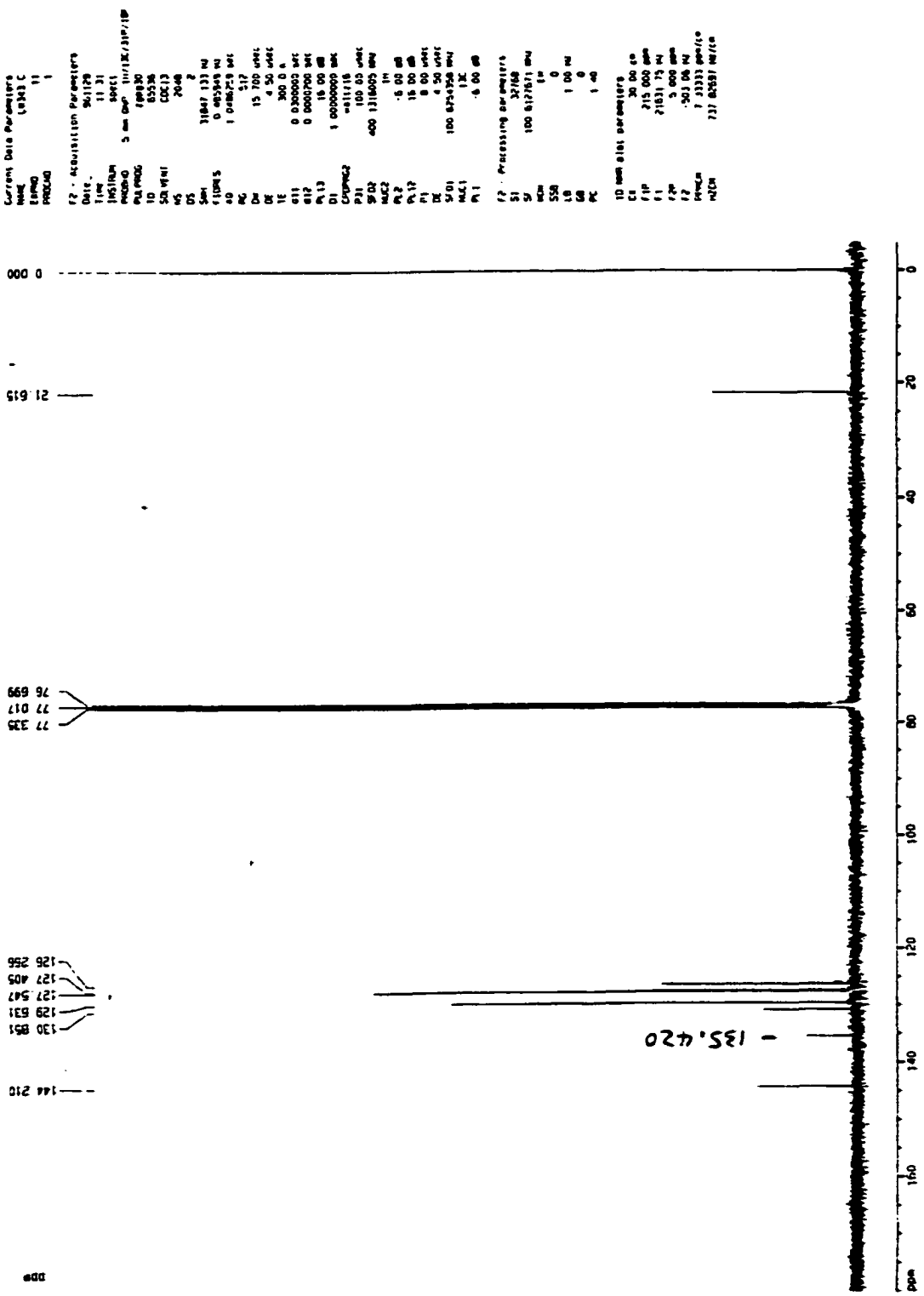

Figure 19-1. ^{1}H NMR ($CDCl_3$) of PPhyl (9)

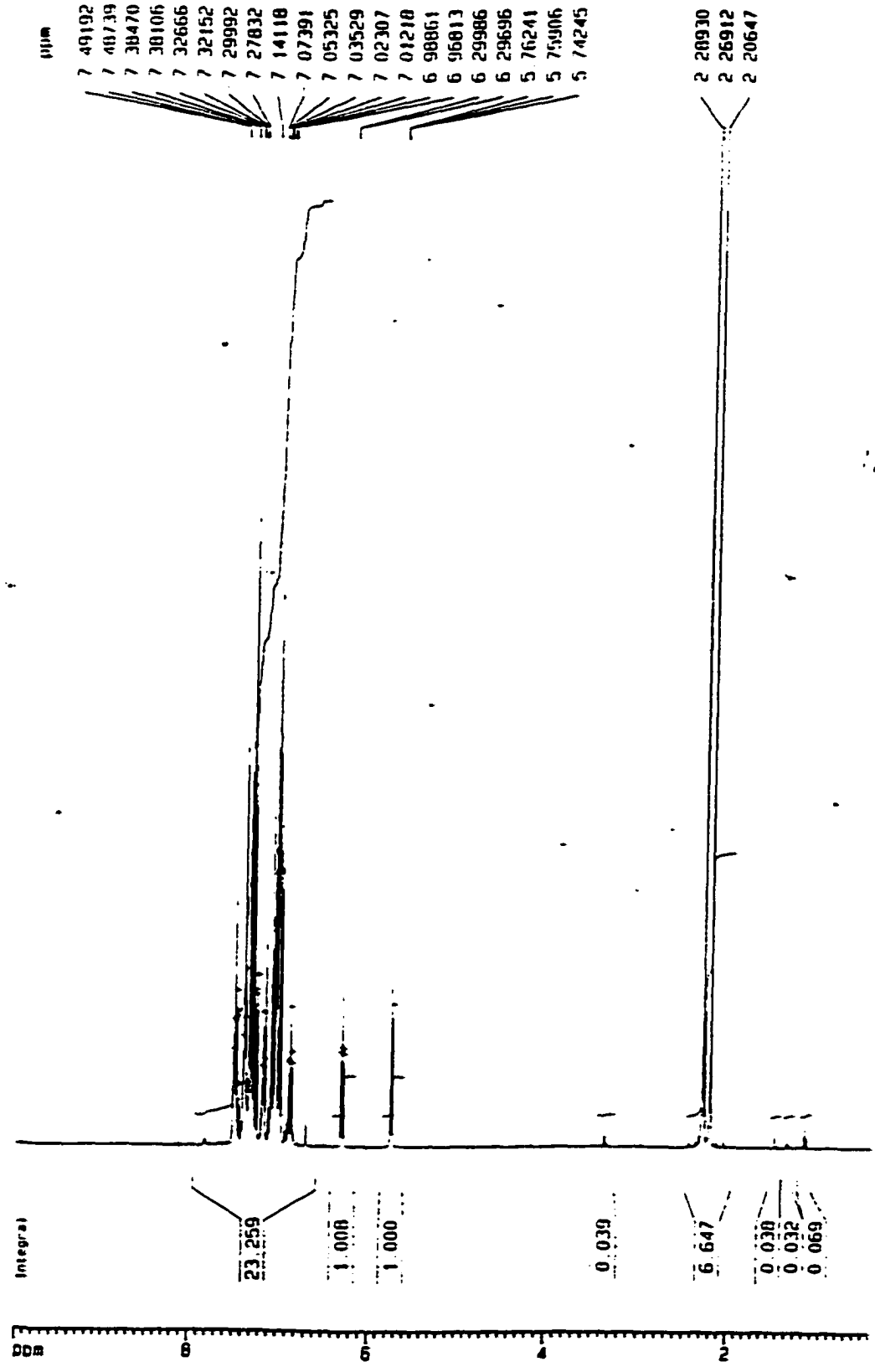

Figure 19-2. ^{31}P NMR ($CDCl_3$) of **PPhyl (9)**

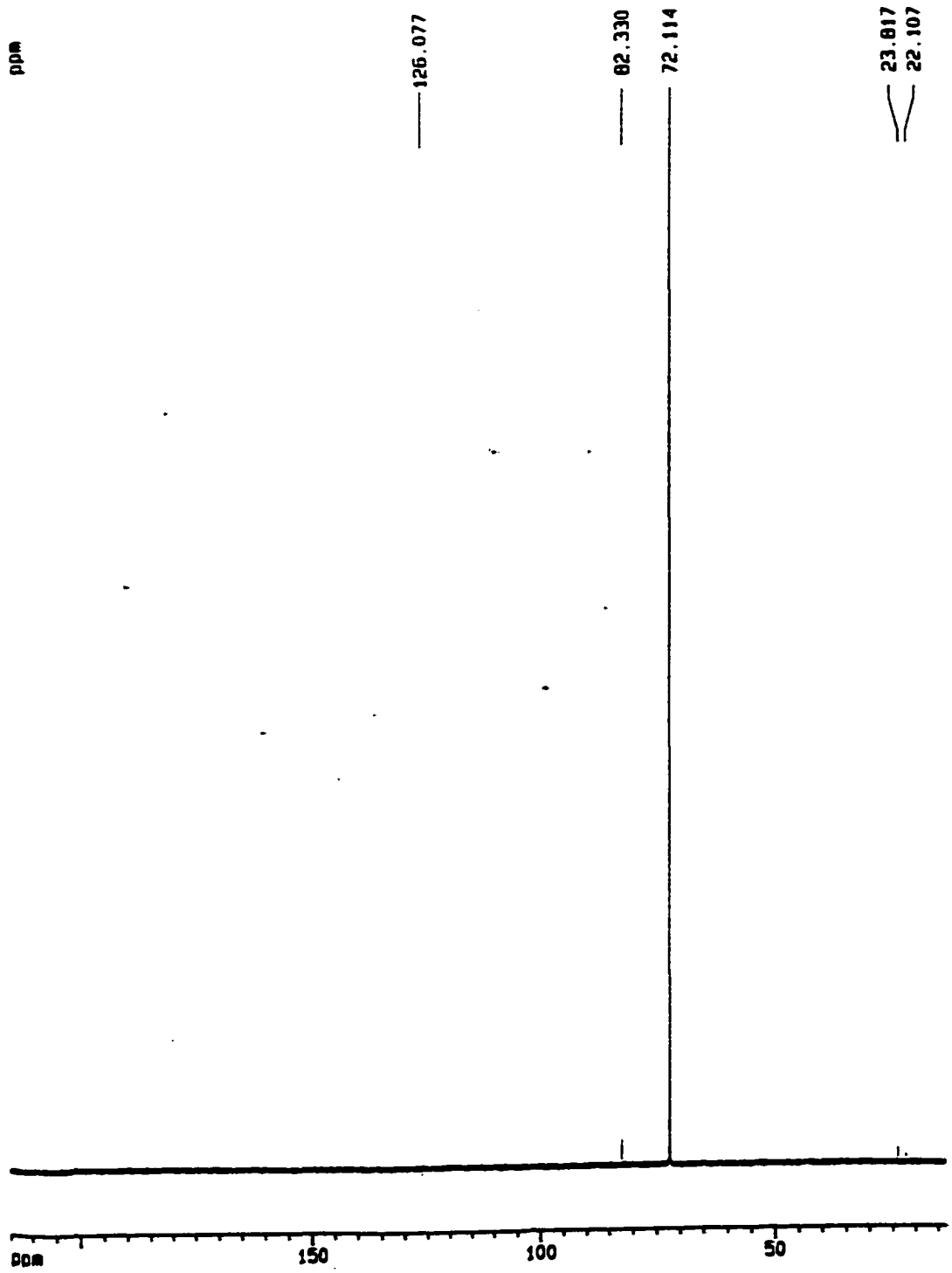

Figure 19-3. ^{13}C NMR ($CDCl_3$) of **PPhyl (9)**

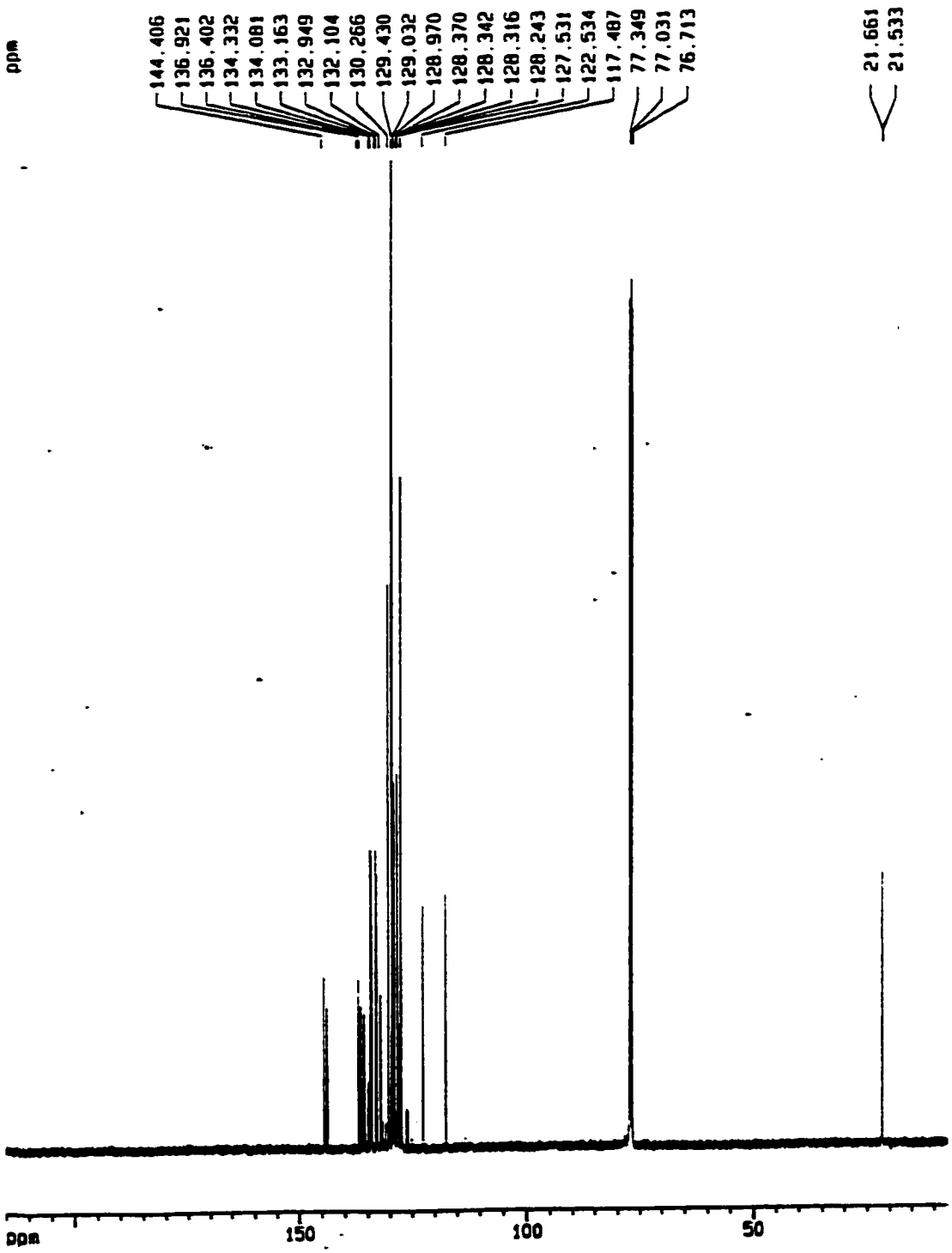

Figure 20-1. ^{1}H NMR ($CDCl_3$) of 1,8-$TsNHC_{10}H_6NHTs$ (10)

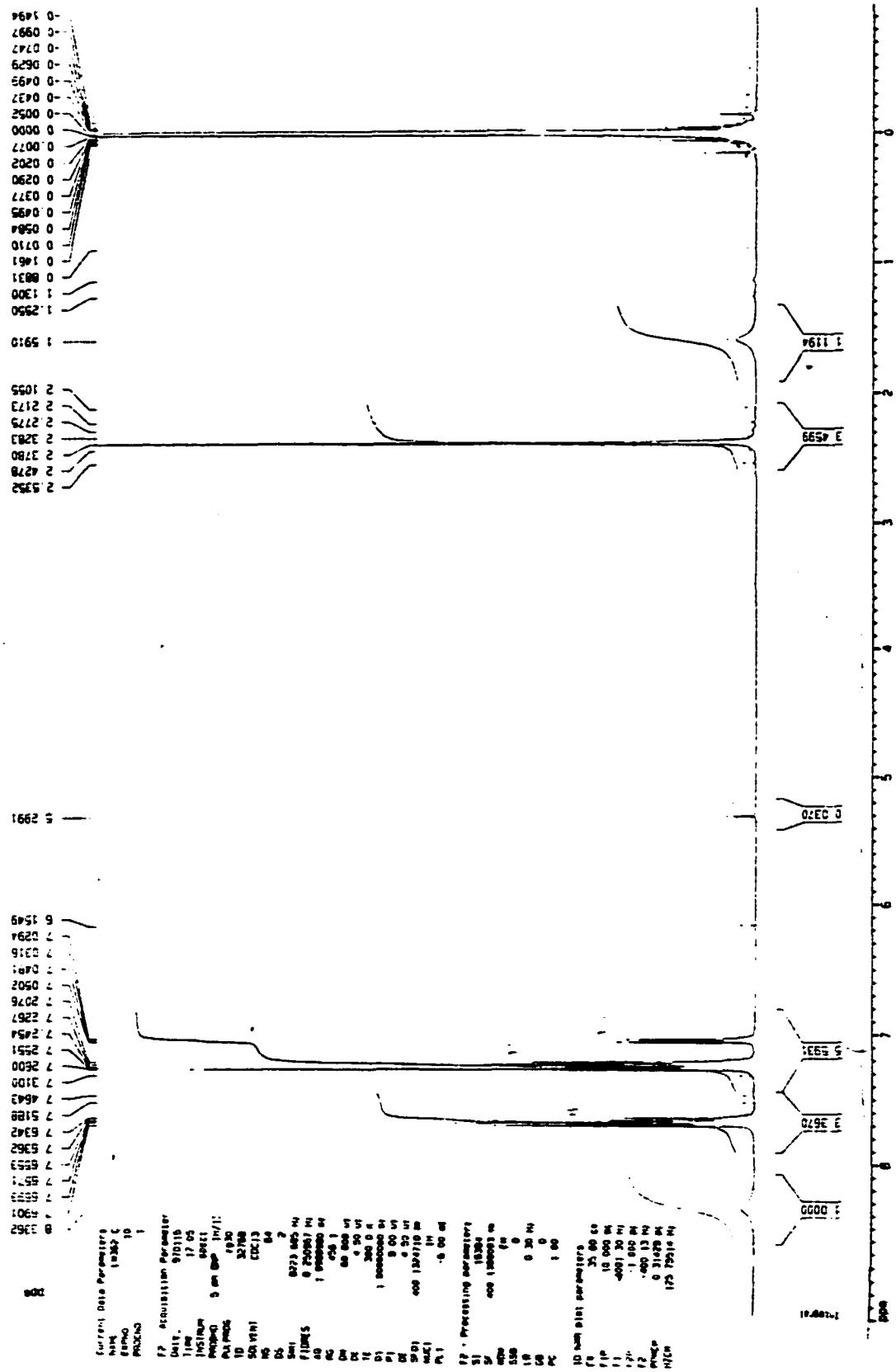

Figure 20-2. ^{13}C NMR ($CDCl_3$) of 1,8-$TsNHC_{10}H_6NHTs$ (10)

Figure 21-1. ^{1}H NMR ($CDCl_3$) of 2,2'-$TsNHC_6H_4C_6H_4NHTs$ (12, BDT)

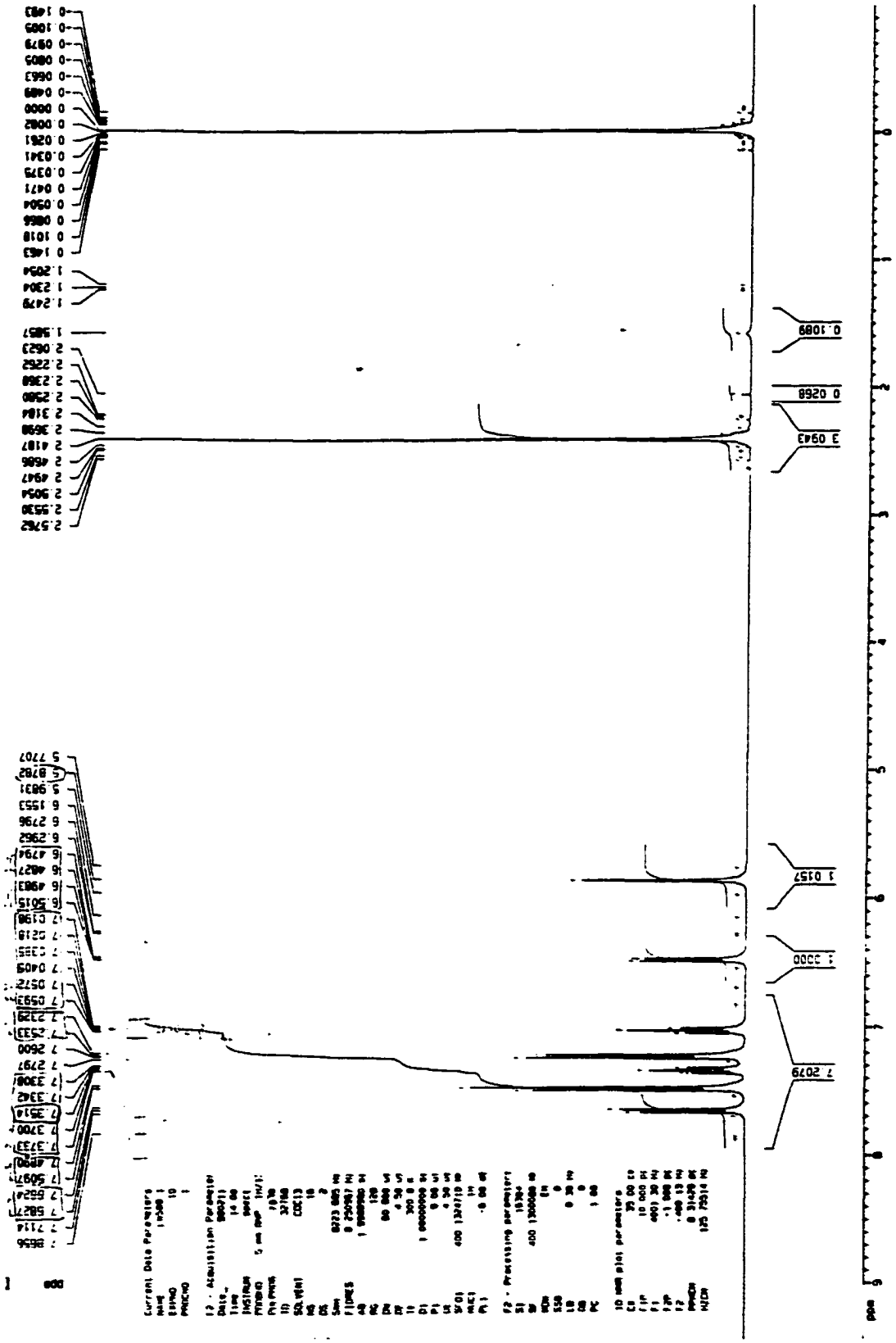

Figure 21-2. ^{13}C NMR ($CDCl_3$) of 2,2'-$TsNHC_6H_4C_6H_4NHTs$ (12, BDT)

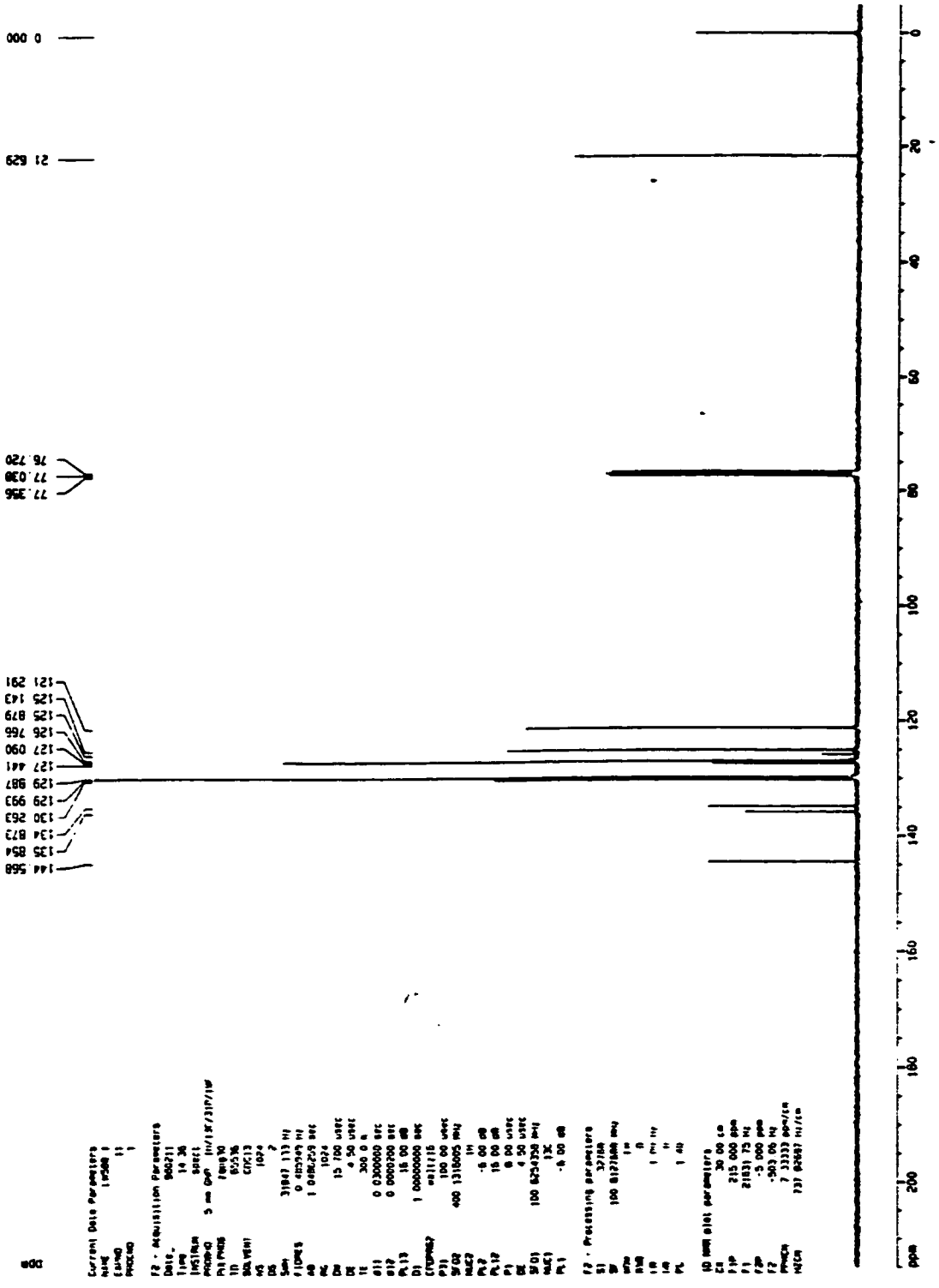

Figure 22-1. ^1H NMR ($CDCl_3$) of $Ts(Ph_2P)NC_6H_4C_6H_4NHTs$ (13, DBT)

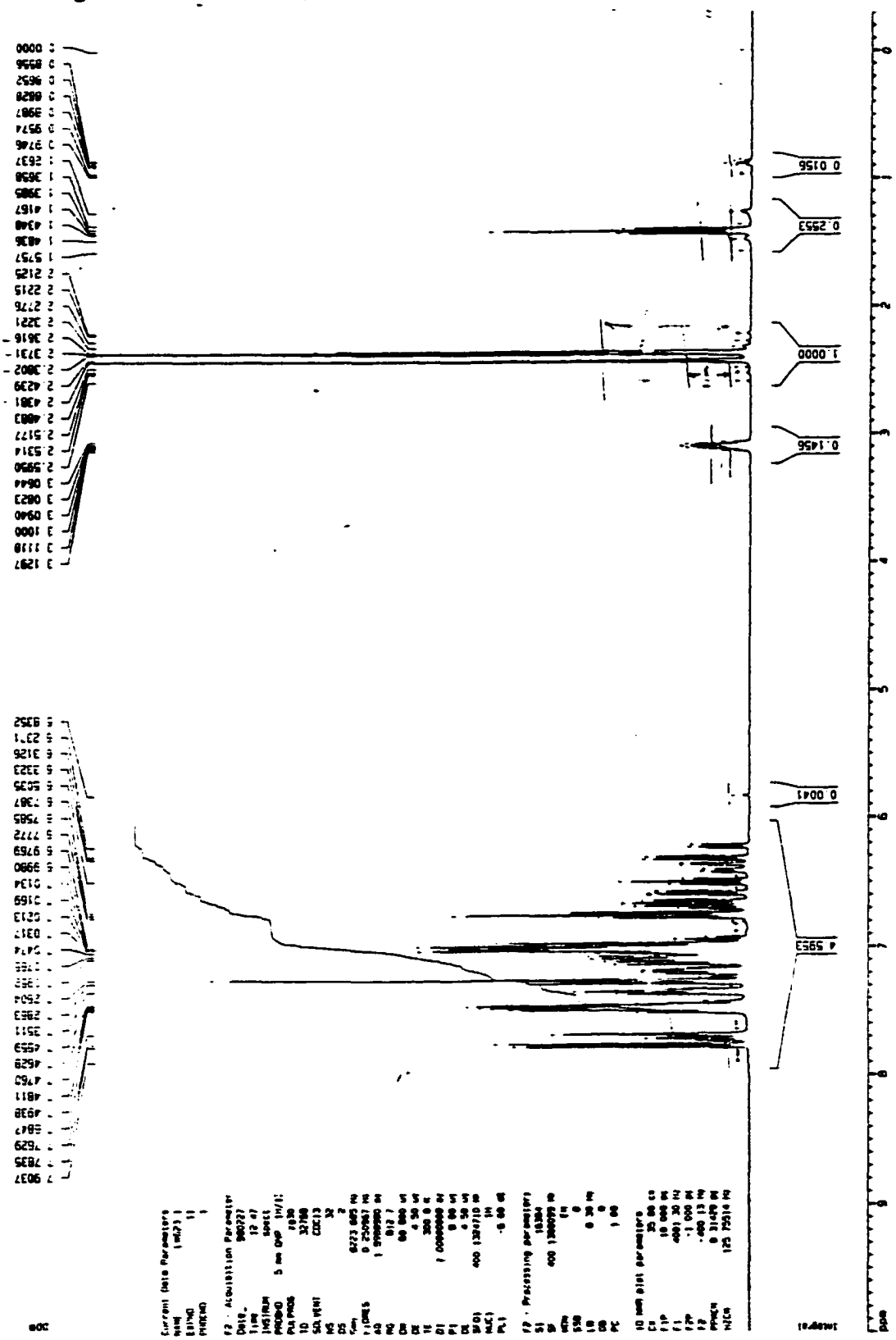

Figure 22-2. ^{31}P NMR ($CDCl_3$) of $Ts(Ph_2P)NC_6H_4C_6H_4NHTs$ (13, DBT)

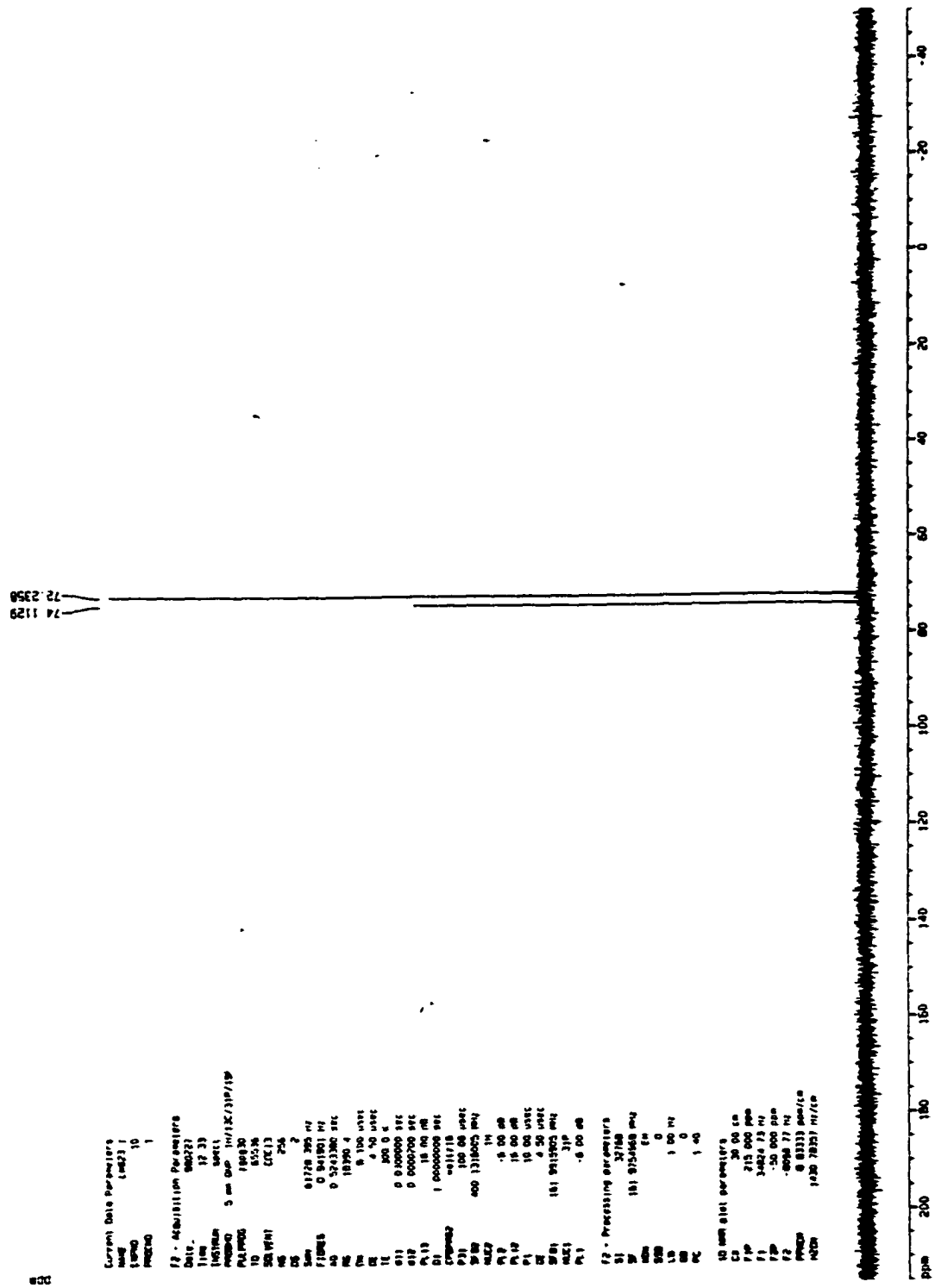

Figure 23-1. ^{1}H NMR ($CDCl_3$) of $MsNHC_6H_4C_6H_4NHMs$ (14, BBMs)

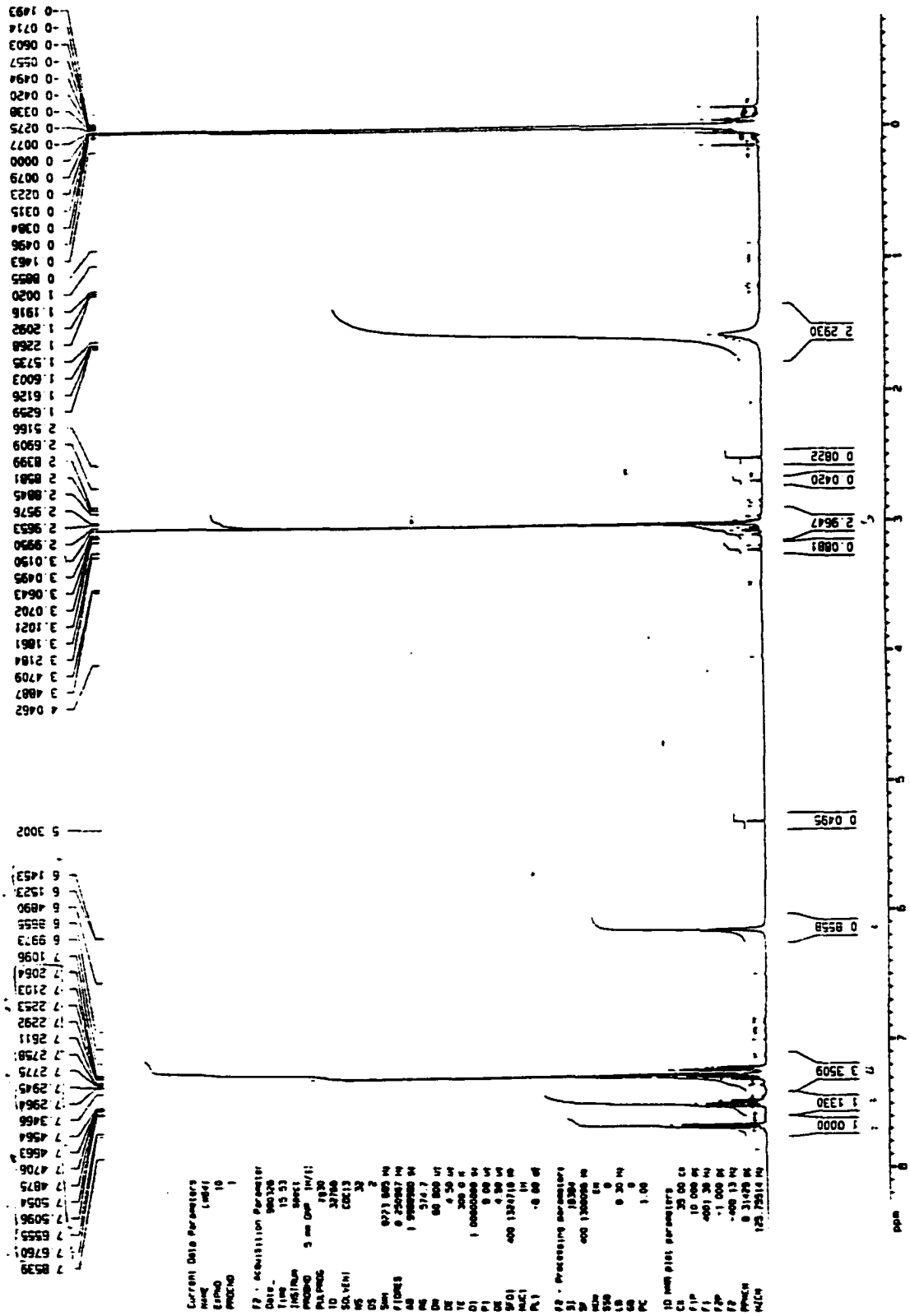

Figure 23-2. ^{13}C NMR ($CDCl_3$) of $MsNHC_6H_4C_6H_4NHMs$ (14, BBMs)

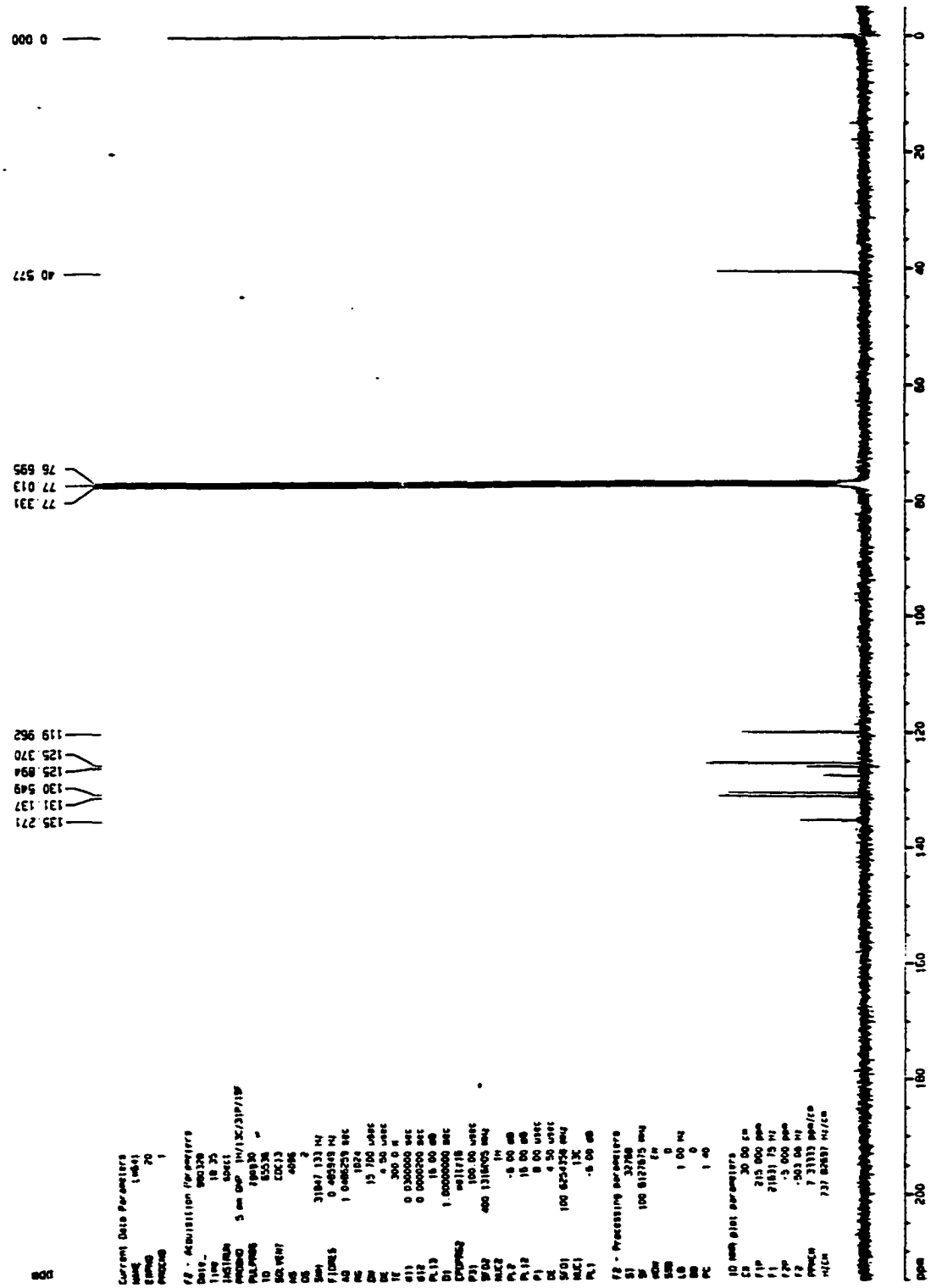

Figure 24-1. ^{1}H NMR ($CDCl_3$) of *trans*-1,2-(*p*-TsNH)$_2$C$_6$H$_{10}$ (15, DTC)

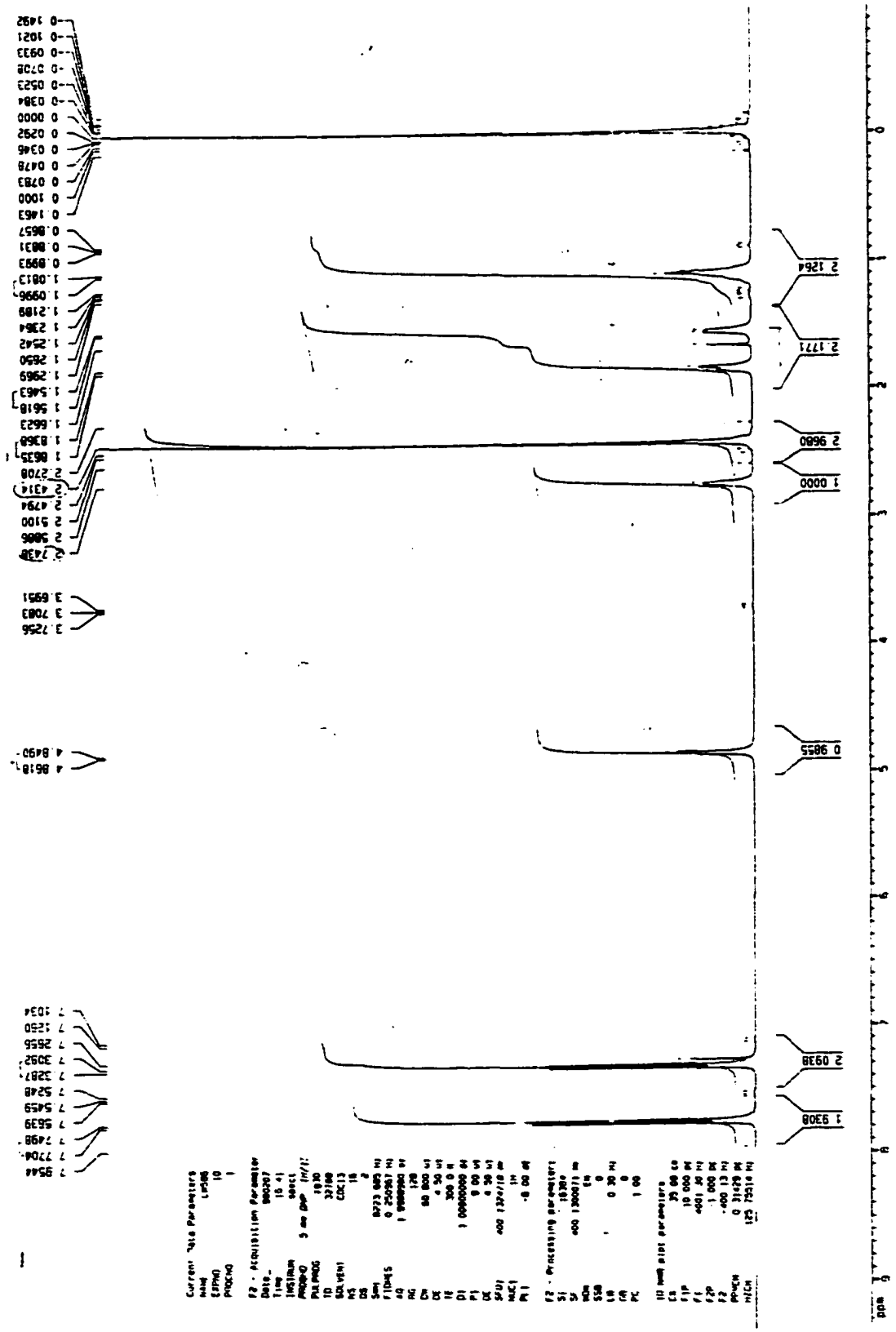

Figure 24-2. ^{13}C NMR ($CDCl_3$) of *trans*-1,2-(*p*-$TsNH)_2C_6H_{10}$ (**15, DTC**)

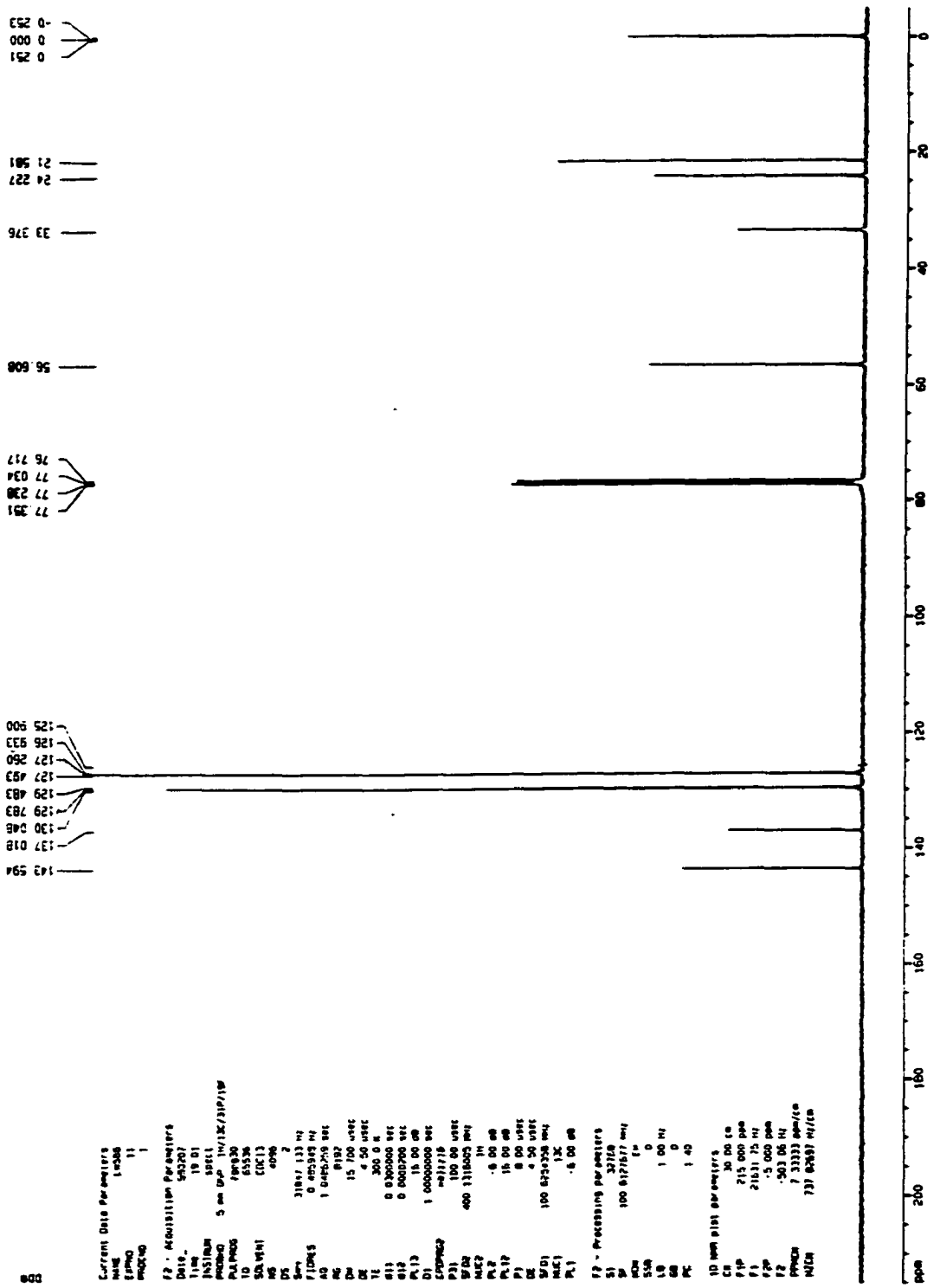

Figure 25-1. ^{1}H NMR ($CDCl_3$) of Rh(acac)$(CO)_2$ (16)

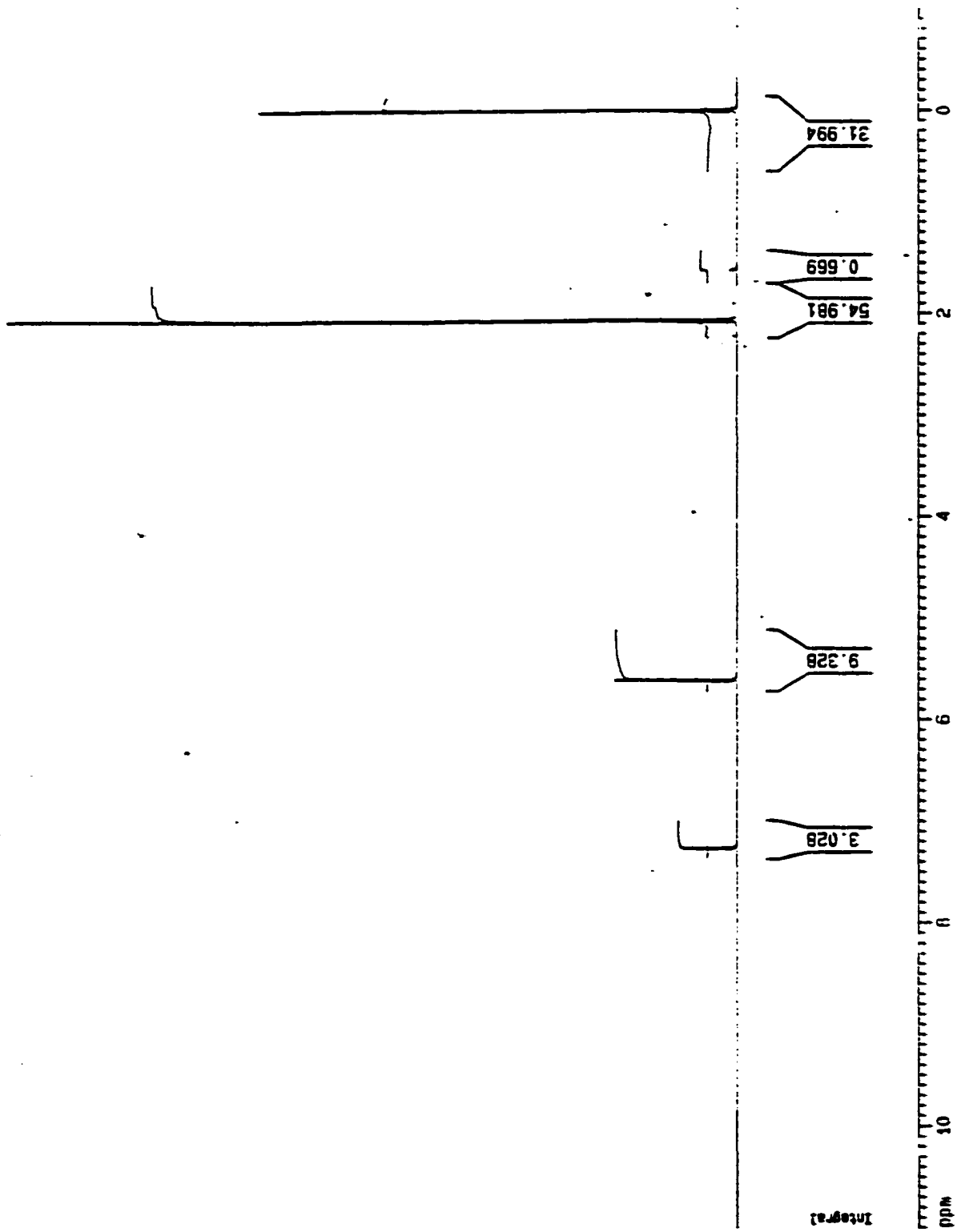

Figure 25-2. ^{13}C NMR ($CDCl_3$) of Rh(acac)$(CO)_2$ (16)

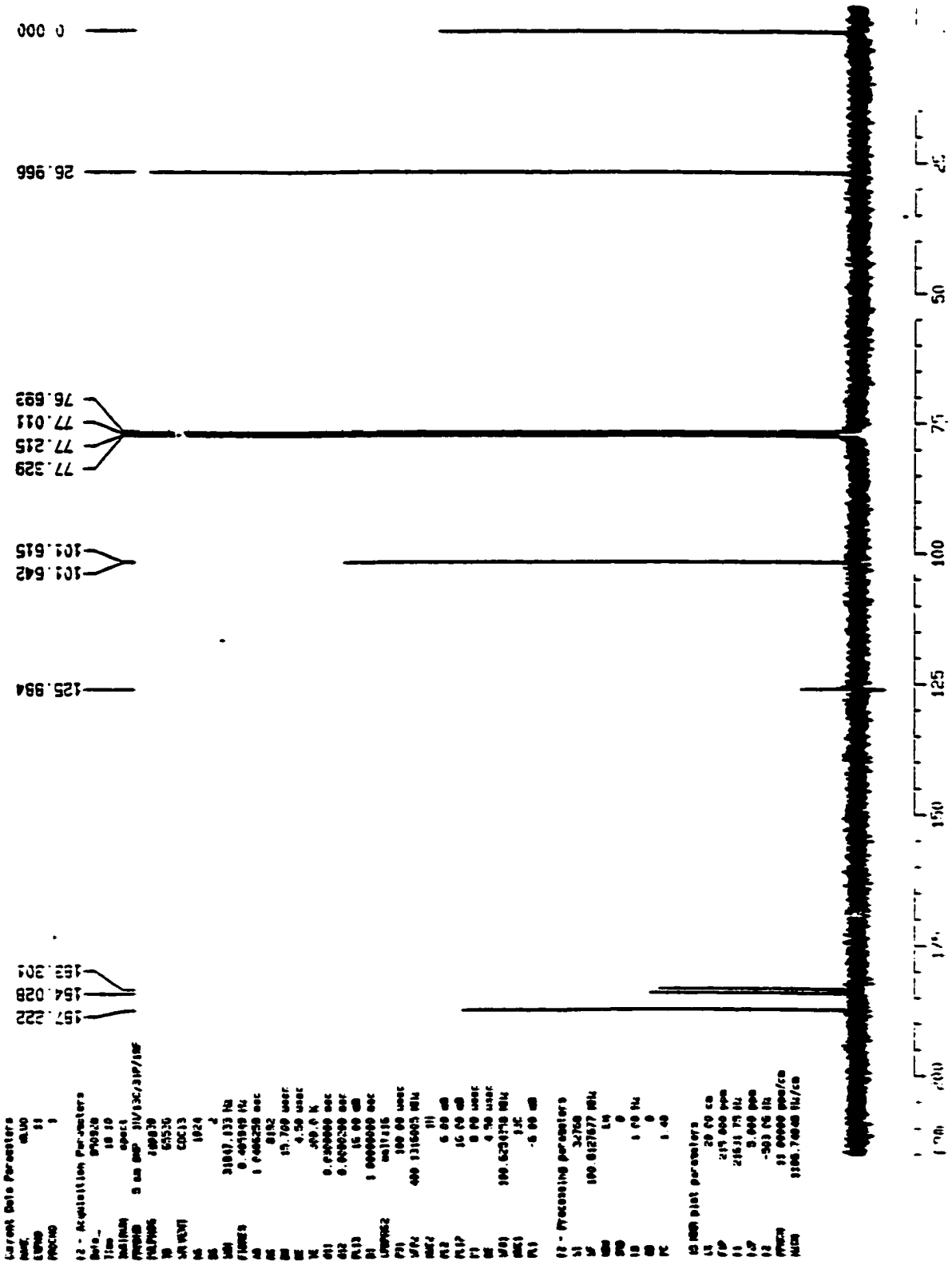

Figure 25-3. IR (Hexane) of $Rh(acac)(CO)_2$ (16)

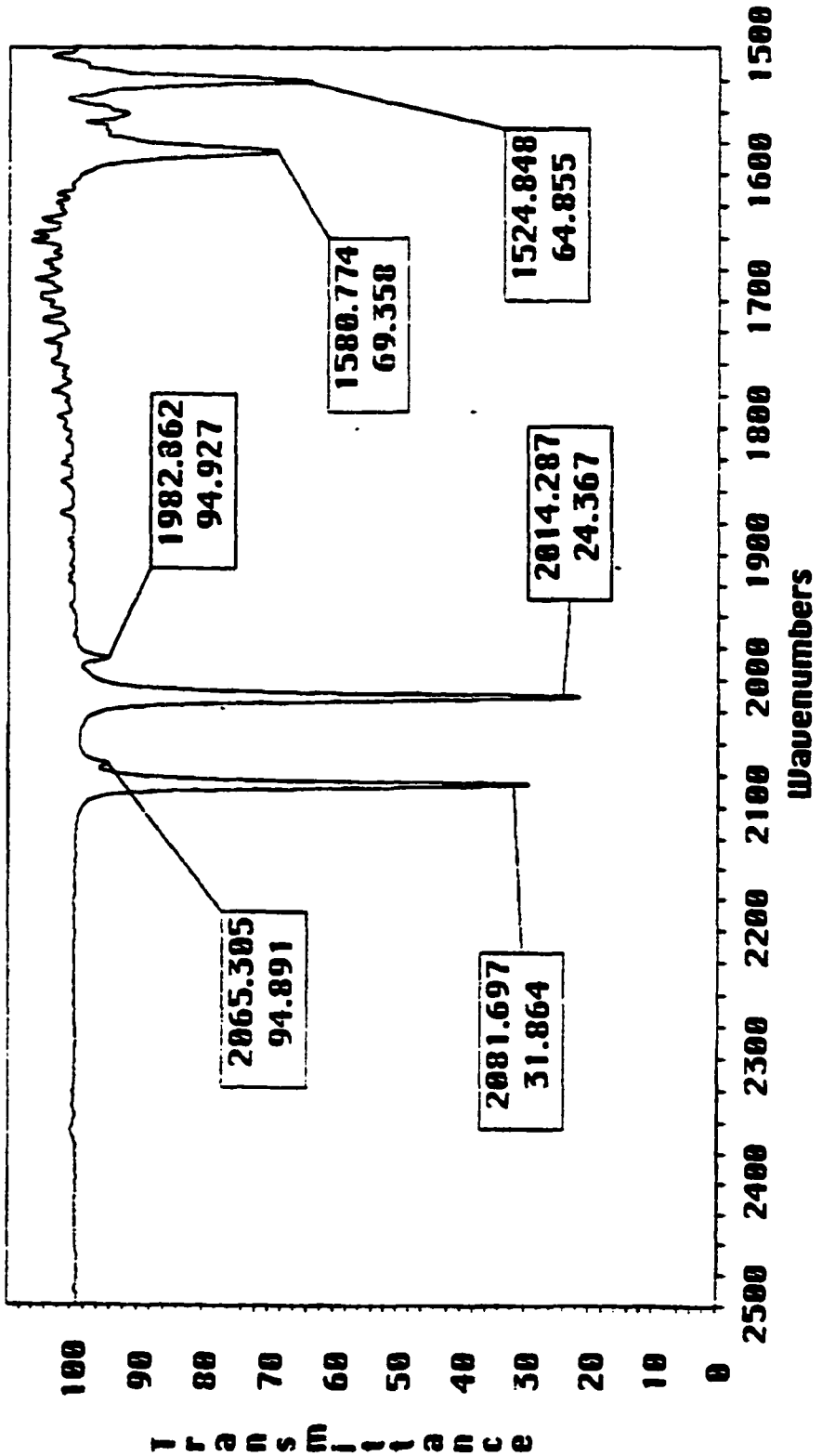

Figure 26. Reaction of TNAP with PPh_2Cl in the presence of Et_3N (17)
a) ^1H; b) ^{31}P ($CDCl_3$)

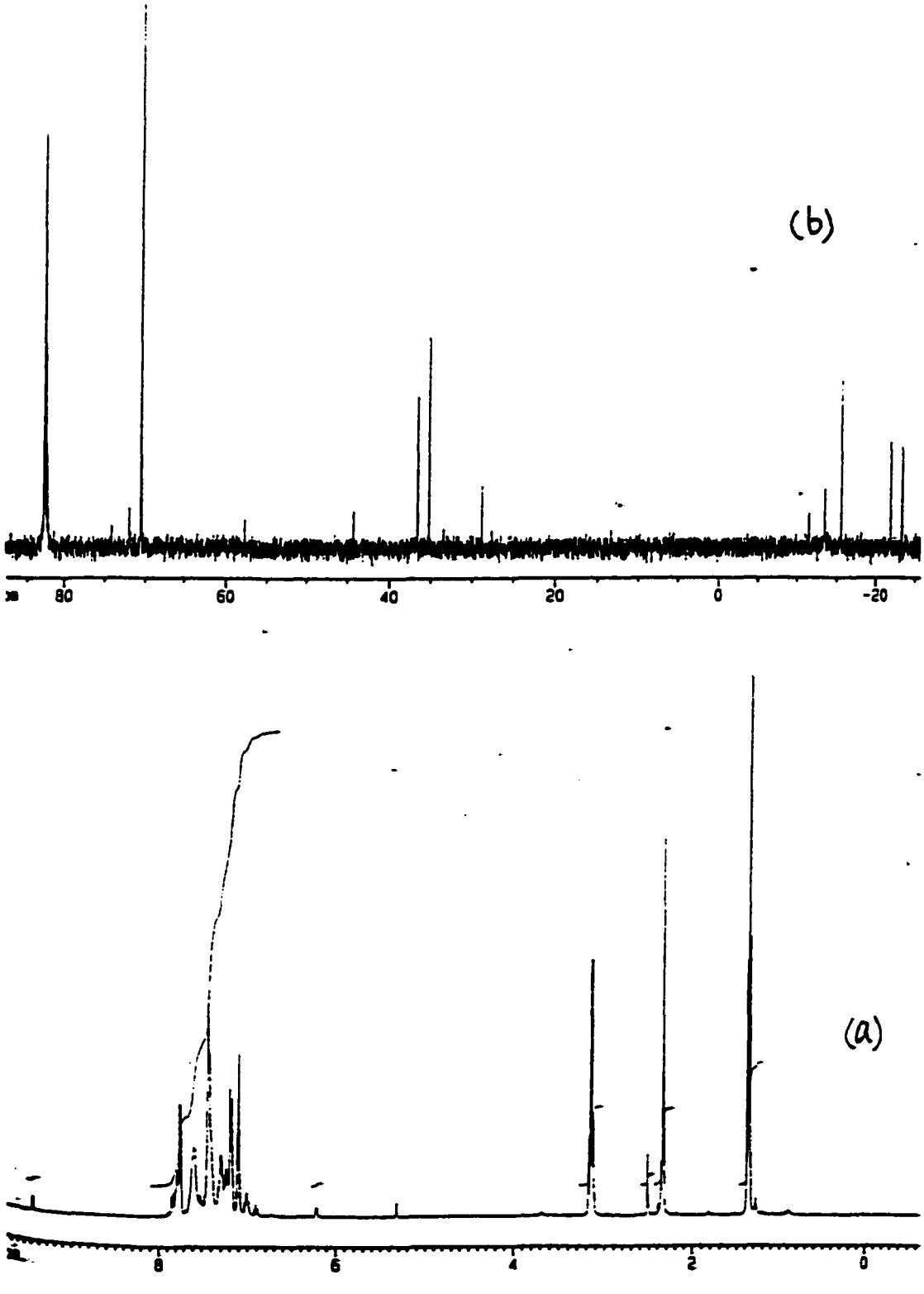

Figure 27-1. ^{1}H NMR ($CDCl_3$) of $Ts(Ph_2P)NC_6H_4C_6H_4N(PPh_2)Ts$ (**18, BBT**)

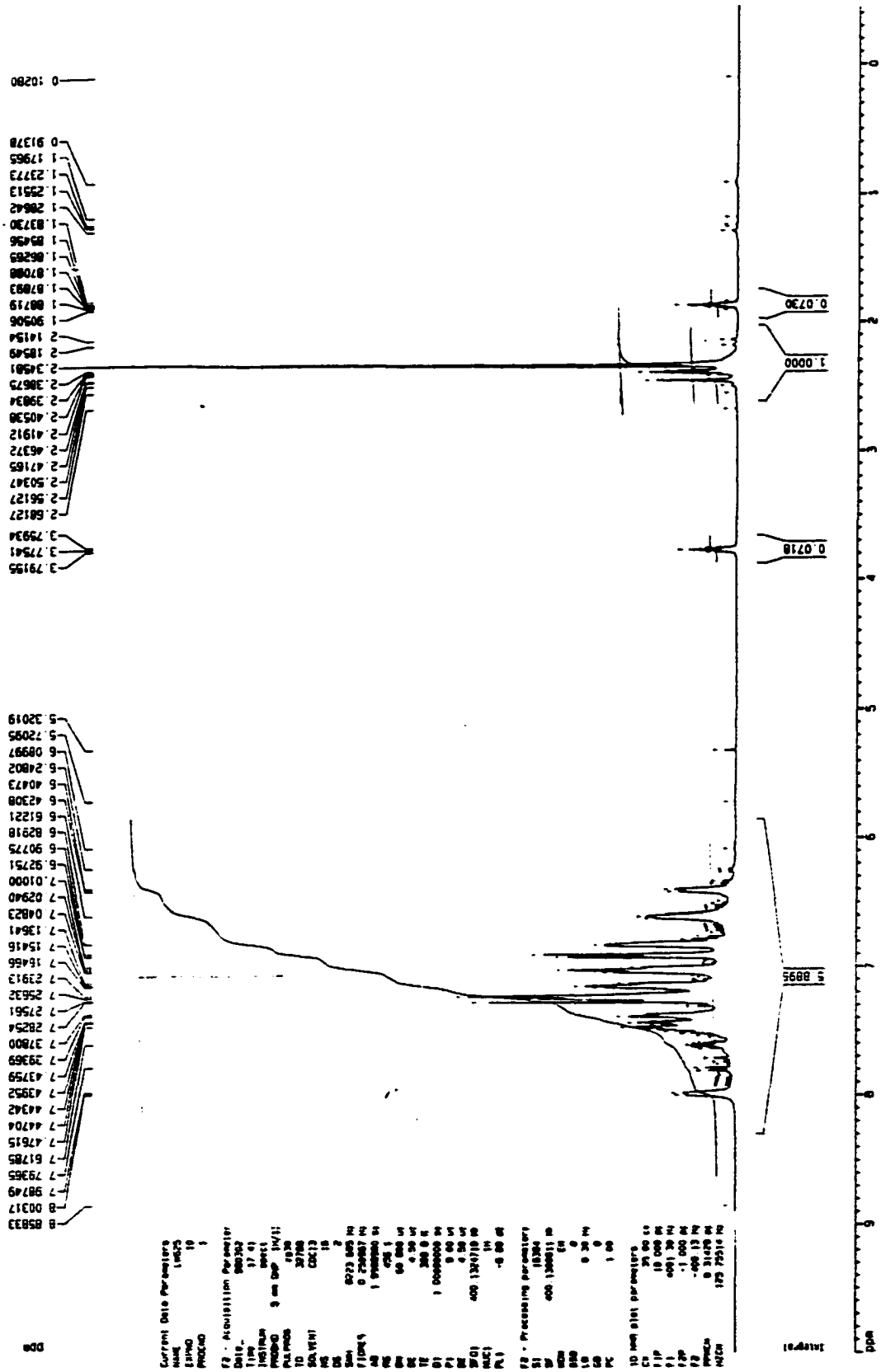

Figure 27-2. ^{31}P NMR ($CDCl_3$) of $Ts(Ph_2P)NC_6H_4C_6H_4N(PPh_2)Ts$ (18, BBT)

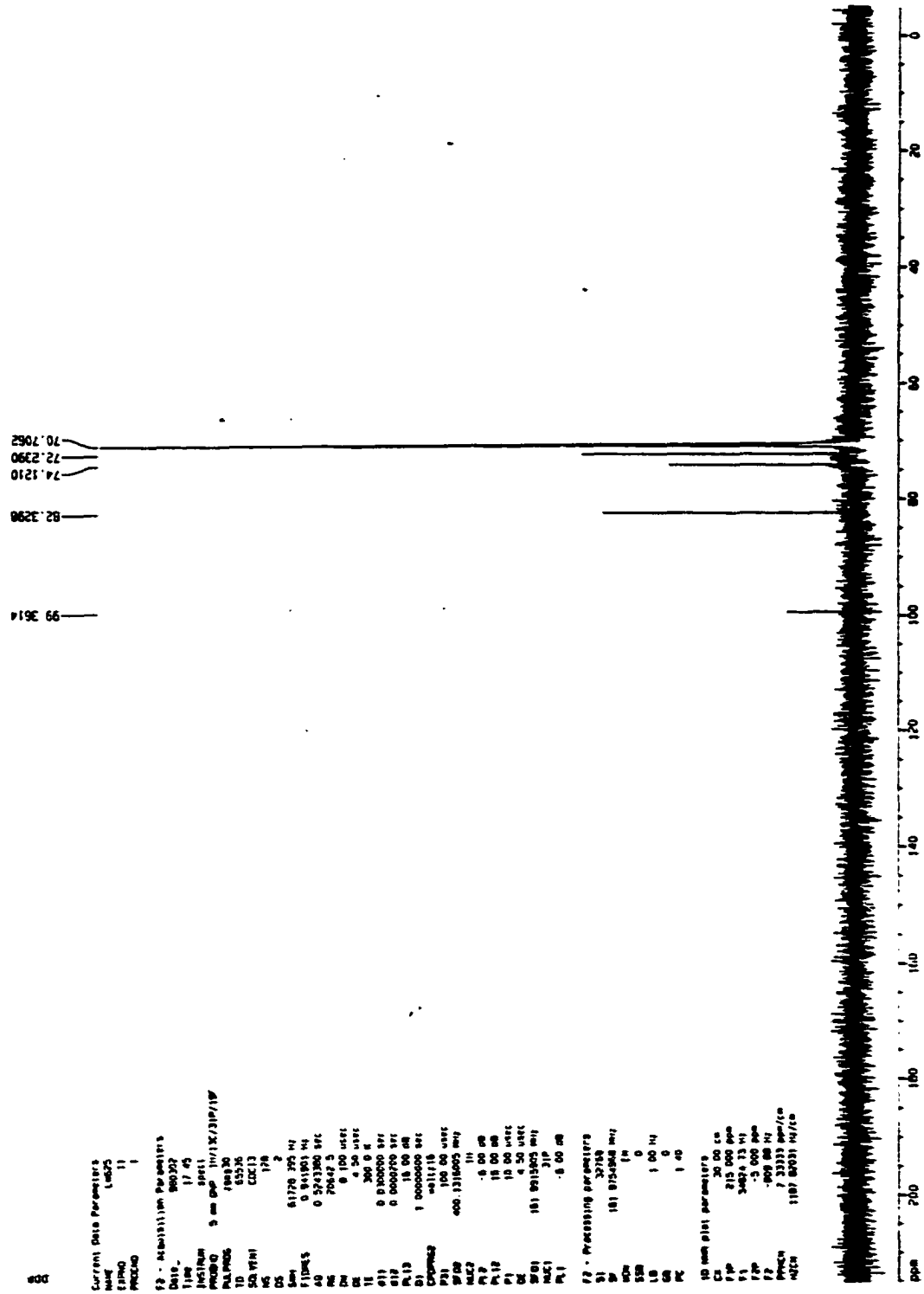

Figure 28-1. ^{1}H NMR ($CDCl_3$) of TosL analog A (19)

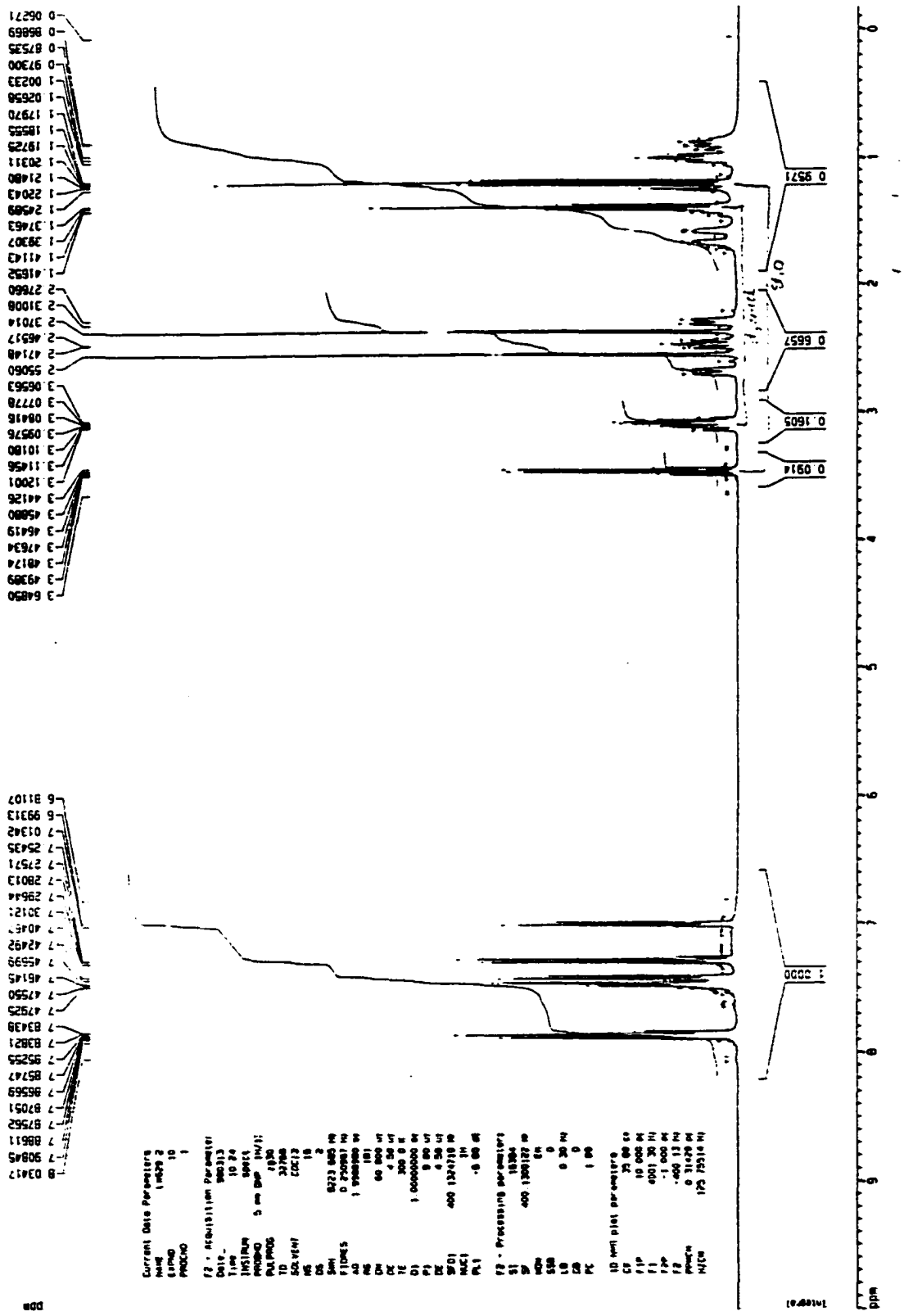

Figure 28-2. ^{31}P NMR ($CDCl_3$) of TosL analog A (19)

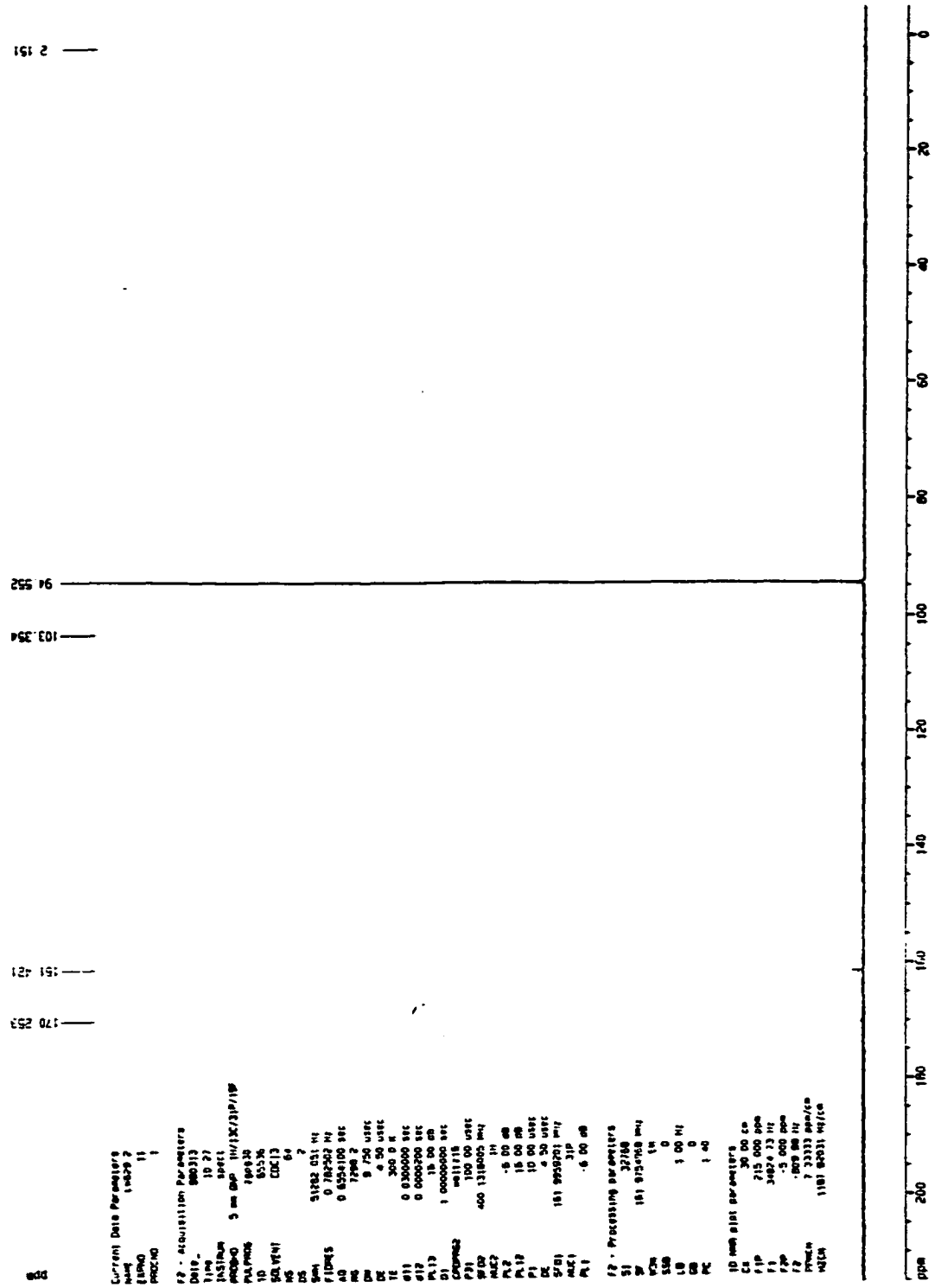

Figure 28-3. ^{13}C NMR ($CDCl_3$) of TosL analog A (19)